

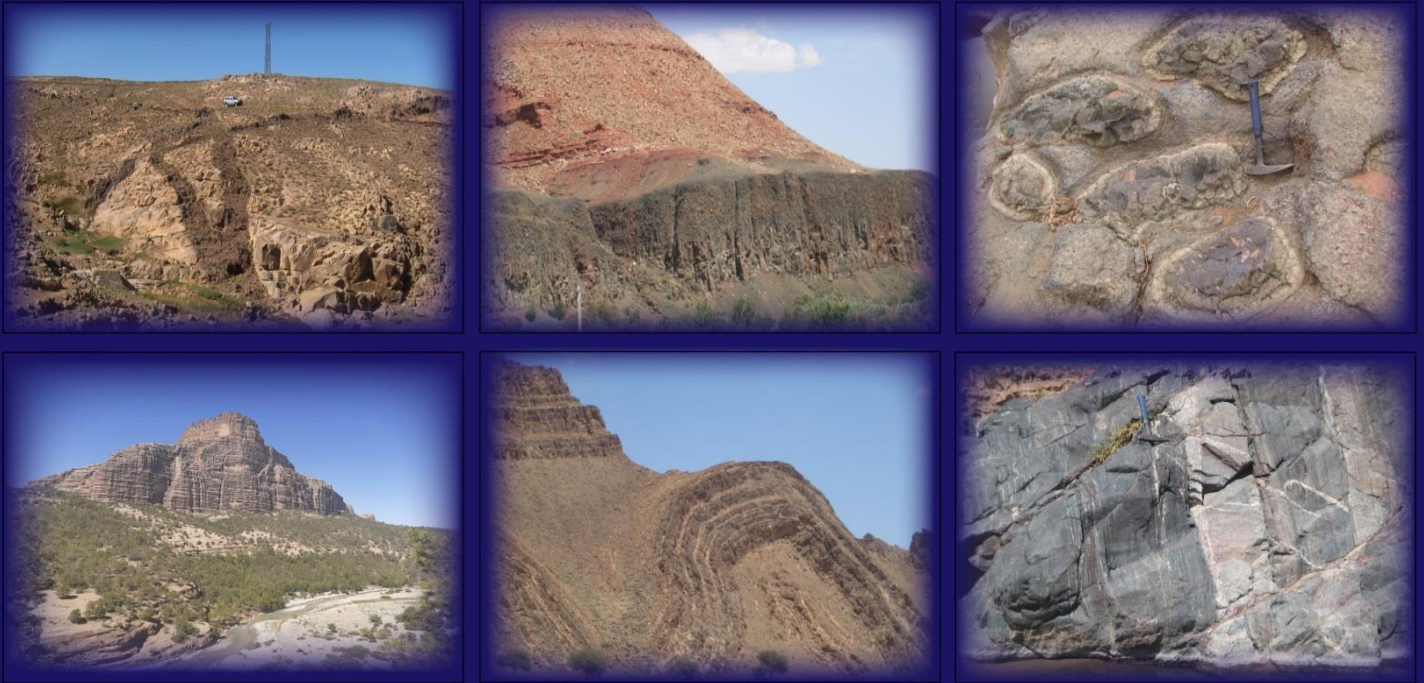


Joint Conference: IDC 8- LIPs 8 - Rodinia 2023

29th May - 16th June 2023, Marrakesh-Morocco

Abstract

Oral presentations and posters



Faculty of Sciences Semlalia and Faculty of Sciences and Techniques



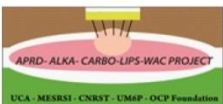
كلية العلوم
السمالية - مراكش
FACULTÉ DES SCIENCES
SEMLALIA - MARRAKECH

DLGR Lab
Dynamics of the Lithosphere and
Genesis of the Resources Laboratory

Managem
Creating value beyond mining



كلية العلوم
والتقنيات - مراكش
FACULTÉ DES SCIENCES ET
TECHNIQUE - MARRAKECH



SDSNT
SDS N T



MOHAMMED VI
POLYTECHNIC
UNIVERSITY

A first in Africa and the Arab world

Marrakesh, Morocco

Joint International, Dyke Conference (IDC 8) - Large Igneous Provinces
(LIPs 8) - Rodinia 2023, Conference

Organized under the theme:

**JOIN US IN A GEOSCIENCE PARADISE:
A VOYAGE THROUGH EARTH HISTORY IN THE KINGDOM
OF MOROCCO**



Prof. H. IBOUH and Prof. N. YOUBI Cadi Ayyad University; Marrakech, Kingdom of Morocco

Dates and Location: 29th May-16th June 2023, Marrakesh (Morocco)



Dispersed pillow lavas associated with hyaloclastites at the bottom of the Intermediate Basalt Formation of the 201 Ma Central Atlantic Magmatic Province (CAMP, High-Atlas, Morocco. Photo Prof. N. YOUNI)

<https://marrakech.sciencesconf.org/>

Our History

Joint International Dyke Conference (IDC 8)-Large Igneous Provinces (LIPs 8)- Rodinia 2023 Conference

International Dyke Conference (IDC 8)

The Eighth International Dyke Conference (IDC8) will concentrate on mafic dyke swarms and related igneous associations, e.g., sills, kimberlites, syenites, carbonatites, volcanics, etc., with a special emphasis on paleogeographic reconstruction based on geological comparison and paleomagnetic studies. The IDC8 continues the every-five-year tradition started in Toronto, Canada in 1985 by Prof. Henry C. Halls (University of Toronto). Subsequent IDCs were held in Australia (1990), Israel (1995), South Africa (2001), Finland (2006), India (2010), and China (2016).

Large Igneous Provinces (LIPs 8)

The Large Igneous Provinces conference series was launched in 2007 in Novosibirsk, Siberia, Russia by Prof. Alexander Borisenko and colleagues, and continued in 2009 – Novosibirsk, Russia; 2011 – Irkutsk, Russia; 2013 - Hanoi, Vietnam; 2015 – Irkutsk, Russia; 2017 - Chengdu, China- Tomsk, Russia ; 2019. The early conferences (2007-2015) were focused on the LIP record of Asia, but the Tomsk and the current focus is more global. The Eighth LIPs conference will again cover all aspects of this rapidly expanding field.

Rodinia 2023

The Rodinia conference series began in the form of Tectonics Special Research Centre symposia (1998-2005) that morphed into dedicated Rodinia conferences in Edinburgh, Scotland (2009); Moscow, Russia (2013); and Townsville, Australia (2017). The planned Rodinia meeting herein will continue this tradition and join forces with the other conference series noted above.

West African Craton's magmatic and tectonic legacy, 2 Ga to present

The last decade has revealed West African craton as a key witness to long-term magmatic and tectonic processes, occupying important locations within ancient supercontinents. Consolidated in the Eburnian tectonic event of ca. 2.0 Ga, the craton was long thought to be devoid of significant igneous and tectonic activity until Pan-African orogenesis 1500 million years later. However, numerous ca. 1.7-1.4 Ga mafic dyke swarms have now been dated by U-Pb on zircon and baddeleyite, both in northern and southern regions of the craton; these swarms may be related to protracted breakup of the Nuna supercontinent. In addition, craton-wide ca. 0.9-Ga mafic magmatism could be related to the Rodinia supercontinent cycle. Lacking direct records of late Mesoproterozoic ("Grenvillian") orogenesis, West African craton has typically been relegated to the outer periphery of Rodinia reconstructions, but recent documentation of Mesoproterozoic detrital zircons within autochthonous cover strata suggests some proximity to Rodinia-forming orogens.

Within the post-Rodinia era, West African craton's margins were all reworked by the ca. 0.6-0.5-Ga Pan-African orogeny, coeval with multiple episodes of glaciation and the widespread Ouarzazate (Peri-lapetus Magmatic Province) LIP. The Pan-African interval can be viewed either as a culmination of Pannotia supercontinent amalgamation, or a subsidiary step toward eventual Pangea assembly at ca. 0.3 Ga. Northern regions of the craton are directly affected by that Hercynian orogenesis. Breakup of Pangea is spectacularly documented by Central Atlantic Magmatic Province (CAMP) magmatism and rift-related sedimentation at ca. 0.2 Ga. At present, post-Alpine subduction has migrated westward to the Strait of Gibraltar, perhaps initiating subduction within the Atlantic realm that will close interior oceans *en route* to the next future supercontinent.

In celebration of all these diverse geological records, spectacular rock exposure, fascinating culture, and friendly people, we invite you to join us in the "Geological Paradise" of Morocco in 2023!

Local Organizing Committee (Cadi Ayyad University, Marrakech, Morocco)

Nasrddine, YOUNI (Leader) (Fac. of Sciences-Semlalia, Cadi Ayyad University, Marrakech, Morocco)

Hassan IBOUH (Co-Leader) (Fac. of Science & Techniques, Cadi Ayyad Uni., Marrakech, Morocco)
El Mostafa, MOUGUINA (Faculty of Sciences-Semlalia, Cadi Ayyad University, Marrakech, Morocco)
Hassan ADMOU (FSSM, Cadi Ayyad University, Marrakech, Morocco) Marrakech, Morocco)
Amina WAFIK (Faculty of Sciences-Semlalia, Cadi Ayyad University, Marrakech, Morocco)
Farid El WAHIDI (Faculty of Science & Techniques, Cadi Ayyad University, Marrakech, Morocco)
My Ahmed, BOUMEHDI, (Faculty of Sciences-Semlalia, Cadi Ayyad University, Marrakech, Morocco)
Abderrahmane SOULAIMANI, (Faculty of Sciences-Semlalia, Cadi Ayyad University, Marrakech, Morocco)
El Hassane CHELLAI (Faculty of Sciences-Semlalia, Cadi Ayyad University, Marrakech, Morocco)

Phd Student Organizing Committee (Cadi Ayyad University, Marrakesh, Morocco)

MGHAZLI Kamal
HADIMI Ismail
IDBAROUD Mohamed
Warda EL MOUME
CHINOUR Marouane
BENDAOU Mohamed
BENJELLOUN Mohamed
FADIL Malika
LAGHRIS Said
MEDIANY Mohamed Achraf
MOUTBIR Oussama
Diallo MAMADOU
AZMI Mohamed
AIT LAHNA Abdelhak
OUKHRO Rachid

National Scientific Committee

Nasrddine, YOUNI (Cadi Ayyad University, Marrakech, Morocco)
Hassan IBOUH (Cadi Ayyad University, Marrakech, Morocco)
Hassan ADMOU (Cadi Ayyad University, Marrakech, Morocco)
El Mostafa MOUGUINA (Cadi Ayyad University, Marrakech, Morocco)
Amina WAFIK (Cadi Ayyad University, Marrakech, Morocco)
Moulay Ahmed BOUMEHDI (Cadi Ayyad University, Marrakech, Morocco)
Mohamed Khalil BENSALAH (Cadi Ayyad University, Marrakech, Morocco)
Abderrahmane SOULAIMANI (Cadi Ayyad University, Marrakech, Morocco)
Mohamed HIBTI (Cadi Ayyad University, Marrakech, Morocco)
El Hassane CHELLAI (Cadi Ayyad University, Marrakech, Morocco)
Hind EL HAIBI (Cadi Ayyad University, Marrakech, Morocco)
Mohamed BOUABDELLA (Mohmed Premier University, Oujda, Morocco)
Mohamed JADID (Mohamed Premier University, Oujda, Morocco)
Youssef DRIOUCH (Sidi Mohamed Ben Abdellah University, Fes, Morocco)
Mohamed BEN ABBOU (Sidi Mohamed Ben Abdellah University, Fez, Morocco)
Mohamed AISSA (Moulay Ismail University, Meknes, Morocco)
Mustapha BOUJEMAAOUI (Moulay Ismail University, Meknes, Morocco)
Hassan EL OUALI (Sidi Mohamed Ben Abdellah University, Fes, Morocco)
Driss OURHACHE (Sidi Mohamed Ben Abdellah University, Fes, Morocco)
Zouheir BARODI (Hassan II University, Casablanca)
Zahour Ghanem (Hassan II University, Casablanca)
Omar SADDIQI (Hassan II University, Casablanca)
Faouziya HAISSAN (Hassan II University, Casablanca)
Hassan ELHADI (Hassan II University, Casablanca, Morocco)
Hasnaa CHENNAOUI A. (Hassan II University, Casablanca Morocco)
Abdelhak BOUABDELLI (University Ibon Toufail, Kenitra, Morocco)

Ahmid HAFID	(Cadi Ayyad University, Marrakech, Morocco)
Ahmed TOUIL	(Cadi Ayyad University, Marrakech, Morocco)
Abdellatif SAIDI	(Cadi Ayyad University, Marrakech, Morocco)
Lhou MAACHA	(Managem, Morocco)
Amine BAJDDI	(Managem, Morocco)
Mohamed ZOHAIR	(Managem, Morocco)
Hind EL HACHIMI	(Chouaib Doukkali University, El Jadida, Morocco)
Ezzoura ERRAMI	(Chouaib Doukkali University, El Jadida, Morocco)
Moha IKKEN	(Ibno Zohr University, Agadir, Morocco)
Elhassane Beraaouz	(Ibno Zohr University, Agadir, Morocco)

International Scientific Committee

ALTERMANN Wladyslaw	(University of Johannesburg, South Africa)
BASEI Miguel Angelo Stipp	(Universidade de São Paulo, USP, Brazil)
BEKKER Andrey	(University of California, Riverside, USA)
BETTS Peter	(Monash University)
BLEIN Olivier	(BRGM, France)
BOURDIER Jean Louis	(ISTO, France)
CHAMBERLAIN Kevin	(University of Wyoming, USA)
COUSENS Brian	(Carleton University, Canada)
DAVIES Joshua	(GeoTop, Université du Québec à Montréal, Canada)
DE KOCK, Michiel	(University of Johannesburg, South Africa)
DE MIN Angelo	(Università degli Studi di Trieste, Italy)
DENYSZYN, Steven	(Memorial University, Canada)
DOBLAS LAVIGNE Miguel de las	(Instituto de Geociencias – IGEO, Spain)
EGLINGTON Bruce	(University of Saskatchewan).
ERNST, Richard E.	(Convenor of the International Committee, Carleton University, Ottawa, Canada & Faculty of Geology and Geography, Tomsk State University, Tomsk, Russia)
EVANS, David	(Yale University, USA)
EL BILALI, Hafida	(Carleton University, Ottawa, Canada)
FLAMENT Nicolas	(University of Wollongong, Australia). The talk will be given remotely
GÄRTNER Andreas	(Senckenberg Naturhistorische Sammlungen Dresden, Germany).
	GLADKOCHUB, Dimitri P (Institute of Earth's Crust, Russian Academy of Sciences, Russia)
HAMIMI Zakaria	(Benha University, Egypt)
HEAD James W., III	(Brown University, USA)
HOLLANDA Maria Helena B. M.	(Universidade de São Paulo, USP, Brazil).
HUSTON David	(Geosciences Australia)
IBOUH Hassan	(Co-Leader of the Joint Conference 2023, Cadi Ayyad University, Marrakech)
JELSMA, Hielke	(Exploration Business and Strategic Planning, Anglo American plc, Johannesburg, South Africa)
JESSELL, Mark	(The University of Western Australia, Australia)
KHALAF Ezz El-din Abdel Hakim	(Cairo University, Egypt).
KUIPER Yvette	(Colorado School of Mines, USA). The talk will be given remotely
LI, Zheng Xiang	(Curtin University, Australia)
LINDEMANN Ulf	(Senckenberg Naturhistorische Sammlungen Dresden, Germany).
LO Khalidou	(University of Nouakchott Al Aasriya, Mauritania).
MAACHA Lhou	(Managem, Morocco)
MADEIRA José	(Universidade de Lisboa, Portugal).
MARZOLI Andrea	(Università degli Studi di Padova, Italy).
MATA João	(Universidade de Lisboa, Portugal).
MORESI Louis	(University of Melbourne)
OKUNLOLA Gbenga	(President of GSAf -Geological Society of Africa, University of Ibadan, Nigeria).

OSSA OSSA Frantz	(Khalifa University, Abu Dhabi, UAE).
OVTCHAROVA Maria	(University of Geneva, Switzerland)
PEARCE Julian	(Cardiff University, Cardiff, United Kingdom)
PEHRSSON Sally	(Natural Resources Canada)
PENG, Peng	(Institute of Geology and Geophysics, CAS, Beijing)
PISAREVSKY, Sergei	(Curtin University & University of Western Australia)
ROSS Mitchell	(Institute for Geology and Geophysics, Beijing).
SALMINEN Johanna	(University of Helsinki)
SCHALTEGGER Urs	(University of Geneva, Switzerland).
SIMON Jowitt	(University of Nevada, Las Vegas, USA)
SÖDERLUND, Ulf	(Lund University, Sweden)
SRIVASTAVA, Rajesh	(Banaras Hindu University, India)
TASSINARI Colombo Celso Gaeta	(Universidade de São Paulo, USP, Brazil)
TCHOUANKOUE Jean Pierre	(University of Yaoundé, Cameroon).
TEGNER, Christian	(Aarhus University, Denmark)
TEIXEIRA Wilson	(Universidade de São Paulo, USP, Brazil).
THIÉBLEMONT Denis	(BRGM, France)
WOTZLAW Jörn-Frederik	(ETH Zürich University, Switzerland).
XU Yigang	(Guangzhou Institute of Geochemistry, China).
YOUBI, Nasrddine	(Leader of the Joint Conference, Vice President of GSAf -Geological Society of Africa for North Africa, Cadi Ayyad University, Marrakech, Morocco & Faculty of Geology and Geography, Tomsk State University, Tomsk, Russia).
ZHANG Shuan-Hong	(Chinese Academy of Geological Science, China)
ZHONG Shije	(University of Colorado)

The Honorary Chairs, who are honored in this conference:

Prof. Henry C., HALLS	(University of Toronto, Toronto)
Prof. Hervé, BERTRAND	(University of Lyon, France)
Prof. Ahmed, EL HASSANI	(Academy Hassan II of Science & Technology)
Prof. El Hassane, CHELLAI	(Cadi Ayyad University)
Prof. Ahmed CHALOUAN	(Mohamed V University)

Keynote speakers

Abstracts

In search of the event-based definition for the Archean-Proterozoic boundary

By

Bekker¹ A. (andrey.bekker@ucr.edu)

1. Department of Earth & Planetary Sciences, University of California, Riverside CA 92521 USA

There is a growing interest to base the Archean-Proterozoic boundary on the synchronous and potentially global surface event. The rise of atmospheric oxygen in the early Paleoproterozoic closely followed the assembly and emergence of large landmasses and associated emplacement of Large Igneous Provinces (LIPs), was bracketed by 3 to 4 Snowball Earth events, and led to the largest and longest positive carbon isotope excursion in seawater composition in Earth's history, the Lomagundi Event (LE). Since each of these events could be globally synchronous and widespread, they hold an eminent potential to define a GSSP that deserves to be considered.

Assembly of the supercraton Superia occurred over a protracted period that started in the late Neoproterozoic and continued to the early Paleoproterozoic, potentially ending at ~2.3 Ga with the Arrowsmith Orogeny in NW Canada. Associated emplacement of LIPs affected all landmasses, but their ages cluster into several discreet groups that individually are not expressed on all continents (Ernst, 2014). The initiation of the GOE, as defined by the disappearance of mass-independently fractionated sulphur (MIF-S) from sedimentary records (Holland, 2002), has been constrained between ~2.45 and 2.43 Ga (e.g., Warke et al., 2020). However, the long-term pattern of MIF-S during the GOE has been recently considered to be either globally asynchronous (Philippot et al., 2018) or to correspond to a series of rises and falls in atmospheric oxygen in association with global glaciations (Gumsley et al., 2017; Bekker et al., 2020; Poulton et al., 2021). The Paleoproterozoic glaciations are generally envisioned to have a global extent since there is strong geological and paleomagnetic evidence for glaciation at sea-level near paleo-equator (Evans et al., 1997). However, diamictites in the Boolgeeda Iron Formation (Martin, 1999) and the Koegas Subgroup (Polteau et al., 2006), if indeed glacial, would correspond to regional-scale glaciations leading to the Snowball events. Although three stratigraphic horizons with glacial diamictites are recorded in the Huronian and Snowy Pass supergroups of Ontario and Wyoming, respectively, other Paleoproterozoic successions bear evidence for two, one, or no glaciations. The record of the fourth glacial event, at ca. 2.22 Ga (Rasmussen et al., 2013), has been recently identified in the Pretoria Group of South Africa. Furthermore, synchronicity of Paleoproterozoic ice ages, in contrast to the Neoproterozoic glaciations, has to be tested with high-precision geochronology. Finally, the LE that was inferred to last between ~2.22 and 2.06 Ga (Karhu and Holland, 1996), might be mistaken for shorter-lived, but similar magnitude excursions leading to the LE and in its aftermath before ~2.0 Ga.

Pending future work testing synchronicity of the early Paleoproterozoic events with high-precision geochronology, it seems premature at this stage to define the GSSP based on any of these events that could be multiple and asynchronous worldwide. In contrast, the conventional approach based on the numerical value for the Archean-Proterozoic boundary avoids potential confusion and provides an independent framework to test synchronicity and global extent of the early Paleoproterozoic events.

ATLA REGIO SUPERPLUME, VENUS

H. El Bilali^{1,2}; R.E. Ernst^{1,2}; K.L. Buchan³; J.W. Head⁴

¹Department of Earth Sciences, Carleton University, Ottawa, Ontario, Canada;

²Faculty of Geology and Geography, Tomsk State University, Tomsk, Russia,

³273 Fifth Ave., Ottawa, Ontario, Canada,

⁴Department of Earth, Environmental and Planetary Sciences, Brown University, Providence, Rhode Island, USA.

Introduction:

Overview of Atla Regio. Atla Regio represents a major mantle plume concentration on Venus, featuring multiple volcanic centres (notably Ozza, Maat and Ongwuti Montes, and perhaps also Sapas Mons), associated coronae, topographic highs, a geoid high and radiating rift system, all classic signatures of terrestrial Large Igneous Province (LIP)-style magmatism associated with an active mantle plume (e.g., Senske et al., 1992; Smrekar, 1994; Shalygin et al., 2012) (Figs. 1-2). Comparable LIP magmatism on Earth consists of major volcanism in the form of shield and plateau basalts, and a plumbing system that includes giant radiating and circumferential dyke swarms (e.g. Ernst et al., 2001; Buchan and Ernst, 2021). Dyke swarms on Venus are expressed as sets of long narrow grabens (and also pit chains) inferred to overlie blind dykes [not reaching the surface] that were, for the most part, laterally emplaced (e.g. Grosfils and Head, 1994; Ernst et al. 1995; Ernst et al., 2003; Studd et al., 2011; Davey et al., 2013; Graff et al., 2018).

Objectives of Analysis. We summarize our detailed mapping of graben systems across Atla Regio which distinguishes multiple radiating, circumferential and linear graben sets (interpreted to mark underlying dyke swarms) and their link with magmatic centres. See El Bilali et al., (2022) for more details of this Atla Regio dyke swarm mapping and criteria to distinguish tectonic from magmatic graben. Several key results are emphasized below, as well as lessons learned that can be applied to dyke-swarm mapping of other major mantle plume centres on Venus.

Dyke Swarms and Magmatic Centres of Atla Regio:

Mapping of Atla Regio graben-fissure systems (interpreted as dyke swarms) is shown in Figure 1, with more than 40,000 lineaments traced to date. Giant radiating and circumferential graben (dyke) systems linked to the four recognized mons (Maat, Sapas, Ozza, Ongwuti), Zemina corona, and unnamed magmatic centres. Grabens from Ongwuti Mons, Unnamed (labelled as such) magmatic centre, Maat and Ozza montes extend for hundreds to thousands of kilometers from the centres, with the Ozza Mons dykes reaching more than 2000 km.

Locating the Plume Centre and Plume Head Size: The transition distance from radiating (due to the underlying plume head) to linear (due to dominance of the regional stress field), is a proxy for plume head size. On this basis, the inferred plume size for Ozza Mons is the largest, with an inferred plume head radius of 1200 km (Fig. 2) (El Bilali et al., 2022). The plume heads of the other three (with sizes 600, 600 and 200 km) are all enclosed within the extent of the Ozza Mons plume head. In addition, Sapas Mons is located at the edge of the outer boundary of the Ozza Mons plume head and could therefore also be related to it. On this basis all the Atla Regio magmatic centres may be related to a single large plume centered on Ozza Mons.

Implications:

Atla Regio is at the Plume Head Stage. An important implication of the above analysis is that Atla Regio is still at the plume head stage, and potentially no older than about 50 myr, based on the maximum duration of plume-caused terrestrial LIPs (see discussion in El Bilali et al., (2022)).

Origin of Multiple Magmatic Centres in a Plume Context. If this plume head interpretation is correct, then an explanation is required for the presence of multiple distinct magmatic centres (e.g. Maat, Sapas, Ozza, Ongwuti, Unnamed). In El Bilali et al. (2022), we consider candidate models involving: 1) shifting of the lithosphere above a stationary plume, 2) lateral shifts of the plume itself, 3) lithospheric controls

(including incipient rifting; and/or 4) breakup of the plume head during ascent into multiple plumes/diapirs.

Lessons for Mapping Dyke Swarms for Other Major Mantle Plume Centres on Venus:

Other Venesian Regios including Beta, Bell, Phoebe, Eistla, are also inferred to be linked with major mantle plumes (e.g. Senske et al., 1992; Ernst et al., 2007). The approach applied herein to interpreting the dyke swarm history of Atla Regio is also being applied to some of these other regios as part of the current detailed mapping of the International Venus Research Group (IVRG) (Ernst et al., 2022).

Below are listed some relevant lessons for other plume-generated regios from the graben-fissure (dyke swarm) mapping of Atla Regio (see also El Bilali et al., (2022)):

Radiating graben-fissure systems (marking dyke swarms) can extend for >2000 km away from the mantle plume centre. This is well recognized on Earth but also true for Venus (Ernst et al., 2001; Buchan and Ernst, 2021; Ernst et al., 2003; Hansen and Olive, 2010) and Mars, where Tharsis-centered radial graben reach a distance of 3000-4000 km from their source (Wilson and Head, 2002). The longest dykes associated with Atla Regio extend greater than 2000 km from the Ozza Mons magmatic centre.

Using Dyke Swarms to Estimate the size of a mantle plume head. A proxy for the edge of the underlying mantle plume head is the distance at which a radiating swarm (influenced by magmatic-induced and uplift stresses) swings into a linear trend (marking the greater influence of regional stresses). The plume head size can also be estimated by the outer boundary of a circumferential dyke swarm (e.g. Buchan and Ernst, (2021)). [This approach may also apply to determining the size of smaller mantle plumes/diapirs associated with smaller magmatic centres.]

Radiating and Circumferential Dyke Swarms can identify Cryptic Magmatic Centres. Mapping of graben fissure systems (interpreted as dyke swarms) is a powerful tool for identifying additional ‘cryptic’ magmatic centres i.e those lacking obvious central volcanism.

Identifying Which Other Regios are also at the Plume Head Stage. It is suggested that Atla Regio is at the plume head stage (rather than at the plume tail stage) on the basis that all its major magmatic centres have radiating graben-fissure (dyke swarm) systems that extend more than several hundred km. Such a scale is consistent with LIP magmatism above a plume head. Magmatism associated with semi-stationary plume tails can also produce large volcanic centres (c.f. the terrestrial example of Iceland), but the lower magmatic flux of plume tail magmatism is observed to be associated with shorter dyke swarms (with a maximum of about 100 km (cf. discussion in El Bilali et al., (2022))).

References:

Buchan, K.L. and Ernst R.E. (2021) *Gond. Res.*, 100, 25-43. Davey S.C. et al. (2013) *Can. J. E. Sci.*, 50, 109-126. Ernst R.E. et al. (1995) *ESR*, 39, 1-58. Ernst R.E. et al. (2001) *Ann. Rev. E & Planet. Sci.*, 29, 489-534. Ernst R.E. et al. (2003) *Icarus*, 164, 282-316. Ernst R.E. et al. (2007). In Yuen, D.A. et al. (eds). *Superplumes: Beyond Plate Tectonics*. Springer-Verlag, pp.537-562. Ernst R.E. et al. (2022) *Ann. Mtg Planet. Mappers #7009*. El Bilali H. et al (2022) *LPSC. Graff J.R. et al. (2018) Icarus*, 306, 122-138. Grosfils E.B., and Head J.W. (1994) *GRL*, 21, 701-704. Hansen V.L. and Olive A. (2010). *Geology*, 38, 467-470. Senske D.A. et al. (1992) *JGR*, 97, 13395-13420. Shalygin, E.V. et al. (2012) *Planet Space Sci.*, 73, 294-301. Smrekar S.E.. (1994) *Icarus*, 112, 2-26. Studd D. et al. (2011) *Icarus*, 215, 279-291. Wilson, L. and Head, J.W. (2002) *J. Geophys. Res.* 107, E8 doi:10.1029/2001JE001593.

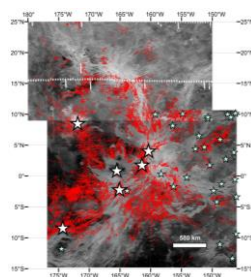


Figure 1: Radiating, circumferential and linear graben systems of Atla Regio inferred from mapping of about 34,000 lineaments to date. Large/small stars mark major/minor magmatic centres.

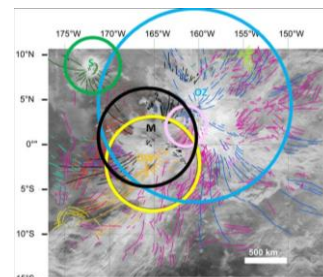


Figure 2: Generalized graben-fissure distributions, showing plume head size estimates for Maat Mons (M), Ozza Mons (Oz), Ongwuti Mons (On), Unnamed centre (U) and Sapas Mons (S), using criterion discussed in the text.

FRONTIERS IN LARGE IGNEOUS PROVINCE RESEARCH (LIP) AND THE STATUS OF THE GLOBAL LIP RECORD

R.E. Ernst^{1,2} and H. El Bilali^{1,2}

¹ Department of Earth Sciences, Carleton University, Ottawa, Canada

² Faculty of Geology and Geography, Tomsk State University, Tomsk, Siberia, Russia

LIP Research Frontiers: Over the past two decades, there has been a dramatic expansion of the global LIP record through precise U-Pb dating, new approaches to geochemical characterization, improved reconstruction constraints (based on paleomagnetism and matching of magmatic events), and a better understanding of LIP plumbing system architecture.

There has also been recognition that LIPs contribute to major geodynamic processes including formation and evolution of lithospheric and mantle, supercontinent breakup, dramatic climate change including mass extinctions, major regional topographic changes, formation of major ore deposits for a range of commodities including critical minerals, a role in oil/gas exploration, and as a planetary analogue.

Dramatic Expansion of the Global LIP Record: The dramatic expansion of the global LIP record has been facilitated by U-Pb dating (and Ar-Ar dating) campaigns, including a major initiative of the ongoing LIPs Industry Consortium (www.supercontinent.org). This wealth of new precise ages has resulted in discovery of numerous LIP events, not only of Precambrian age, but also surprisingly even some new Phanerozoic LIPs. As a result, most of the continental blocks on Earth are at least partially LIP-barcode which allows the LIP record to be efficiently used along with paleomagnetism in global reconstructions.

Continued U-Pb dating campaigns will facilitate the next steps of determining the full extent of LIPs within a crustal block (and between crustal blocks through reconstructions), and locating a mantle plume centre (typically as the focus of giant radiating and/or circumferential mafic dyke swarms).

We provide an overview of the current status of the global LIP record and associated dyke swarms (through time, including into the Archean), and current understanding of their geodynamic impacts.

Broader Goal of Integrating Earth's Magmatic (LIP) History with the Climatic History Recorded in Sedimentary Rocks. It is increasingly clear that LIPs are a major driver of climate change including mass extinction events in the Phanerozoic. LIPs have also become a leading candidate as a proxy for natural geochronological boundaries in the Proterozoic and Archean. The expanding pace of high precision CA-IDTIMS zircon dating applied to LIPs of all ages will allow further correlations of LIP events with the climatic change record by isotopic proxies / facies changes in the sedimentary record and lead to greater integration between igneous and sedimentary geology and with climate and environmental change.

Strategies for utilizing dyke swarms in pre-Pangea cratonic reconstructions

David Evans^{1,*}

¹ *Department of Earth and Planetary Sciences, Yale University, New Haven, CT 06511, USA*

* *Email: david.evans@yale.edu*

Ever since the advent of procedures for routine dating mafic dykes with U-Pb methods on baddeleyite grains, dyke swarms have become one of the primary geologic features used in pre-Pangea cratonic reconstructions. In order of increasing spatial precision, (1) the swarms' ages can be compared across several cratons to generate "bar-code" diagrams that potentially identify matches among once-neighboring cratons, possibly supplemented by geochemical matches; (2) the dyke orientations, if inferred to radiate from a plume source, can provide azimuthal constraints on the juxtapositions, and possibly locking into unique configurations when two or more ages of swarms are considered; and (3) paleomagnetic data can provide an independent test of proposed fits from the first two methods, as long as magnetic remanences can be demonstrated as primary and representative of an axial-dipolar time-averaged geomagnetic field.

In order for the third method to be employed successfully, numerous field- and laboratory-based strategies are recommended. Here I describe field strategies learned during the course of four extensive sampling campaigns by my research group in the last decade across five regions with highly variable conditions of dyke exposures: Western Australia, central Sweden, Angolan shield, the Moroccan Anti-Atlas Mountains, and Wyoming craton USA. The Western Australian region is perhaps ideal for identifying dyke swarms, because of high-resolution aeromagnetic imagery coupled with reasonable exposure, either natural or in quarries. If an individual dyke can be traced unambiguously along strike with aeromagnetism, then even sporadic outcrops can be tied confidently to one swarm or another. It should be noted, however, that standard-level aeromagnetic imaging of dyke intersections does not typically permit assignment of cross-cutting relationships, which are best assessed with direct field observations and perhaps supplemented by field measurements of magnetic susceptibility or portable X-ray fluorescence. In the Dalarna region of central Sweden, only rare exposures of dykes emerge from beneath a pervasive Quaternary till cover. In that area, recognition of swarms is permitted by excellent aeromagnetic coverage, and the outcrops are identified by a comprehensive database curated by the national geological survey. Exposed dyke intersections are exceedingly rare, however, and U-Pb dating is critically required to develop a regional magmatic stratigraphy. This situation is similar to many northern-subpolar shield areas. In southern Angola, high-resolution aeromagnetic data aren't available (to my group's knowledge) but the Namib desert's aridity shows the extent of most dykes at great distances along their lengths, using Google Earth satellite imagery. The southern African continent's elevated topography denudes large areas of colluvium and allows numerous exposures of dykes in ephemeral stream channels. As with Western Australia and Sweden, then, the fresh, in-situ outcrops demanded by paleomagnetic methods – though rare – can be linked confidently into swarm groupings because of the complementary geospatial map datasets.

The Moroccan Anti-Atlas Mountains and Wyoming craton present more difficult challenges for reconstructions, because in both regions the Precambrian basement exposures are isolated from each other due to younger tectonism. In the case of the Anti-Atlas, the uplifts ("boutonnieres") are autochthonous, resulting from broad folding during Hercynian orogenesis. There is little concern about substantial relative rotations between the boutonnières, so dyke trends and paleomagnetic declinations can confidently be taken at face value. Google Earth imagery is high-enough resolution, and with low-enough vegetative cover, to show distinct groups of dykes based on trends, which can then be investigated with integrated paleomagnetism, U-Pb geochronology, and geochemistry. Dykes exposed along the

edges of the boutonnières, however, would require modest tilt corrections based on nonconformably overlying strata in the broad fold limbs. In Wyoming craton, Precambrian dykes are exposed in large but geographically distinct uplifts (“Laramide”), most of them riding atop Cretaceous thrust faults and separated by thick sedimentary basins that preclude geophysical correlation of individual dykes from one uplift to the other. There is a distinct chance of local vertical-axis rotation, especially near the along-strike terminations of each uplifted block. Quantifying those rotations requires confident assignment of the dykes to particular swarms, and ideally, integrated comparison of both dyke trends and paleomagnetic declinations from one uplift to another.

Using these variable conditions of exposure and correlatability, one common lesson learned from the study of these regions is that many dykes need to be sampled in order to understand the complexity of magmatic stratigraphy and paleomagnetic remanences. Dyke intersections should be sought out and carefully examined for unambiguous cross-cutting relationships. Once established, the intersections are amenable to the paleomagnetic baked-contact test (BCT), which when successful can demonstrate primary remanence in the younger intrusion and a more ancient remanence in the host rock. Confounding rock-magnetic behavior is common in ancient rocks, however, so many attempts at BCTs end up being inconclusive. Sampling campaigns should devote extra time to allow for multiple BCTs across a given region. In many regions, dyke swarms extend from cratonic areas into adjacent orogenic forelands. There can also be kind of an inverse BCT (in a very loose sense) where increasing proximity to the orogen correlates to an increasing likelihood that the dykes are overprinted at the time of orogeny. Such a pattern would give confidence that the more cratonic areas carry older paleomagnetic remanences.

In the laboratory, detailed stepwise demagnetization is needed to isolate vector components of different remanence generations in ancient rocks that have had opportunities for partial remagnetization during secondary events such as orogenesis, hydrothermal alteration, weathering (modern or ancient), etc. Both alternating-field and thermal methods are useful in cases of magnetite, but thermal methods are preferred when attempting to fully demagnetize goethite and hematite, due to those minerals’ high magnetic coercivities. Magnetite is the usual remanence carrier in mafic dykes, but shallow-level intrusions can also contain maghemite or hematite, which may be considered primary for the purposes of tectonic reconstructions if formed early enough by deuteric alteration. The challenge in such cases would be for the paleomagnetist to demonstrate that the oxidation formed immediately after dyke emplacement.

After obtaining robust paleomagnetic directions from the various generations of dykes (or other rocks) from each craton, the results can be integrated into a coherent paleogeographic model. Reconstructions that only consider a single age will likely be incompatible with integrated kinematic models; thus it is important to utilize reconstruction software that explicitly deals with plate kinematics, such as GPlates. The most plausible reconstruction models will consider not only magmatic barcodes, dyke orientations, and paleomagnetic data; but also consider the stratigraphic records of sedimentary basins and orogenesis.

Setting the lower mantle free: Assembly of the basal mantle structure beneath Africa

Nicolas Flament¹, Ömer Bodur¹, Simon E. Williams² and Andrew Merdith^{3,4}

¹*GeoQuEST Research Centre, School of Earth, Atmospheric and Life Sciences, University of Wollongong, Wollongong, New South Wales, Australia.*

²*Department of Geology, Northwest University, Xi'an, China.*

³*UnivLyon, Université Lyon 1, ENS de Lyon, CNRS, UMR 5276 LGL-TPE, Villeurbanne, France.*

⁴*Present address: School of Earth and Environment, University of Leeds, Leeds, UK.*

Plate tectonics shapes Earth's surface, and is linked to motions within its deep interior. Cold oceanic lithosphere sinks into the mantle, and hot mantle plumes rise from the deep Earth, leading to volcanism. Volcanic eruptions over the past 320 million years have been linked to two large structures at the base of the mantle presently under Africa and the Pacific Ocean. This has led to the hypothesis that these basal mantle structures could have been stationary over geological time, in contrast to observations and models suggesting that tectonic plates, subduction zones and mantle plumes have been mobile. Here we reconstruct mantle flow from one billion years ago to the present day to show that the history of volcanism is statistically as consistent with mobile basal mantle structures as with fixed ones. In our reconstructions the structure beneath Africa progressively assembled from 400 million years ago, pushed by sinking oceanic lithosphere, to become a coherent structure as recently as 60 million years ago. In contrast to previous suggestions, our mantle flow models suggest that basal mantle structures are mobile, and aggregate and disperse over time, similarly to continents at Earth's surface. Our models also predict the presence of continental material in the mantle beneath Africa, consistent with geochemical data.

Appalachian ‘terrane’ and connections with NW Africa

Yvette D. Kuiper¹ ; Sandra M. Barr² ; André Michard³

¹: *Department of Geology and Geological Engineering, Colorado School of Mines, Golden, CO, 80401, USA*

²: *Department of Earth and Environmental Science, Acadia University; Wolfville, NS, B4P 2R6, Canada*

³: *Université Paris-Saclay (Orsay), 10 rue des Jeûneurs, 75002 Paris, France*

The eastern part of the northern Appalachian orogen in North America generally consists of exotic terranes, terrane assemblages, or domains with Gondwanan and/or Baltican affinities. From west to east they are named Ganderia, Avalonia and Meguma. In the eastern part of the southern Appalachians, exotic terrane assemblages are Carolinia, and the Suwannee (Florida) terrane to the south. A brief overview of each area is presented, as well as for smaller crustal blocks with possible NW African affinity, and two possibly exotic terranes in Morocco: the Sehoul Block in the north, and the western part of the Oulad Dlim massif of the northern Mauritanides to the south.

Ganderia consists of latest Ediacaran to early Paleozoic volcanic arc/back-arc systems, with local Ediacaran arc basement, and Ediacaran-early Paleozoic clastic sedimentary cover rocks. Ganderian rocks are distributed between Newfoundland, Canada, and southern New England, USA. Ganderia rifted from Gondwana in the Cambrian and accreted to Laurentia in the Late Ordovician and Silurian. Prior to accretion, Ganderia was extended and split in a leading edge and a trailing edge, separated by two sequential back-arc oceanic basins in the late Cambrian and early-mid Ordovician. Accretion of the leading edge, as well of Laurentian arcs to Laurentia caused the Cambrian-Ordovician Taconic orogeny, while accretion of the trailing edge caused the Silurian Salinic orogeny. In general, the detrital zircon signature of Ganderia shows a large ~750–500 Ma population and minor age populations distributed between the Archean and Neoproterozoic, suggesting Amazonian affinity.

(West) Avalonia is located east of Ganderia and, similarly, stretches between Newfoundland and southern New England. The oldest sedimentary rocks may be as old as Tonian. Extensive Ediacaran arc magmatism occurred throughout Avalonia, as well as local extensional magmatism, and the Ediacaran rocks are locally overlain by Cambrian cover. Rifting occurred in the late Ediacaran and Ordovician, and accretion to Laurentia during the latest Silurian to Middle Devonian Acadian orogeny. Based on detrital zircon signatures of metasedimentary rocks, inherited zircon in plutonic and volcanic rocks, and Nd model ages, Avalonia is interpreted as having a predominately late Mesoproterozoic basement. Detrital zircon from Avalonian rocks show a predominant ~750–500 Ma population, and scattered ages back to the Archean. Detrital zircon age population differences with Ganderia are subtle. For Avalonia, the ~630 Ma population is larger than the ~540 Ma population, whereas the reverse is generally true for Ganderia. Furthermore, the Mesoproterozoic population is larger for Avalonia relative to other populations than for Ganderia, especially in southeastern New England. However, this difference may be obscured in samples where the ~750–500 Ma population is dominant. Based on detrital zircon U-Pb and Lu-Hf data and paleomagnetism, Avalonia has most recently been interpreted as having a mixed Amazonian/Baltican origin.

The Meguma terrane of Nova Scotia, Canada, consists of latest Ediacaran to Early Ordovician turbiditic metasandstone and slate, unconformably overlain in the southwestern part of the terrane by early Silurian to Early Devonian bimodal metavolcanic rocks, slate, metasilstone, ironstone, and quartzite. The Meguma terrane departed from Gondwana in the early Silurian, based on ~440 Ma within-plate rift volcanic rocks. Early to Middle Devonian deformation under greenschist to amphibolite facies conditions was related in part to accretion of the terrane to Laurentia, but also likely to subduction on the east related to the approaching collision with Gondwana. The terrane is intruded by Middle to Late Devonian distinctive peraluminous subduction-related granitic plutons. The detrital zircon in various units of the Meguma terrane, including the oldest Cambrian unit, has a strong West African signature with large ~2.2–1.9 Ga and ~700–500 Ma populations, and minor ~1.5–0.9 zircon.

In the southern Appalachians, Carolina is a collection of Neoproterozoic to early Paleozoic magmatic arc and sedimentary terranes stretching from central Virginia to Alabama. It generally consists of ~670–610 Ma arc rocks overlain by younger clastic sedimentary rocks, and ~560–<532 Ma arc magmatic and intra-arc sedimentary rocks. Inherited zircon in volcanic and volcanoclastic rocks yielded 965–1229 Ma dates. Detrital zircons in clastic sedimentary rocks from Carolina reveal clusters of ages at 0.6–0.65, 0.8–1.3, 1.5–1.8, and 2.2–2.6 Ga. Based on detrital and inherited zircon ages, and on Nd isotopic data, Carolina is interpreted as having Amazonian affinity. Carolina rifted from Gondwana in the early Cambrian and accreted to Laurentia in the Late Ordovician to early Silurian. Carolina thus has an origin similar to Avalonia, but a Paleozoic geological history more similar to Ganderia.

Farther south, the Suwannee terrane consists of Neoproterozoic igneous rocks and high-grade metamorphic rocks, overlain by unmetamorphosed and undeformed Cambrian–Ordovician to Middle Devonian sandstone and minor oolitic ironstone and black shale of the Suwannee Basin. Accretion of the Suwannee terrane probably occurred in the Carboniferous-Permian, but possibly as early as the Late Devonian. Detrital zircon grains are dominated by large ~2250–2000 Ma and ~650–510 Ma populations, suggesting West African sources. The age distribution of >1 Ga detrital zircon is similar to that of the Meguma terrane, but their Paleozoic histories were apparently different.

Metasedimentary rocks from the bottom of a ~5 km deep well below the Georges Bank in offshore Massachusetts, USA, yielded a detrital zircon signature dominated by a ~2.2–2.0 Ga population, almost and uniquely identical to that of the Paleoproterozoic Taghdout quartzite of the Anti-Atlas of Morocco, which is part of a Paleoproterozoic passive margin sequence that exists directly on top of the Archean–Paleoproterozoic West African Craton. Because the Anti-Atlas was adjacent to southeastern New England at the time of Pangea, the simplest interpretation is that the crustal block remained behind after the breakup of Pangea. Alternatively, it may have arrived earlier, like other Gondwanan terranes. For example, it may be basement to the Meguma terrane to the north.

Other Proterozoic sedimentary rocks with detrital zircon signatures characteristic of the Paleoproterozoic Taghdout Group in the Anti-Atlas of Morocco have been discovered in coastal Maine, USA, and on Grand Manan Island offshore of southwestern New Brunswick, Canada. These areas are located between otherwise eastern Ganderian rocks and may have arrived at different times than the rocks below the Georges Bank. Other possible NW African rocks are ~800–730 Ma arc-related igneous rocks in the Mount Ephraim block in Nova Scotia, and ~760 Ma mafic rocks associated with marble in the fault-bounded Burin Group of eastern Newfoundland. Rocks interpreted as Avalonia in New Brunswick (Hammondvale Metamorphic Suite) and Rhode Island, USA (Newport Block), include ~770–730 Ma detrital zircon. The ~770–730 Ma rocks and zircon ages may be related to the Pan-African I orogeny recorded in the Anti-Atlas region of Morocco. Other orogenies of that age are not known in West Africa, and arc-related igneous rocks of that age are rare in Baltica and Amazonia. The timing and mechanisms of emplacements of these possible NW African crustal fragments in Ganderia and Avalonia remain a topic of investigation.

In northern Morocco, the Sehoul Block consists of early-middle Cambrian and Ordovician quartz-phyllites with local, interbedded meta-carbonate rocks. They are intruded by the ~367 Ma Rabat granite. The detrital zircon signature shows a predominate ~650–500 Ma population with a smaller ~2.2–2.0 Ga population, and scattered other Proterozoic and Archean grains, consistent with a NW African origin. However, the block has been interpreted as having a shared history with Avalonia, based on evidence for Acadian deformation, not otherwise recorded in NW Africa.

Silurian-Devonian granitoids and gneisses are predominant in the western part of the Oulad Dlim Massif in southern Morocco. In the same domain are highly deformed Ediacaran granites, several metasedimentary formations, and minor late Carboniferous rocks. To the west, recent sediments cover the crystalline bedrock. Sedimentary rocks in this domain contain significant Mesoproterozoic zircon that may suggest an exotic origin for these rocks, similar to Avalonia, Ganderia, or Carolina. However, these zircon populations may alternatively have been derived from rocks of the Mauritanide belt or Taoudeni basin southeast of the Oulad Dlim massif in Mauritania.

LIP Printing and its Application to Moroccan Dykes from the Central Atlantic Magmatic Province (CAMP)

Pearce, J.A.^{1,2}, Ernst, R.E³

¹*School of Earth and Environmental Sciences, Cardiff University, UK*

²*London Centre for Ore Deposits and Exploration (LODE), Natural History Museum, London, UK*

³*Dept. of Earth Sciences, Carleton University, Ottawa, Canada*

LIP printing is a term adapted from forensic science to describe the use of geochemical proxies for tectonic and petrogenetic fingerprinting of Large Igneous Provinces (LIPs). In its original form (Pearce et al, 2021), it focused on the LIP printing of basic lavas, sills and dykes using two immobile element proxies: Th/Nb, a crustal input proxy, to monitor subduction-metasomatism and crustal assimilation; and Ti/Yb, a residual garnet proxy, to monitor depth and degree of melting. The LIP printing diagram, a plot of Th/Nb against Ti/Yb for intraplate, plume-derived magmas, is characterized by two distinct arrays: a subduction-modified lithospheric mantle (SZLM) array and a MORB-OIB-OPB (plume) array (where OPB = oceanic plateau basalt). Continental lithosphere also plots predominantly in the SZLM array. LIP basalt suites divide into three categories on this diagram: Type I plots entirely within the MORB-OIB-OPB array indicative of a significant plume source; Type II plots entirely within the SZLM array indicative of a significant subcontinental lithospheric mantle source; and Type III plots on a variety of trends between the two arrays indicative of significant plume-lithosphere interactions. Modelling demonstrates how the three LIP types, and the observed trends within and between individual LIPs, can be explained by (a) differences in the compositions and relative contributions of lithospheric and asthenospheric (plume) mantle, (b) the temperature and depth of melting, and (c) the extent and nature of magma-crust interactions. This large genetic, and hence compositional, variability within and between LIPs relates to differences in geological and geodynamic setting and supports the forensic concept that ‘no two LIP prints are alike’

Follow-up work (Pearce et al., 2022) has incorporated a further proxy (the fractionation proxy, -Ni) to help distinguish crustal from mantle lithosphere inputs in Type III trends. The result is a LIP printing suite of projections made up of four diagrams (Fig. 1): three focusing in turn on the individual crustal, melting and fractionation proxies, with the fourth (the LIP printing diagram (Th/Nb v Ti/Yb) summarizing all the key features on a single projection. Further studies have revealed that the projections can also be effective for LIP printing of ultramafic and mafic cumulates, provided concentrations are above quantification limits and samples affected by fractionation involving magnetite are excluded.

Work carried out to date highlights three types of application: 1) geochemical correlation of LIP events within and between cratons to produce geochemical barcodes that extend the existing age-based barcodes; 2) geochemical (petrogenetic) tracing of individual LIPs in time and space; and 3) identification of the distinctive features of magmas directly related to mineralization. This presentation focusses on the second of these, specifically on continental Phanerozoic LIPs and their similarities and differences. Those featured in this talk are Columbia River Basalt Group, Afar, NAIP, HALIP, Kerguelen, Parana, Karoo and Ferrar, CAMP, Siberian Traps, Emeishan and Tarim, all taken from quality-checked published data and, where possible, model-checked by reference to isotope data. The results highlight a large intra-LIP and between-LIP variation. Notably, LIP printing demonstrates that some LIPs are dominated by plume magma sources (Type I LIP prints), some by SZLM sources (Type II LIP prints), and some by interaction between both magma sources (Type III LIP prints). Superimposed on this is a wide variation in the nature and magnitude of crustal contamination.

The focus LIP for this presentation, the CAMP LIP is an example of a LIP that has both plume and mantle sources with a marked spatial variation. According to the LIP printing projections, the centre of the CAMP province (NE South America and the southern part of Western Africa) is dominated by plume-type sources, while the peripheral regions such as SW USA and Europe) are dominated by SZLM-type sources. The Durham Basin in SW USA is the only Type III LIP, having characteristics of a depleted plume source that has experienced variable interaction with lithosphere. Thanks, in particular, to the comprehensive study by Marzoli et al (2019), the Moroccan CAMP LIP provides an excellent opportunity to test the LIP printing methodology. On a regional scale, the Moroccan LIP magmas most resemble the peripheral LIPs, notably

many of the SW American basin-hosted sheeted intrusions on its original ‘conjugate’ margin. The LIP prints can be interpreted most simply in terms of shallow, small to moderate degrees of melting of metasomatized, mostly undepleted lithospheric mantle. The fact that much of the magma actually classifies as SHMB (siliceous high-Mg basalt) and HMA (high-Mg andesite) in Mg-TAS space is also consistent with shallow, possibly hydrous, melting leading to incongruent melting of orthopyroxene. Apart of the late (Recurrent) magmatic unit, with its more depleted source, LIP printing identifies stratigraphic variations that are significant, but nonetheless very small in the context of the whole CAMP LIP. Compared to the multi-element, multi-isotope work of Marzoli et al. (2019), LIP printing provides a different perspective, lacking the detail and complexity provided by, for example, isotopes and echoing many of the conclusions, but also giving some potentially useful additional insights that will be presented for discussion at this meeting.

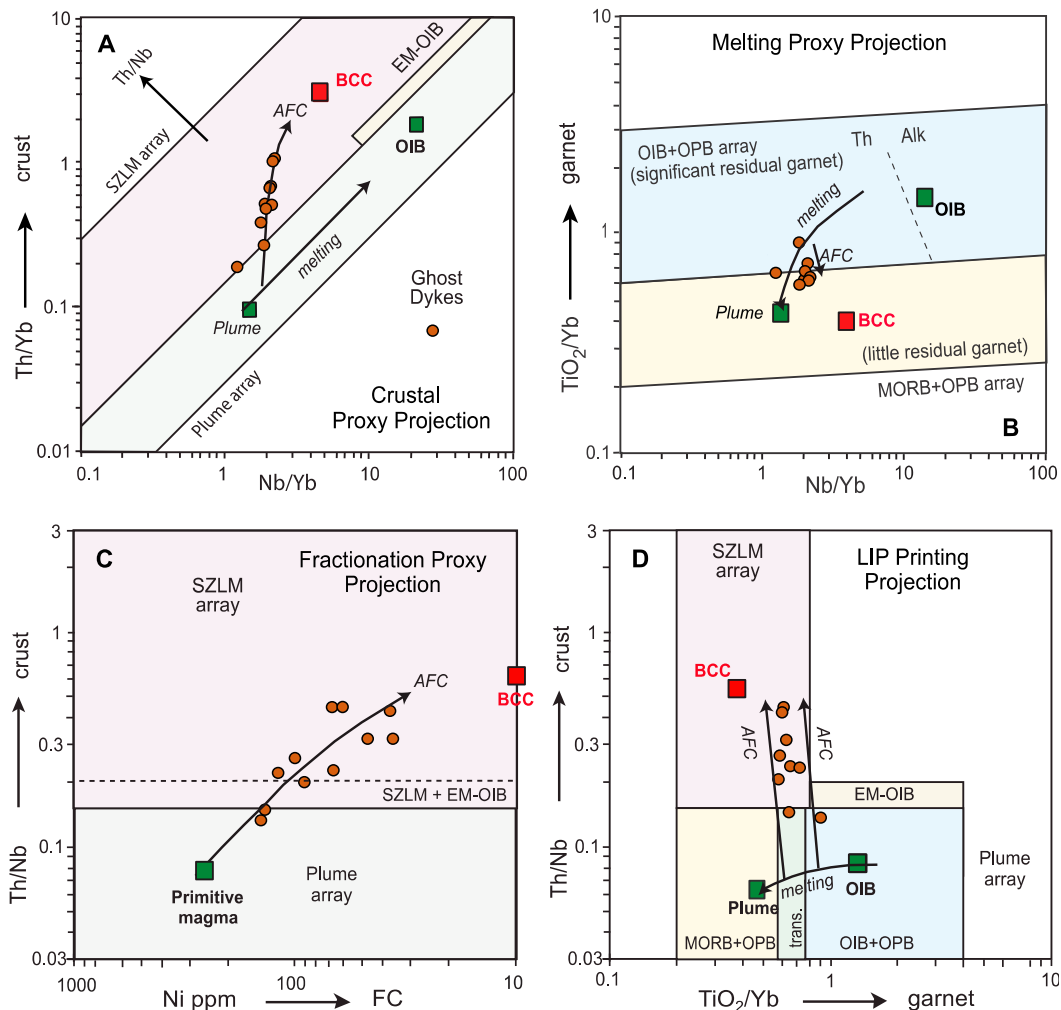
References:

Pearce, J.A., Ernst, R.E., Peate, D.W. and Rogers, C., (2021). LIP printing: Use if immobile element proxies to characterize large igneous provinces in the geologic record. *Lithos* 392. 106068.

Pearce, J.A., and Ernst, R.E. (2022). LIP printing: Theory and applications. *Goldschmidt Conference 2022, Abstract No. 11945.*

Marzoli, A. et al., (2019). The Central Atlantic Magmatic Province (CAMP) in Morocco. *J. Petrol.* 60, 945-996.

Figure 1: A simple example of LIP Printing using four projections: a crustal proxy projection (A), a melting proxy projection (B), a fractionation proxy projection (C) and an integrated (LIP printing) projection (D). This example shows a dyke swarm formed from magma generated by an intermediate degree of plume melting (some residual garnet) followed by extensive assimilation and fractional crystallization (AFC) at basic compositions. The result is a Type II LIP print extending from the plume into the SZLM (also continental crust) field. In this presentation, we examine the LIP prints of magmas related to CAMP magmatism and, in particular, Moroccan CAMP magmatism using published data.. BCC is bulk continental crust



From Yanliao mafic sill swarms in the North China Craton to 1.4–1.3 Ga large-scale continental rifting in the Columbia (Nuna) supercontinent

Shuan-Hong Zhang¹; Richard E. Ernst^{2,3}; Yue Zhao¹; Jun-Ling Pei¹

¹: Institute of Geomechanics, Chinese Academy of Geological Sciences, MLR Key Laboratory of Paleomagnetism and Tectonic Reconstruction, Beijing 100081, China

²: Department of Earth Sciences, Carleton University, Ottawa, Ontario K1S 5B6, Canada.

³: Faculty of Geology and Geography, Tomsk State University, Tomsk 634050, Russia.

The Yanliao basin in the northern North China Craton (NCC) hosts the standard section for late Paleoproterozoic–Mesoproterozoic strata in China (Lu et al., 2008). Large volumes of dolerite sill swarms are common within the late Paleoproterozoic–Mesoproterozoic strata, especially the black shales of the Xiamaling Formation. SIMS U-Pb/Pb-Pb baddeleyite dating of 23 sill samples has yielded crystallization ages between 1330±4 Ma and 1305±11 Ma with a weighted mean age of 1323±2 Ma (Li et al., 2009; Zhang et al., 2012a, 2017a; Wang et al., 2014; Su et al., 2016; Zhu et al., 2020). The Yanliao dolerite sills are distributed over a region >600 km long and >200 km wide; they have an areal extent >120,000 km² and a cumulative thickness ranging from 50 m to >1800 m and constitute a large igneous province (LIP) (Zhang et al., 2017).

Comparisons with coeval LIPs in other continents combined with paleomagnetic results show that the Yanliao LIP in the NCC and the Derim Derim-Galiwinku LIP in the North Australian Craton (NAC) represent portions of the same LIP separated by continental breakup, suggesting a connection (or at least near neighbors) between the NCC and NAC during the early Mesoproterozoic period (Zhang et al., 2017; Bodorkos et al., 2021). A comparison of major mafic magmatic events and black shales in Paleo-Mesoproterozoic successions of the NCC and NAC shows that the northern–northeastern margin of the NCC was connected to the northern margin of the NAC from 1800 Ma to 1300 Ma during the late Paleoproterozoic to Mesoproterozoic (Zhang et al., 2022a). This long-lived connection lasted for at least 500 million years until separation of the NCC and NAC between ca. 1320 and ca. 1230–1220 Ma, likely associated with the ca. 1320 LIP event. The long-lived connection between the NCC and NAC from 1800 Ma to 1300 Ma during the late Paleoproterozoic to Mesoproterozoic is supported by paleomagnetic results obtained in these two cratons (Zhang et al., 2012b; Xu et al., 2014; Wang et al., 2019; Kirscher et al., 2021).

The 1.4–1.3 Ga LIPs (and smaller intraplate mafic magmatic events interpreted as LIP fragments/remnants) and REE-rich carbonatites are common in many cratons within the Columbia (Nuna) supercontinent (Ernst, 2014; Zhang et al., 2022b). Spatial and temporal distributions of the 1.4–1.3 Ga LIPs (and the interpreted LIP fragments/remnants) in the refined paleogeographic reconstruction map of Columbia supercontinent reveal a 1.4–1.3 Ga large-scale continental rift zone along western Laurentia, western-northern Siberia, southeastern Baltica, western-northern West Africa, southwestern Amazonia, southern-eastern Congo/São Francisco, eastern Kalahari, northern North China and northern North Australia. The 1.4–1.3 Ga continental rift system extends about 15,000 km across the Columbia supercontinent and is considered as the main indicator and a proximal reason for final breakup of the Columbia supercontinent. This newly identified huge continental rift zone system also controlled the distributions of Bayan Obo (zircon Th-Pb age of 1.33–1.30 Ga, Zhang et al., 2017b, 2022; Li et al., 2018), the world's first and largest REE-Nb deposit in northern North China and Mountain Pass, the world's second largest REE deposit in western Laurentia (monazite Th-Pb ages of carbonatite ranging from 1396±16 Ma to 1371±10 Ma, Poletti et al., 2016). These new observations more broadly suggest this rift zone as a favorable metallogenic belt for other carbonatite-related REE(-Nb) deposits, and other commodity types such as giant clastic-dominated

Zn-Pb-Ag deposits. Future work should focus on a more systematic comparison of the 1.4–1.3 Ga rift system with the entire Atlantic rift system, the mechanism and deep processes for formation of this huge rift system and global environmental effects of the 1.4–1.3 Ga large-scale rift system.

This research was financially supported by the National Natural Science Foundation of China (41920104004, 41725011, U2244213).

References:

- Bodorkos, S., Crowley, J.L., Claoué-Long, J.C., Anderson, J.R., Magee, C.W., Jr., 2021. Precise U-Pb baddeleyite dating of the Derim Derim Dolerite, McArthur Basin, Northern Territory: Old and new SHRIMP and ID-TIMS constraints. *Australian Journal of Earth Sciences*, 68, 36–50.
- Ernst, R.E., 2014. *Large Igneous Provinces*. Cambridge University Press, Cambridge. 653 p.
- Kirscher, U., Mitchell, R.N., Liu, Y., Nordsvan, A.R., Cox, G.M., Pisarevsky, S.A., Wang, C., Wu, L., Murphy, J.B., Li, Z.-X., 2021. Paleomagnetic constraints on the duration of the Australia-Laurentia connection in the core of the Nuna supercontinent. *Geology*, v. 49, 174–179.
- Li, H.K., Lu, S.N., Li, H.M., Sun, L.X., Xiang, Z.Q., Geng, J.Z., Zhou, H.Y., 2009. Zircon and baddeleyite U-Pb precision dating of basic rock sills intruding Xiamaling Formation, North China. *Geological Bulletin of China*, 28, 1396–1404 (in Chinese with English abstract).
- Li, Q., Liu, Y., Tang, G., Wang, K., Ling, X., 2018. Zircon Th–Pb dating by secondary ion mass spectrometry. *Journal of Analytical Atomic Spectrometry*, 33, 1536–1544.
- Lu, S.N., Zhao, G.C., Wang, H.C., Hao, G.J., 2008. Precambrian metamorphic basement and sedimentary cover of the North China Craton: A review. *Precambrian Research*, 160, 77–93.
- Poletti, J.E., Cottle, J.M., Hagen-Peter, G.A., Lackey, J.S., 2016. Petrochronological constraints on the origin of the Mountain Pass ultrapotassic and carbonatite intrusive suite, California. *Journal of Petrology* 57, 1555–1598.
- Su, L., Wang, T.G., Li, X.H., Song, S.G., Yang, S.W., Zhang, H.Y., Zhong, L.X., 2016. Petrogenesis and emplacement age of the gabbro-dolerite sills within the Mesoproterozoic Xiamaling Formation in Yanliao rifting zone. In: Sun, S., Wang, T.G. (eds.), *Meso-Neoproterozoic geology and oil and gas resources in eastern China*, Science Press, Beijing, p. 325–342.
- Wang, Q., Yang, H., Yang, D., Xu, W., 2014. Mid-Mesoproterozoic (~1.32 Ga) diabase swarms from the western Liaoning region in the northern margin of the North China Craton: Baddeleyite Pb–Pb geochronology, geochemistry and implications for the final breakup of the Columbia supercontinent. *Precambrian Research*, 254, 114–128.
- Wang, C., Li, Z.-X., Peng, P., Pisarevsky, S., Liu, Y., Kirscher, U., Nordsvan, A., 2019. Long-lived connection between the North China and North Australian cratons in supercontinent Nuna: paleomagnetic and geological constraints. *Science Bulletin*, 64, 873–876.
- Zhang, S.H., Zhao, Y., Santosh, M., 2012a. Mid-Mesoproterozoic bimodal magmatic rocks in the northern North China Craton: Implications for magmatism related to breakup of the Columbia supercontinent. *Precambrian Research*, 222–223, 339–367.
- Zhang, S., Li, Z., Evans, D.A.D., Wu, H., Li, H., Dong, J., 2012b. Pre-Rodinia supercontinent Nuna shaping up: A global synthesis with new paleomagnetic results from North China. *Earth and Planetary Science Letters*, 353–354, 145–155.
- Zhang, S.H., Zhao, Y., Li, X.H., Ernst, R.E., Yang, Z.Y., 2017a. The 1.33–1.30 Ga Yanliao large igneous province in the North China Craton: Implications for reconstruction of the Nuna (Columbia) supercontinent, and specifically with the North Australian Craton. *Earth and Planetary Science Letters*, 465, 112–125.
- Zhang, S.H., Zhao, Y., Liu, Y., 2017b. A precise zircon Th–Pb age of carbonatite sills from the world's largest Bayan Obo deposit: implications for timing and genesis of REE-Nb mineralization. *Precambrian Research* 291, 202–219.
- Zhang, S.H., Ernst, R.E., Munson, T.J., Pei, J.L., Hu, G.H., Liu, J.M., Zhang, Q.Q., Cai, Y.H., Zhao, Y., 2022. Comparisons of the Paleo-Mesoproterozoic large igneous provinces and black shales in the North China and North Australian cratons. *Fundamental Research*. 2(1), 84–100.
- Zhang, S.H., Ernst, R.E., Yang, Z.Y., Zhou, Z.Z., Pei, J.L., Zhao, Y., 2022b. Spatial distribution of 1.4–1.3 Ga LIPs and carbonatite-related REE deposits: evidence for large-scale continental rifting in the Columbia (Nuna) supercontinent. *Earth and Planetary Science Letters*. 597, 117815.
- Zhu, Y.-S., Yang, J.-H., Wang, H., Wu, F.-Y., 2020. Mesoproterozoic (~1.32 Ga) modification of lithospheric mantle beneath the North China craton caused by break-up of the Columbia supercontinent. *Precambrian Research*, 342, 105674.

From Rodinia's dispersal to the amalgamation of Gondwana: Correlation of Precambrian to Lower Palaeozoic rock units of the Cadomian orogen of Western-Central Europe with the Anti-Atlas in Morocco by U-Pb ages of detrital and magmatic zircon

Ulf Linnemann¹, Andreas Gärtner¹, Maria Ovtcharova², Nasrddine Youbi³, Ezzoura Errami⁴, Nasser Ennih⁵, Mandy Hofmann¹, Jessica Gärtner¹, Johannes Zieger¹, Katja Mende¹, Rita Krause¹

¹Senckenberg Naturhistorische Sammlungen Dresden, GeoPlasmaLab, Königsbrücker Landstraße 159, 01109 Dresden, Germany. Email: ulf.linnemann@senckenberg.de, andreas.gaertner@senckenberg.de, mandy.hofmann@senckenberg.de, jessica.gaertner@senckenberg.de, johannes.zieger@senckenberg.de, katja.mende@senckenberg.de, rita.krause@senckenberg.de

²Département des Sciences de la Terre, University of Geneva, Genève, Switzerland. Email: maria.ovtcharova@unige.ch

³Department of Geology, Faculty of Sciences - Semlalia, Cadi Ayyad University, P.O. Box 2390, Prince Moulay Abdellah Boulevard, Marrakech, Morocco. Email: youbi@uca.ac.ma

⁴Université Cadi Ayyad, Faculté Polydisciplinaire de Safi, B.P. 4162, 46 000 Safi, Morocco. Email: errami.e@ucd.ac.ma

⁵Université Chouaïb Doukkali, Faculté des Sciences, EGGPG, B.P. 20, 24000 El Jadida, Morocco. Email: ennih.n@ucd.ac.ma

The correlation of Lower Palaeozoic sedimentary rocks from Central and Western Europe with age-equivalent strata from the Anti-Atlas was practiced since the Sixties and Seventies of the last century by making use of key fossils, fossil assemblages, and the sedimentary deposits of the Hirnantian glaciation happened during the Upper Ordovician. The deposits of the latter were often used as a prominent key horizon in lithostratigraphic columns. Here, we present new U-Pb ages of detrital and magmatic zircon from Precambrian and Lower Palaeozoic rocks from the basement units of the Anti-Atlas and its European counterpart. Oldest useful rocks for a correlation are represented by cratonic basement rocks from the Anti-Atlas referred to as the Palaeoproterozoic aged Eburnean Basement. Equivalents of this occur in the Armorican and in the Bohemian Massifs of Western and Central Europe. Zircon ages of such rocks scatter around 2050 Ma. Another very useful tool for correlation purposes are glacial diamictites and surfaces of striated rocks in a time period of c. 565 Ma. Occurrences of the Upper Ediacaran Glacial Period are known from the Quarzazate (e.g. (Vernet et al. 2012), Tiddiline, and Saghro Groups in the Anti-Atlas and from the Cadomian Basement in Spain (Lower Alcludian Group), France (Granville Formation), and Germany (Weesenstein and Clanzschwitz Groups) (Linnemann et al. 2018, 2021). Another good method for the correlation of Precambrian and Lower Palaeozoic rocks from West Africa and Central-Western Europe is the detrital zircon record. Distribution patterns of U-Pb ages of detrital zircon from both areas show a strong relation to each other. The overall geotectonic setting for the origin of Ediacaran to Lower Palaeozoic rocks from the Anti-Atlas and Central-Western Europe is the amalgamation of the Gondwana supercontinent during Lower Ediacaran time followed by lateral extrusion tectonics during the Upper Ediacaran. Lower Palaeozoic volcano-sedimentary sequences display a rift-drift regime and the rift-off of peri-Gondwanan terranes.

Linnemann U, Pidal AP, Hofmann M, Drost K, Quesada C, Gerdes A, Marko L, Gärtner A, Zieger J, Ulrich J, Krause R, Vickers-Rich P and Horak J (2018) A ~565 Ma old glaciation in the Ediacaran of peri-Gondwanan West Africa. *International Journal of Earth Sciences* 107, 885–911.

Linnemann U, Hofmann M, Gärtner A, Gärtner J, Zieger J, Krause R, Haenel R, Mende K, Ovtcharova M, Schaltegger U, Vickers-Rich P (2021) An Upper Ediacaran Glacial Period in Cadomia: the Granville tillite (Armorican Massif) – sedimentology, geochronology and provenance. *Geological Magazine*, 159, 999-1013.

Vernhet E, Youbi N, Chellai EH, Villeneuve M and El Archi A (2012) The Bou-Azzer glaciation: evidence for an Ediacaran glaciation on the West African Craton (Anti-Atlas, Morocco). *Precambrian Research* 196–197, 106–112.

Morphology, architecture and emplacement of the Central Atlantic Magmatic Province (CAMP) basaltic successions in Morocco, and comparisons with the Deccan (India) and Parana (Brazil) traps. Proposal of a new facies model for the emplacement of the Continental Flood Basalt.

Nasrddine Youbi¹, Mohamed Khalil Bensalah^{1,2}, José Madeira², Moulay Ahmed Boumebdi^{1,2}, Hind El Hachimi³, Hetu Sheth⁴, Raymond Duraiswami⁵, João Mata², El Hassane Chellai¹, Andrea Marzoli⁶, Hervé Bertrand⁷, Fida Medina⁸.

¹*Department of Geology, Faculty of Sciences-Semlalia, Cadi Ayyad University, Prince Moulay Abdellah Boulevard, P.O. Box 2390, Marrakech, 40 000, Morocco, e-mail: youbi@uca.ma; boumebdi@uca.ac.ma;*

²*Instituto Dom Luiz, Faculdade de Ciências, Universidade de Lisboa, 1749-016 Lisboa, Portugal. Email : jmadeira@fc.ul.pt; jmata@fc.ul.pt*

³*Department of Geology, Faculty of Sciences, Chouaib Doukkali University, 24000 El Jadida, Morocco. Email : elhachimi_hind@yahoo.fr*

⁴*Department of Earth Sciences, Indian Institute of Technology Bombay, Mumbai, India. Email: hcsheth@iitb.ac*

⁵*Department of Geology, Savitribai Phule Pune University, Pune 411 007, India. Email: raymond.duraiswami@gmail.com*

⁶*Dipartimento di Geoscienze, Università di Padova, 35131 Padova, Italy. Email : andrea.marzoli@unipd.it*

⁷*Laboratoire de Géologie de Lyon, ENS de Lyon, Université Lyon 1, CNRS, UMR 5276, Lyon 69364, France. Email : herve.bertrand@ens-lyon.fr*

⁸*Moroccan Association of Geosciences, Rabat, Morocco*

Once considered to be composed by monotonous stacks of basaltic lava, continental flood basalt (CFB) provinces are now known to display considerable diversity in lava flow morphology. Whereas most initial studies of flood basalt morphology and emplacement focused on younger provinces such as the Columbia River Basalt (e.g., Self et al. 1996; Thordarson and Self 1998), subsequent investigations have also targeted older provinces such as the Central Atlantic Magmatic Province (CAMP, e.g., Kontak, 2008; Martins et al., 2008; El Hachimi et al., 2011), Parana-Etendeka (Jerram et al., 1999a, b; Waichel et al., 2006; Waichel et al., 2008; Waichel et al., 2012; Rossetti et al., 2014), and the Deccan Volcanic Province (DVP, e.g., Keszthelyi et al. 1999; Duraiswami et al., 2001, Duraiswami et al., 2003; Bondre et al., 2004a,b; Sheth 2006; Sheth et al., 2011; Duraiswami et al., 2014). It is becoming increasingly clear that every CFB province is unique in terms of its tectono-magmatic evolution as well as in the types of lava flows and their proportions. Bondre et al. (2004a,b) have cautioned against using only the Columbia River Basalt province as an analogue for all CFB provinces. They stressed the need to document the morphology of lava flows from each individual province in order to obtain insights into their emplacement and eruptive histories. An important reason for documenting flow morphology in older provinces is to uncover lava types and modes of emplacement that are not observed in younger and active volcanic provinces. Indeed, recent studies from CFB provinces have led to the recognition of distinct lava types that have few young analogues (e.g. rubbly pahoehoe; Keszthelyi et al. 2006). Here we compare the morphology, architecture and emplacement of the CAMP basaltic successions in Morocco with the DVP (India) and Parana (Brazil) traps and propose a new facies model for the emplacement of the CFB. Our comparison on the physical volcanology of these key provinces and others CFB indicate that they do not have a simple, 'layer-cake stratigraphy', but contain complex internal and external architectures. Such architectures are governed by the volume of individual eruption events, the location and abundance of volcanic centers, and the evolution of these centers through time. The architecture of most, if not all, CFB provinces reveals that the production of compound pahoehoe flows was followed by flows with a simpler, sheet-like geometry indicating a fundamental temporal change in the emplacement process of lava flows. Accordingly, it appears that flood basalt volcanism initially starts out at relatively low effusion rate, which gradually accelerate to high effusion rate, high-volume eruptions. This worldwide similarity suggests that the magma genesis and/or magma ascension processes are similar in all CFB provinces (Jerram 2002; Jerram et al. 1999a, b; Planke et al. 2000; White et al. 2009; Jerram and Widdowson 2005; Martins et al., 2008; El Hachimi et al., 2011; Waichel et al., 2012; Rossetti et al., 2014; Duraiswami et al., 2014), although local conditions (coeval regional geomorphology, surface

and underground water availability) may constrain the details of the internal architecture of each province (Luchetti et al., 2014; El Ghilani et al., 2017).

References

- Bondre NR, Duraiswami RA, Dole G (2004a) Morphology and emplacement of flows from the Deccan Volcanic Province, India. *Bull Volcanol* 66:29-45
- Bondre NR, Duraiswami RA, Dole G (2004b) A brief comparison of lava flows from the Deccan Volcanic Province and the Columbia-Oregon Plateau flood basalts: Implications for models of flood basalt emplacement. In: Sheth HC, Pande K (eds) *Magmatism in India through time. Proc Ind Acad Sci (Earth and Planet Sci)* 113:809-817.
- Duraiswami RA, Bondre NR, Dole G, Phadnis VM, Kale VS (2001) Tumuli and associated features from the western Deccan Volcanic Province, India. *Bull Volcanol* 63:435-442.
- Duraiswami RA, Dole G, Bondre NR (2003) Slabby pahoehoe from the western Deccan Volcanic Province: evidence for incipient pahoehoe-aa transitions. *J Volcanol Geotherm Res* 121:195-217.
- Duraiswami, R.A., Purva Gadpallu, Shaikh, T.N. and Neha Cardin (2014). Pahoehoe-a'a transitions in the lava flow fields of the western Deccan Traps, India- implications for emplacement dynamics, flood basalt architecture and volcanic stratigraphy. *Jour. Asian Earth Sci.*, v.84, pp.146-166
- El Ghilani, S.; Youbi, N.; Madeira, J.; Chellai, E.H.; Lopez-Galindo, A.; Martins, L. and Mata, J. (2017) Environmental implication of subaqueous lava flows from a continental Large Igneous Province: examples from the Moroccan Central Atlantic Magmatic Province (CAMP). *J. African Earth Sci.* 127: 211–221.
- El Hachimi H, Youbi N, Madeira J, Bensalah MK, Martins L, Mata J, Bertrand H, Marzoli A, Medina F, Munhá J, Bellieni J, Mahmoudi A, Ben Abbou M, Assafar H (2011) Morphology, internal architecture, and emplacement mechanisms of lava flows from the Central Atlantic Magmatic Province (CAMP) of Argana basin (Morocco). In: Van Hinsbergen DJJ, Buitter SJH, Torsvik TH, Gaina C, Webb SJ (eds) *The Formation and Evolution of Africa: A Synopsis of 3.8 Ga of Earth History. Geol Soc Lond Spec Publ* 357, 167-193.
- Jerram DA, Mountney N, Stollhofen H. (1999a) Facies architecture of the Etjo Sandstone Formation and its interaction with the Basal Etendeka flood basalts of NW Namibia: Implications for offshore analogues. In: Cameron N, Bate R, Clure V (eds) *The Oil and Gas Habitats of the South Atlantic. Geol Soc Lond Spec Publ* 153, 367-380.
- Jerram DA, Mountney N, Holzförster F, Stollhofen H (1999b) Internal stratigraphic relationships in the Etendeka Group in the Huab Basin, NW Namibia: understanding the onset of flood volcanism. *J Geodyn* 28, 393-418.
- Jerram, D. A. & Widdowson, M. (2005). *The anatomy of Continental Flood Basalt Provinces: geological constraints on the processes and products of flood volcanism. Lithos*, 79, 385-405.
- Jerram, D. A. (2002). *Volcanology and facies architecture of flood basalts. In: Menzies, M. A., Klemperer, S. L., Ebinger, C. J. & Baker, J. (eds) Volcanic Rifted Margins. Geological Society of America, Boulder, Special Paper*, 362, 121-135.
- Keszthelyi L, Self S, Thordarson T (1999) Application of Recent studies on the emplacement of basaltic lava flows to the Deccan Traps. In: Subbarao KV (ed) *Deccan Volcanic Province, Mem Geol Soc Ind* 43, 485-520.
- Keszthelyi L, Self S, Thordarson T (2006) Flood lavas on Earth, Io and Mars. *J Geol Soc Lond* 163, 253-264.
- Kontak DJ (2008) On the edge of CAMP: Geology and volcanology of the Jurassic North Mountain Basalt, Nova Scotia. In: Dostal J, Greenough JD, Kontak DJ (eds) *Rift-related Magmatism. Lithos* 101, 74-101.
- Luchetti, A.C.F.; Nardy, A.J.R.; Machado, F.B.; Madeira, J. & Arnósio, J.M. (2014) New insights on the occurrence of peperites and sedimentary deposits within the silicic volcanic sequences of the Paraná Magmatic Province, Brazil. *Solid Earth* 5, 121-130.
- Martins LT, Madeira J, Youbi N, Munha J, Mata J., Kerrich R (2008) Rift-related magmatism of the Central Atlantic Magmatic Province in Algarve, Southern Portugal. In: Dostal J, Greenough JD, Kontak DJ (eds) *Rift-related Magmatism. Lithos* 101, 102-124.
- Planke, S., Symonds, P. A., Alvestad, E. & Skogseid, J. (2000). Seismic volcanostratigraphy of large-volume basaltic extrusive complexes on rifted margins. *Journal of Geophysical Research*, 105, 19,335-19,351.
- Rossetti, L.M.L.M., Lima, E.F.E.F., Waichel, B.L.B.L., Scherer, C.M.C.M., Barreto, C.J.C.J., 2014. Stratigraphical framework of basaltic lavas in Torres syncline main valley, southern Parana-Etendeka Volcanic Province. *J. S. Am. Earth Sci.* 56:409-421.
- Self S, Thordarson T, Keszthelyi L (1996) A new model for the emplacement of Columbia River basalts as large, inflated pahoehoe lava flow fields. *Geophys Res Lett* 23:2689–2692.
- Sheth HC (2006) The emplacement of pahoehoe lavas on Kilauea and in the Deccan Traps. *J Earth Syst Sci* 115, 615-629.
- Sheth HC, Ray JS, Senthil Kumar P, Duraiswami RA, Chatterjee RN, Gurav T (2011) Recycling of flow-top breccia crusts into molten interiors of flood basalt lava flows: Field and geochemical evidence from the Deccan Traps. In: Ray J, Sen G, Ghosh B (eds) *Topics in Igneous Petrology. Springer, Ch 8*, 161-180.

- Thordarson T, Self S (1998) The Roza Member, Columbia River Basalt Group: A gigantic pahoehoe lava flow field formed by endogenous processes? J Geophys Res 103:27411-27445*
- Waichel PL, Lima EF, Lubachesky R, Sommer CA (2006) Pahoehoe flows from the central Parana Continental Flood Basalts. Bull Volcanol 68, 599-610*
- Waichel PL, Scherer CMS, Frank HT (2008) Basaltic lava flows covering active aeolian dunes in the Parana Basin in southern Brazil: Features and emplacement aspects. J Volcanol Geotherm Res 171, 59-72.*
- Waichel, B.L., Lima, E.F., Viana, A.R., Scherer, C.M., Bueno, G.V., Dutra, G., (2012). Stratigraphy and volcanic facies architecture of the Torres Syncline, Southern Brazil, and its role in understanding the Parana-Etendeka Continental Flood Basalt Province. J. Volcanol. Geotherm. Res. 216, 74-82.*
- White, J. D. L., Bryan, S. E., Ross, P. S., Self, S. & Thordarson, T. (2009). Physical volcanology of large igneous provinces: update and review. In: Thordarson, T., Self, S., Larsen, G., Rowland, S. & Hoskuldsson, A. (eds) Studies in Volcanology: The Legacy of George Walker. Special Publications of IAVCEI, 2. Geological Society, London, 291-321.*

Global plate reconstruction since 2 billion years: The start of the supercontinent cycle, evolving mantle dynamics, and new constraints on absolute paleolongitude

Zheng-Xiang Li¹; Yebo Liu¹; Richard Ernst²

¹: Earth Dynamics Research Group, School of Earth and Planetary Sciences, The Institute for Geoscience Research, Curtin University, GPO Box U1987, Perth, WA 6845, Australia

²: Department of Earth Sciences, Carleton University, Ottawa, ON K1S 5B6, Canada

An advanced understanding of how tectonic plates have moved since deep time is essential for understanding how Earth's geodynamic system has evolved and interacted with the plate tectonic system, i.e., the longstanding question of what "drives" plate tectonics. In this work, we take advantage of the rapidly improving database and knowledge about the Precambrian world, and the conceptual breakthroughs both regarding the presence of a supercontinent cycle and possible dynamic coupling between the supercontinent cycle and mantle dynamics, to establish a full-plate global reconstruction back to 2000 Ma. We utilise a variety of global geotectonic databases to constrain our reconstruction, and use palaeomagnetically recorded true polar wander events and global plume records to help evaluate competing geodynamic models regarding the origin and evolution of first-order mantle structures, and provide new constraints on the absolute longitude of continents and supercontinents. After revising the configuration and life span of both supercontinents Nuna (1600–1300 Ma) and Rodinia (900–720 Ma), we present here a 2000–540 Ma animation featuring the rapid assembly of large cratons and supercratons (or megacontinents) between 2000 Ma and 1800 Ma after billion years of dominance by many small cratons, that kick started the ensuing Nuna and Rodinia supercontinent cycles and the emergence of hemisphere-scale (long-wavelength) degree-1/degree-2 mantle structures. We further use the geodynamically-defined type-1 and type-2 inertia interchange true polar wander (IITPW) events, which likely occurred during Nuna (type-1) and Rodinia (type-2) times as shown by the palaeomagnetic record, to argue that Nuna assembled at about the same longitude as the latest supercontinent Pangea (320–170 Ma), whereas Rodinia formed through introversion assembly over the legacy Nuna subduction girdle either ca. 90° to the west (our preferred model) or to the east before the migrated subduction girdle surround it generated its own degree-2 mantle structure. Our interpretation is broadly consistent with the global LIP record. Using TPW and LIP observations and geodynamic model predictions, we further argue that the Phanerozoic supercontinent Pangea assembled through extroversion on a legacy Rodinia subduction girdle with a geographic centre at around 0°E longitude before the formation of its own degree-2 mantle structure, the legacy of which is still present in present-day mantle.

Work published in:

Li, Z.-X., Liu, Y., Ernst, R. (2023). A dynamic 2000–540 Ma Earth history: From cratonic amalgamation to the age of supercontinent cycle. *Earth-Science Reviews* 238, 104336. (Open access at: <https://doi.org/10.1016/j.earscirev.2023.104336>).

Biospheric oxygenation through time 2.0: A new look at ecological coevolution and solid-Earth drivers

Timothy W. Lyons, Department of Earth and Planetary Sciences, University of California, Riverside, CA USA (timothy.lyons@ucr.edu)

The relationships between first-order tectonic processes and evolution of the Earth surface system have long been of interest. Supercontinent cycling and LIP events, including those related to continental breakup, are among the key tectonic drivers. Related consequences are the interweaving of dramatic climatic warming and cooling, shifting biospheric redox, and biotic extinctions. Despite a long history of related study, key questions remain about the temporal fabric of first- and higher-order processes and products—in part because our understanding of environmental evolution, including ocean-atmosphere oxygenation and the overall ecological landscape, is still emerging. Critical unknowns center on the history of nutrient cycling, including bioessential trace metals, and the myriad feedbacks among diverse biotic and abiotic processes. However, new methods and data from new locations are exposing a textured history of biospheric oxygenation and environmental evolution more generally. Recent discoveries include the persistence of low-oxygen conditions in the deep oceans well into the Paleozoic and the highly protracted and dynamic nature of redox transitions, most notably at the GOE and NOE. Transitions traditionally viewed as steps or events are now known to be long, complex, and oscillatory intervals spanning a range of time scales, while at the same time comparatively short episodes of rising and falling oxygen are now mapped on top of the longer-term trends. This talk will lay out the latest views of biospheric evolution, including fundamental advances in the evolution of life that may link to episodes of major tectonic/LIP reorganization. Even more rigorous mechanistic explorations of the patterns and cause-and-effect relationships among the evolving solid Earth, surface environments, and life are on the list of remaining research frontiers.

JCM_2023
IDC8-LIPS8-Rodinia 2023
Marrakesh Morocco
Abstracts
oral presentation

Venusian Crust: Insights from Study of a Major Normal Fault in Dali Chasma, SW of Atla Regio

A. Ait Lahna¹ ; H. El Bilali^{2,3} ; R.E. Ernst^{2,3} ; N. Youbi¹

¹: Cadi Ayyad University, Marrakech, Morocco; aitlahna.abdelhak@gmail.com, youbi@uca.ac.ma

²: Department of Earth Sciences, Carleton University, Ottawa, Ontario; hafidaelbilali@cunet.carleton.ca, richard.ernst@ernstgeosciences.com,

³: Faculty of Geology and Geography, Tomsk State University, Tomsk, Russia

The 7,500 km-long Diana - Dali Chasmata is a rift system that connects the SW side of Atla Regio with Thetis Regio in the west. These rifts host the steepest and deepest troughs on Venus (Ford and Pettengill, 1992), having gradients of more than 30° (Hansen and DeShon, 2002). As a result of the steep chasmata walls, landslide deposits may be seen in both. A ~ 390 km long portion of Dali Chasma is the focus of this study. Previous 1:5 million-scale mapping by Hansen and DeShon (2002) covers the western part of the study area; however, only the 1:10 M global mapping of Ivanov and Head (2011) covers the eastern half of the study area. Herein, we map the study area at a higher resolution of 1:500,000.

The focus of this abstract is a 4 km thick section of Venusian crust that was exposed in Diana Chasma as a result of asymmetric rifting and normal faulting. The rift, which is 190°E / 10°S, ~ 390 km in length and 30–70 km wide, trends NE in line with the overall trend of the chasmata (Figs. 1-2). Asymmetrical dip-slip movement occurs on the normal faults, with more of it occurring on the rift's northwest than its southeast side. In this study, we specifically focus on one of these normal faults (Figs. 2A and B), which has a NE-SW trend, a 36° steep gradient, and which is interpreted to expose a 4 km stretch of the crust. Figure 2A, C-E shows the exposed crustal portion, where a radar brighter 3 km layer overlies a radar darker 1 km layer. Locally, the radar brighter section reveals parallel lineations that may be horizontal layering, possibly reflecting a flood basalt sequence or sequence of sills (locations b in Fig. 2D). On the slope, steep lines (shown in red in Fig. 2E) are also depicted, which might either be evidence of debris sliding down the slope or the trace of dykes. The deeper exposed part is characterized by irregular regions (radar darker), which may indicate crosscutting intrusions (such as lopoliths) (locations c and d in Fig. 2D). Irregular units that are thought to be talus have accumulated near the base of the exposed escarpment (location a in Fig. 2C) as a result of mass wasting. As seen in Fig. 2B, closing the rift causes the various graben trends (each with a different color) to have a more consistent trend across the rift, indicating that these various graben systems were in existence before the rifting.

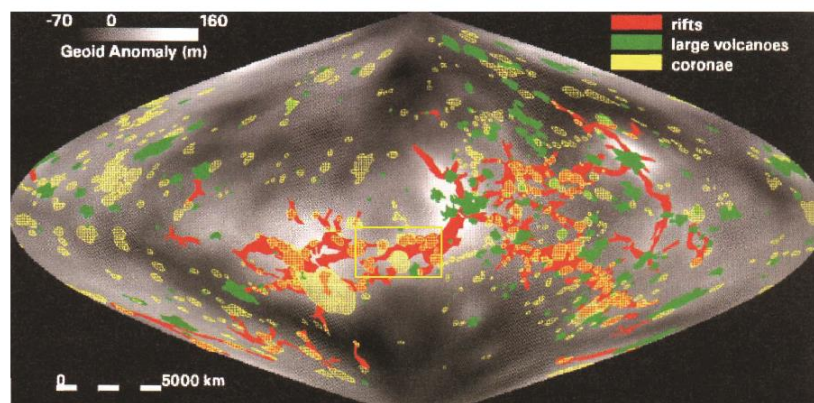


Figure 1: Study area, located on global map of Herrick (1999).

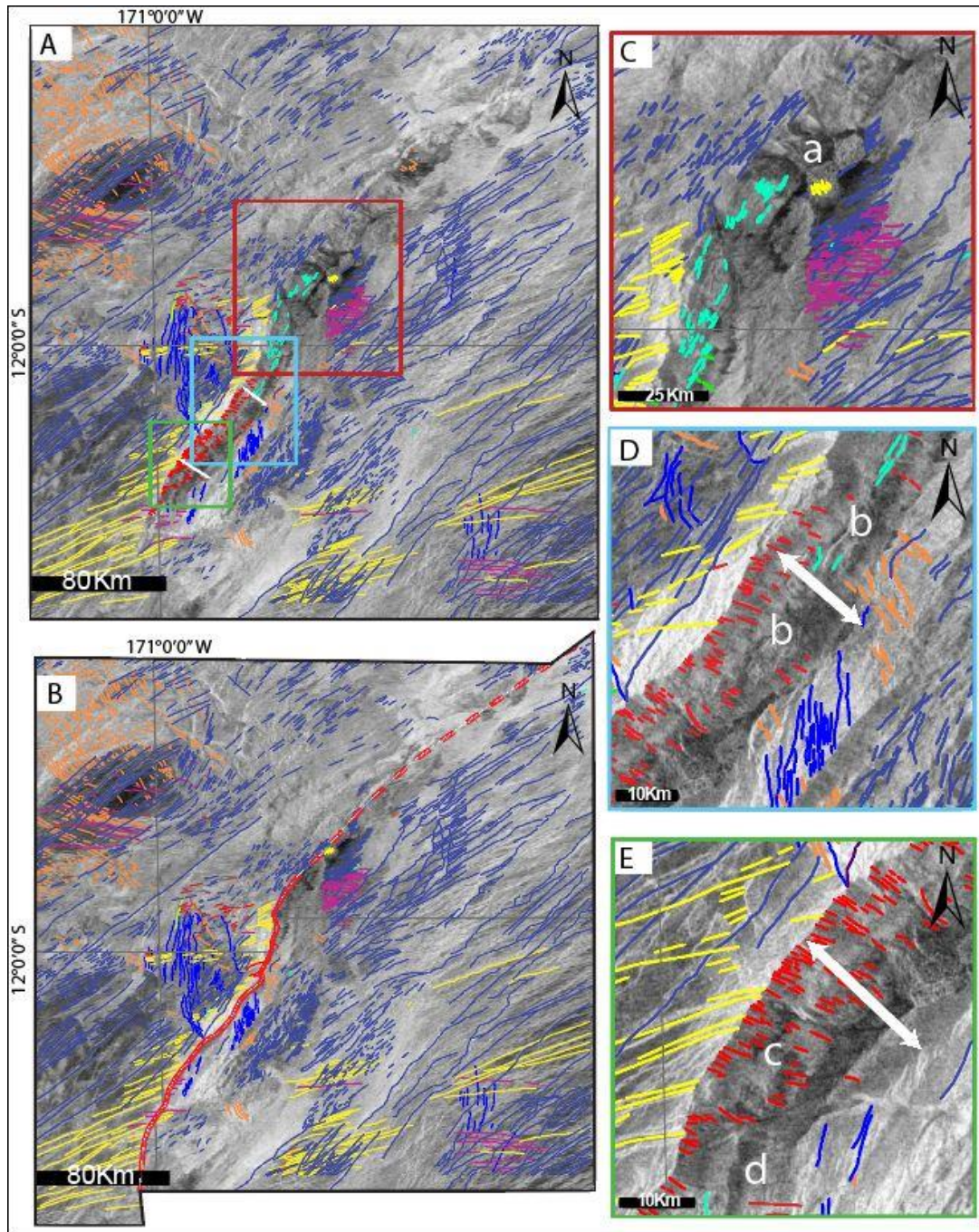


Figure 2: (A) Mapping of graben-fissure sets of various trends on both sides of the asymmetric rift (distinguished by color). The direction of the rift opening is indicated by white double-headed arrows. (B) A map showing the closure of the rift by relocating the SE side of the rift by around 30 km to the NW (C-E) Enlargements of important locations with lowercase letters indicating specific items of importance mentioned in the text.

References

Ait Lahna A. et al. (2022). LPSC 1657.
 Ford, P.G. and Pettengill, G.H. (1992). JGR, 97(E8), 13103.
 Hansen, V.L. and DeShon, H.R. (2002). USGS SIM I-2752.
 Herrick, R.R. (1999). Geophysical Research Letters, v. 26, p. 803-806.
 Ivanov, M.A. and Head, J.W. (2011). Planetary and Space Science, v. 59, p. 1559–1600

The intra-oceanic Assif n'Bougmmane arc complex (Bou Azzer inlier, Central Anti-Atlas, Morocco): petrology, geochemistry, U-Pb geochronology, and geodynamic implications.

Ait Lahna A.¹, Youbi N.^{1,2}, Tassinari C. C. G.³, Admou H.¹, Mata J.⁴, Gärtner A.⁵, El Moume W.¹, Hadimi I.¹, Basei M. A. S.⁶, Sato K.³, Boumehdi M.A.^{1,4}

1: Department of Geology, Faculty of Sciences-Semlalia, Cadi Ayyad University, Prince Moulay Abdellah Boulevard, P.O. Box 2390, Marrakech, Morocco. aitlahna.abdelhak@gmail.com; youbi@uca.ac.ma; admou@uca.ac.ma warda.elmoume@gmail.com; ismail.hadimi@gmail.com; boumehdi@uca.ac.ma

2: Faculty of Geology and Geography, Tomsk State University, 36 Lenin Ave, Tomsk, 634050, Russia

3: Centro de Pesquisas Geocronológicas (CPGeo), Instituto de Geociências (IG), Universidade de São Paulo-USP, Caixa Postal 11348, CEP 05422-970, São Paulo (SP), Brazil. ccgtassi@usp.br; keisato@usp.br

4: Instituto DomLuiz, Faculdade de Ciências, Universidade de Lisboa, 1749-016 Lisboa, Portugal. jmata@fc.ul.pt

5: Senckenberg Naturhistorische Sammlungen Dresden, Museum für Mineralogie und Geologie, Sektion Geochronologie, GeoPlasma Lab, Königsbrücker Landstraße 159, 01109, Dresden, Germany. andreas.gaertner@senckenberg.de

6: Instituto de Geociências (IG), Departamento de Mineralogia e Geotectônica (GMG), Universidade de São Paulo- USP, Rua do Lago, 562 Cidade Universitária 05508-080 São Paulo - SP – Brasil. baseimas@usp.br

The Assif n'Bougmmane gneiss complex comprises meta-igneous units, paragneiss, schist, and muscovite-bearing granite. The complex occurs at Bou Azzer, Oumlil, Tazigzaout, Hassi El Mnissi, and Assif n'Bougmmane windows in the southern part of the Bou Azzer inlier in the Central Anti-Atlas (Morocco). To determine the tectonomagmatic setting, the origin, and review the age of the Assif n'Bougmmane arc complex mafic (hornblende gabbro, garnet-hornblende gabbro, and hornblendite) and felsic rocks, we collected samples from mafic and felsic units for major and trace element analyses. Geochemical analyses from previous works are used for comparison. Three samples were dated using SHRIMP U-Pb zircon geochronology.

Tectonic discrimination diagrams reveal that the Bougmmane arc complex rocks were formed in an island-arc or volcanic-arc environment. The samples of host granodioritic gneiss fall within the field of "syn-collision granite" and "volcanic arc granite" in the Rb versus Y + Nb and the Rb versus Yb + Ta diagrams and belong also to "volcanic arc granite" in the Ta versus Yb and the Nb versus Y. The Hornblende gabbro and the garnet hornblende gabbro from this complex were generated from primary magmas originating from N-MORB and E-MORB sources, with no influence of subduction-related chemical components and slight influence of enriched OIB-type material. In contrast, the hornblendite is compatible with a genesis from primary magmas originating from depleted N-MORB, with the influence of subduction-related chemical components.

The complex was originally interpreted, on the basis of lithological similarity with rocks of the nearby Zenaga Massif and its intense deformation, as the Eburnean basement of the West African Craton (WAC) dated to 2 Ga or older age and onto which the Precambrian ophiolites of Bou Azzer and Siroua were obducted (Choubert, 1963, Leblanc, 1975, and Saquaque et al., 1992). The recent geochronological data confirmed their Neoproterozoic ages. The dating of gneiss at an age of ca. 745Ma, corroborates with the previously obtained ages in the Tazigzaout complex (D'lemos et al., 2006), in the Oumlil window (EL Hadi et al., 2010), in the Bou Azzer area (Blein et al., 2014), and in the Assif n'Bougmmane area (Triantafyllou et al., 2018). In addition, the obtained age of 767.9 ± 3.7 Ma for a garnet-bearing gabbro in the Assif n'Bougmmane area indicates the presence of a crust of this age probably the equivalent of the oceanic crust described in Siroua inlier.

References

Choubert, G., 1963. Histoire géologique de l'Anti-Atlas de l'archéen à l'aurore des temps primaires. Notes et Mémoires du Service Géologique du Maroc, v. 62, p. 350–352.

- Leblanc, M., 1975. *Ophiolites précambriennes et gîtes arsénites de cobalt (Bou Azzer, Maroc)*. Ph.D. thesis, université. Paris VI, p. 329.
- Saquaque, A., 1992. *Un Exemple de Suture-Arc: Le Précambrien de l'Anti-Atlas centre oriental (Maroc)*. Ph.D. Thesis, Université Cadi Ayyad, Marrakech, Morocco, 342p.
- D'Lemos, R.S., Inglis, J.D., Samson, S.D., 2006. A newly discovered orogenic event in Morocco: Neoproterozoic ages for supposed Eburnean basement of the Bou Azzer inlier, Anti-Atlas Mountains. *Precam. Research* 147, 65-78.
- El Hadi, H., Simancas, J.F., Martínez-Poyatos, D., Azor, A., Tahiri, A., Montero, P., Fanning, C.M., Bea, F., González-Lodeiro, F., 2010. Structural and geochronological constraints on the evolution of the Bou Azzer Neoproterozoic ophiolite (Anti-Atlas, Morocco). *Precambrian Research*, v. 182, p. 1–14.
- Blein, O., Baudin, T., Chèvremont, P., Soulimani, A., Admou, H., Gasquet, P., Cocherie, A., Egal, E., Youbi, N., Razin, P., Bouabdelli, M., Gombert, P., 2014. Geochronological constraints on the polycyclic magmatism in the Bou Azzer-El Graara inlier (Central Anti-Atlas Morocco). *Journal of African Earth Sciences*, v. 99, p.287–306.

The contribution of both MORB- and OIB-type mantle sources in the petrogenesis ca. 1.89 Ga Bastanar mafic dyke swarm, Bastar craton, India,

Ankur Ashutosh, Amiya K. Samal, Gulab C. Gautam, Rajesh K. Srivastava

Department of Geology, Banaras Hindu University, Varanasi 221005, India.

The Bastar craton of the Indian shield hosts nine distinct mafic dyke swarms of various trends and compositions with a period from 2.7 Ga to 1.42 Ga. The geochemistry and geochronology of the ca. 1.89 Ga NW- to NNW-trending Bastanar swarm are among those that have received the most attention (e.g., Srivastava and Singh, 2004; French et al., 2008; Shellnut et al., 2018). Most samples in this swarm show LREE enriched with almost flat HREE patterns, but intriguingly, a few samples exhibit an overall inclined REE pattern (e.g., Shellnut et al., 2018). The variable REE pattern raises a genuine concern about the potential contribution of a heterogeneous mantle source. Therefore, the present study is undertaken to provide a detailed geochemical characterization and petrogenetic interpretation of the ca. 1.89 Ga Bastanar swarm, particularly to examine – whether the parental magma of this swarm is derived from subcontinental lithospheric mantle (SCLM) as proposed by Shellnut et al. (2018) or metasomatized SCLM plays a significant role in the petrogenesis of this swarm. Furthermore, this work will also confirm whether the variation in REE pattern is because of melting of different mantle sources or something else. Based on geochemistry, samples of this swarm are classified into two distinct groups; the Group 1 samples have higher TiO_2 (average 1.6), $(\text{La}/\text{Yb})_N$ (7.2 – 8.6), $(\text{Gd}/\text{Yb})_N$ (1 – 2.37), Nb (10–16.6 ppm), Th (1.23 – 4.42 ppm) and Zr (104 – 171 ppm), whereas the Group 2 samples have lower TiO_2 (average 1.1), $(\text{La}/\text{Yb})_N$ (0.96 – 3.24), $(\text{Gd}/\text{Yb})_N$ (1 – 1.3), Nb (2.4 – 6.2 ppm), Th (0.18 – 2.72 ppm) and Zr (49 – 105 ppm) contents. Moreover, the REE patterns and variations in HFSE content of the Group 1 samples suggest its derivation from an OIB-type deeper and enriched mantle source. This is further substantiated by its higher TiO_2/Yb , Zr/Nb and Nb/Y ratios. On the other hand, the geochemical attributes of the Group 2 samples suggest its derivation from a shallower MORB-type depleted mantle source. The involvement of variable mantle sources is confirmed by observed variation in Dy/Yb and Gd/Yb ratios of samples of both the groups suggesting their derivation from a variable depth of a peridotitic mantle source in the garnet + spinel stability field. The absence of consistent negative Nb-Ta-Ti anomalies in the Group 1 samples attests to its uncontaminated nature and precludes any role of crustal contamination, whereas, the Group 2 samples display negative Nb-Ta-Ti anomalies with enriched LREE and LILE patterns, which suggesting a role of crustal components in its evolution. We propose that the Group 1 samples of 1.89 Ga mafic dykes are derived by a partial melting of an OIB-type deeper mantle source with rapid emplacement, whereas the Group 2 samples are derived by melting of MORB-type shallower mantle source. Based on geochemical characteristics observed in both the Group of samples, it is suggested that melts responsible for genesis of these mafic dykes are likely to be interacted with a metasomatized mantle source, where the source enrichment is brought about by fluids from a subducted slab.

References

- Shellnut, J. G., Hari, K. R., Liao, A. C. Y., Denyszyn, S. W. and Vishwakarma, N. 2018. A 1.88 Ga giant radiating mafic dyke swarm across southern India and Western Australia; *Precamb. Res.*, 308, 58–74.
- Srivastava, R. K. and Singh, R. K., 2004. Trace element geochemistry and genesis of Precambrian sub-alkaline mafic dikes from the central Indian craton: Evidence for mantle metasomatism; *J. Asian. Earth. Sci.*, 23, 373–389.
- French, J. E., Heaman, L. M., Chacko, T. and Srivastava, R. K., 2008. 1891–1883 Ma Southern Bastar–Cuddapah mafic igneous events, India: A newly recognized large igneous province; *Precamb. Res.*, 160, 308–322.

Totally molten magma chambers may grow in Earth's crust in months to years

Catherine Annen¹, Rais Latypov², Sofya Chistyakova², Alexander R. Cruden³ and Troels F. D. Nielsen⁴

¹Institute of Geophysics of the CAS, Prague 4, Czech Republic. ²School of Geosciences, University of the Witwatersrand, Johannesburg, South Africa. ³School of Earth, Atmosphere and Environment, Monash University, Melbourne, Australia. ⁴Department of Petrology and Economic Geology, Geological Survey of Denmark and Greenland, Copenhagen, Denmark.

Knowledge of magma emplacement timescales is critical for understanding how volcanic and igneous plumbing systems operate in the Earth's crust. The timescales of processes that create space for magma chambers are particularly poorly constrained. The vertical growth rate of basaltic magma chambers remains largely unknown with available estimates (0.5 to 20 cm/yr) being highly uncertain. Here, we propose a novel approach to address this issue using petrological constraints from the Skaergaard layered intrusion, Greenland – a classic example of closed-system differentiation in a ~4 km thick magma body with a total volume of ~300 km³. The onion-skin chemical structure of the Skaergaard intrusion indicates a parallel evolution in liquidus parageneses, suggesting that it crystallized from all margins inwards after it had been completely filled with magma (Nielsen, 2004). This evidence can be used to thermally calculate the minimum rate of magma emplacement that kept the growing Skaergaard magma chamber completely molten (<1% crystals). Our numerical simulations indicate that the required vertical growth rate was on the order of several 100s to a few 1000s m/yr, corresponding to volumetric flow rates of 10s to 100s of km³/yr (Annen et al. 2022). These rates are several orders of magnitude higher than other estimates (Menand et al. 2015) and were likely achieved by catastrophically rapid subsidence of the floor rocks along faults lubricated by magma (Nielsen, 2004, Cruden and McCaffrey, 2001). We propose that the Skaergaard and possibly other layered intrusions can be viewed as plutonic equivalents of super-eruptions, or catastrophic intrusions that grow via extremely rapid magma emplacement into the crust from staging chambers at depth, producing shallow crustal and totally molten magma chambers in a matter of a few months to dozens of years (Annen et al. 2022).

Nielsen, T. F. D. *The shape and volume of the Skaergaard intrusion, Greenland: implications for mass balance and bulk composition. J. Petrol.* 45, 507–530 (2004).

Menand, T., Annen, C. and de Saint Blanquat, M. *Rates of magma transfer in the crust: Insights into magma reservoir recharge and pluton growth. Geology.* 43, 199–202 (2015).

Cruden, A. R. and McCaffrey, K. J. W. *Growth of plutons by floor subsidence: implications for rates of emplacement, intrusion spacing and melt-extraction mechanisms. Physics and Chemistry of the Earth, Part A: Solid Earth and Geodesy.* 26, 303–315 (2001).

Annen, C., Latypov, R., Chistyakova, S., Cruden, A. R. and Nielsen, T. F. D. *Catastrophic growth of totally molten magma chambers in months to years. Science Advances* 8 (38), (2022).

Identification of Hidden Volcanic Centers from the Emanating Pattern of Lava Channel and Tubes from the Aurangabad Plateau in Deccan Volcanic Province in Maharashtra, India

Anshuman Misra¹; K. S. Misra²

¹: Department of Geology, Doon University, Dehradun n.

²: Department of Petroleum Engineering and Earth Sciences, University of Petroleum and Energy Studies, Dehradun

Mapping of remnants of lava channels and tubes has emerged as an important methodology for identification of hidden volcanic vents covered by the younger flows. An integrated arterial system comprising lava tubes and channels, through them molten basaltic lava has flowed long distances in the Deccan region of western India, has been reported by Misra (2002 a). This study suggested multi-central effusion in large Deccan Volcanic Province, with the development of local lava stratigraphy around them. This has also indicated futility of establishing long distance regional correlation based on very subtle chemical signatures. Remnants of lava tubes and channels are identified not only in Deccan Province but also in associated Cretaceous Volcanic Provinces such as Malwa, Mandla, Saurashtra, Kutch, Rajahmundry and Rajmahal (Misra, 2008). Over years these remnants are identified in more than three hundred and fifty places. Asolia Dongar hill was identified as an effusive centre from the radiating pattern of the lava channels by Misra (2002b). The present study suggests identification of effusive centres in areas covered by the younger flows. It has emerged that the extensive Deccan Plateau is composed of several smaller plateaus. The most prominent is the Aurangabad plateau, dissected in to number of smaller ones, from where a number of remnants are seen radially emanating from a large hidden volcano. On western side a quite prominent remnant of lava channel is seen emerging from the Tisgaon Tanda area and narrows towards west right up to Tisgaon locality (Fig. 1).



Fig. 1 Remnant of lava channel emerging out from the Aurangabad plateau near Tisgaon Tanda towards the west up to Tisgaon locality.

On north-north-west side a very complex pattern of lava channels is mapped approximately two km east of Ghusur village. Smaller distributary channels can also be seen emerging from the trunk channel (Fig. 2).



Fig. 2 Complex pattern of remnants of lava channels emanating from the Aurangabad plateau towards northern side can be seen.

Similarly in the cliff portion on the northern side of the Kannad Ghat, a long remnant of lava channel is described (Misra 2002a and 2002b). The channel proceeds and tappers in northerly direction with a number of gentle meanders (Fig.3).



Fig.3 Remnant of lava channel emanating towards north can be seen close to Kannad Ghat section.

References

1. Misra, K.S., 2002 (a), Arterial system of Lava tubes and channels within Deccan Volcanics of western India. *Journal Geological Society of India*, v. 59, pp. 115–124.
2. Misra, K. S. 2002 (b) Arterial system of Lava tubes and channels within Deccan Volcanics of western India. *Discussion; Journal Geological Society of India*, v.60, pp. 595-600.

Detailed Mapping of Unnamed Volcanic Event in Northern Themis Regio, Venus

E.G. Antropova¹, C.H.G. Braga^{1,2}, R.E. Ernst^{1,2}, H. El Bilali^{1,2}, K. L. Buchan³

¹: Faculty of Geology and Geography, Tomsk State University, Russia

²: Department of Earth Sciences, Carleton University, Ottawa, Canada

³: 273 Fifth Ave., Ottawa, Canada

Detailed (1:400,000 scale) geological mapping using full resolution (50-100 m/pixel resolution) Left-Look Magellan SAR images and altimetry data (10-20 km/pixel horizontal resolution, on average) has allowed grouping of several independent magmatic features into a single volcanic event (Fig. 1). The study area is more than 400 km across and is centered on 0.6°N, 277.8°E in the eastern part Beta-Atla-Themis (BAT) Region, Venus. Preliminary geological mapping in the region was carried out as part of the Devana Chasmata (V-29) Quadrangle mapping at a 1:5,000,000 scale by (Tandberg and Bleamaster, 2010).

Main volcanic center. The most prominent topographic feature of the map area is an intermediate size volcano (20x15 km²) (**C₁** in Fig. 1, b) with a maximum elevation of +2650 m. It has been previously classified as a fluted or modified dome (Antropova et. al., 2021).

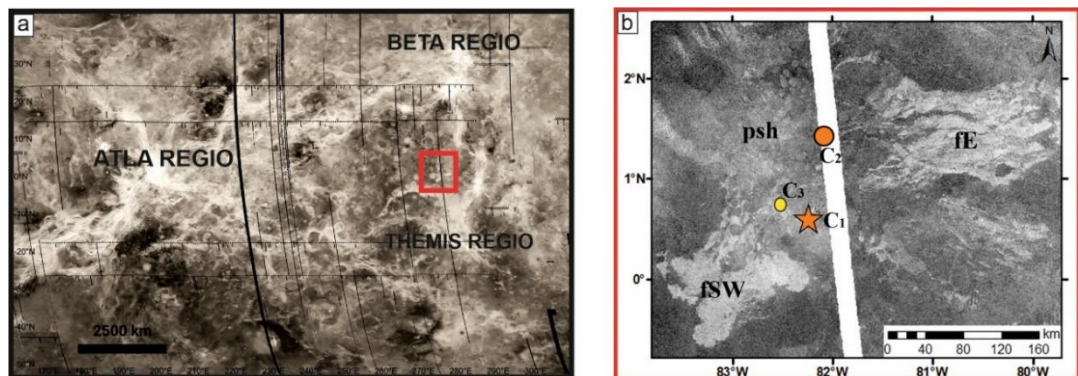


Figure 1 – Global Magellan SAR image of the Beta-Atla-Themis Regio on Venus (a). Location of the study area (b).

Lava flow fields. There are two major lava flows fields in the area (Fig. 1, 2, 3). The first flow field (**fE**) trends downslope in an east or northeasterly direction for ~250 km and includes multiple overlapping individual flows (Figs. 1, 2). The oldest flow unit (**fE₁** in Fig. 2) appears to originate from the main volcano (**C₁**). The younger **fE₂** flow unit appears to be sourced farther north at **C₂**. Even younger radar dark flow units (**fE₃** and **fE₄**) partially cover the earlier flows. Flow unit **fE₃** could be sourced from either **C₁** or **C₂** (Antropova et. al., 2021).

The second flow field (**fSW**) trends in a southwesterly direction for ~100 km, covering older tessera units (Figs. 1, 3). There appear to be local areas of lava breakout (Wilson et al. 1993; Parfitt et al. 1995). Flow unit **fSW₁** may originate from the main volcano (**C₁**). Alternatively, a smaller volcano (**C₃**) nearby could be its source. **C₃** is the source for local radar bright lavas (not shown). The source for flow unit **fSW₂** is unknown.

Shield field. An intense field of shield volcanoes (**psh**) is mainly concentrated within an area ~150 km across (Figs. 1, 4). However, more widely scattered shield volcanoes are also observed beyond this area (Fig. 5). These volcanoes have gentle slopes and small sizes (5-10 km in diameter), typical of many other Venusian shield fields (Hansen, 2005; Ivanov and Head, 2004). A detailed analysis of shield volcanoes showed that six main groups of volcanoes are distinguished within the boundaries of the study area, in accordance with their brightness. Some groups of volcanoes are concentrated in certain areas, for example, radar-dark volcanoes (blue circle) are distributed mainly in the northern part, and the radar-darkest ones (purple circle) tend to be distributed in the eastern part of the territory. Volcanoes marked with yellow and pink circles are unevenly distributed throughout the area.

We assume that the location and distribution of different groups of volcanoes may reflect age relationships between each other and between the rest of the geological units in the area. Thus, the volcanoes marked with a blue circle may be among the youngest, since they are confined to the youngest radar-dark stream spreading over the northern part of the study area. While the volcanoes shown as

yellow and pink circles are the most ancient, as most of the younger lava flows surround them from different sides, but do not overlap.

References

Antropova, E.G., Braga, C.H.G., Ernst, R.E., Buchan, K.L., El Bilali, H. (2021). Geological Mapping of Unnamed Volcanic Event (Centered at 0.6° N and 277.8° E) in Eastern Part of BAT Region, Venus. // Lunar and Planetary Science Conference (LPSC XXIII), Abstract number #1402.

Hansen, J.E., (2005), A slippery slope: How much global warming constitutes "dangerous anthropogenic interference"? An editorial essay. *Climatic Change*, 68, 269-279, doi:10.1007/s10584-005-4135-0.

Ivanov, M., and J. Head (2004), Stratigraphy of small shield volcanoes on Venus: Criteria for determining stratigraphic relationships and assessment of relative age and temporal abundance, *J. Geophys. Res.*, 109, E10001.

Parfitt, E.A., Wilson, L., Neal, C.A. (1995) Factors influencing the height of Hawaiian lava fountains: implications for the use of fountain height as an indicator of magma gas content. *Bulletin of Volcanology*, 57 (6), 440–450, doi:10.1007/bf00300988.

Tandberg, E.R. and Bleamaster, L.F. (2010). Geologic Mapping of the Devana Chasma (V-29) Quadrangle, Venus: Preliminary Report. // Lunar and Planetary Science Conference (LPSC XLI), Abstract #2751.

Wilson, M. (1993), Magmatic differentiation. *J. Geol. Soc. London*, 150, 611–624.

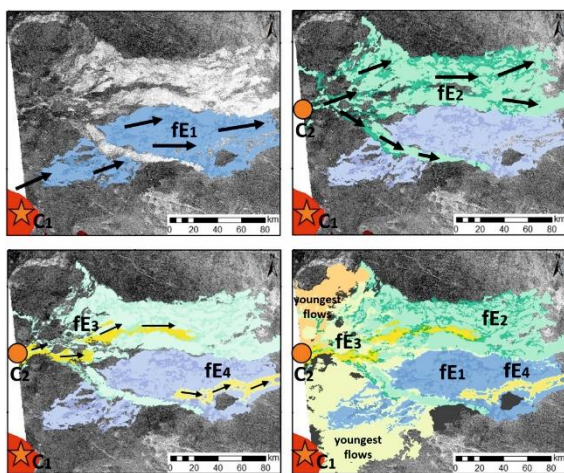


Figure 2 – Geological map of the eastern flow field (fE) which is subdivided into flow units fE₁–fE₄. C₁ = main volcano; C₂ = second source.

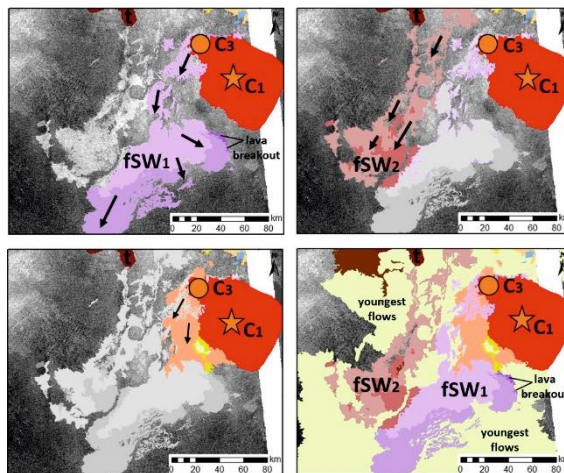


Figure 3 – Geological map of the southwest flow field (fSW) which is provisionally subdivided into flow units fSW₁, fSW₂. C₁ = main volcano; C₃ = small volcano.

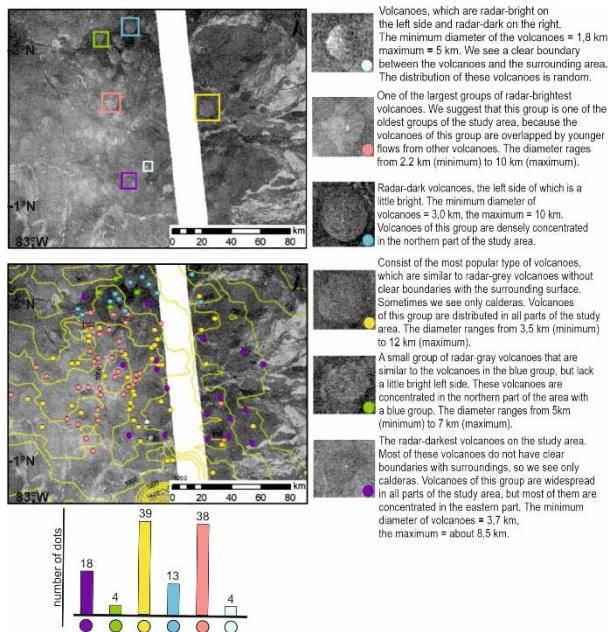


Figure 4 – Geological interpretation of the shield volcanoes of the study area.

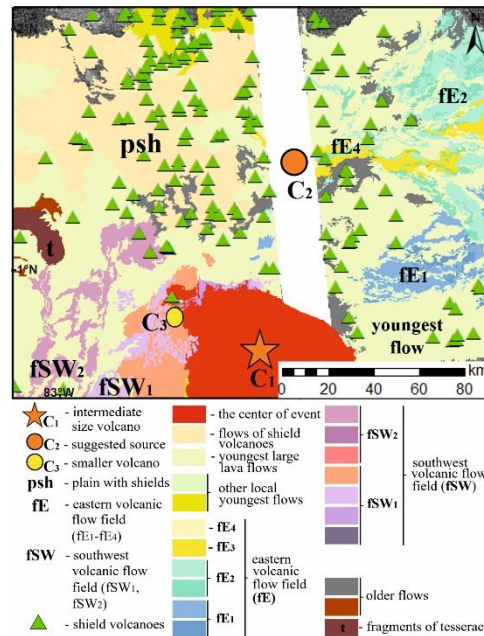


Figure 5 – Geological map of the central part of the study area.

Baddeleyite (ZrO₂) for isotope U-Pb (ID-TIMS) dating of multimetal (Cu-Ni, PGE, Ti-Cr-V) Paleoproterozoic deposits on continental (plume) and oceanic (subduction) crust (Fennoscandian shield, Arctic region) and supercontinental reconstructions

Tamara Bayanova^{1,2}, Yury Neradovsky¹, Evgeniy Kunakkuzin¹, Ekaterina Steshenko¹, Elena Borisenko¹

¹Geological Institute, Kola Science Centre, Russian Academy of Sciences; 14 Fersman street, Apatity, 184209 Russia; tamara@geoksc.apatity.ru

²Institute of Geosphere Dynamics, Russian Academy of Sciences; 38 Bld. 1 Leninsky prospect, Moscow, 119344 Russia; tamara@geoksc.apatity.ru

Baltic or Fennoscandian Shield contains oldest TTG and gray gneisses with 3.7-3.2 Ga on zircon SHRIMP and U-Pb (ID-TIMS) data (Bayanova et al., 2020). Oldest relicts of the rocks are coeval to another almost Hadean Shields (Kranendonk et al. 2019). In Paleoproterozoic time Baltic Shield are characterized by originating multimetal deposits and considered LIP according to (Ernst. 2017). Commercial Cu-Ni, PGE and Ti-Cr-V deposits – Pados, Pechenga and Kolvitsa were formed on oceanic crust in subduction substance (Barkov et al. 2021) with Paleoproterozoic ages. All new isotope U-Pb dating on baddeleyite and zircon are shown in (Fig. 1) and zircon grains have more discordances and xenocryst nature compared with baddeleyite.

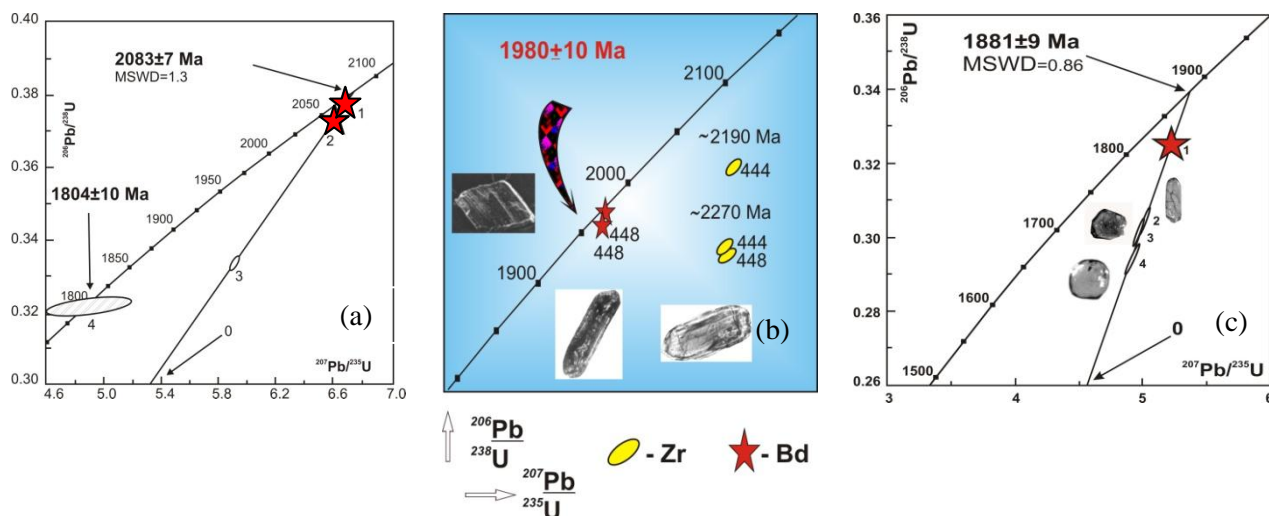


Fig. 1. Isotope U-Pb diagrams for baddeleyite and zircon from (a) Pados-Tundra Cr-deposit gabbro; (b) Pechenga gabbro from Cu-Ni Zdanov deposit. Sizes of zircon – baddeleyite grains vary within 100-150 μm, and (c) for single grain baddeleyite (1) and zircons (2-4) from clinopyroxenite Ti-Mag ores from the Kolvitsa deposit. Sizes of zircon-baddeleyite grains are 130-150 μm.

In Paleozoic time there are more than 20 alkaline massifs multimetal deposits with super large Khibina, Lovozero and Kovdor. The isotope U-Pb (ID-TIMS) age of baddeleyite from Kovdor phoscorite ore is 382±3 Ma and 379.2 ± 0.3 Ma (single grains) of baddeleyite according to new U-Pb method with artificial ²⁰⁵Pb/²³⁵U spike (Bayanova et al. 2014). Points 3-7 on the plot are very discordant and reflect presence ²³¹Pa and exceeded ²⁰⁷Pb according to (Ivanov et al. 2021).

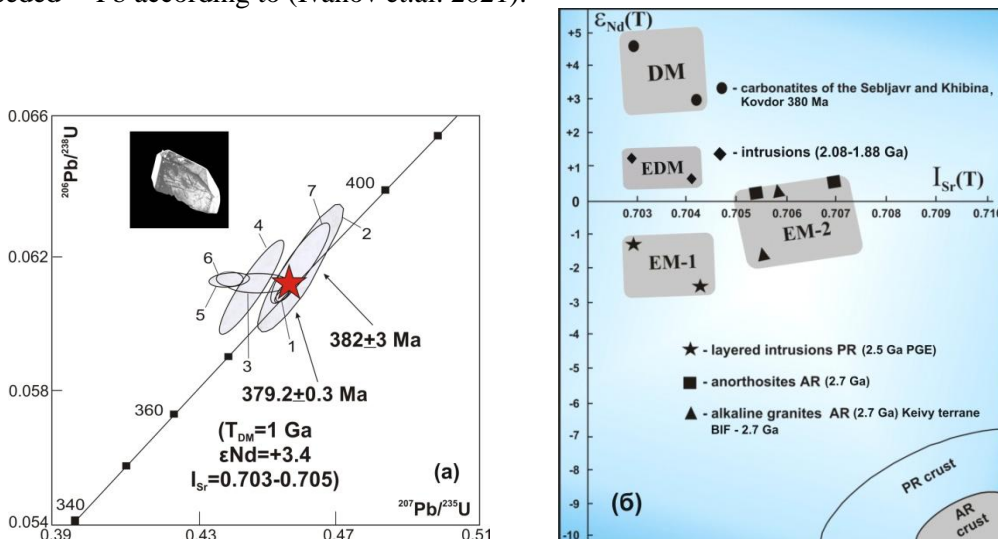


Fig. 2. Isotope U-Pb data for baddeleyite from the Kovdor phosphorite ore (a) and ϵNd - ISr diagram for rocks of the Fennoscandian Shield (b).

All new summarizing isotope U-Pb ages mostly on baddeleyite from multimetalliferous deposits from Archaean to Paleozoic time are shown on (Fig. 3).

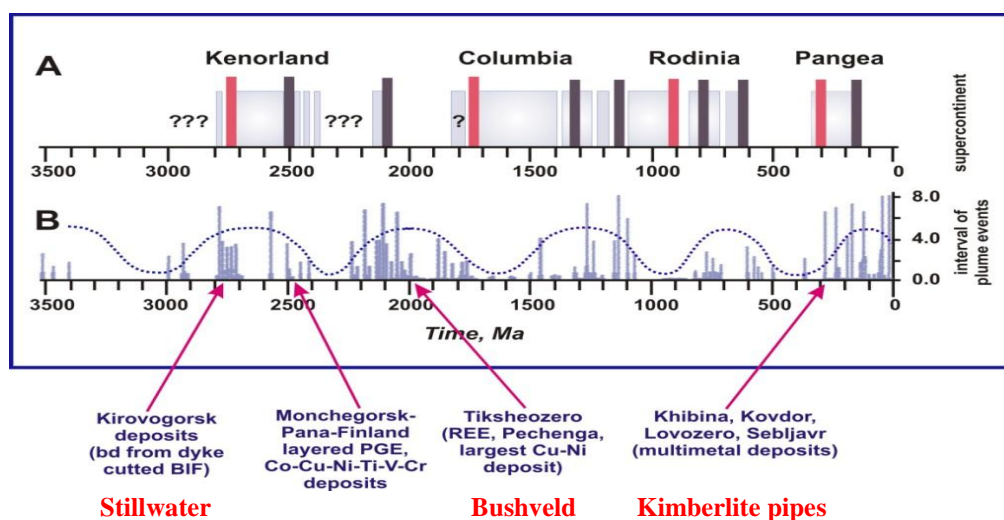


Fig. 3. Correlation of supercontinental cycles (A) with period 750-900 Ma for mantle-plume (B) activity, according to (Lubnina, 2009; Ernst, 2014). For East-European craton from Neoproterozoic to Paleozoic time based on paleomagnetic data.

Isotope precise U-Pb ages on baddeleyite from multimetalliferous Paleoproterozoic deposits are most important compared with zircon, due to mostly magmatic genesis. First occurrences of baddeleyite grains inside orthomagmatic orthopyroxene crystals were found in thin section in Kivakka layered PGE intrusion in Karelia region and reflected primary origin (Balashov et al., 1993).

In the framework of these studies, baddeleyites were sampled from important Paleoproterozoic Cu-Ni and Pt-Pd layered intrusions in the East Scandinavian LIP. Analyses of the sampled minerals indicated their primary magmatic genesis and U-Pb geochronology, baddeleyite is important in indicating the formation time and duration of the magmatic activity. It is also crucial for the reconstruction of the supercontinents in the geological history of the Earth.

Funding: All investigations are supported by Scientific Research Contracts No. 0226-2019-0053, Russian Science Foundation 21-17-00161.

REFERENCES

- Bayanova T.B., Mitrofanov F.P., Serov P.A., Nerovich L.I., Yekimova N.A., Nitkina E.A., Kamensky I.L. Layered PGE Paleoproterozoic (LIP) intrusions in the NE part of the Fennoscandian Shield – isotope Nd-Sr and $^3\text{He}/^4\text{He}$ data summarizing U-Pb ages (on baddeleyite and zircon), Sm-Nd data (on rock-forming and sulfide minerals), duration and mineralization. In *Geochronology – methods and case studies* / Ed. N.-A. Mörmner: INTECH, P. 143–193, 2014.
- Bayanova T.B., Kunakkuzin E.L., Serov P.A., Steshenko E.N., Borisenko E.S., Larionov A.N., Turkina O.M. The Oldest Grey Gneisses and Tonalite-Trondhjemite Granodiorites in the Fennoscandian Shield: ID-TIMS and SHRIMP Data // *Open Journal of Geology*. No 10. P.124-136. 2020. DOI: 10.4236/ojg.2020.102007
- Barkov A.Y., Nikiforov A.A., Barkova L.P., Korolyuk V.N., Martin R.F. Zones of PGE–chromite mineralization in relation to crystallization of the Pados-Tundra ultramafic complex, Serpentinite Belt, Kola Peninsula, Russia // *Minerals*, V. 11(1). 68. 2021.
- Balashov Y.A., Bayanova T.B., Mitrofanov F.P. Isotope data on the age and genesis of layered basic-ultrabasic intrusions in the Kola Peninsula and northern Karelia, northeastern Baltic Shield // *Precambrian Research*. V. 64. P. 197-205. 1993.
- Ernst R.E. *Large Igneous Provinces*; Cambridge University Press: Cambridge, UK. 653p. 2014.
- Ivanov A.V., Corfu F., Kamenetsky V.S., Marfin A.E., Vladykin N.V. ^{207}Pb -excess in Carbonatitic Baddeleyite as the Result of Pa Scavenging from the Melt // *Geochemical Perspectives Letters*. V.18. P. 11-15. 2021. DOI: 10.7185/geochemlet.2117
- Lubnina N.V., *East European Craton from Neoproterozoic to Paleozoic: paleomagnetic data*, Doctor Sci. (Geol. Miner.) Dissertation, Moscow, 275 P. 2009. (In Russian)
- Van Kranendonk M. J., Bennett V. C., Hoffmann J. E. *Earth's Oldest Rocks*. // Amsterdam: Elsevier. 1112 P. 2019.

Graben-Fissure Systems (Dyke Swarms) and Channelized lava Flows of Quetzalpetlatl and interior Boala Coronae Region, in Lada Terra Rise, Venus.

M. Ben Marzoug¹, H. El Bilali^{2,3}, R.E. Ernst^{2,3}, K.L. Buchan⁴, N. Youbi¹

¹: Department of Geology, Faculty of Sciences-Semlalia, Cadi Ayyad University, Marrakesh, Morocco, m.benmarzoug.ced@uca.ac.ma

²: Department of Earth Sciences, Carleton University, Ottawa, Ontario, Canada, hafidaelbilali@cunet.carleton.ca, RichardErnst@cunet.carleton.ca

³: Faculty of Geology and Geography, Tomsk State University, Tomsk, Russia.

⁴: 273 Fifth Ave., Ottawa, Ontario, kbuchan33@gmail.com

Introduction: Lada Terra rise, is a 2000-km-wide circular topographic feature that is elevated 2.5–3 km above the mean planetary radius in the southern hemisphere of Venus (Ivanov and Head, 2010). It is the site of numerous coronae including one of the largest on Venus, Quetzalpetlatl Corona (Fig. 1), (Stofan et al., 1992). Quetzalpetlatl Corona is 850 km in diameter, and hosts an interior corona, Boala Corona (350 km x 250 km in diameter).

Previous studies of the Quetzalpetlatl Corona area include reconnaissance-scale mapping (1:5,000,000 scale) of Mylitta Fluctus Quadrangle (V-61) (Ivanov and Head, 2006; 2010). The latter provided an overview of the geological units and general characteristics of the Quetzalpetlatl Corona area in order to understand the origin and nature of the Lada Terra rise, which the authors concluded represented a long-lived mantle upwelling, that was also associated with recent volcanic activity on Venus.

Channelized flows (including Canali, Sinuous Rilles and Valley networks) are common on Venus (Baker et al., 2015) and exhibit a wide variety of morphological characteristics (Gulick, et al., 1992). Simple channels generally consist of a single, sinuous main channel, whereas complex channels display branching, anastomosing, braided, or distributary patterns (Gulick, et al., 1992; Komatsu et al., 1993).

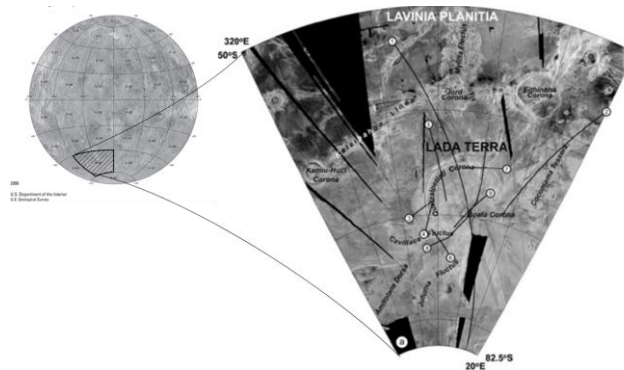


Figure 1. Location of study area.

Goals: Our broad research goal is to map Quetzalpetlatl Corona, both its graben-fissure systems (interpreted to overlie dyke swarms) and lava flows at 1:500,000 scale and to characterize its detailed geological history. In this abstract we present two aspects: 1) Preliminary characterization of the dyke swarms of Quetzalpetlatl and its interior Boala Corona. 2) Mapping the channelized flow systems (cf. (Baker et al., 2015) that are spatially associated with Boala Corona and assess their relationship with the corona.

Methods: Geological mapping was carried out using full-resolution (75 m/pixel) Magellan SAR images (Left and Right look) and its altimetry data in ArcGIS Pro v. 2.8.

Dyke Swarms: More than 14000 graben-fissure lineaments have been mapped and grouped into radiating and circumferential systems (Fig. 2). An impressive radiating system is centred on Quetzalpetlatl Corona. It can be divided into 4 subswarms, each focused on a slightly distinct sub-centre within Quetzalpetlatl (Fig. 2B). In addition, a radiating system is centred on Boala Corona (Fig. 2B). Furthermore, graben-fissure systems circumscribe two of the radiating sub-centres, one belonging to Quetzalpetlatl Corona and the other to Boala Corona. The Boala Corona circumferential graben are clearly linked to underlying dykes, because they are observed to be the source of several channelized flows, as discussed below. To the east of Boala Corona, other small circumferential systems identify four additional centres (Fig. 2).

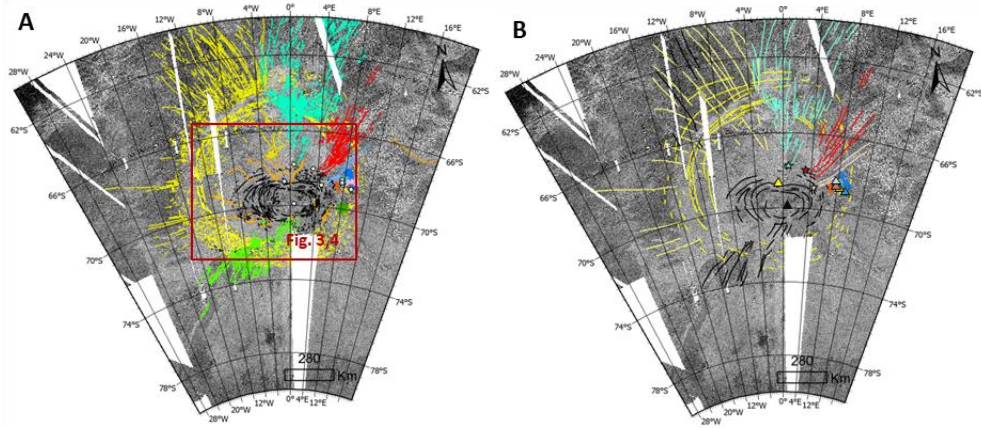


Figure 2. Distribution of graben colour-coded by swarm. A) detailed lines. B) Generalized lines with different colours for each centre and associated dyke swarm.

Channelized flows: We mapped approximately 15 channelized lava flows around the Boala Corona (Fig. 3). They typically trend downslope from sources in the outermost circumferential graben of the circumferential system, which is located along the elevated rim of Boala Corona. Based on altimetry data, the elevation of the sources ranges from 2158 to 2649 m (Fig. 3). The flows vary in length from 50 to at least 200 km. In some cases, flows begin within a circumferential graben, but then become channelized for a time along a radiating graben (and possibly even a second circumferential graben) before spilling out along a more irregular channel (e.g., Fig. 3B). Several channels branch in the downslope direction, or occasionally upslope. Oblique views of the Boala Corona topography and associated channelized flows are shown in (Fig. 3).

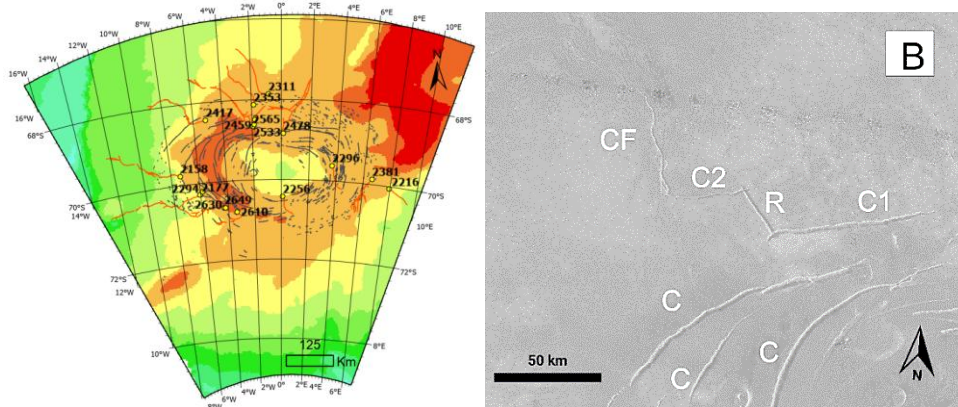


Figure 3. A) Distribution of channelized lavas (red lines) on Magellan topography. Yellow dots locate sources. Numbers indicate elevations (in metres) of sources. B) Magellan SAR image showing channelized flow starting at a circumferential graben (C1) but following a radiating graben (R) downslope before following another possible circumferential graben (C2) and then continuing downslope to the NNW as a channelized flow (CF). The location of the centre of the image is 68.55 deg S, 354.51 deg E.

Acknowledgments: Magellan SAR images obtained from <https://astrogeology.usgs.gov/search/?pmi-target=venus> based on the data from <https://pdsimaging.jpl.nasa.gov/volumes/magellan.html#mgnFMAP>.

References:

- Baker, V.R. et al. (2015) *Geomorph (Amst)* 245: 149–182.
- Gulick, V.C., et al. (1992) *LPSC Abstr.* 1231.
- Ivanov, M.A. & Head, J.W. (2006) *USGS Sci. Invest. Map* 2920.
- Ivanov, M.A., Head, J.W. (2010) *Planet. Space Sci.* 58, 1880-1894.
- Komatsu, G. et al. (1993). *Icarus* 102, 1–25.

WHAT IS THE EXTENT OF THE ARTEMIS TECTONOMAGMATIC FEATURE INFLUENCE ACROSS THE HENIE QUADRANGLE (V-58), SOUTHERN VENUS?

H.N. Bley¹, K.J.E. Boggs¹, C. Pendleton¹, J. Shackman¹ J., E. Varga¹, S. Herrington¹, P. Fontaine¹, H.G. Wehnes¹, R.E. Ernst^{2,3}, H. El Bilali^{2,3} and, E.M. Bethell⁴,

¹Department of Earth and Environmental Sciences, Mount Royal University, 4825 Mount Royal Gate se, Calgary, Alberta, Canada T3E 6K6;

²Department of Earth Sciences, Carleton University, 1125 Colonel By Drive, Ottawa, Ontario, Canada K1S 5B6;

³Faculty of Geology and Geography, Tomsk State University, 36 Lenin Avenue, Tomsk, Russia 634050;

⁴Department of Earth and Environmental Sciences, University of Ottawa, 75 Laurier Avenue E, Ottawa, Ontario, Canada K1N 6N5.

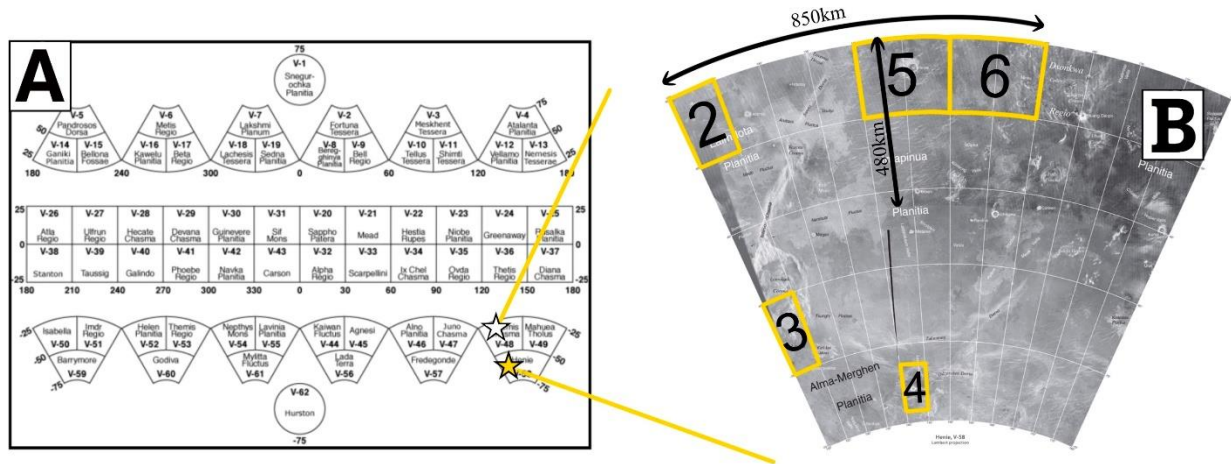


Figure 1: Study Area. The Henie Quadrangle (V-58), in southern Venus, is directly south of the Artemis Tectonomagmatic Feature. The boxes outline the locations for Figures 2, 3, and 4. Boxes 5 and 6 have been mapped by Herrington and Fontaine.

Keywords: Artemis Tectonomagmatic Feature, Wrinkle Ridges, Henie Quadrangle (V-58), Venus

Introduction: Artemis, a 2400 km diameter circular feature, is one of the largest tectonomagmatic features in our solar system. It is proposed to have formed above a deep mantle plume [1]. A concentric wrinkle ridge suite (13,000 km diameter) and a radiating dike swarm (12,000 km diameter) have been linked to the Artemis system [1]. Venusian grabens are long extensional lineaments generally appearing in linear, radial or circumferential patterns, and are widely interpreted to be a surface expression of underlying dyke swarms such as those associated with the Artemis Feature [2]. Wrinkle ridges are undulating elevated (possibly) compressional features. Here we investigate the extent of the influence of the Artemis tectonomagmatic feature, across the Henie Quadrangle that is located south of the eastern portion of the Artemis Quadrangle (Fig. 1), to determine the extent of the Artemis tectonomagmatic influence.

Methodology: Files were downloaded from the Planetary Data System for Magellan data. Mapped topographical features were categorized by qualities such as radar brightness, and orientation. Detailed mapping of Venusian geological features was traced out using ArcGIS at a scale of 1:500,000.

Results: The northwesternmost quadrant of the Henie Quadrangle (Fig. 1a) is crosscut by three graben swarms (353-173°; 340-160°; 010-190°), with their relative relationships outlined in the Table. In the region of the Latmikaik Corona (Fig. 3) there is one north-south graben swarm (015 to 195°) and two more north-south graben swarms around the Gilliani Impact Crater (Fig. 4; 351-171°; 005-185°). Wrinkle ridges are inconsistent across the western margin of the Henie Quadrangle being common in the northwest (Fig. 2), minimal to non-existent around the Latmikaik Corona (Fig. 3) and then patchy around the Gilliani Impact Crater (Fig. 4).

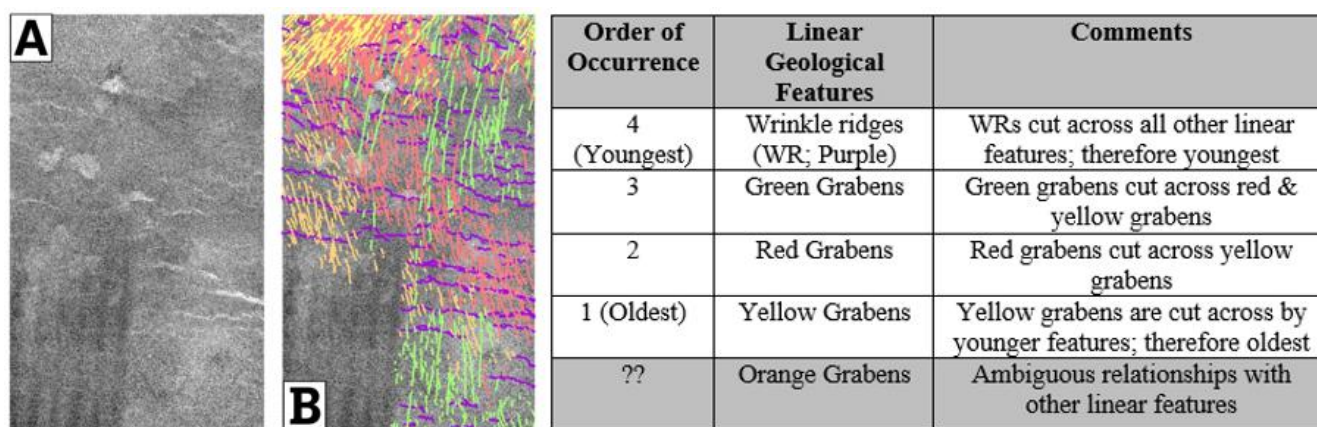


Figure 2: Northwestern quadrant of Henie quadrangle (Box 2 in Fig. 1). This quadrant has three graben swarms ($353-173^\circ$; $160-340^\circ$; $010-190^\circ$) traced in red, orange, and green respectively (Fig. 2.B) which align with grabens in the Artemis system to the north. The purple wrinkle ridges ($105-275^\circ$) are suggested to be part of the southeastern margin of the Artemis suite. In the middle of the Henie Quadrangle, WRs extend 850km to the east and 480km to the south (see lines in Fig. 1). The fourth yellow graben swarm ($045-225^\circ$) is likely not related to Artemis as these are oriented away from Artemis.

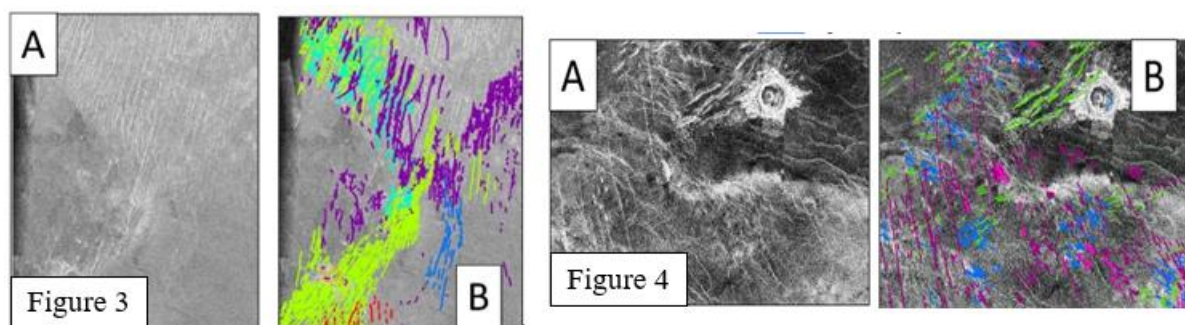


Figure 3: Southern portion of the Latmikaik Corona (Box 3 in Fig. 1). The purple graben swarm ($015-195^\circ$) could be related to Artemis, but still needs to be connected between boxes 3 and 4 in Figure 1. Here the teal graben swarm appears to be controlled by the Latmikaik Corona as they bend 25° to the west ($355-175^\circ$ to $318-138^\circ$) as they cross into the annulus for this corona. There are no observed wrinkle ridges in this quadrant.

Figure 4: Gilliani Impact Crater (Box 4 in Fig. 1). Here the purple ($351-171^\circ$) and pink ($005-185^\circ$) graben swarms could be related to Artemis, but more work is needed to connect these grabens with those in Figures 2 and 3. There is a patch of wrinkle ridges surrounding the Gilliani Impact Crater ($290-110^\circ$) which are unlikely to be associated with Artemis as they appear to be restricted to the radar dark lava flow surrounding the crater.

Discussion and Conclusion: The five graben swarms that extend north-south from the northwestern quadrant of the Henie quadrant through the Latmikaik Corona to the Gilliani Impact Crater could possibly join together across the entire length of the Henie quadrangle. It is very challenging to connect the wrinkle ridges across the western Henie Quadrangle from the northwestern quadrant (Fig. 2) to the Gilliani Impact Crater (Fig. 4) because WRs are not continuous in the western Henie Quadrangle. However, in central Henie Quadrangle ($850\text{km} \times 480\text{km}$ zone marked with lines in Fig. 1), WRs are continuous, appear to wrap around the southern flank of the Artemis feature and are therefore attributed to the influence of the Artemis tectonomagmatic feature.

Future Work: Our team is working towards completing the geological map of the Henie Quadrangle at a scale of 1;500,000. We are working towards connecting the grabens across the Henie Quadrangle.

Acknowledgements. We greatly appreciate the PDS data from the Magellan Mission.

References: [1] Hansen, V. L., & Olive, A. (2010). Artemis, Venus: The largest tectonomagmatic feature in the solar system? *Geology*, 38(5), 467-470. <https://doi.org/10.1130/G30643.1>

[2] Ernst, R.E., et al. (1995). Giant radiating dyke swarms on Earth and Venus. *Earth-Science Reviews* 39, 1-58. <https://www.sciencedirect.com/science/article/abs/pii/0012825295000175>

Mount Royal University, Henie Quadrangle (V-58, Southern Venus), and Large Igneous Provinces

Boggs, K.J.E.¹, Shackman, J.¹, Demorcy, J.¹, Pendleton, C.¹, Hall, J.¹, Chowdhury, M.¹, Bley, H.¹, Varga, E.¹, Shustova, J.², Dear, B.¹, Fontaine, P.², Dhimi, L.¹, Herrington, S.¹, Ernst, R.^{3,4}, El Balil, H.^{3,4}, Bethel, E.⁵, and Hanmer, S.⁶

¹Department of Earth and Environmental Sciences, Mount Royal University, 4825 Mount Royal Gate se, Calgary, Alberta, Canada T3E 6K6; ²Department of Geoscience, University of Calgary, 2500 University Drive nw, Calgary, Alberta, Canada T2N 1N4; ³Department of Earth Sciences, Carleton University, 1125 Colonel By Drive, Ottawa, Ontario, Canada K1S 5B6; ⁴Faculty of Geology and Geography, Tomsk State University, 36 Lenin Avenue, Tomsk, Russia 634050; ⁵Department of Earth and Environmental Sciences, University of Ottawa, 75 Laurier Avenue E, Ottawa, Ontario, Canada K1N 6N5; ⁶Retired Research Scientist, Geological Survey of Canada, Ottawa, Ontario, Canada.

Introduction: The NASA Magellan Mission produced a valuable resource that planetary geologists continue to use three decades later to unravel the geological characteristics of Venusian Large Igneous Provinces. The ability to be the first to map the surface of Venus is a powerful engagement tool to inspire the next generation of planetary geologists. Here we present an overview of the main geological features across the Henie Quadrangle (V58; Fig. 1; described in greater detail in [1, 2, 3, 4, 5]) and highlight the work done by other members of our team [6,7] who were unable to make it to Marrakesh. We would appreciate your comments and feedback before we submit the first papers from the Mount Royal University Venus geology mapping team.

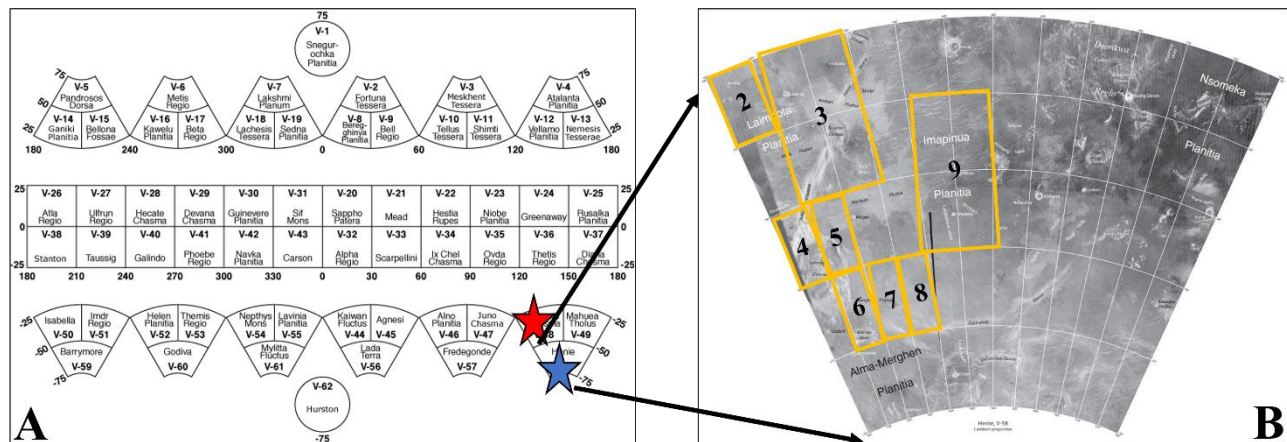


Figure 1: Study area location and team projects A) Henie Quadrangle (V-58; blue star) is south of the Artemis Quadrangle (red star). B) The orange rectangles outline the locations mentioned (e.g. Fig. 2). The top left quadrant (#2) is directly south of the Artemis tectonomagmatic feature, which is perfectly situated to determine the extent of the influence of Artemis [1]. The Latmikaik Corona is being mapped by #4 [6], #5 [7], #6 [3], while #3 is examining the relationship between two coronae, two dorsa, a fluctus and at least five lava flows [4]. Canali extend across the entire quadrangle [2], with mapping in #9 that revealed two generations of canali along with one canali segment originating from a circumferential graben associated with the Fotla Corona (see Fig. 2).

Methodology and Team: Mount Royal University (MRU) is an undergraduate university. Students out of first year geology courses are recruited into our team (now 25 from MRU and 3 from the larger research-focused University of Calgary), as an engagement hook for attracting students into geology programs, while giving them opportunities to publish a peer-reviewed journal article before graduation. In year one (Y1) the students learn how to use ArcGIS, how to identify and map the various Venusian geological features while completing the geological map of their quadrant (e.g #s in Fig. 2), and unravelling the relative order of geological events. In Y2 or Y3, the students present a poster at either an internal MRU (e.g. Pendelton & Chowdhury [6], Shustova [7]) or an external conference (e.g. Bley [1], Demorcy [2], Hall [3], Shackman [4], Varga [5] in Marrakesh).

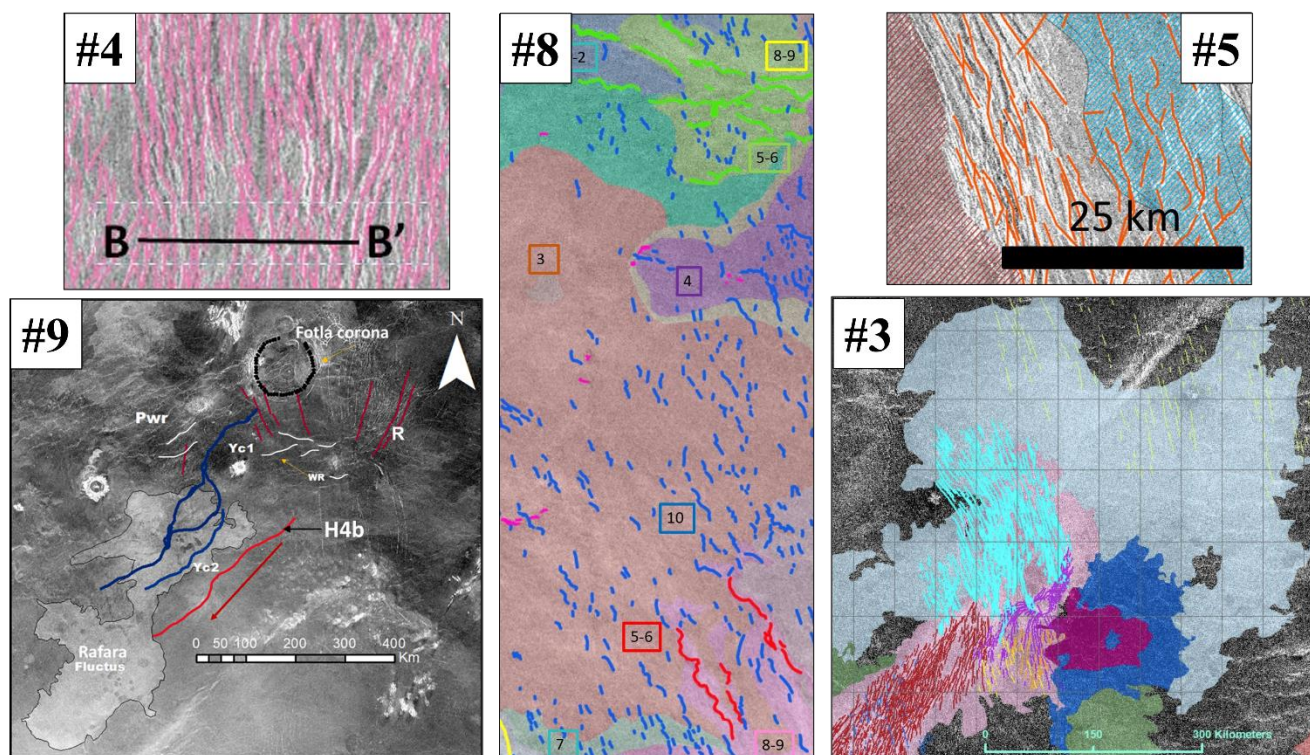


Figure 2: Results/Discussion from Mount Royal University geological mapping of the Henie Quadrangle (#s in white boxes correspond to the numbers in orange boxes in Fig. 1). Collectively we are exploring for evidence of strain localization into master faults as is typically observed on Earth (#4 [6] and #5 [7] detailed analysis of the Latmikaik Corona show no evidence for master faults with grooves evenly distributed at 1.5 to 2.5km). In #8) there are seven lava flows with two populations of wrinkle ridges (WR) in bright green and bright red. The green WRs have been linked to the formation of the Artemis feature north of the Henie Quadrangle, while the source of the strain that formed the red WRs is unknown [5]. There is no evidence for master faults associated with WRs. There are at least two generations of canali (#9 [2]). The Rafara Fluctus (RF) flowed over canali segment H4b suggesting that H4b is older than RF. Canali segment Yc2 cut across RF, suggesting that Tc2 is younger than RF. Note that canali segment Yc1 originates from a Fotla Corona circumferential graben [2]. Detailed mapping of the Xcacau Corona (#3) revealed an ambiguous relationship between the Arubani Fluctus (pale grey) and the Sunna Dorsa (radar bright in top centre of figure). It is possible that the dorsa is the source of the lava for the fluctus, suggesting a fissure eruption to form this fluctus.

Future Work – Our MRU team is working towards completing the geological map for the Henie Quadrangle. This needs to be completed in order to compile the relative order of all geological events between the Artemis feature, coronae (Latmikaik, Xcacau, Fotla), dorsa, fluctus, laval flows, wrinkle ridges and grabens. Further detailed analysis of WRs, grabens, and groove belts will be used to model the amounts of compression and extension necessary to form these features.

References: [1] Bley et al., 2023. What is the extent of the Artemis tectonomagmatic feature influence across the Henie Quadrangle (V-58), Southern Venus? Abstract for Large Igneous Provinces (LIPs 8) Conference, Marrakesh. [2] Demorcy et al., 2023. The relationship of Canali with Coronae, WR, and Lava Flows across the Henie Quadrangle (V-58), southern Venus. Abstract for LIPs 8 Conference, Marrakesh. [3] Hall et al., 2023. Latimikaik Corona Annulus Groove Belts, Katl-imi Mons, Henie Quadrangle (V-58), Southern Venus. Abstract for LIPs 8 Conference, Marrakesh. [4] Shackman et al., 2023. Geology of the Latmikaik and Xcacau Coronae in the Henie (V-58) Quadrangle, Venus. Abstract for LIPs 8 Conference, Marrakesh. [5] Varga et al., 2023. Wrinkle Ridges, Henie Quadrangle (V-28), Southern Venus. Abstract for LIPs 8 Conference, Marrakesh. [6] Pendleton & Chowdhury, 2023. Venus and Earth: Two Sister Planets with Unique Tectonic Processes. Abstract for MRU Faculty of Science and Technology (FST) Research Day. [7] Shustova et al. 2023. Coronae and associated lava flows, Henie Quadrangle (V58), southern Venus. Abstract for MRU FST Research Day.

Geological History of Atira Mons: a Large Shield Volcano on Venus

C.H.G. Braga¹, E.G. Antropova², R.E. Ernst^{1,2}, H. El Bilali^{1,2}, J. W. Head³, K. L. Buchan⁴

¹: Department of Earth Sciences, Carleton University, Ottawa, Canada

²: Faculty of Geology and Geography, Tomsk State University, Russia

³: Department of Earth, Environmental and Planetary Sciences, Brown University, Providence, U.S.A.

⁴: 273 Fifth Ave., Ottawa, Canada

Atira Mons (Fig. 1a) is a large shield volcano centered at 51.4°N, 272.9°E (92.9°W) in the NW portion of Beta Regio, a major mantle plume center (Basilevsky and Head, 2007). In the global context, the volcano is located between Kawelu and Guinevere Planitiae, and superposed on groove belts (gb), regional plains (rp₁₋₂) and plains with shield volcanoes (psh) (Ivanov and Head, 2011).

Being highly voluminous lava flows that occur in an intraplate setting, large flow fields such as this are frequently compared to terrestrial large igneous provinces (LIPs) on Earth (Head and Coffin, 1997; Magee and Head, 2001; Buchan and Ernst, 2021; Ernst, 2014), which makes Atira Mons an ideal target for detailed geologic mapping using SAR (synthetic aperture radar) images from the Magellan mission (Ford et al, 1993). The main objective is to characterize this volcanic center and reconstruct its geologic history following the example of MacLellan et al. (2021) and the principles described in Tanaka (1994). This was accomplished by compiling a 1:500,000 geologic map that includes a characterization of all the visible geologic units related to, or located in the vicinity of, Atira Mons. Furthermore, where possible, sources for each unit (underlying magma reservoir, dykes, small shield volcanoes, etc.) were determined, and a stratigraphic column was compiled based on cross-cutting and embayment relationships.

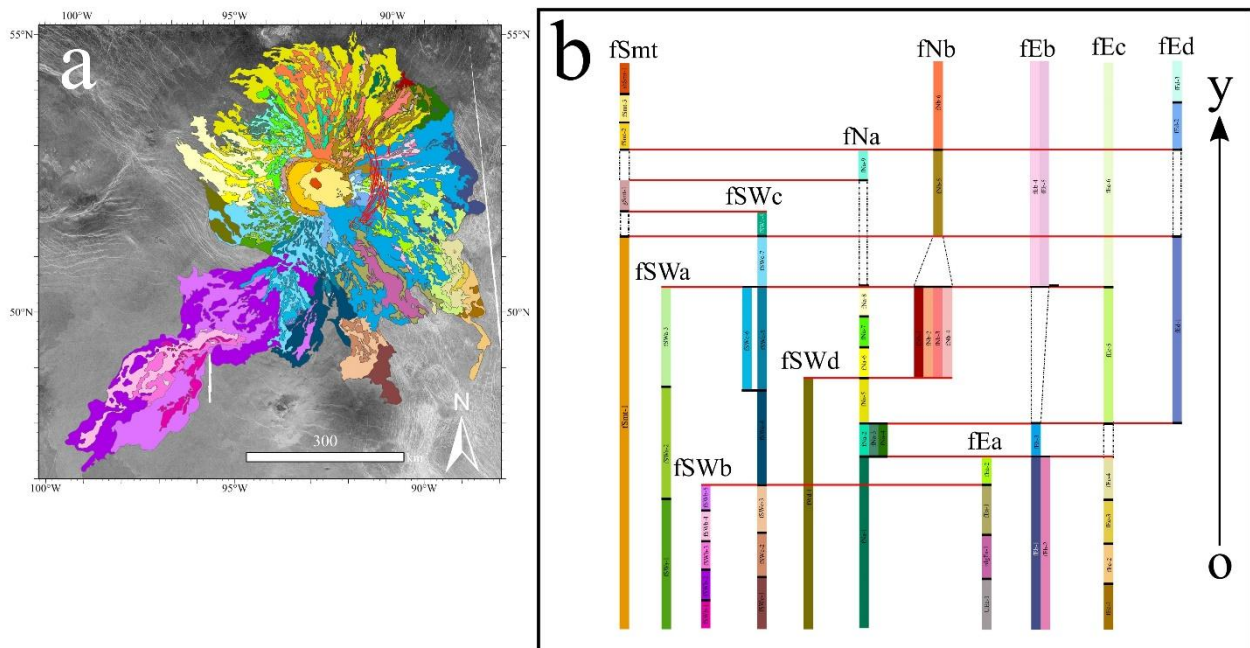


Figure 1 – a) Geologic map of Atira Mons. Each color represents one of the sixty areal geologic units, while the red lines correspond to the circumferential fractures on the eastern flank; b) Age relationships between areal units depicted in (a) with flow groups indicated by the prefix “f”. The arrow points to the younging direction (y), while red lines represent observed relative age relationships between different flow groups.

The results of geologic mapping are summarized in the map shown in Fig. 1b. A total of sixty-four geologic units were described, with sixty being areal units (lava flows, landslides, structural-material units, etc.), and four being linear units (arcuate fractures, polygonal fractures, wrinkle ridges, etc.). The main volcanic edifice covers an area of ~300,000 km², has a width of ~680 km, a length of ~1035 km and a height of 1.1 km. Atira Mons is also capped by a multiple-event, resurgent, asymmetric and elliptical basaltic caldera (Kargel et al, 1993; Cole et al, 2005) that is from ~115 km to ~140 km across and has its eastern side dropped lower. Its slopes are shallow, varying from ~0° to ~7.5° and averaging ~0.26°. The eastern flank of Atira Mons also contains a prominent system of circumferential fractures spanning an arc angle of ~90° with a radius of curvature of ~110 km.

The age relationships of the different geologic units are outlined in the stratigraphic column (Fig. 1b). Analysis of the relationships between fifty-five of the areal units show a complex and multi-episodic eruption history. The most voluminous flows are concentrated on the early stages of evolution of this volcanic center (e.g., fSWb-2 and fEb-3, Fig. 1b), while younger flow pulses (e.g., fEd-3, fSmt-3, Fig. 1b) are shorter and less voluminous, which indicates a waning of the volcanic activity over time. The development of the summit region appears to be the closing episode of Atira Mons' activity, as evidenced by the position of the summit flows on the stratigraphic column. Furthermore, one of the youngest units (fSmt-3, Fig. 1b) appears to be flowing uphill, judging by the current topography. This suggests that one of the last episodes of caldera collapse took place after the emplacement of these flows.

Mapping also revealed that most flows (representing most of the areal extent and volume of the volcano) are sourced or likely to be sourced from the summit region. Flank eruptions also occur. For instance, fSWb-2, fNa-9, fEc-5, fEc-6 (Fig. 1b). fEc-5 and fEc-6 appear to be fed from the circumferential fractures on the volcano's eastern flank, which could be considered evidence that they are not purely tectonic but overlie dykes (Ernst et al, 1995; Grosfils and Head, 1994). Flow fEc-6 is one of the youngest units on the volcano, and coupled with the fact the summit experienced a collapse episode after the emplacement of one of its youngest flows, fSmt-3, opens up the possibility that some of the eastern flank flows were emplaced by lateral movement of magma after a caldera collapse episode, as described by Gudmundsson et al, 2016 for the Bárðarbunga volcano in Iceland.

With the mapping complete, a series of questions are now being considered, such as:

— How to estimate the volume of Atira Mons, its load on the lithosphere and its potential volcanic time-volume release of volatiles?

— What are the limitations of the current data sets and how can the new missions to Venus (VERITAS, EnVision, DAVINCI+, Venera-D, Shukrayaan-1) help us improve detailed mapping efforts of large volcanic centers on the planet?

References

- A. T. Basilevsky, J. W. Head, *Beta Regio, Venus: Evidence for uplift, rifting, and volcanism due to a mantle plume*. *Icarus*, V. 192, Issue 1, 167-186 (2007).
- K. L. Buchan, R. E. Ernst, *Plumbing systems of large igneous provinces (LIPs) on Earth and Venus: investigating the role of giant circumferential and radiating dyke swarms, coronae and novae, and mid-crustal intrusive complexes*, *Gondwana Research*, V. 100, 25-43 (2021).
- J. W. Cole et al, *Calderas and caldera structures: a review*. V. 69, Issues 1-2, 1-26 (2005).
- R. E. Ernst, *Large Igneous Provinces*. Cambridge University Press, 653p (2014).
- R. E. Ernst et al, *Giant radiating dyke swarms on Earth and Venus*. *Earth-Science Reviews*, V. 39, Issues 1-2 (1995).
- J. P. Ford et al, *Guide to Magellan Image Interpretation*. JPL Publication 93-24 (1993).
- E. B. Grosfils, J. W. Head, *Emplacement of a Radiating Dike Swarm in Western Vinmara Planitia, Venus: Interpretation of the Regional Field Orientation and Subsurface Magmatic Configuration*. *Earth, Moon, and Planets*, V. 66, Issue 2, 153-171 (1994).
- M. T. Gudmundsson et al, *Gradual caldera collapse at Bárðarbunga volcano, Iceland, regulated by lateral magma outflow*. *Science*, V. 353, Issue 6296 (2016).
- J. W. Head, M. F. Coffin, *Large Igneous Provinces: a planetary perspective*. In "Large Igneous Provinces: Continental, Oceanic, and Planetary Flood Volcanism. J. J. Mahoney and M. F. Coffin (eds). AGU Geophysical Monograph 100, 411-438 (1997).
- M. A. Ivanov, J. W. Head, *Global geological map of Venus*, *Planetary and Space Science*, V. 59, Issue 13, 1559-1600 (2011).
- J. S. Kargel et al, *The Volcanology of Venera and Vega Landing Sites and the Geochemistry of Venus*, *Icarus*, V. 103, 253-275 (1993).
- L. MacLellan et al, *Volcanic history of the Derceto large igneous province, Astkhik Planum, Venus*. *Earth-Science Reviews*, V. 220, 103619 (2021).
- K. P. Magee, J. W. Head, *Large flow fields on Venus: Implications for plumes, rift associates, and resurfacing*". In "Mantle plumes: their identification through time" R. E. Ernst, K. L. Buchan (eds) (2001).
- K. L. Tanaka, *The Venus Geologic Mappers' Handbook*. USGS Publications, Open-File Report 94-438, (1994).

Does a supercontinent have a ‘megacontinent’ stage during formation?

Chong Wang¹, Ross N. Mitchell^{1,2}, Peng Peng^{1,2}

¹ State Key Laboratory of Lithospheric Evolution, Institute of Geology and Geophysics, Chinese Academy of Sciences, Beijing, China 100029

² College of Earth and Planetary Sciences, University of Chinese Academy of Sciences, Beijing 100049, China

Global oceanic subduction and continental collision leads to the formation of a supercontinent (Mitchell et al., 2021). Supercontinent formation is a protracted process with a duration of ~300 Myr or longer. Understanding the dynamics of such a long period is key to answering how and why supercontinents assemble. The well-known supercontinent Pangea was built off of the major and early-forming building block of Gondwana. A similarly massive landmass known as Nuna (the Paleoproterozoic connection of Laurentia–Baltica–Siberia) also came into existence before the final formation of supercontinent Columbia. Recent studies have speculated about the early assembly of Umkondia (Mesoproterozoic connection of India–Kalahari–São Francisco/Congo–Amazonia–West Africa) before the formation of supercontinent Rodinia (Choudhary et al., 2019; Evans, 2021; Bispo-Santos et al., 2023). Present-day Eurasia (with recently added India and arguably imminently colliding Australia) could be regarded as a core of the future supercontinent Amasia. According to these basic observations, we infer that “Rome was not built in a day”, i.e., that the formation of a supercontinent unfolds in quantized stages rather than being a constant activity of assembly. We suggest that a “megacontinent” forms as a precursor ~200 Myr prior to the appearance of its larger supercontinent (Fig. 1; Wang et al., 2021). The geodynamics of megacontinents even may induce large-amplitude true polar wander (Wang and Mitchell, 2023). In summary, a megacontinent could be regarded as a basic paleogeographic and geodynamic unit for interpreting supercontinent dynamics and mantle convection.

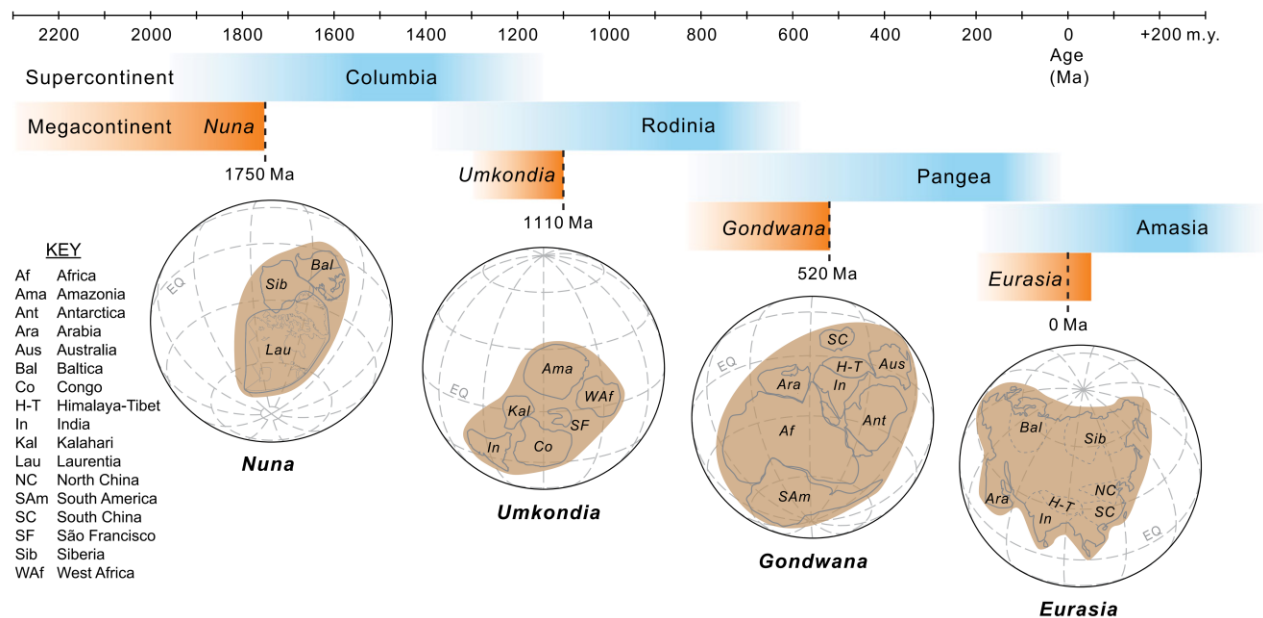


Figure 1 Megacontinents through time

References

- Bispo-Santos, F., D'Agrella-Filho, M.S., de Almeida, R.P., Ruiz, A.S., Patroni, O.A.L., Silva, J.M., 2023. Paleomagnetic study of the 1112 Ma Huanchaca mafic sills (SW Amazonian Craton, Brazil) and the paleogeographic implications for Rodinia supercontinent. *Precambrian Res.* 388, 107013.
- Choudhary, B.R., Ernst, R.E., Xu, Y.-G., Evans, D.A.D., de Kock, M.O., Meert, J.G., Ruiz, A.S., Lima, G.A., 2019.

Geochemical characterization of a reconstructed 1110 Ma Large Igneous Province. Precambrian Res. 332, 105382.

Evans, D.A.D., 2021. Meso-Neoproterozoic Rodinia supercycle. 549-576.

Mitchell, R.N., Zhang, N., Salminen, J., Liu, Y., Spencer, C.J., Steinberger, B., Murphy, J.B., Li, Z.-X., 2021. The supercontinent cycle. Nature Reviews Earth & Environment 2, 358-374.

Wang, C., Mitchell, R., 2023. True polar wander in the Earth system. SCIENCE CHINA Earth Sciences. doi.org/10.1007/s11430-022-1105-2

Wang, C., Mitchell, R.N., Murphy, J.B., Peng, P., Spencer, C.J., 2021. The role of megacontinents in the supercontinent cycle. Geology 49, 402-406.

Volcanism of the Baikal Rift as evidence of melting of mafic lithology in lithospheric mantle

Elena I. Demonterova, Alexei V. Ivanov

Institute of the Earth's Crust, Siberian Branch of the Russian Academy of Sciences, Irkutsk, Russia,
dem@crust.irk.ru, aivanov@crust.irk.ru

The Baikal rift locates in the middle of continent Eurasia and the beginning of its pronounced development is associated with the impact of the Indo-Asian collision on the continent (Molnar, Tapponier 1975). During the collision, the movement of crustal blocks led to the counterclockwise rotation of the Amur Plate and the development of extensional regions along the southern margin of the Siberian Craton (Zonenshain, Savostin 1981). With the time of development of the rift, volcanic eruptions of predominantly basalt composition occurred. In the southwest of the rift system, volcanism manifested itself over a wider area (more than 450 km in diameter) within the basins and on their shoulders, as well as in areas without visible extension structures. In the northeast of the rift system, there are two separate volcanic fields (~ 100 km across) - Udokan and Vitim. The first of them is located on the southern shoulder of the Chara basin, and the second is in the area of small basins outside the axis of the rift system. According to the data summarized in (Ivanov et al. 2015), volcanic activity associated with the Baikal extension stage began in the Late Mesozoic (~74 Ma), but the peak of volcanism occurred in the Miocene (18-9 Ma). Volcanic rocks throughout the territory are characterized by a close major and trace element compositions and more varying Sr-Nd-Pb isotopes. In the TAS diagram (Le Bas et al. 1986) the most of samples (~90%) fall into the field of basalt and trachybasalt. Basanites, tephrites, and phonotephrites are less common. Silica-saturated varieties such as trachyandesites and trachytes are observed in the Udokan volcanic field only. If rocks with SiO₂ over 55 wt.% are excluded from consideration, the volcanic rocks of the Baikal rift are characterized by K₂O+Na₂O = 3.8–10 wt.% and, according to the K₂O to SiO₂ ratio, belong to high potassium basalts. We consider that major-element compositional variations of the studied rocks are due to the various degrees of partial melting of geochemically variable mantle sources. Several authors point out that mafic lithologies (eclogite, pyroxenite, hornblendite) play the key role in derivation of basaltic melts (Sobolev et al. 2005; Pilet et al. 2008). For example, the crystallization of orthopyroxenites in the mantle, as a source for subsequent basalt melts, is associated with the transformation of olivine from peridotite to orthopyroxene due to the reaction with an acidic melt, which is formed during the melting of eclogite (Sobolev et al., 2005; Wang et al., 2020). Basaltic melts formed by the melting of pyroxenites will show a different behavior of the elements compared to if they were formed from a peridotite mantle (Herzberg, 2006; Pilet et al., 2011). According to the experimental data of fractional melting, the melts from pyroxenites (mafic lithologies) and peridotites will differ in the content of major oxides (for example, SiO₂, CaO, MgO, TiO₂ et al.) and their ratios (Herzberg 2006; Herzberg & Asimov 2008). The chemical composition of the lavas of the Baikal rift shows that they were derived from mafic source lithologies. Only a part of the volcanic melts from the Udokan volcanic field falls within the area of derivation from the peridotite source. Previously, the melting of a pyroxenite was used to explain the genesis of the Vitim and Udokan volcanic fields (Johnson et al. 2005; Yarmolyuk et al. 2023). In some volcanic fields, the major and trace element, and isotopic compositions change when moving from one tectonic block to another, while the predominant source of melting everywhere remains as mafic. This suggests that we see a predominance of lithospheric sources, and do not see any common component that could be attributed to a mantle plume or a plume-fed asthenosphere. This indicates that volcanism, at least in the Baikal rift, was caused by tectonic events and is controlled by passive rifting. Collision processes could control not only the movements and rotation of crustal blocks, but also the redistribution of upper mantle flows by reducing the distance between the margins of lithospheric plates (Schellart et al. 2019). Depending on the position of various tectonic blocks, the contrast in the thickness of the lithosphere between neighboring blocks, the orientation of crustal

stresses and upper mantle flows, each block reacted to destabilization in different ways, which explains why the temporal evolution of volcanism in Central Asia was complex and formless. Tectonic restructuring of the region throughout the rift evolution imposed by isostatic rise due to the removal of glacial load in some regions during interglacials, etc., the appearance of a melt and its subsequent eruption create thermal or chemical imbalances that lead the lithosphere from one unstable state to another (Lee et al. 2017). The destabilization of the lithosphere leads to the formation of lithospheric faults that play the role of channels, but not the direct penetration of asthenospheric melts, as modelled by Koptev et al. (2021), but the creation of metasomatic zones (Wang et al. 2020; Roy 2023). The melting of such metasomatic zones ultimately leads to the appearance of low-volume volcanism, which is widespread over a vast territory.

Herzberg, C., 2006. *Petrology and thermal structure of the Hawaiian plume from Mauna Kea volcano*. *Nature* 444, 605–609.

Herzberg, C., Asimow P.D., 2008. *Petrology of some oceanic island basalts: PRIMELT2.XLS software for primary magma calculation*. *Geochem., Geophys., Geosyst.* 9, Q09001, doi:10.1029/2008GC002057.

Ivanov, A.V., Demonterova, E.I., He, H., Perepelov, A.B., Travin, A.V., Lebedev, V.A., 2015. *Volcanism in the Baikal rift: 40 years of active-versus-passive model discussion*. *Earth-Sci. Rev.* 148, 18–43.

Johnson, J.S., Gibson, S.A., Thompson, R.N., Nowell, G.M., 2005. *Volcanism in the Vitim Volcanic Field, Siberia: Geochemical evidence for a mantle plume beneath the Baikal Rift zone*. *J. Petrol.* 46, 1309–1344.

Koptev, A., Cloetingh, S., Kovács, I.J., Gerya, T., Ehlers, T.A., 2021. *Controls by rheological structure of the lithosphere on the temporal evolution of continental magmatism: Inferences from the Pannonian Basin system*. *Earth and Planetary Science Letters* 565, 116925.

Le Bas, M.J., LeMaitre, R.W., Streckeisen, A., Zanettin, B., 1986. *A chemical classification of volcanic-rocks based on the total alkali silica diagram*. *J. Petrol.* 27, 745–750.

Lee, C.-T. A., Caves, J., Jiang, H., Cao, W., Lenardic, A., McKenzie, N.R., Shorttle, O., Yin, Q.-Z., Dyer, B., 2018. *Deep mantle roots and continental emergence: implications for whole-Earth elemental cycling, long-term climate, and the Cambrian explosion*. *Inter. Geol. Rev.*, 60:4, 431–448.

Molnar, P., Tapponnier, P., 1975. *Cenozoic tectonics of Asia: effects of a continental collision: Features of recent continental tectonics in Asia can be interpreted as results of the India-Eurasia collision*. *Science* 189, 419–426.

Pilet, S., Baker, M.B., Stolper, E.M., 2008. *Metasomatized lithosphere and the origin of alkaline lavas*. *Science* 320, 916–919.

Pilet, S., Baker, M.B., Müntener, O., Stolper, E.M., 2011. *Monte Carlo Simulations of Metasomatic Enrichment in the Lithosphere and Implications for the Source of Alkaline Basalts*. *J. Petrol.* 52, 1415–1442.

Roy, M. 2022. *Assessing the role of thermal disequilibrium in the evolution of the lithosphere–asthenosphere boundary: an idealized model of heat exchange during channelized melt transport*. *Solid Earth*, 13, 1415–1430.

Schellart, W.P., Chen, Z., Strak, V., Duarte, J.C., Rosas, F.M., 2019. *Pacific subduction control on Asian continental deformation including Tibetan extension and eastward extrusion tectonics*. *Nature Communications* 10, 4480.

Sobolev, A.V., Hofmann, A.W., Sobolev, S.V., Nikogosian, I.K., 2005. *An olivine-free mantle source of Hawaiian shield basalts*. *Nature* 434, 590–597. <https://doi.org/10.1038/nature0341>.

Wang, C., Lo Cascio, M., Liang, Y., Xu, W., 2020. *An experimental study of peridotite dissolution in eclogite-derived melts: Implications for styles of melt-rock interaction in lithospheric mantle beneath the North China Craton*. *Geochim. Cosmochim. Acta* 278, 157–176.

Yarmolyuk, V.V., Savatenkov, V.M., Kozlovsky, A.M., Stupak F.M., Kuznetsov M.V., Shpakovich L.V., 2023. *Crystallization Parameters, Genesis of Melts, and Sources of Magmas of the Late Cenozoic Udokan Volcanic Plateau, Central Asia*. *Petrology* 30 (Suppl 1), S1–S24.

Zonenshain, L.P., Savostin, L.A., 1981. Geodynamics of the Baikal rift zone and plate tectonics of Asia. Tectonophysics 76, 1–45. [https://doi.org/10.1016/0040-1951\(81\)90251-1](https://doi.org/10.1016/0040-1951(81)90251-1).

The relationship of Canali with Coronae, WR, and Lava Flows across the Henie Quadrangle (V-58), southern Venus.

Demorey, J.¹, Boggs K.J.E.¹, Shackman J.¹, Ernst, R.^{2,3}, El Bilali, H.^{2,3}, Bethell, E.⁴, and Wehnes, H.⁵

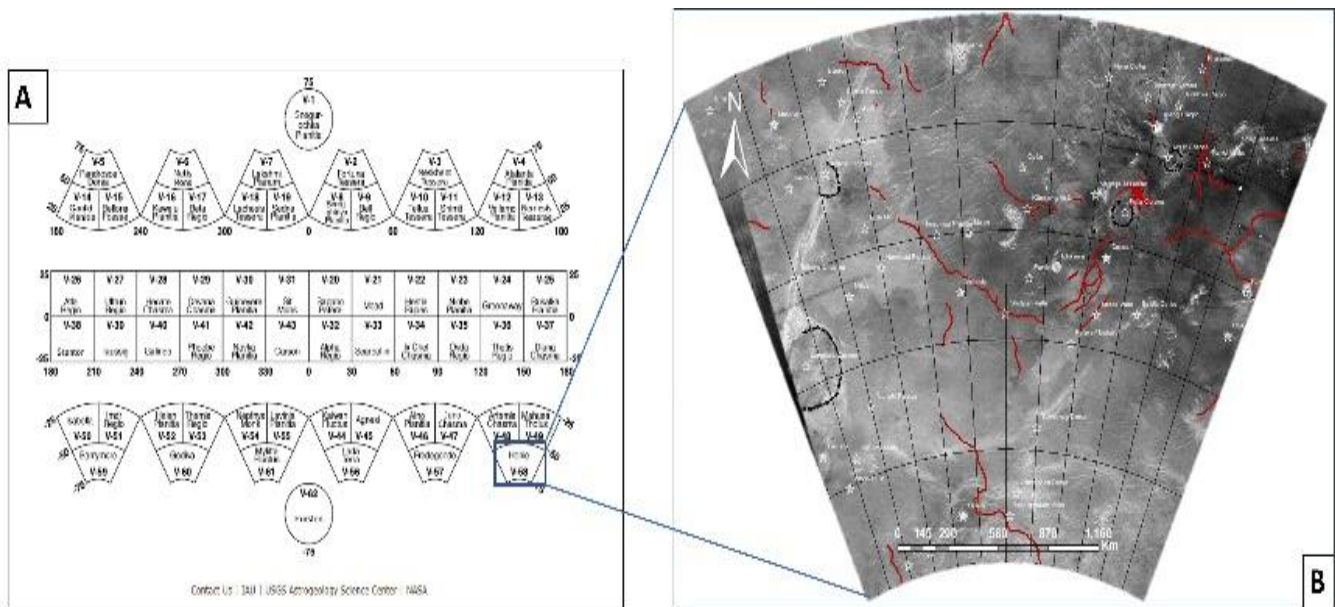
¹Department of Earth and Environmental Sciences, Mount Royal University, 4825 Mount Royal Gate se, Calgary, Alberta, Canada T3E 6K6; ²Department of Earth Sciences, Carleton University, 1125 Colonel By Drive, Ottawa, Ontario, Canada K1S 5B6; ³Faculty of Geology and Geography, Tomsk State University, 36 Lenin Avenue, Tomsk, Russia 634050; ⁴Department of Earth and Environmental Sciences, University of Ottawa, 75 Laurier Avenue E, Ottawa, Ontario, Canada K1N 6N5; ⁵Faculty of Mathematics, University Waterloo, 200 University Avenue West, Waterloo, Ontario N2L 3G1.

Introduction:

Lava channels, or canali, are long, narrow features with parallel sides that cross ~25% of Venus's surface [4]. They are typically <1-3km wide and are concentrated in lowland plain regions ([1,2,4]). Several studies indicate these lava channels were created before topographic uplift [1,3]. Studies show that the lengths and widths of the canali on Venus can provide insight into the lava composition of these channels. Narrower and shorter channels have been suggested to indicate low viscosity and basaltic composition [2]. Generally, younger canali features have sharper curves and more complex patterns than older features [2]. Canali morphologies and the three Wrinkle Ridge (WR)-canali relationships are illustrated in Figure 2.

This study describes the detailed mapping of canali segments across the Henie Quadrangle (V-58) in southern Venus. Outstanding questions include: i) What is the source of these canali segments? ii) What is the relationship between canali and WRs? iii) How many generations of canali are there?

Methods: Synthetic Aperture Radar (SAR) images were obtained by the NASA Magellan spacecraft (1990-94) and were downloaded from the Planetary Data System (PDS). Canali, WR, and coronae were



mapped at 1:500,000 using ArcGIS software.

Figure 1: Study area - Henie Quadrangle (V-58) in southern Venus (1A). The red lines on 1B are canali segments. The dark lines outline coronae. Segments Yc1/Yc2, and H6 emerge from a graben adjacent to Fotla Corona. A sinuous rille channel emerges from Huang Daopo Crater. Valley network channels occur adjacent to Fotla Corona (Fig 2a, b and c).

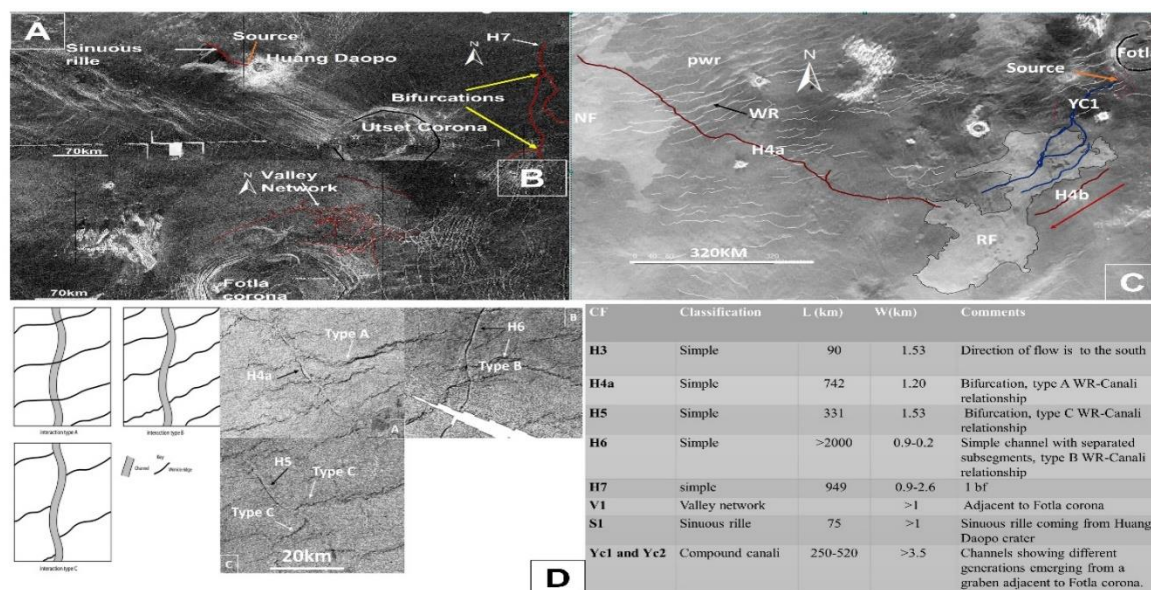


Figure 2 Results: Canali segments and their relationships with WRs are described in Table. There are four types of canali: i) simple canali channels with some bifurcation (2A), ii) valley network channels (2B), iii) sinuous rilles (2A); and iv) compound channels that cut across Rafara fluctus (RF; 2C). The compound channel starts at a graben adjacent to Fotla corona (2C). Canali fragments Yc1/Yc2 cut across RF and are therefore younger than RF. RF partially flows over segment H4b, suggesting that RF is younger than H4b. The three relationships between WRs and canali (2D; [3]) are: i) WR cuts across canali (canali older), ii) Canali cuts across WRs (either formed at the same time or canali younger), and iii) Ambiguous, either canali cuts across end of WR or WR are offset across canali [3].

Discussion and conclusion:

Most canali segments in this study have gentle curves suggesting that they are older [2]. They are also mostly narrower (<2km wide), supporting basaltic lava composition [2,3]. There are at least two generations of canali (Fig. 2C); segments Yc1 and Yc2 are younger than RF, while H4a is older than RF (Fig 2C). All three relationships exist between WRs and canali (Fig. 2, [3]). WRs cut across canali segment H4a (Type A), suggesting segment H4a is older than this WR. Type B and C are ambiguous with respect to relative order. Three canali segments (Yc1, Yc2, H6) originate at features associated with coronae. More work is needed to link all canali segments back to their origin.

Acknowledgments:

Thank you to Katherine Boggs, the MRU Venus research team, and the International Venus Research Group for many discussions, your input and your support. We also appreciate the PDS Magellan SAR images.

References:

- [1] Baker, V. R., Komatsu, G., Parker, T. J., Gulick, V. C., Kargel, J. S., & Lewis, J. S. (1992). Channels and valleys on Venus: Preliminary analysis of Magellan data. *Journal of Geophysical Research: Planets*, 97(E8), 13421-13444.
- [2] Bray, V. J., D. B. J. Bussey, R. C. Ghail, A. P. Jones, and K. T. Pickering. "Meander Geometry of Venusian Canali: Constraints on Flow Regime and Formation Time." *Journal of Geophysical Research* 112, no. E4 (April 25, 2007): E04S05. <https://doi.org/10.1029/2006JE002785>.
- [3] Lang, Nicholas P., and Vicki L. Hansen. "Venusian Channel Formation as a Subsurface Process." *Journal of Geophysical Research* 111, no. E4 (2006): E04001. <https://doi.org/10.1029/2005JE002629>.
- [4] Williams- Jones, G., Williams- Jones, A. E., & Stix, J. (1998). The nature and origin of Venusian canali. *Journal of Geophysical Research: Planets*, 103(E4), 8545-8555.

The Kelly Large Igneous Province: Evidence for horizontal tectonics in the form of a 3317 Ma magmatic suite

Steven W. Denyszyn¹ ; Andreas Petersson² ; Anthony I. S. Kemp³

¹: Department of Earth Sciences, Memorial University of Newfoundland, St. John's, Canada

²: Department of Geosciences and Natural Resource Management, University of Copenhagen, Copenhagen, Denmark

³: School of Earth Sciences, University of Western Australia, Perth, Australia

In order for the lateral motion of rigid lithospheric plates (i.e., 'horizontal tectonics') to be realistically considered, the mantle needs to be cool enough to allow the lithosphere to be sufficiently viscous for an efficient transfer of stress, and the lithosphere must be viscous enough to accommodate sedimentary basins and a network of brittle fractures. Linear dykes in large swarms therefore indicate crust rigid enough to facilitate horizontal accretion. While the onset of plate tectonics has been proposed as far back as the Hadean, there is no evidence for rigid crust that can accommodate linear dyke swarms until ~ 2700 Ma in the Pilbara Craton, and at ~ 2500 Ma in most other Archean cratons. Here, we provide a precise baddeleyite U–Pb age determination and litho-geochemistry for mafic dykes from the regionally extensive Kelly dyke swarm that feeds the voluminous Euro Basalt in the East Pilbara Terrane (Fig. 1), and establish this as part of perhaps the oldest Large Igneous Province (LIP) on Earth. This is the first time that a dyke swarm has been used as evidence for rigid crust prior to 3000 Ma, as it suggests that lithospheric conditions appropriate for plate tectonics existed at least as far back as the Paleoarchean.

A baddeleyite ²⁰⁷Pb/²⁰⁶Pb age of 3317.0 ± 1.1 Ma (MSWD = 1.5, n = 10) was obtained for one of the Kelly dykes (Fig. 2). Chondrite-normalized REE patterns of samples of this dyke have flat profiles with (La/Yb)_N ranging between ~1.5 and 2.5, and primitive mantle normalized trace-element profiles are also flat with (Th/Yb)_N ranging between ~0.1 and 0.5. All analyzed samples plot within the geochemical field defined by the related flood basalts.

Our 3317 Ma age of the Kelly dykes offers a minimum age for the Euro basalt (Fig. 1), which comprises a widespread ≤ 1.5 km thickness of komatiite and ~5 km of overlying komatiitic and tholeiitic basalt (Van Kranendonk et al., 2007). Similar geochronology and lithology suggests a correlation to the Kromberg Formation of the Onverwacht Group of the Kaapvaal craton; this connection would make the scale of the Euro basalt at least 1 000 000 km² (Hickman, 2021). The baddeleyite U–Pb data also provide an age for the related lithospheric extension, the period of which saw alternating deposition of thick basaltic successions and shallow water sediments, interpreted to suggest crustal uplift during mantle plume impingement, and basin deepening during crustal extension (e.g., Van Kranendonk et al., 2007). The Euro and Charteris Basalts make up a significant volume of the volcanic stratigraphy in the area, and this potential LIP requires a substantial network of magmatic conduits, apparently represented by the Kelly dykes. Furthermore, the temporal association with the nearby 3313 ± 9 Ma Carbara Pool monzogranite (Fig. 1, Barley and Pickard, 1999) and the coeval felsic volcanic Wyman Formation, intercalated with the Euro and Charteris basalts, implies a cogenetic suite of intrusive and extrusive mafic and felsic rocks that collectively represent the oldest well-defined Large Igneous Province in the geological record and the oldest preserved differentiated igneous suite.

Substantial deepening of the basin during accumulation of the Kelly Group volcanic rocks suggests that these eruptions were accompanied by crustal extension, in turn facilitating numerous dyke

intrusion into straight, brittle fissures — definitive signs of rigid-crust tectonic activity. All the criteria that define a rigid lithosphere as listed by Cawood et al., (2018) – brittle features, dyke swarms and large-scale sedimentary basins – are identified during the ~3430–3320 Ma time period that spans the deposition of the Strelley Pool Formation and the intrusion of the Kelly dyke swarm. This rigid crust is a prerequisite for horizontal tectonics and is likely also an important criterion for the development of thick basaltic crust and LIPs. Considering the combined thickness and areal extent of the Euro and Charteris basalts, a significant abundance of non-transient brittle fissures to accommodate these large volumes of basaltic and komatiitic magma to ascend is necessary. A rigid lithosphere is also an important element for allowing thick basaltic crust to be built, which can subsequently re-melt to generate felsic magmas, further promoting stability of proto-cratonic crust. The ~3000 Ma period is a critical period with respect to the onset of plate tectonics. However, until now there has been limited evidence for a lithosphere rigid enough to accommodate horizontal accretion during the Paleoproterozoic, and hence horizontal plate tectonics, as required by these models. The Kelly dyke swarm of the Pilbara Craton indicates the existence of rigid crust at ~3300 Ma, as required for a >3000 Ma onset of plate tectonics.

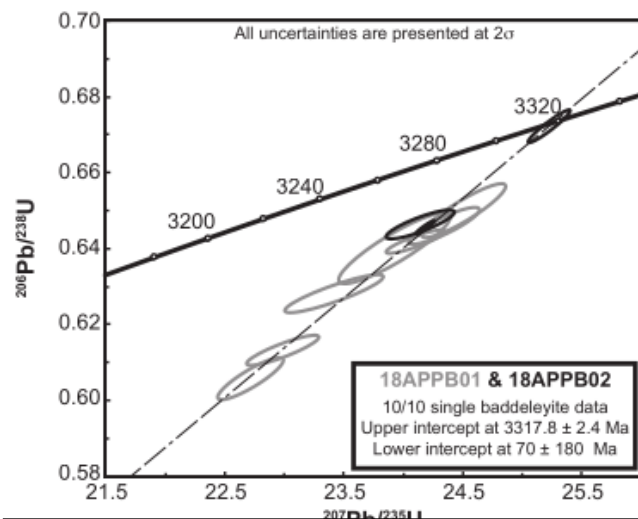
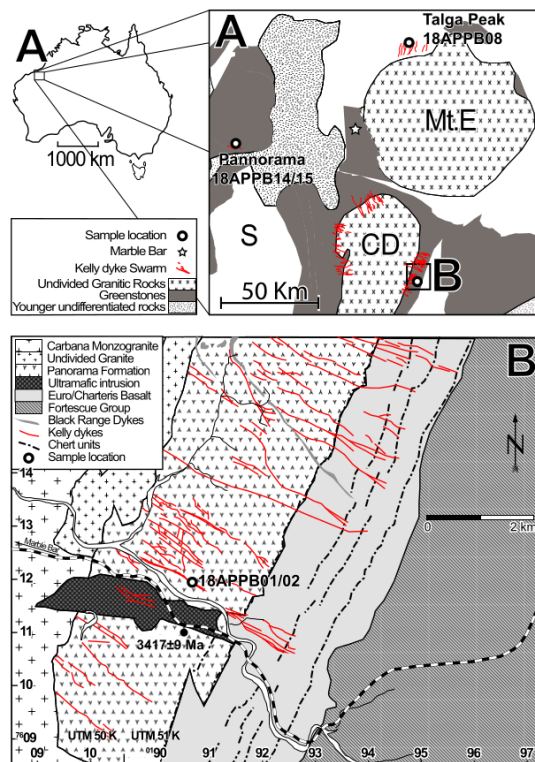


Figure 1. Simplified map of the sample localities. Mt.E = Mount Edgar Granite Complex, S = Shaw Granite Complex and CD = Corunna Downs Granite Complex. (B) Kelly dyke type locality.

Figure 2. Concordia plot of U-Pb data from baddeleyites of a Kelly dyke.

References

- Barley M. E. & Pickard, A. L. 1999. An extensive, crustally-derived, 3325 to 3310 Ma silicic volcanoplutonic suite in the eastern Pilbara Craton: evidence from the Kelly Belt, McPhee Dome and Corunna Downs Batholith. *Precambrian Research* **96**(1–2), 41–62.
- Cawood P. A., Hawkesworth C. J., Pisarevsky S. A., Dhuime B., Capitano F. A. & Nebel O. 2018. Geological archive of the onset of plate tectonics. *Philosophical Transactions of the Royal Society A: Mathematical, Physical and Engineering Sciences* **376**(2132), 20170405.
- Hickman A. H. 2021. East Pilbara Craton: a record of one billion years in the growth of Archean continental crust. *Geological Survey of Western Australia, Report* **143**, 1–187.
- Peterson, A., Kemp, A.I.S. and Denyszyn, S.W., 2022. The Kelly Dyke swarm, Pilbara craton: A 3317 Ma large igneous province? *Australian Journal of Earth Sciences*, **69**(8), 1207-1214.
- Van Kranendonk M. J., Smithies R. H., Hickman A. H. & Champion D. C. 2007. Paleoproterozoic development of a continental nucleus: the East Pilbara terrane of the Pilbara Craton, Western Australia. *Developments in Precambrian Geology* **15**, 307–337.

Late Paleoproterozoic and Mesoproterozoic extensional events in the Siberian craton marked by mafic dykes

Tatiana Donskaya¹, Dmitrii Gladkochub¹, Richard Ernst^{2,3}, Sergei Pisarevsky⁴, Elena Demonterova¹

¹: Institute of the Earth's Crust, Siberian Branch of the Russian Academy of Sciences, Irkutsk, Russia

²: Department of Earth Sciences, Carleton University, Ottawa, Ontario, Canada

³: Faculty of Geology and Geography, Tomsk State University, Tomsk, Siberia, Russia

⁴: Earth Dynamics Research Group, The Institute for Geoscience Research (TIGeR), School of Earth and Planetary Sciences, Curtin University, WA, Australia

The geological, geochronological, and paleomagnetic data suggest that Siberia and Laurentia could be close to each other between 1850 and 720 Ma, and probably were parts of the Paleo-Mesoproterozoic Nuna supercontinent and the Neoproterozoic Rodinia supercontinent (Ernst et al., 2016a; Pisarevsky et al., 2021; Elming et al., 2021 etc.). During this time interval, Late Paleoproterozoic and Mesoproterozoic mafic intrusions were emplaced in different parts of the Siberian craton. All these emplacements were in intracontinental extension settings and did not lead to the separation of the Siberian craton from other continents (or supercontinents). New geochemical and Nd isotopic data from Late Paleoproterozoic and Mesoproterozoic intrusions were obtained in recent years. These data show that Late Paleoproterozoic and Mesoproterozoic mafic rocks were produced from sources of different composition, despite a similar geodynamic setting.

1.78–1.75 Ga mafic dykes are widespread in different part of the Siberian craton (Baikal uplift, Aldan and Anabar shields). All of them belong to Timpston LIP and include Chaya, Doros, Timpston-Algamay, and East Anabar dyke sub-swarms (Gladkochub et al., 2010, 2022; Donskaya et al., 2014; McClelland, 2013; Ernst et al., 2016a). The dolerites demonstrate similar geochemical affinities and are characterized by negative Nb–Ta and Ti anomalies in multi-element spectra as well as mainly negative $\epsilon\text{Nd(T)}$ between 0.1 and –7.0 (Donskaya et al., 2014; McClelland, 2013; Gladkochub et al., 2022). Geochemistry and Nd isotope systematics of these mafic intrusions indicate the subcontinental lithospheric mantle source, or mantle source contaminated by crustal material.

1.64–1.61 Ga dolerite sills are locally exposed in the Biryusa uplift in the southern part of the Siberian craton (Ernst et al., 2016a; Gladkochub et al., 2021). These dolerites have slightly negative Nb-Ta anomalies in multi-element spectra and negative $\epsilon\text{Nd(T)}$ between –2.2 and –2.5 (Gladkochub et al., 2021). Geological, geochemical and Nd isotopic data suggest that the dolerites were generated from a mantle source produced by interaction between OIB and metasomatized lithosphere.

1.50–1.47 Ga mafic dykes and sills are widely distributed only in the northern part of the Siberian craton (Anabar shield and Olenek uplift) and belong to the Kuonmaka LIP (Ernst et al., 2000; Wingate et al., 2009; Ernst et al., 2016b). These dolerites correspond to sub-alkaline and alkaline tholeiitic basalts and don't show Nb–Ta and Ti anomalies in multi-element diagrams (Ernst et al., 2016b; Gladkochub et al., 2016). The dolerites of Olenek uplift are characterized by $\epsilon\text{Nd(T)} = +0.6 \dots -0.8$ (Gladkochub et al., 2016). All Kuonamka LIP dolerites are suggested to be mainly of OIB affinity with a minimum of crustal and lithospheric contamination (Ernst et al., 2016b; Gladkochub et al., 2016).

1.42 Ga Gornostakh dyke is located in the southeastern Siberian craton (Malyshev et al., 2021). Malyshev et al. (2021) showed that tholeiitic dolerites of this dyke have a negative Nb–Ta anomaly and were generated from metasomatically enriched subcontinental lithospheric mantle source.

1.39–1.38 Ga mafic dykes are located in the northern part of the Siberian craton (Anabar shield and Udzha paleo-rift) and grouped as the Chieress LIP (Ernst et al., 2000; Malyshev et al., 2018). The Udzha tholeiitic dolerites lack Nb–Ta anomalies in multi-element spectra. Geochemistry of these mafic dykes indicates a mantle source similar to OPB (oceanic plateau basalt) (Gladkochub et al., 2009).

1.35–1.34 Ga mafic dykes of the Listvyanka LIP are located in the Irkutsk Promontory in the southern part of the Siberian craton (Listvyanka and Goloustnaya locations) (Ernst et al., 2016a). The dolerites of these dykes correspond to sub-alkaline tholeiitic basalts. They are characterized by positive Nb-Ta and Ti anomalies in multi-element diagrams and by $\epsilon\text{Nd(T)}$ values between –0.9 and +1.5 (Donskaya et al., 2018). Geochemical and isotopic affinities of these dolerites suggest their generation from the OIB-type source.

1.26 Ga Srednecheremshansk dyke-shaped intrusion is locally distributed in the Sharyzhalgay uplift of the southern part of the Siberian craton (Ernst et al., 2016a; Gladkochub et al., 2023). This intrusion is composed of ultramafic and mafic rocks, which is geochemically close to subalkaline peridotite gabbro and gabbro. These rocks are characterized by negative Nb–Ta and Ti anomalies in multi-element spectra, as well

as negative $\epsilon\text{Nd}(T)$ values range from -6.3 to -6.9 (Gladkochub et al., 2023). The rocks of this intrusion might be derived from a subcontinental lithospheric mantle source.

Thus, the syntheses of geochemical and Nd isotope data on the Late Paleoproterozoic and Mesoproterozoic mafic intrusions of the Siberian craton led us to the conclusion that only Mesoproterozoic intrusions with ages of 1.50–1.47, 1.39–1.38 and 1.35–1.34 Ga were generated from mantle sources similar to OIB or OPB (possibly plume-dominated) source. In the global paleogeographic reconstructions, the Siberian craton during 1.50–1.34 Ga was located in the core of Nuna supercontinent (Elming et al., 2021). The 1.78–1.75 Ga and 1.26 Ga intrusions, originated from subcontinental lithospheric mantle sources, were intruded during the assembly and breakup of Nuna correspondingly (Elming et al., 2021).

Donskaya, T.V., Gladkochub, D.P., Shokhonova, M.N., Mazukabzov, A.M., 2014. Late Paleoproterozoic basites of the northern Baikal area: composition and melt sources. *Russ. Geol. Geoph.* 55 (11), 1278–1294.

Donskaya, T.V., Gladkochub, D.P., Ernst, R.E., Pisarevsky, S.A., Mazukabzov, A.M., Demonterova, E.I. Geochemistry and petrogenesis of Mesoproterozoic dykes of the Irkutsk Promontory, southern part of the Siberian craton. *Minerals* 8 (12), 545.

Elming, S.-Å., Salminen, J., Pesonen, L.J., 2021. Paleo-Mesoproterozoic Nuna supercycle, in: Pesonen, L.J., et al., eds., *Ancient Supercontinents and the Paleogeography of the Earth*. Amsterdam, Elsevier, Chapter 16, pp. 499–548.

Ernst, R.E., Buchan, K.L., Hamilton, M.A., Okrugin, A.V., Tomshin, M.D., 2000. Integrated paleomagnetism and U-Pb geochronology of mafic dikes of the eastern Anabar Shield region, Siberia: Implications for mesoproterozoic paleolatitude of Siberia and comparison with Laurentia. *J. Geology* 108, 381–401.

Ernst, R.E., Hamilton, M.A., Söderlund, U., Hanes, J.A., Gladkochub, D.P., Okrugin, A.V., Kolotilina, T., Mekhonoshin, A.S., Bleeker, W., LeCheminant, A.N., Buchan, K.L., Chamberlain, K.R., Didenko, A.N., 2016a. Long-lived connection between southern Siberia and northern Laurentia in the Proterozoic. *Nature Geosc.* 9 (6), 464–469.

Ernst, R.E., Okrugin, A.V., Veselovskiy, R.V., Kamo, S.L., Hamilton, M.A., Pavlov, V., Söderlund, U., Chamberlain, K.R., Rogers, C., 2016b. The 1501 Ma Kuonamka Large Igneous Province of northern Siberia: U-Pb geochronology, geochemistry, and links with coeval magmatism on other crustal blocks. *Russ. Geol. Geoph.* 57, 653–671.

Gladkochub, D.P., Stanevich, A.M., Travin, A.V., Mazukabzov, A.M., Konstantinov, K.M., Yudin, D.S., Kornilova, T.A., 2009. The Mesoproterozoic Udzha paleorift (northern Siberian craton): New data on age of basites, stratigraphy, and microphytology. *Doklady Earth Sci.* 425A (3), 371–377.

Gladkochub, D.P., Pisarevsky, S.A., Ernst, R., Donskaya, T.V., Söderlund, U., Mazukabzov, A.M., Hanes, J., 2010. Large igneous province of about 1750 Ma in the Siberian craton. *Doklady Earth Sci.* 430 (2), 168–171.

Gladkochub, D.P., Donskaya, T.V., Mazukabzov, A.M., Pisarevsky, S.A., Ernst, R.E., Stanevich, A.M., 2016. The Mesoproterozoic mantle plume beneath the northern part of the Siberian craton. *Russ. Geol. Geoph.* 57, 671–685.

Gladkochub, D.P., Donskaya, T.V., Pisarevsky, S.A., Salnikova, E.B., Mazukabzov, A.M., Kotov, A.B., Motova, Z.L., Stepanova, A.V., Kovach, V.P., 2021. Evidence of the latest Paleoproterozoic (~1615 Ma) mafic magmatism the southern Siberia: extensional environments in Nuna supercontinent. *Precamb. Res.* 354, 106049.

Gladkochub, D.P., Donskaya, T.V., Pisarevsky, S.A., Ernst, R.E., Söderlund, U., Kotov, A.B., Kovach, V.P., Okrugin, A.V., 2022. 1.79–1.75 Ga mafic magmatism of the Siberian craton and late Paleoproterozoic paleogeography. *Precamb. Res.* 370, 106557.

Gladkochub, D.P., Donskaya, T.V., Pisarevsky, S.A., Kotov, A.B., Salnikova, E.B., Mekhonoshin, A.S., Sklyarov, E.V., Demonterova, E.I., Mazukabzov, A.M., Stepanova, A.V., Konstantinov, K.M., 2023. Mesoproterozoic (ca. 1.26 Ga) Srednecheremshansk mafic-ultramafic intrusion in the southern Siberia: Signature of the Mackenzie event in Siberia. *Precamb. Res.* 390, 107038.

Malyshev, S.V., Pasenko, A.M., Ivanov, A.V., Gladkochub, D.P., Savatenkov, V.M., Meffre, S., Abersteiner, A., Kamenetsky, V.S., 2018. Geodynamic significance of the Mesoproterozoic magmatism of the Udzha paleo-rift (northern Siberian craton) based on U-Pb geochronology and paleomagnetic data. *Minerals* 8, 555.

Malyshev, S.V., Ivanov, A.V., Khudoley, A.K., Marfin, A.E., Kamenetsky, V.S., Kamenetsky, M.B., Lebedeva, O.Yu., 2021. Global implication of Mesoproterozoic (~1.4 Ga) magmatism within the Sette-Daban Range (Southeast Siberia). *Scientific Reports* 11, 20484.

McClelland, S.J., 2013. *The Geochemical Study of 1750 Ma Siberian Dykes. A thesis of the degree of Bachelor of Science. Department of Earth Sciences, Carleton University, Ottawa.*

Pisarevsky, S.A., Gladkochub, D.P., Donskaya, T.V., 2021. Precambrian paleogeography of Siberia, in: Pesonen, L.J., et al., eds., *Ancient Supercontinents and the Paleogeography of the Earth*, Chapter 8: Amsterdam, Elsevier, pp. 263–275.

Wingate, M.T.D., Pisarevsky, S.A., Gladkochub, D.P., Donskaya, T.V., Konstantinov, K.M., Mazukabzov, A.M., Stanevich, A.M., 2009. Geochronology and paleomagnetism of mafic igneous rocks in the Olenek Uplift, northern Siberia: implications for Mesoproterozoic supercontinents and paleogeography. *Precamb. Res.* 170, 256–266.

Geochemical and mineralogical characterization of gold distribution in Bou Azzer El Graara – Inlier, for forecasting of its processing and environmental impact, Central Anti-Atlas, Morocco

M. EL GHORFI¹⁻², L. MAACHA³, A. EL GHALI², H. EL BILALI⁴, R. ERNST⁴, H. IBOUH¹ AND T. OBERTHÜR⁵

1 Lab. Geo-Resources, Geo-Environment and Civil Engineering, Faculty of Sciences and Technology, Cadi Ayyad University, Bd A. Elkhattabi, BP549, Marrakesh, Morocco

2 Geology and Sustainable Mining Institute (UM6P/GSMI), Mohammad VI Polytechnic University, Lot 660. Hay Moulay Rachid, 43150, Ben Guerir, Morocco

3 Group Managen, Twin Center Tour A – Angle Bd.Zerktoni & Massira Khadra BP. 5199 – Casa Blanca , Morocco.

4 Carleton University, 2115 D Herzberg Building, 1125 Colonel By Drive, Ottawa, ON K1S 5B6

5 Federal Institute for Geosciences and Natural Resources, Stilleweg 2, 30655 Hannover, Germany

email: m.elghorfi@uca.ac.ma

The cobalt ores of Bou Azzer are associated with the Precambrian green stone belt along the southern Moroccan Atlasic fault. It was mined from 1930 and has yielded 70000 t Co and 5 t of Gold. Currently, Managem has annual production capacity 2500 t metal Co 10000 t As, 300 t metal Ni and 250 kg gold. The cobaltiferous mineralization occurs in the form of lodes and pockets at the contact of serpentinites and quartz-diorite, mainly consists of arsenides, sulfarsenides of [Co-Ni-Fe] and sulphides. Gangue minerals are quartz, calcite, dolomite, chlorite, and rutile.

Samples from surface, drill core, and underground workings in operating mines (up -640 m) were analyzed by Actlabs, using ICP-OEM and NiS fire assay-INAA methods. At BGR in Germany and UM6P/GSMI Morocco, light and SEM Mineral Liberation Analysis (MLA) using automated mineralogy system (TIMA), and electron microprobe analysis (EPMA) of selected minerals were performed. Gold and all mineral phases were analysed using (EPMA) and X-ray chemical distribution maps were completed.

Whole rock analyses of ore samples from different mining sites of the Bou Azzer district show that gold is irregularly distributed in the ores (0.5-49 g/t Au). However, maximum contents of Ag, Pt and Pd are successively 338 g/t Ag, 43 mg/t Pt and 45.2 mg/t Pd, while gold contents are between 0.5 and 50 g/t. deep investigation based on SEM, and EPMA approved that the ores of the western part of the district, show native gold inclusions with varying size from 5 to 50µm, those inclusions are found in skutterudite, cobaltite, gersdorffite, rammelsbergite, chalcopyrite, and molybdenite associated with brannerite-uraninite. In ores of the eastern part (F51-F53-F56), two types of gold are observed: (i) Primary gold with size varying from 2 to 15 µm, associated to niccolite and rammelsbergite, (ii) abundant free grains of gold (5–50 µm) occurs with (oxides-chlorite) disseminated in listwaenite rock; this gold is probably related to a late remobilisation phase along fracture zones. Gold analyses in EPMA show a wide range of compositions [7-83.78 wt.% Ag] and up to 8.03 wt.% Hg.

Physical volcanology and geochemistry of the Oued El Maleh ridge basaltic pile (Middle Atlas, Morocco)

Hind El Hachimi¹, Abedlilah Fekkak¹, Abdellatif Jouhari¹, Nasrddine Youbi², Said Haidatte¹, Mina Bouhsis¹.

¹Geology Department, Faculty of Sciences, Chouaib Doukkali University, 24000, El Jadida, Morocco. e-mail: elhachimi.h@ucd.ac.ma

²Geology Department, Faculty of Sciences-Semlalia, Cadi Ayyad University, Prince MoulayAbdellah Boulevard, P.O. Box 2390, Marrakech, Morocco, e-mail: youbi@uca.ac.ma

The Central Atlantic Magmatic Province (CAMP) is a large igneous province (LIP) covering an area in excess of 10 million km² with an estimated total volume of more than 3 million km³ (Marzoli et al., 2018, 2019). It is composed of mafic dykes, sills, layered intrusions and lava flows in the four continents surrounding the Atlantic Ocean. One of the oldest and best-preserved sub-provinces of the CAMP is located in Morocco. This work aims to study the morphology, internal architecture and geochemistry of the Central Atlantic Magmatic Province (CAMP) of the Oued El Maleh ridge in the Middle Atlas.

The Oued El Maleh ridge is located in the central part of the folded Middle Atlas (Morocco), limited by the village of Boulemane to the North East, Timahdite to the West, Achlouj to the South and Ait Hamza to the East part. Despite the disturbance of the original basaltic pile by tectonics, three volcanic formations were identified based on volcanological and geochemical data. The three formations are conventionally designated by the terms "Lower Formation, Intermediate Formation, and Upper Formation" and correspond to three volcanic episodes. These are geochemically correlative to the Lower, Intermediate and Upper Formations of the Moroccan High Atlas, where the sequence is the most complete. According to Walker's (1971) nomenclature and on the basis of volcanological criteria (the vesiculation pattern, the jointing style, the petrographic texture), it is established that the CAMP flows of Oued El Maleh Ridge can be grouped into compound pahoehoe flows and simple flows. However, it is not rare to observe lava flows of intermediate type between the pahoehoe and aa, such as lava flows with a "flow top breccia" based on the Keszthelyi's (2002) classification.

Although some elements have been mobilized by alteration processes (LOI from 2.2 to 4.7 wt%), the tholeiitic affinity of all the analysed lava flows from the study area is attested by the immobile elements: low TiO₂ (1.01–1.42 wt%) and P₂O₅ (1.97–2.57 wt%) contents; high Zr/P₂O₅ (915.55–1050) and Y/Nb (1.88–4.35) ratios. The observed geochemical variations between the three formations could be explained by a limited crustal assimilation. Source mineralogy and degree of melting are probably the main components responsible for the observed difference in REE ratios. The magmas of the three formations of the Oued El Maleh ridge cannot be affected by closed system fractional crystallization processes, but probably request parent magmas or crustal assimilation processes.

Sr-Nd-Pb isotope ratios in the CAMP formations from the Oued El Maleh ridge have fairly homogeneous compositions and show high similarities to other CAMP sub-provinces. These ratios indicate that the basaltic magmas were compositionally enriched relative to the mid-ocean ridge basalts and yet differed in composition from the Atlantic Ocean Island basalts and suggest a significant enrichment of the mantle-source regions by subducted crustal components.

References

- Keszthelyi, L., 2002. Classification of the mafic lava flows from OPD Leg 183. In: FREY, F.A., Coffin, M.F., Wallace, P.J. & Quality, P.G. (eds.), *Proceedings of the Ocean Drilling Program. Scientific Results*, 183, 1-28.
- Hofmann, A.W., White, W.M., 1982. Mantle plumes from ancient oceanic crust. *Earth Planet. Sci. Lett.* 57, 421–436.

Marzoli, A., Bertrand H., Youbi, N., Callegaro, S., Merle, R., Reisberg, L., Chiaradia, M., Brownlee, S., Jourdan, F., Zanetti, A., Davies, J., Cuppone, T., Mahmoudi, A. Medina, F., Renne, P. R. , Bellieni, G., Crivellari, S., El Hachimi, H., Bensalah, M. K., Meyzen C. M., Tegner, C. (2019). *The Central Atlantic Magmatic Province (CAMP) in Morocco*. *Journal of Petrology*, 60(5), 945–996. doi: 10.1093/petrology/egz021

Marzoli, A., Callegaro, S., Dal Corso, J., Davies, J. H. F. L., Chiaradia, M., Youbi, N., Bertrand, H., Reisberg, L., Merle, R. & Jourdan, F. (2018). *The Central Atlantic Magmatic Province (CAMP): A review*. In: Tanner, L. H. (ed.) *The Late Triassic World. Topics in Geobiology* 46. Heidelberg: Springer, pp. 91–125.

Walker, G.P.L., 1971. *Compound and simple lava flows and flood basalts*. *Bulletin Volcanologique*, 35, 579–590.

Ediacaran biota from Ougnat Massif (Eastern Anti-Atlas, Morocco): Paleoenvironmental and stratigraphic constraints

Jamal El Kabouri¹, Ezzoura Errami^{1,2}, Bruno Becker-Kerber³, Nasser Ennih¹, Ulf Linnemann⁴, Clémentine Fellah⁵, Antoine Triantafyllou⁵, Youbi Nasrddine^{6,7}

¹:Faculté des Sciences, Université Chouaib Doukkali, EGGPG, B.P. 20, 24000, El Jadida, Morocco

²:Faculté Polydisciplinaire de Safi, Université Cadi Ayyad, Got, B.P. 4162, 46 000, Safi, Morocco

³:Brazilian Synchrotron Light Laboratory (LNLS), Brazilian Center for Research in Energy and Materials (CNPEM), 13083-970, Campinas, Sao Paulo, Brazil

⁴:Senckenberg Naturhistorische Sammlungen Dresden, Museum für Mineralogie und Geologie, GeoPlasmaLab, Königsbücker Landstraße 159, D-01109, Dresden, Germany

⁵:Lyon Geology laboratory - Earth, Planets and Environment (LGL-TPE), Université Lyon 1, ENS de Lyon, CNRS, UMR, 5276, Villeurbanne, France

⁶:Department of Geology, Faculty of Sciences Semlalia, Cadi Ayyad University, Prince Moulay Abdellah Boulevard, P.O. Box 2390, Marrakech, Morocco

⁷: Faculty of Geology and Geography, Tomsk State University, 36 Lenin Ave, Tomsk 634050, Russia.

The Ediacaran period records the appearance of the first multicellular and complex organisms in Earth's history (Knoll et al., 2006; Narbonne et al., 2012). However, the West African Craton (WAC) is commonly regarded as one of the cratons where the Ediacaran biota (metazoans and microfossils) is still poorly documented. Within the West African Craton just a few simple discoidal structures have been previously reported within the supposed Ediacaran successions.

Here, we describe for the first time a slightly diversified Ediacaran assemblage of micro- and macrofossils from Ediacaran volcano-sedimentary rocks of Northwest Africa. Fossils occur in shallow water carbonate-bearing siliciclastic sediments of the Izelf Formation (567–550 Ma), in the Moroccan Anti-Atlas. Macrofossils are represented by *Aspidella*, ivesheadiomorphs and other problematic structures with putative biotic origin. The macrofossil assemblage is dominated by taphomorphs that indicate different degrees of preservation due to progressive decaying processes, possibly extending the effacement preservation mode outside of Avalonia assemblages. Microbially induced sedimentary structures (MISS), stromatolites and spheroidal microfossils are also reported. In particular, spheroidal microfossils may occur as isolated individuals or as concatenated spheres with potentially cell-division processes and were preserved through carbonate and silica permineralization. Morphologically, spheroidal microfossils are compared to sphaeromorph acritarchs and sulfur-oxidizing bacteria such as genus *Thiomargarita*.

The depositional environment and age interval provide new information concerning paleogeographic and paleoenvironmental conditions of Ediacaran biota living on the West African Craton; thus, fills a gap in the Precambrian fossil record from the WAC.

References.

Knoll, A.H., Wornle, S., Kah, L.C., 2013. Covariance of microfossil assemblages and microbialite textures across an upper Mesoproterozoic carbonate platform. *Palaios* 28 (7), 453–470.

Narbonne, G.M., Xiao, S., Shields, G.A., Gehling, J.G., 2012. The Ediacaran Period. *The geologic time scale 1*, 413–435.

DYKE AND CANALI HISTORY OF ITUANA CORONA REGION, LLORONA PLANITIA, VENUS.

K. Eloualda¹, H. El Bilali^{2,3}, R.E. Ernst^{2,3}, K.L. Buchan⁴, N. Youbi¹.

¹Department of Geology, Faculty of Sciences-Semlalia, Cadi Ayyad University, Marrakesh, Morocco;

²Department of Earth Sciences, Carleton University, Ottawa, Ontario, Canada;

³Faculty of Geology and Geography, Tomsk State University, Tomsk, Russia, ⁴273 Fifth Ave., Ottawa, Canada.

Introduction: Ituana Corona (centred at 19.5 N, 153.5 E) is a prominent feature in eastern Llorona Planitia, Venus, with a rim diameter of about 150-200 km. Extensive flows extend more than 700 km from the centre, and channelized flows are interpreted to radiate outward from the raised rim of the corona. Most of the features associated with Ituana Corona are located in northwestern Quadrangle V-25 (Young and Hansen, 2003), but portions of it are also present in northeastern Quadrangle V-24 [2] and southwestern Quadrangle V-13 [3].

Research Goals: Previous mapping in Quadrangles V-25, V24, V-13 was at a scale 1:5,000,000 (Young and Hansen, 2003; Ivanov and Head, 2005; Lang and Hansen, 2010). In this research we aim to produce a much more detailed map (1:500,000) of the graben-fissure systems and lava flows in order to develop a detailed geological history of this impressive corona.

Herein, we report on graben-fissure mapping (which we interpret as overlying mafic dykes). A total of 11,276 graben-fissure lineaments have been mapped in the study area, and grouped into radiating, circumferential, and linear swarms.

Methods: Full resolution (up to 75 m/pixel) right-and left-looking Synthetic Aperture Radar (SAR) images obtained by the Magellan spacecraft were downloaded from the Planetary Data System (PDS). The ArcGIS software suite was used to trace the graben-fissure systems and other features. Detailed linework is shown in Figure 1 and generalized in Figure 2.

Dyke Swarms: The graben-fissure systems are interpreted to overlie dykes and define two circumferential and one radiating system (Figs. 1, 2). In addition, two major linear systems (interpreted as swarms) have been identified in the area, trending NE and SW (Figs. 1,2)

Ituana Circumferential Swarm(s): Circumferential graben are associated with Ituana Corona's raised rim and with a broad area west of the corona rim. In detail, the graben define two overlapping circumferential dyke swarms, a smaller eastern (reddish-brown) swarm, and a larger western (red) swarm that extends west of the raised corona rim (Fig. 2; enlarged in Fig. 3). The centres of the circumferential swarms are located ~65 km apart. Extensive flooding by lava appears to have obscured parts of the circumferential systems.

Ituana Radiating Swarm: A graben-fissure system (light blue) radiates from the southwestern edge of the western circumferential swarm, extending out about 300 km from the centre (Figs. 2,3). It is very sparse on the northern and eastern side, perhaps because of the extensive distribution of late lava flows. In addition, there is a localized, radiating wrinkle ridge system on the west side (dark blue lines) of the corona.

Linear NE-Trending Swarm: An extensive NE-trending graben-fissure set (greenish-blue) extends across much of the map area (Fig. 2), and is likely linked to a magmatic centre (as yet unidentified) outside the map area. The swarm is especially dense on the Oya-Dorsa ridge system.

Linear NW-Trending swarm: An extensive NW-trending graben-fissure set (black) extends across the map area (Fig. 2), and is likely linked to a magmatic centre (as yet unidentified) outside the map area.

Channelized flows associated with Ituana corona: We have mapped in detail channelized flows (Baker et al., 2015), which radiate away from Ituana Corona (Fig. 3; see discussion in Young and Hansen (2003)). In general, the flows run downslope away from the corona rim. There is a spatial relationship between the channelized flows and the circumferential graben swarm on the NW side of Ituana Corona and possibly on the SE side. This suggests that these channelized flows may be fed from the circumferential graben overlying dykes. Lava flows from circumferential graben of coroneae have been reported in other studies (Sanchez et al., 2020).

Canali: Long canali channels (Baker et al., 2015) that have been reported in earlier studies (e.g., (Young and Hansen, 2003)) occur in several parts of the study area. They are mapped (in purple) in Figure 2, and include Martuv, Jutrzenka, Ikhwesi, and Tai-pe canali.

Ituana Lava Flows: Extensive flows radiate in all directions from the centre of Ituana Corona. We are currently mapping these in detail (1:500,000) in order to determine their sources, their relationship with the channelized flows, and their relationship to cycles of filling and emptying of the central corona depression.

Shield volcanoes: There is a concentration of shield volcanoes (yellow dots) within and in the vicinity of Ituana Corona (Figs. 2,3). They are also abundant to the west and east of the corona (Young and Hansen, 2003).

References:

Baker V. R. et al. (2015) *Geomorphology (Amst)*, 245, 149-182.
 Ivanov, M.A., Head, J.W. (2005) *USGS Sci. Invest. Map 2870 with pamphlet*.
 Lang, N.P., Hansen, V.L. (2010). *USGS Sci. Invest. Map 3089 with pamphlet*.
 Sanchez J.C. et al (2020) *LPSC 52*, 2548.
 Young, D.A., Hansen, V.L. (2003) *USGS Geol. Invest. Series I-2783*.

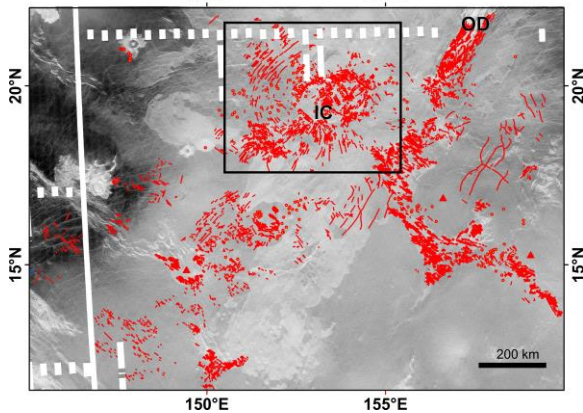


Figure 1: Study area with detailed mapping of graben-fissure systems (11,276 graben-fissure lineaments mapped). Box locates Fig. 3. IC = centre of Ituana corona. OD – Oya Dorsa.

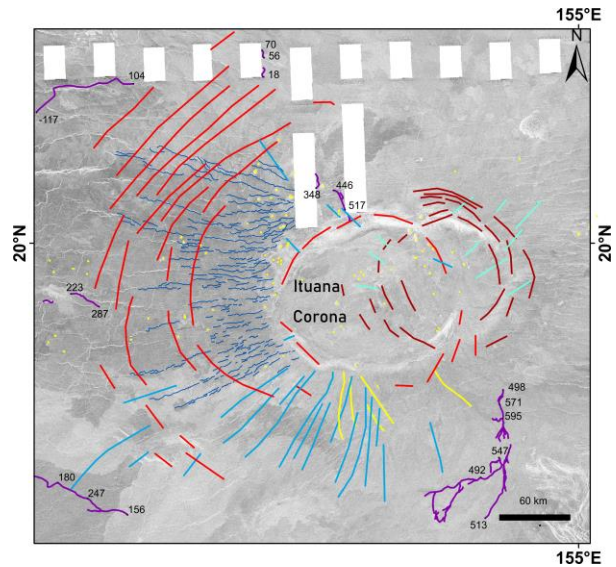


Figure 3. Enlargement of the Ituana corona area, showing generalized graben-fissure systems (dyke swarms). Fanning dark blue lineaments are wrinkle ridges. Numbers are elevations along channelized flows.

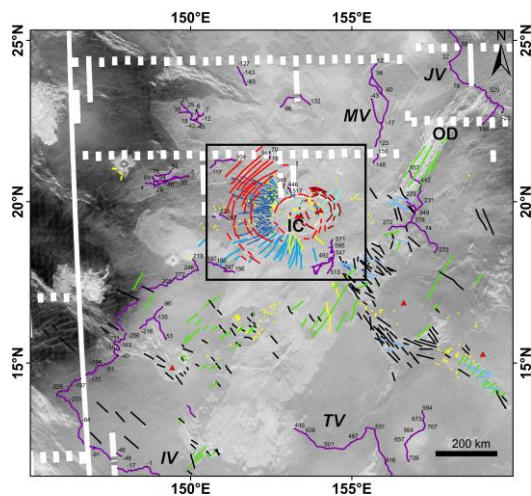


Figure 2. Generalized linework with different colours for different inferred dyke swarms. Fanning distribution of wrinkle ridges (dark blue) is located west of IC. Channelized flows and canali are in purple, and numbers give elevations at points along these features. Canali are labelled: MV = Martuv, JV = Jutrzenka, IV = Ikhwesi, and TV = Tai-pe. Other labels: IC = Ituana corona, and OD = Oya Dorsa. Box shows location of Figure 3.

Irkutsk Large Igneous Province (725–710 Ma) as a signature of the Franklin event in Siberia

Dmitrii Gladkochub¹, Tatiana Donskaya¹, Richard Ernst^{2,3}, Sergei Pisarevsky⁴

¹: Institute of the Earth's Crust, Siberian Branch of the Russian Academy of Sciences, Irkutsk, Russia

²: Department of Earth Sciences, Carleton University, Ottawa, Ontario, Canada

³: Faculty of Geology and Geography, Tomsk State University, Tomsk, Siberia, Russia

⁴: Earth Dynamics Research Group, The Institute for Geoscience Research (TIGeR), School of Earth and Planetary Sciences, Curtin University, WA, Australia

The ~720 Ma Franklin Large Igneous Province (LIP) in North America includes numerous dyke swarms and sill complexes, which are located on an area of more than 3 million km² mainly in northern Canada and northwestern Greenland (Ernst et al., 2016). Traditionally, it is believed, that this magmatic event records a global rifting associated with the breakup of Rodinia. Several ~730–710 Ma mafic complexes within the marginal regions of the western and southern flanks of Siberian craton and in the same adjacent terranes of the Central Asian Orogenic Belt (CAOB) could be also caused by the Franklin event.

These complexes (listed below) are exposed over a huge territory.

1. Igarka Uplift (NW margin of the Siberian craton): the ~715 Ma mafic volcanites with geochemical characteristics of intraplate basalts (Kochnev et al., 2022).

2. Yenisei Ridge (SW margin of the Siberian craton): the 725–710 Ma rift-related magmatic formations are represented by a wide range of igneous rocks from granitoids and felsic A-type volcanites to basalts with typical intraplate geochemical characteristics and carbonatites (Nozhkin et al., 2008; Likhanov, Santosh, 2019 etc.).

3. Sayan-Baikal dyke belt (S–SW margin of the Siberian craton): Neoproterozoic dolerites are widely distributed within the marginal salients of the Siberian craton basement, forming dyke swarms so-called as Biryusa, Sharyzhalgay, Goloustnaya and Baikal.

3.1. The 718±6 Ma (U-Pb zircon) Biryusa dyke swarm (Romanov et al., 2021) is represented by numerous dolerite sills and dykes produced by contamination of the mantle source material with continental crust (Gladkochub et al., 2006, 2007).

3.2. The Sharyzhalgai swarm U-Pb combines dolerite dykes exposed in three areas: Kitoy, Circum-Baikal and Listvyanka. The Kitoy dolerites could have been formed by melting of a mantle source similar in composition to the basalts of oceanic plateaus with the addition of subcontinental lithospheric mantle material. The original mafic melts of dolerite dykes of the Circum-Baikal and Listvyanka sites were formed as a result of contamination of the mantle source with crustal material.

3.3. Neoproterozoic dolerite dykes are found in the Goloustnaya area, their geochemical characteristics indicate formation due to melting of the subcontinental lithospheric mantle enriched with subduction components.

3.4. Ca. 715 Ma (U-Pb, baddeleyite) Baikal dyke swarm, located in the central part of the Baikal basement salient of the Siberian craton. These dolerites were formed by melting of a mixture of the mantle-like component of oceanic plateaus and subcontinental lithospheric mantle. An addition of continental crust material to the mantle source is suggested for some dykes.

Coeval analogues of the Franklin event are also present in the CAOB terranes adjacent to the southern margin of the Siberian craton. In particular, the 730–710 Ma mafic complexes include the massifs of the Kingash intrusive complex of the Kan terrane (Ernst et al., 2016), the Tartai massif of the Alkhadyr terrane (Polyakov et al., 2013), the Dovyren intrusive complex, including the Yoko-Dovyren massif of the Olokit terrane (Ariskin et al., 2013). The major difference between these CAOB intrusions and the coeval mafic intrusions of the marginal parts of the Siberian craton is the enrichment of the CAOB mafic intrusions with PGE, Cu and Ni, which made it possible to unite the CAOB mafic complexes into the East Siberian Metallogenic Province (Polyakov et al., 2013).

Thus, we could suggest that mafic complexes coeval to the Franklin extension event are widely represented both within the Siberian craton and in the adjacent CAOB terranes. These rocks demonstrate wide variations in petrochemical, geochemical and isotopic characteristics and cannot be characterized by a single universal set of geochemical features.

Paleomagnetic data obtained for mafic intrusions of the Siberian craton allowed us to propose paleogeographic reconstructions with close spatial position of the southern flank of the Siberian craton and the north of Laurentia in the structure of Rodinia supercontinent (Pisarevsky et al., 2013; Evans, 2021).

However, the absence of reliable paleomagnetic data from the CAOB terranes hampers their positioning on such reconstructions.

The research was partly supported by grant 23-17-00196 from the Russian Science Foundation and partially supported by Canadian NSERC Grant CRDPJ 523131-17.

Ariskin, A.A., Kostitsyn, Yu.A., Konnikov, E.G., Danyushevsky, L.V., Meffre, S., Nikolaev, G.S., McNeill, A., Kislov, E.V., Orsoev, D.A., 2013. Geochronology of the Dovyren intrusive complex, Northwestern Baikal area, Russia, in the Neoproterozoic. *Geochem. Int.*, 51 (11), 859-875.

Ernst, R.E., Hamilton, M.A., Söderlund, U., Hanes, J.A., Gladkochub, D.P., Okrugin, A.V., Kolotilina, T., Mekhonoshin, A.S., Bleeker, W., LeCheminant, A.N., Buchan, K.L., Chamberlain, K.R., Didenko, A.N., 2016. Long-lived connection between southern Siberia and northern Laurentia in the Proterozoic. *Nature Geosciences* 9 (6), 464–469.

Evans, D.A.D., 2021. Meso-Neoproterozoic Rodinia supercycle, in: Pesonen L.J., Salminen J., Elming S.-Å., Evans D.A.D., Veikkolainen T. (Eds.) *Ancient Supercontinents and the Paleogeography of the Earth*. Amsterdam, Elsevier, Chapter 17, 549–576.

Gladkochub, D.P., Donskaya, T.V., Mazukabzov, A.M., Stanevich, A.M., Sklyarov, E.V., Ponomarchuk, V.A., 2007. Signature of Precambrian extension events in the southern Siberian craton. *Russ. Geol. Geophys.* 48 (1), 17–31.

Gladkochub, D.P., Wingate, M.T.D., Pisarevsky, S.A., Donskaya, T.V., Mazukabzov, A.M., Ponomarchuk, V.A., Stanevich, A.M., 2006. Mafic intrusions in southwestern Siberia and implications for a Neoproterozoic connection with Laurentia. *Precamb. Res.* 147, 260–278.

Kochnev, B.B., Khudoley, A.K., Priyatkin, N.S., Dufrene, S.A., Pokrovsky, B.G., Kuznetsov, A.B., Kaurova, O.K., Marusin, V.V., 2022. Neoproterozoic evolution of the northwestern margin of the Siberian Platform. *Precamb. Res.* 382. Art. No. 106877.

Likhanov, I.I., Santosh, M., 2019. A-type granites in the western margin of the Siberian craton: Implications for breakup of the Precambrian supercontinents Columbia/Nuna and Rodinia. *Precamb. Res.* 328, 128–145.

Nozhkin, A.D., Turkina, O.M., Bayanova, T.B., Berezhnaya, N.G., Larionov, A.N., Postnikov, A.A., Travin, A.V., Ernst, R.E., 2008. Neoproterozoic rift and within-plate magmatism in the Yenisei Ridge: implications for the breakup of Rodinia. *Russ. Geol. Geophys.* 49 (7), 503–519.

Pisarevsky, S.A., Gladkochub, D.P., Konstantinov, K.M., Mazukabzov, A.M., Stanevich, A.M., Murphy, J.B., Tait, J.A., Donskaya, T.V., Konstantinov, I.K., 2013. Paleomagnetism of Cryogenian Kitoi mafic dykes in South Siberia: Implications for Neoproterozoic paleogeography. *Precamb. Res.* 231, 372–382.

Polyakov, G.V., Tolstykh, N.D., Mekhonoshin, A.S., Izokh, A.E., Podlipskii, M.Yu., Orsoev, D.A., Kolotilina, T.B., 2013. Ultramafic-mafic igneous complexes of the Precambrian East Siberian metallogenic province (southern framing of the Siberian craton): age, composition, origin, and ore potential. *Russ. Geol. Geophys.* 54, 1319–1331.

Romanov, M., Sovetov, Ju.K., Vernikovskiy, V.A., Rosenbaum, G., Wilde, S.A., Vernikovskaya, A.E., Matushkin, N.Yu., Kadilnikov, P.I., 2021. Late Neoproterozoic evolution of the southwestern margin of the Siberian craton: evidence from sedimentology, geochronology and detrital zircon analysis. *Int. Geol. Review* 63 (13), 1658–1681.

Ca. 2580-2574 Ma mafic magmatism in the Zimbabwe and Kaapvaal cratons: implications for their amalgamation along the Limpopo Belt

Ashley Gumsley¹, Michiel de Kock², Martin Klausen³, Emilie Larsson⁴, Beata Marciniak-Maliszewska⁵, Dominika Niezabitowska⁶, Johan Rådman⁴, Ulf Söderlund⁴, Tomasz Krzykawski¹

¹: Institute of Earth Science, University of Silesia in Katowice, Sosnowiec, Poland

²: Department of Geology, University of Johannesburg, Johannesburg, South Africa

³: Stellenbosch University, Stellenbosch, South Africa

⁴: Department of Geology, Lund University, Lund, Sweden

⁵: Faculty of Geology, University of Warsaw, Warsaw, Poland

⁶: Institute of Geophysics, Polish Academy of Science, Warsaw, Poland

The timing of the amalgamation of the Zimbabwe and Kaapvaal cratons in southern Africa along the Limpopo Belt has long been debated. Arguments for this timing range from the Neoproterozoic through to the Paleoproterozoic. Most arguments are interpreted through the timing of metamorphic events and deformational history within the Limpopo Belt itself and usually suggest a Neoproterozoic origin for amalgamation (e.g., Zeh and Kirchenbaur, 2022). However, studies utilising the large igneous province (LIP) barcode technique suggest amalgamation either in the Paleoproterozoic based on matches between the Mashonaland Sill Province (LIP) and the ca. 1.9-1.8 Ga LIP events within Kaapvaal (i.e., the Black Range dykes, Waterberg sills, Soutpansberg sills and Soutpansberg lavas (Söderlund et al., 2010). However, paleomagnetic studies of these different mafic magmatic units between Zimbabwe and Kaapvaal have been used to argue for an even later amalgamation (Hanson et al., 2011). Here we present new U-Pb ID-TIMS crystallisation ages on baddeleyite of ca. 2574-2580 Ma from an ENE-trending mafic dyke and a mafic sheet on the southeasternmost region of the Kaapvaal Craton in northern KwaZulu-Natal. These units cut across a ca. 2646 Ma NNE-trending mafic dyke (also dated by U-Pb ID-TIMS on baddeleyite), likely unrelated to the White Mfolozi Dyke Swarm in the region, due to differences in age, geochemistry and orientation. These ca. 2574-2580 Ma ages are coeval with the ca. 2574-2579 Ma Great Dyke of the Zimbabwe Craton, as well as the related Umvimeela and East satellite dykes. Using further petrographic, geochemical, paleomagnetic and rock magnetic studies on these mafic intrusions, we can show that the Kaapvaal Craton and the Zimbabwe Craton did not assemble in the Neoproterozoic along the Limpopo Belt. Instead, it is more likely that the Kaapvaal Craton and Zimbabwe Craton assembled much later, in the Paleoproterozoic, during supercontinent Columbia assembly.

This study acknowledges financial support through a grant from the National Science Centre (Naradowe Centrum Nauki; NCN), Poland (SONATINA 3 grant no. UMO-2019/32/C/ST10/00238).

Reference(s):

Hanson, R.E., Rioux, M., Gose, W.A., Blackburn, T.J., Bowring, S.A., Mukwakwami, J., Jones, D.L., 2011. Paleomagnetic and geochronological evidence for large-scale post-1.88 Ga displacement between the Zimbabwe and Kaapvaal cratons along the Limpopo belt. *Geology*, 39, 487-490.

Söderlund, U., Hofmann, A., Klausen, M.B., Olsson, J.R., Ernst, R.E., Persson, P.-O. 2010. Towards a complete magmatic barcode for the Zimbabwe craton: Baddeleyite U-Pb dating of regional dolerite dyke swarms and sill complexes. *Precambrian Research* 183, 388-398.

Zeh, A., Kirchenbaur, M., 2022. Zircon U-Pb-Hf isotope systematics of Limpopo Belt quartzites and igneous rocks, implications for Kaapvaal – Zimbabwe Craton accretion. *Precambrian Research* 373, 106631.

Geodynamic Significance of The Permian Intermediate and Felsic Dyke Swarms and Sill Complexes from the Western Meseta and the High Atlas (Morocco) based on U-Pb Geochronology and Geochemistry Data.

Hadimi Ismail¹; Mohamed Khalil Bensalah^{1,2}; Nasrddine Youbi¹; Abdelhak Ait Lahna¹; Colombo Celso Gaeta Tassinari³; Oussama Moutbir¹; Moulay Ahmed Boumehti^{1,2}; Miguel Angelo Stipp Basei⁴; Kei Sato³; El Mostafa Aarab¹

¹Department of Geology., Faculty of Sciences-Semlalia, Cadi Ayyad University, Prince Moulay Abdellah Boulevard, P.O. Box 2390, Marrakech, Morocco.

²Instituto Dom Luiz, Faculdade de Ciências, Universidade de Lisboa, 1749-016 Lisboa, Portugal.

³Centro de Pesquisas Geocronológicas (CPGeo), Instituto de Geociências (IG), Universidade de São Paulo- USP, Caixa Postal 11348, CEP 05422-970, São Paulo (SP), Brazil.

⁴Instituto de Geociências (IG), Departamento de Mineralogia e Geotectônica (GMG), Universidade de São Paulo- USP, Rua do Lago, 562 Cidade Universitária 05508-080 São Paulo - SP – Brasil.

A conspicuous dyke swarms of intermediate dykes (microdiorites) and felsic dykes (microgranites) cross-cuts hercynian plutons and paleozoic metasedimentary basement of Rehamna, Jbilets (Western Meseta) and Azegour (High Atlas). The microdiorites dykes dominantly alkaline (presence of kaersutite, $Ti/V = 61-85$; $Zr/Y = 2-12$ and $La/Yb = 15-23$) show also some calco-alkaline characters and are Post-Autunian and ante-Triassic in age on the basis of field observations. They are never observed to cut the lower Permian sedimentary successions. They have a volcanic equivalents in others paleozoic massifs of Morocco and the West of Europe. They are interpreted here as the result of Late to Post-hercynian distensions which occurred during the Upper Permian or Lower Triassic (“second eruptive Permian cycle”) within a continental pre-rifting system in relation to intracontinental rifting preceding the opening of Central Atlantic basin. By contrast, the microgranite dykes by their chemical nature (within-plate/calco-alkaline) and emplacement age (sample SRYN37-1 from Rehamna: 285.4 ± 6.1 Ma, U-Pb on zircon, SIMS method and samples AZB-13: 283.8 ± 2.2 Ma and AZB-2: 272.4 ± 4.0 Ma, U-Pb on zircon, SHRIMP method) are part of the “first Permian calc-alkaline eruptive cycle” that occur largely in the Western Meseta and Western Europe. Both intermediate and felsic dyke swarms and sill complexes from the Western Meseta and the High Atlas belong to the so-called European North West African Magmatic Province (EUNWA or EUNWAMP) (e.g., Doblas et al., 1998; see also Wilson et al., 2004) This Large Igneous Province was emplaced during Carboniferous-Permian times, and three main pulses can be distinguished at ca. 300 Ma, 290-275 Ma, and 250 Ma, and each of these pulses can be considered a separate LIP within the overall EUNWA LIP group. This “compound” LIP has been linked to the gravitational collapse of the previously overthickened and weakened Hercynian (Variscan) orogenic belt (the initial stages of the disruption of the Pangaeon supercontinent). The whole Variscan edifice collapsed through simple-pure shear low-angle extensional detachments during the late Variscan, giving rise to Basin and Range type extensional province in Europe, and northwestern Africa involving major low angle detachment faulting, unroofing of large metamorphic core complexes, and synextensional plutonic bodies, dyke swarms and sill complexes and volcanic successions. Coevally with an extensional scenario, Europe, and northwestern Africa were affected by a complex system of conjugate strike slips faults (NE-SW sinistral and NE-SE dextral) which partially disrupted the Variscan edifice, resulting in new Permo-Carboniferous stress pattern with the principal compressional axis oriented N-S (Arthaud and Matte, 1975; 1977). This episode was accompanied by sediment deposition and volcanism in transtensional and pull-apart basins (Youbi et al., 1995; Doblas et al., 1998). This episode resulted from dextral transcurrent movement along an intracontinental zone located between Gondwana and Laurussia an early proposal of Van Hilten (1964) later reinterpreted by Arthaud and Matte (1975; 1977).

References

Arthaud F. & Matte P. (1977). Late Paleozoic strike-slip faulting in southern Europe and northern Africa result of a right-lateral shear zone between the Appalachians and Urals. *Geological Society of America Bulletin*, v. 88, pp. 1305-1320.

- Arthaud, F., & Matte, P. (1975). *Les décrochements tardi-hercyniens du Sud-Ouest de l'Europe. Géométrie et essai de reconstitution des conditions de la déformation. Tectonophysics*, v. 25, pp. 139-171.
- Doblas, M., Lopez-Ruiz, J., Cebria, J.M., Youbi, N., & Degroote, E. (2002). *Mantle insulation beneath the west African craton during the Precambrian-Cambrian transition, Geology*, v. 30, pp. 839-842.
- Van Hilten, D. (1964). *Evaluation of some geotectonic hypotheses by paleomagnetism. Tectonophysics 1 (1)*, pp. 3-71
- Wilson, M., Neumann, E.-R., Davies, G.R., Timmerman, M.J., Heeremans, M., & Larsen, N.T. (2004). *Permo-carboniferous magmatism and rifting in Europe: introduction. In: Wilson, M., Neumann, E.-R., Davies, G.R., Timmerman, M.J., Heeremans, M., & Larsen, B.T. (Eds.), Permo-Carboniferous Magmatism and Rifting in Europe. Geological Society of London, Special Publications*, v. 223, pp. 1–10.
- Youbi, N., Cabanis, B., Chalot-Prat, F. & Cailleux, Y. (1995). *Histoire volcano-tectonique du massif permian de Khenifra (Sud-Est du Maroc Central). Geodynamica Acta.*, v. 8, no. 3, pp.158-172.

NOTT CORONA REGION, ISABELLA QUADRANGLE (V-50), VENUS: DETAILED MAPPING OF GRABEN-FISSURE SYSTEMS IDENTIFIES CRITICAL TARGETS FOR FUTURE MISSIONS.

Hadimi I.¹; El Bilali H.^{2,3}; Ernst R.E.^{2,3}; Youbi N.^{1,3}

¹: Department of Geology, Faculty of Sciences-Semlalia, Cadi Ayyad University, Marrakesh, Morocco; ismail.hadimi@gmail.com,

²: Department of Earth Sciences, Carleton University, Ottawa, Ontario, Canada;

³: Faculty of Geology and Geography, Tomsk State University, Tomsk, Russia.

Coronae are abundant and widely distributed features on Venus and are of critical importance to understanding Venus geological and geodynamic evolution; however, many unanswered questions remain (Grindrod and Hoogenboom, 2006). Detailed geologic mapping at the 1:500,000 scale provides new insights into these features and identifies targets for future observations to help address these outstanding questions (Grindrod and Hoogenboom, 2006). Nott Corona, located within Isabella Quadrangle (V- 50), is 3000 km south of Atla Regio, east of Aditi Dorsa, southwest of Wawalag Planitia and north of Nsomeka Planitia (Fig. 1) Nott Corona has a central depression with dimensions of 110 x 80 km and a depth of about 250 m. Nott Corona has been described in initial reconnaissance mapping of Quadrangle V-50 (e.g., Bleamaster, 2006, 2008), and briefly discussed in Basilevsky et al., (2009). Isabella (175 km diameter) is the second largest impact crater on Venus and has been characterized in detail (Miyamoto and Sasaki, 2000). Abundant magmatic features in the region include Nott and Epon Corona, Libby Patera, Tursa Tholus, as well as multiple graben-fissure systems. We have geologically mapped the Nott corona region in detail (1:500,000 scale) and constructed a geological history that integrates the volcanic features (lava flows and magmatic centres) along with graben fissure systems, producing features that we interpret to be dyke swarms (c.f. Buchan and Ernst, 2021)

Of particular interest are the detailed mapping results for the radiating graben-fissure systems in the region and our grouping of these into several different and distinctive swarms. As seen in Fig. 2(A and B) our mapping reveals the impressive radiating swarm associated with Nott corona and additional centres (Nos. 1 and 2, in Fig.2B), and circumferential swarms associated with Libby Patera and Epona corona, as well as addition linear swarms (e.g. blue, red and brown, in Fig. 2B) whose source is not yet identified, but could belong to major swarms fed from distal magmatic centres outside the study area (currently under investigation). A major outstanding question concerning coronae in general, and our mapped features in detail is the question of confidently distinguishing between purely tectonic structures (graben from uplift and lineaments) and those that might have originated from shallow dike induced deformation forces (for example extension above a shallow dike to induce graben formation). Improved image resolution and significantly enhanced altimetry horizontal and vertical resolution are essential to provide the conclusive evidence to support or modify the radial and concentric dike emplacement process at the major centres identified in Fig. 2B. In addition, significantly improved topographic data should be obtained over Nott Corona in order to improve quantitative modeling of its topographic and geologic evolution to assess the temporal evolution of the central caldera-like structure. Furthermore, ongoing detailed mapping (1: 500 000 scale) of the associate lava flows and their history, is permitting the identification of magmatic sources, but higher-resolution image data is required to confidently assign many of the fissures/graben to a dike-related origin. We have also identified candidate fissure-fed flows from graben (circumferential and radial) and from shallow collapse features (Buchan and Ernst, 2021), and some apparently from circular fractures associated with caldera collapse MacLellan et al., (2021). We are preparing these key targets in the form of thematic lists that can be used in the planning of the international armada of upcoming Venus missions.

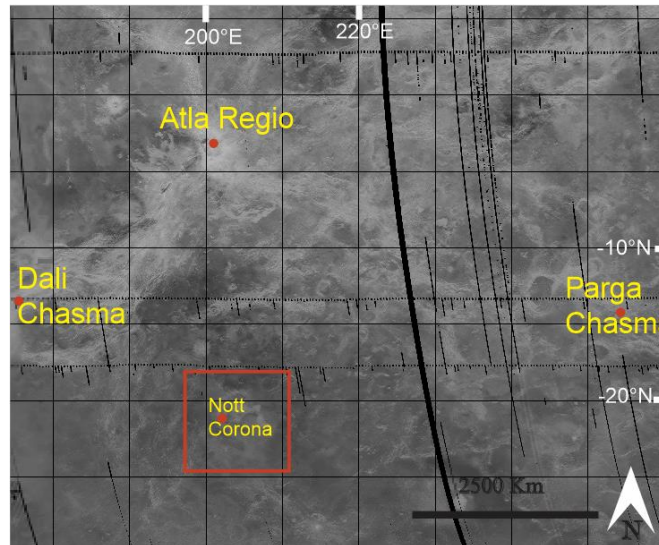


Figure 1: Regional setting of study area.

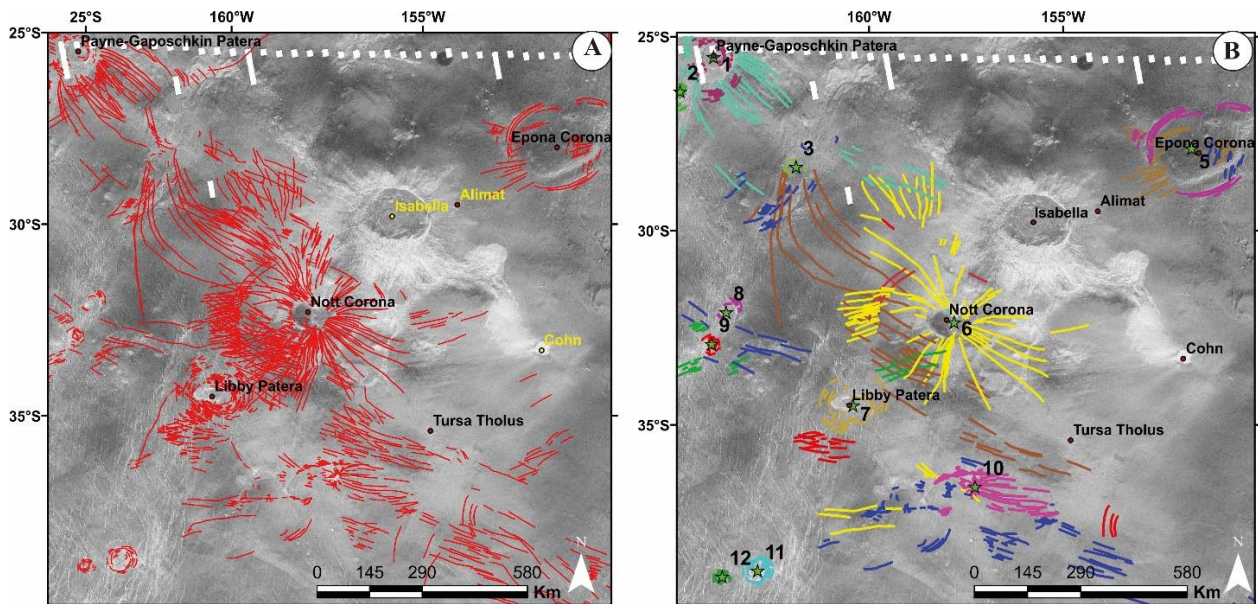


Figure 2: (A) Detailed graben-fissure mapping for parts of the study area. N = Nott Corona, L = Libby Patera, E = Epona Corona, T = Tursa Tholus, U = Unnamed Centre, and I = Isabella Impact Crater. Other impact craters are labelled in yellow font. Background is Cycle 1 Magellan SAR image. NW-trending narrow white rectangular bands indicate missing data. (B) Generalized trends for some sets of grabenfissure lineaments mapped in (A) Colours correspond to different generations of interpreted sets and interpreted to likely overlie dykes (Miyamoto and Sasaki, 2000) . Labels same as in Fig. 1. Background is Left-looking Cycle 1 Magellan SAR image. NW-trending narrow white bands are areas of missing radar data.

References

- Grindrod, P. M. and Hoogenboom, T. (2006) *Astronomy & Geophysics*, 47(3), 3-16.
 Bleamaster L.F. (2006) 37th LPSC, Abstract # 2233.
 Bleamaster L.F. (2008) *Abstr. Ann. Mtg. Planet. Geol. Mappers*.
 Basilevsky A.T., et al. (2009) 40th LPSC, Abstract # 1827.
 Miyamoto H., Sasaki, S. (2000) *Icarus*, 145, 533-545.
 Buchan K.L. and Ernst R.E. (2021). *Gond. Res.*, 100, 25-43.
 MacLellan L.M., et al. (2021). *Earth-Sci. Rev.*, 220. 103619.

Latmikaik Corona Annulus Groove Belts and Katl-Imi Mons, Henie Quadrangle (V-58), Southern Venus

Hall, J.¹, Boggs, K.J.E.¹, Shackman, J.¹, Demorcy, J.¹, Pendleton, C.¹, Chowdhury, M.¹, Bley, H.¹, Varga, E.¹, Dhami, L.¹, Shustova, J.², Ernst, R.^{3,4}, El Balil, H.^{3,4}

¹Department of Earth and Environmental Sciences, Mount Royal University, 4825 Mount Royal Gate SE, Calgary, Alberta, Canada T3E 6K6; ²Department of Geoscience, University of Calgary, 2500 University Drive NW, Calgary, Alberta, Canada T2N 1N4; ³Department of Earth Sciences, Carleton University, 1125 Colonel By Drive, Ottawa, Ontario, Canada K1S 5B6; ⁴Faculty of Geology and Geography, Tomsk State University, 36 Lenin Avenue, Tomsk, Russia 634050.

Introduction: The formation of many tectonomorphic features on Venus, such as tesserae and coronae, are debated. Tesserae are deformed terrain that are thought to be the oldest rocks on Venus. They are characterized by regionally high topography and intersecting lineaments (Bindschadler and Head, 1991). Coronae are large circular to oval-shaped features up to 60-2000km across, bordered by an annulus consisting of densely packed grooves and ridges (Guseva and Ivanov, 2022, Shackman et al, 2023). Mons is the term used to classify topographically raised structures such as volcanos and mountains. This study defines the distribution and density of groove belts within the Latmikaik Corona annulus, and the characteristics of the Katl-Imi Mons.

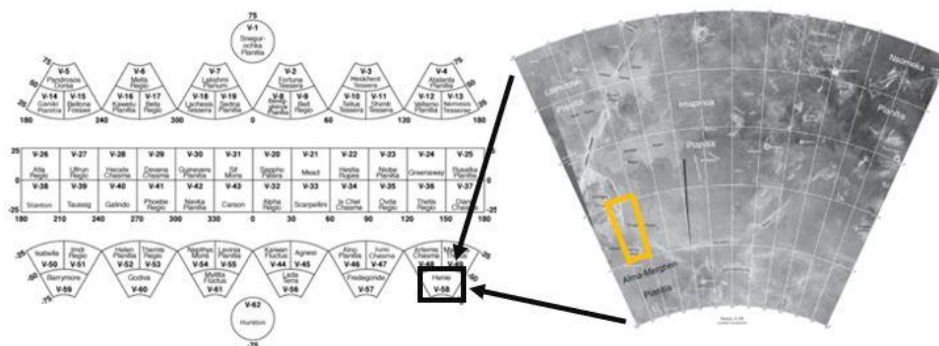


Figure 1: Henie V-58 Quadrangle in southern Venus. Primary study area is outlined in yellow.

Methodology: The Planetary Data System (PDS) was used to download radar image files from the NASA Magellan mission. Geological features were mapped out using ArcGIS, at a scale of 1:500,000.

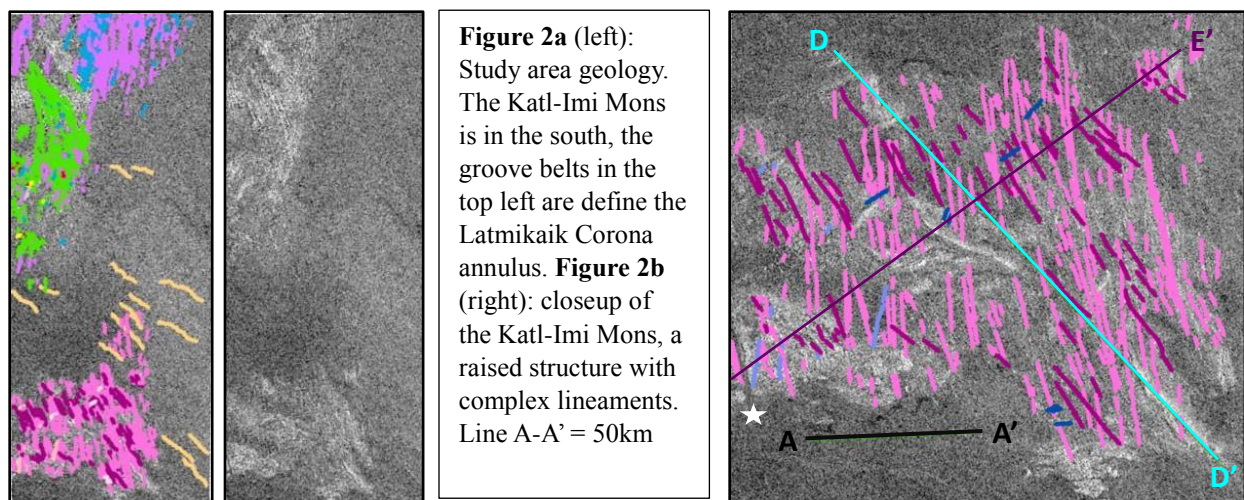


Figure 2a (left): Study area geology. The Katl-Imi Mons is in the south, the groove belts in the top left are define the Latmikaik Corona annulus. **Figure 2b** (right): closeup of the Katl-Imi Mons, a raised structure with complex lineaments. Line A-A' = 50km

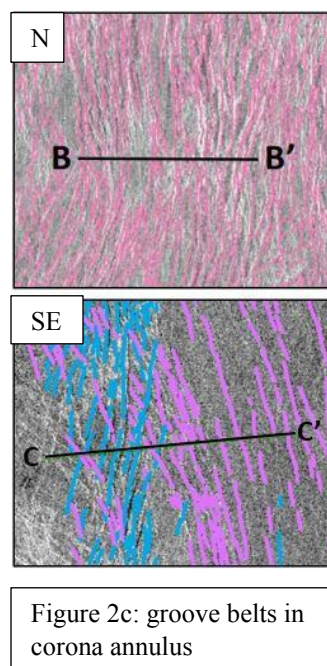


Figure 2c: groove belts in corona annulus

Results: In the N and SE portions of the Latmikaik Corona annulus (Fig. 2c), there is an average of 20-25 grooves per 50 km (lines B-B' and C-C'), spaced between 2-2.5km with no observed master fault (Pendleton and Chowdhury, 2023). South of the Latmikaik Corona, the radar-bright Katl-Imi Mons (Fig. 2b) is crossed by four distinct orientations of lineaments – N-S (bright pink), NE-SW (light blue), NW-SE (dark pink), and E-W (dark blue). A channel-like feature (white star) measuring 26x2km with parallel borders cuts NW-SE across the SW edge of the structure. The topographic profile constructed along lines D-D' and E-E' shows the structure stands topographically high (around ~400m tall), with steep changes in elevation towards the base.

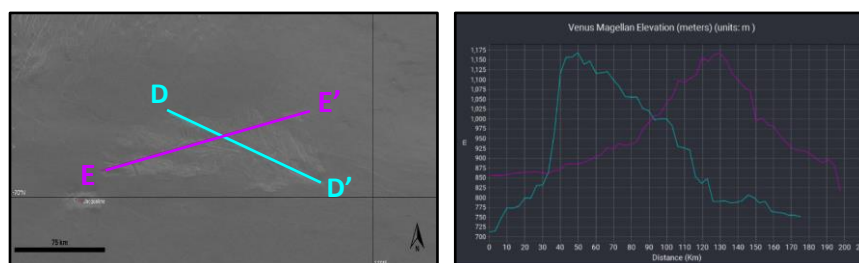


Figure 3: Topographic profile of Katl-Imi Mons. Created using JMARS.

Discussion/Conclusion: Grooves/groove belts were determined to be relatively evenly distributed across the mapped portions of the Latmikaik Corona. A lack of observed master faults related to extensional grooves and grabens suggests a fundamental difference in lithological responses to regional strain on Venus. This could be related to the elevated surface temperatures on Venus. There are at least four orientations of lineaments across the surface of the Katl-Imi Mons that all intersect each other at varying angles. The presence of these dense intersecting lineaments and areas of radar-brightness are characteristic of tessera terrain, and while the structure is of smaller scale than other defined tessera, it could be more correct to call it as such.

Future work: Next steps include a) finishing the mapping of the Henie Quadrangle, b) identifying the possible source(s) for the formation of groove belts, and c) further examination and comparison of the Katl-Imi Mons to other montes and tesserae, as well as further mapping of radar-bright areas and potential other lineament orientations.

Acknowledgements: I would like to thank Dr. Katherine Boggs and the rest of the MRU Venus Mapping Team, for their knowledge, support, and feedback during this project.

References:

- Bindschadler, D. L., and Head, J. W. (1991), Tessera Terrain, Venus: Characterization and models for origin and evolution, *J. Geophys. Res.*, 96(B4), 5889– 5907, doi:10.1029/90JB02742.
- Guseva, E.N., Ivanov, M.A. Coronae of Venus: Geological, Topographic and Morphometric Characteristics. *Sol Syst Res* 56, 76–83 (2022). <https://doi.org/10.1134/S0038094622020046>
- Hanmer, S., 2023, Basic structural geology of Venus: A review of the gaps and how to bridge them: *Earth-Science Reviews*, v. 237, p. 104331, doi:<https://doi.org/10.1016/j.earscirev.2023.104331>.
- Pendleton & Chowdhury, 2023. Venus and Earth: Two Sister Planets with Unique Tectonic Processes. Abstract for MRU Faculty of Science and Technology (FST) Research Day
- Shackman et al, 2023, Geology of the Latmikaik and Xcacau Coronae, Venus, Abstract for LIPs 8 Conference, Marrakesh

DYKE SWARM HISTORY OF EASTERN OVDA REGIO, VENUS

N. Hannour¹, H. El Bilali^{2,3}, R.E. Ernst^{2,3}, K.L. Buchan⁴, N. Youbi¹

¹: Department of Geology, Faculty of Sciences-Semlalia, Cadi Ayyad University, Marrakesh, Morocco\n.hannour.ced@uca.ac.ma

²: Department of Earth Sciences, Carleton University, Ottawa, Ontario, Canada.

³: Faculty of Geology and Geography, Tomsk State University, Tomsk, Russia.

⁴: 2723 Fifth Ave., Ottawa, Ontario, Canada.

Introduction: Tesserae represent ~8% of Venus surface and are characterized by having multiple intersecting sets of tectonic landforms (wrinkle ridges, graben, fractures, folds etc.) which contribute to high radar backscatter; they are also stratigraphically the oldest units and typically have high elevations relative to local plains (e.g., (Ivanov and Head, 1996; Hansen and Willis, 1998; Ivanov & Head, 2015; Gilmore and Head, 2018). Their origin and formation processes remain under debate. A key question is whether they record a short duration geological history (because of crater count ages similar to the post tesserae units) (Ivanov and Head, 2015). There is a possibility that they have a protracted geological history and capture the transition (the proposed Great Climate Transition) from a more habitable climate that may have included oceans and plate tectonics to the current hyper greenhouse conditions with no water cycle and no erosion (e.g., (Khawja et al., 2020; Wayet et al., 2022). Detailed mapping of tesserae can help assess whether a protracted history is present and help characterize that geological and tectonic history.

Overview of dyke swarms in the Eastern Onda: In this study we focus on Eastern Onda Regio, which is characterized by a complex tectonic evolution (e.g., (Dean et al., 2022, 2023; Hansen et al., 1999; Chetty et al., 2010; Romeo and Capote, 2011; Hansen and Lopez, 2018). It includes a large tessera terrain with intra-tessera basins, fracture (shear) zones, fold belts and extensional linear features. The latter type of feature had previously been considered a result of deformation (e.g. Hansen et al., 1999), but we interpret herein as graben overlying dykes (based on the analysis by Hanmer (2020). Our detailed mapping of >100,000 lineaments (*Fig. 1A*) using the full resolution of Magellan SAR images has resulted in the recognition of six distinct graben sets that we interpret to overlie dyke swarms (except possibly for the oldest set (see discussion below). To show the trend patterns more clearly, the line work is generalized in (*Fig. 1B*). The interpreted dyke swarms are widespread on the tessera, but not observed in the surrounding smooth volcanic plains to the north and south, indicating that they were emplaced syn- or post-tessera development, but prior to flooding of the adjacent plains. In the study area, the dense dyke swarms exhibit broadly linear geometries (although future mapping to the north and south of the study area could reveal more complex swarm geometries, such as radiating or circumferential). The different swarms intersect, demonstrating that they are of different ages and not part of a single event. We have also mapped pits and pit chains in association with the dyke swarms.

Detailed mapping of graben sets in the central region of eastern Onda Regio: We have identified six distinct graben sets, whose relative ages are determined from crosscutting relationships. From youngest to oldest they are:

NE-SW (red) grabens (Figs. 1A, B): This set is the most widespread in the study area and is characterized by thin, straight lineaments. The dykes seem to swing slightly in trend, and there is one portion of this trend that seems to slightly converge to the north.

NW-SE (green) grabens (Figs. 1A, B): The set is parallel to blind dykes (based on mapped pit chains).

E-W (dark blue) grabens (Figs. 1A, B): This linear set is restricted to the eastern side of the area, and crosscuts the N-S (light blue) set.

N-S (light blue) grabens (Figs. 1A, B): This set displays minor deformation; some of the graben are 'wiggly' compared to the graben sets discussed above. This set is crosscut by the E-W dark blue set.

NNE (dark purple) grabens (Figs. 1A, B): These grabens are shorter and thinner than the younger grabens previously discussed, which are crossed by the NNW trending light blue colour grabens.

NNW (purple) grabens (Figs. 1A, B): This is the oldest set and is limited to the central region. The grabens are very radar-bright, and are very irregular in trend, which might indicate some minor tectonic deformation and even strike slip movement. Short-wavelength folds that are parallel to this set suggest

contraction of a complex layered crust (I. Romeo, R. Capote. (2011). The NE-trending red graben lines are perpendicular to the folds crests of this set.

Potential Erosion: In some local areas (Fig. 1C), some graben sets appear to be missing. This could reflect erosion of the grabens, or geological or tectonic constraints on the graben set distributions. Further studies are in progress to better understand the full distribution and geometry of the different graben systems that are interpreted as dyke swarms in Eastern Onda Regio.

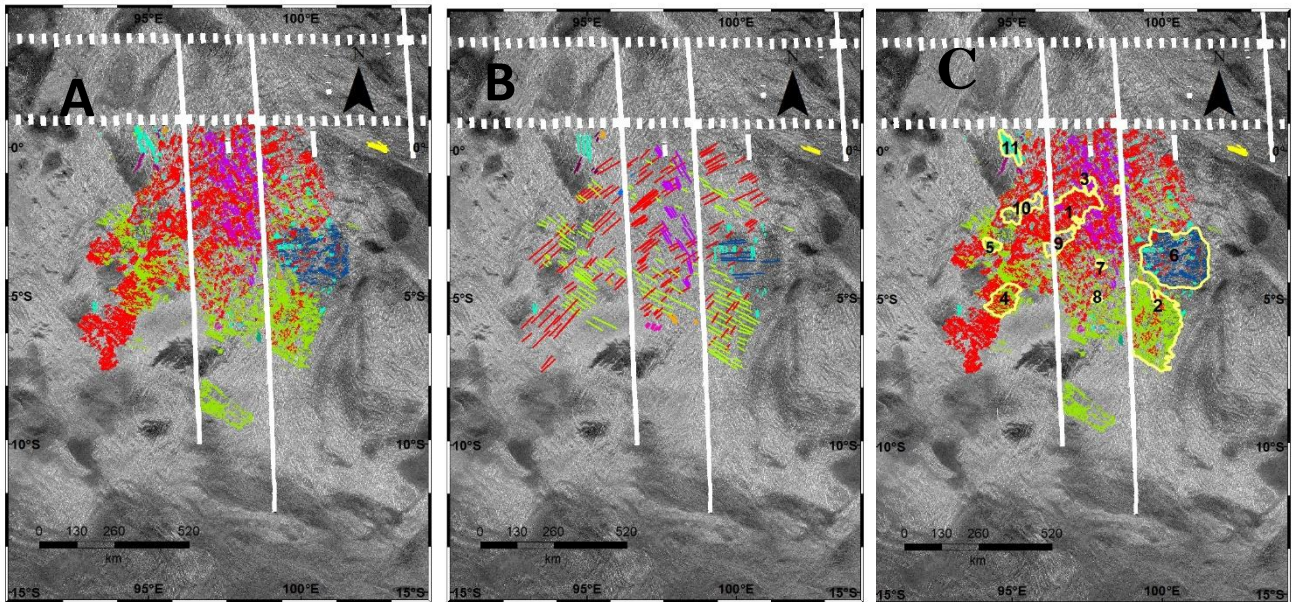


Figure 1: Detailed mapping of graben sets in Eastern Onda Regio. A) Distribution of $>100,000$ graben, distinguished using different colours(B) Generalized trends of the graben sets. (C) Different domains (labelled by number) where there is a dominance of one trend over the other, as well as the areas where there are no grabens, **1** abundance of red set with some purple lineaments, **2** the dominance of green set with a few red lineaments, **3** the oldest set (mapped in purple), **4** the presence of both green and red sets, **5** only green set, **6** dark and light blue sets with some red lines and near absence of green set, **7, 8** the dominance of complicated tectonic structures that are part of the deformation associated with the tessera, **9, 10** absence of lineaments that may represent an erosion process, **11** the dominance of the light blue set.

References:

- Chetty, T.R.K. et al. (2010) *Planet. Space Sci.*, 58, 1286-1297
 Dean, R. et al. 2022, 2023 LPSC abstract (need citation for 2022 and 2023 separately)
 Hanmer, S. (2020) *E. Sci. Rev.* 201, 103077.
 Gilmore, M. & Head, J.W. (2018) *Planet. Space Sci.* 154 (2018) 5–20
 Hansen, V. L., & Willis, J.J. (1998)
 Hansen, V.L. et al. (1999) *Geology*,
 Hansen, V. & Lopez, I. (2018) *JGR* 10.1029/2018 27, 1071-1074 I.
 Romeo, R. Capote. (2011) *Planet. Space Sci.* 59, 1428–1445.
 Ivanov M. & Head J. (1996) *JGR*, 101, 14861-14908 *Icarus* 132, 321–343. *Geology*, 27, 1071-1074.
 Ivanov & Head, (2015) *Planet. Space Sci.* 113-114 10–32.
 Khawja et al. (2020) *Nat. Comm.*, 11, 5789
 Way, M. et al. (2022) *Planet Sci J* 3(4):92

The chronology and distribution of Mesoproterozoic magmatic thermal events in three continental blocks of China (North China, Yangtze and Tarim)

Hongwei Kuang, Yuansheng Geng, Lilin Du, Yongqing Liu
Institute of Geology, Chinese Academy of Geological Sciences

Mesoproterozoic magmatic rocks widely occur in three Chinese blocks of China (North China, South China and Tarim blocks). Based on a large number of geochronologic data, the Mesoproterozoic magmatic events in the North China Block can be divided into five stages (1.78Ga, 1.70Ga, 1.63Ga, 1.32Ga, 1.23Ga), in which 1.78Ga and 1.32Ga magmas have a large influence range and form the large igneous provinces, respectively. The Mesoproterozoic magmatic rocks in the North China Block formed in the intracontinental extensional environment indicating that North China Block was not involved in the assembly process of the Rodinia supercontinent. The Mesoproterozoic magmatic events in the South China Block can be divided into six stages (1.78Ga, 1.72Ga, 1.67Ga, 1.5Ga, 1.42Ga, 1.0Ga), the four stages of magmatic events from 1.78Ga to 1.5Ga were formed in extensional environment. The sporadic 1.4Ga magmatic rocks likely formed in an assembly setting in local area. The magmatic stages around 1.0Ga performed differently in different parts of the South China Block, indicating the different blocks have been aggregated together. The Mesoproterozoic magmatic events in the Tarim block can be subdivided into four stages (1.78Ga, 1.5Ga, 1.43Ga, 1.12Ga). The magmatic events of 1.78Ga and 1.5Ga are only locally distributed, and they formed in the extensional setting. 1.4Ga magmatic events performed differently in the northern and southwestern margins of the Tarim Block, i.e., continental magmatic arc setting in the northern margin and extensional environment in the southwestern margin. ~1.12Ga magmatic events only developed in the southwestern margin of Tarim Block with the characteristics of A2-type granite and in the extensional setting. The difference of magmatic rock assemblages in different locations and stages of the Tarim Block denotes that the Tarim Block originally is not a unified block, but likely assembled by different massifs in different periods. The differential evolutions of the Mesoproterozoic magmatic rocks reveal their independent processes in the North China, South China and Tarim blocks in this period.

This study was supported by the National Key Research and Development Program of China (Grant Nos. 2022YFF0800302, 2016YFC0601001), the China Geological Survey Program (Grant Nos. DD20221649, DD20190005), the National Natural Science Foundation of China (Grant No. 42072135), the Beijing International Innovation and Resource Cooperation Program (Grant No. Z201100008320007).

Key words: Mesoproterozoic magmatism; North China Block; South China Block; Tarim Block; Differential evolution; Tectonic setting

GRABEN-FISSURE SYSTEMS HISTORY OF CORONA ALONG HECATE CHASMATA IN THE VICINITY OF SOBRA FLUCTUS, VENUS.

H. Houane¹; H. El Bilali^{2,3}; R.E. Ernst^{2,3}; J.W. Head⁴; N. Youbi¹

¹: Department of Geology, Faculty of Sciences Semlalia, Cadi Ayyad University, Marrakesh, Morocco
hicham.houane@gmail.com

²: Department of Earth Sciences, Carleton, Ontario, Canada;

³: Faculty of Geography, Tomsk State University, Tomsk, Russia

⁴: Department of Earth, Environmental and Planetary Sciences, Brown University, Providence, RI, USA.

Introduction: Coronae are common tectono-magmatic features on Venus (Stofan et al., 1992; Smrekar and Stofan, 1999; Grindrod and Hoogenboom, 2006; Gülcher et al., 2020). They typically have a quasi-circular/elliptical annulus of graben (or occasionally compressional ridges) with diameters ranging from 60 to 2600 km (mean ~300 km). Recent studies suggest that a terrestrial analogue of corona may be circumferential swarms associated with mantle plumes or diapirs (Buchan and Ernst, 2021).

To improve our understanding of the nature of coronae and their links with rifting, we have been researching an area along Hecate Chasmata near Sorba Fluctus (Fig. 1). Quadrangle scale (1:5,000,000) mapping is available for the eastern half of the study (Stofan et al., 2012), and our goal is more detailed mapping (1:500,000 scale) and interpretation.

Methods: Our approach begins with detailed 1:500,000 scale mapping of graben-fissure lineaments, which are then grouped into sets based on trends, and provisionally interpreted as radiating, circumferential and linear dyke swarms. Radiating and circumferential swarms can be directly associated with magmatic centres. Where we can establish such relationships, we link distal linear swarms to verified magmatic centres outside the study area; remaining abundant long linear segments are linked to rift zone faulting. Geological mapping is being carried out using full-resolution (75 m/pixel) Magellan SAR images and its altimetry data in ArcGIS ArcMap v. 10.8. JMARS (Christensen et al., 2009) is also used for reconnaissance.

Dyke Swarms: Our preliminary detailed mapping of more than 45800 graben-fissure lineaments reveals the occurrence of 9 coronae with circumferential and radiating structures interpreted as the surface deformation associated with the shallow intrusion of dyke swarms (Fig. 2), an interpretation strengthened by the observed co-existence of lava flows emanating from graben and fissures. The generalized map of the interpreted dyke swarms of the region and their associated magmatic centres is shown in Figure 3. The northern part of the study area belongs to a WSW-ENE trending segment of the Hecate chasmata rift system, along which multiple coronae (7-9 in Fig. 3) are aligned. Figures 4 and 5 provide an enlarged view of the graben-fissure systems interpreted as dyke swarms, and associated with centres 2, 7 and 9, 5, respectively. The southern part of the area is covered by the large Sobra Fluctus, a huge fluctus which may be fed by coronae. We are currently assessing whether this fluctus is genetically linked to this system.

Future Work: Mapping (at 1:500,000 scale) of dykes and lava flows is in progress to complete the tectonic and geological history of the region and evaluate the link with Hecate chasmata rifting. The lava flow history of the region will be determined from 1:500,000 scale mapping and integrated with the interpreted dyke swarm history. The first target for detailed mapping will be the areally extensive Sobra Fluctus.

References:

Buchan K.L., & Ernst R.E. (2021) *Gond. Res.* 100, 25–43.

Christensen, P. R. et al. (2009) AGU Fall Meeting, Abstract #IN22A-06
 Grindrod P.M. & Hoogenboom T. (2006). *Astron. Geophys.* 47, 3-16.
 Gülcher et al. (2020) *Nat. Geosci.*, 13, 547–554.
 Herrick R.R. (1999) *GRL*, 26, 803–806.
 Smrekar S.E. & Stofan E.R. (1999). *Icarus*, 139, 100-115.
 Stofan et al. (2012) *Scientific Investigations Map 3163*.
 Stofan et al. (1992) *JGR*, 97, 13347-13378.

[1] [2] [3] [4] [5] [6] [7] [8]

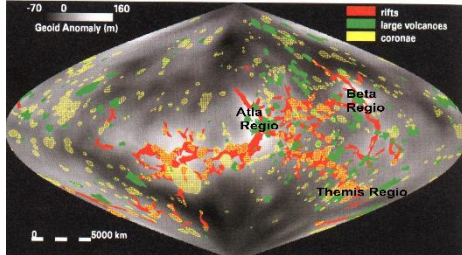


Fig.1: Study area (white square) on base-map of (Herrick, 1999) .

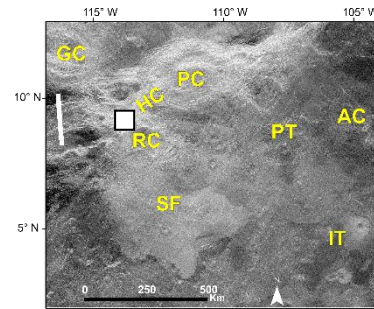


Fig.2: Study area on Magellan Sea floor. Labels: GC = Gashan-Ki corona, HC = Hecuba corona, PC = Pagan Yan Thon corona, RC = Rind corona, PT = Prthivi, AC= Ak-Ene, SF = Sifon, IT = Ithaca.

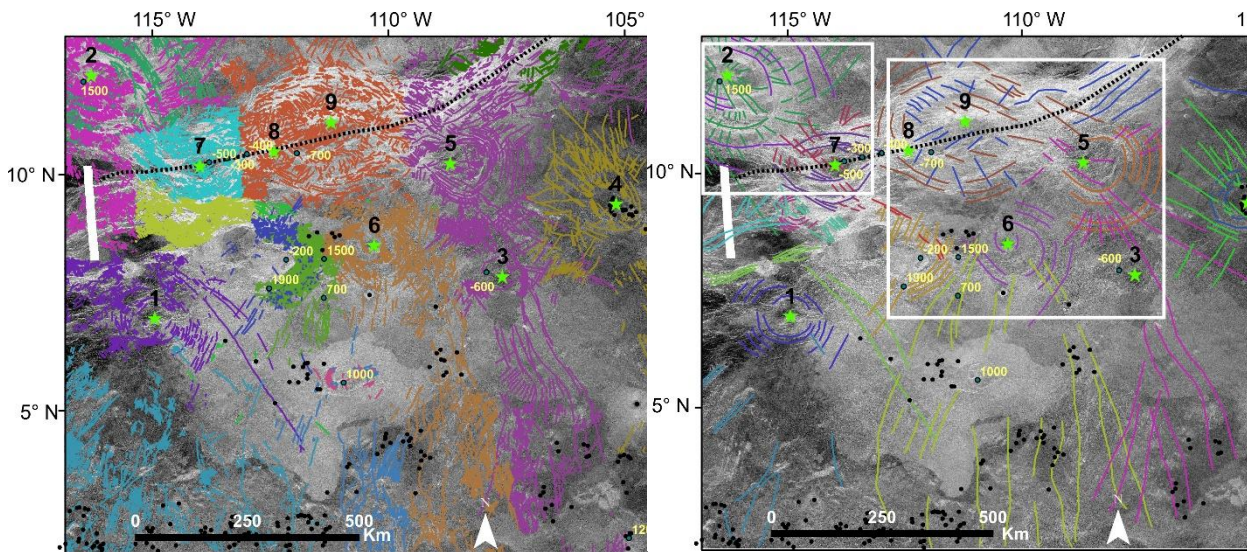


Fig.3: Left: Detailed mapping of graben-fissure lineaments (45800 mapped to date). Right: Generalized distribution of graben systems (colour coded to represent different radiating, circumferential and linear swarms). Centre 2 is Gashan-Ki corona, Centre 6 is Rind corona and Centre 9 is Prthivi corona. White boxes corresponding to detailed maps shown in Figures 4 and 5. Numbers indicate selected elevations associated with magmatic centres.

Fluid-rock interactions as the main ore-forming process at the origin of the Oumjrane copper deposit (Eastern Anti-Atlas, Morocco)

IDBAROUD Mohamed¹, BOUABDELLAH Mohammed², LEVRESSE Gilles³, MOUGUINA El Mostafa¹, MATHUR Ryan⁴, MELCHIORRE Erik⁵, YANS Johan⁶, JINARI Abdessamad¹, SYAD Sghir⁷, MAACHA Lhou⁷

¹: Department of Geology, Cadi Ayyad University, B.P. 2390, Marrakech 40000, Morocco

²: Laboratoire des Gîtes Minéraux, Hydrogéologie & Environnement, Faculté des Sciences, Oujda 60000, Morocco

³: Programa de Geofluidos, Centro de Geociencias UNAM-Campus Juriquilla, AP 1-253, Querétaro Mexico CP 76230, Mexico

⁴: Geology Department, Juniata College, 1700 Moore Street, Huntingdon, PA 16652, USA

⁵: Geology Department, California State University, San Bernardino, CA 92405, USA

⁶: Institute of Life-Earth-Environment (ILEE), University of Namur, 61 rue de Bruxelles, B-5000 Namur, Belgium

⁷: Managem Group, Twin Center, Tour A, Angle Boulevard Zerktouni et Al Massira Al Khadra, B.P. 5199, Casablanca 20000, Morocco

The Oumjrane Cu-Pb-Zn-Ba district, in eastern Anti-Atlas of Morocco, is one of the top three major copper producers in North Africa with an annual production exceeding 260,000 tons at an average grade of 1.4% Cu. The host rocks consist of a succession of Ordovician lower greenschist-facies phosphorous-bearing siliciclastic metasediments of the Ktaoua Group (Lower Sandbian-Katian) and second Bani Group (Hirnantian), conformably overlain by Silurian organic-rich black-shales. The orebodies consist of transtensional, mostly NE- to EW-trending, sub-vertical fault veins, veinlets, and “en echelon” tension gashes and breccia veins. Based on textural relationships and mineral assemblages, two major sulfide fault-vein infill stages are recognized. The early Cu-(Ni-Fe)-rich stage consists predominantly of chalcopyrite (>90% vol. %) with subordinate pyrite and magnetite along with gersdorffite set in a gangue of apatite and quartz. The late Pb-Zn-Ba-rich stage comprises galena, sphalerite, and barite along with apatite as a subordinate phase.

The occurrence of apatite, gersdorffite and magnetite in the mineral paragenesis along with the trace element composition of apatite from the early copper stage reflect the involvement of regional circulation of Cl⁻ and F⁻ rich hydrothermal basinal brines in a dominantly rock-buffered system. High fluid-rock ratios would have resulted in mobilization of Cu and Ni, among other metals, and their transport into the hydrothermal system. Conversely, apatite chemistry from the late Pb-Zn-Ba stage is consistent with a magmatic-hydrothermal origin.

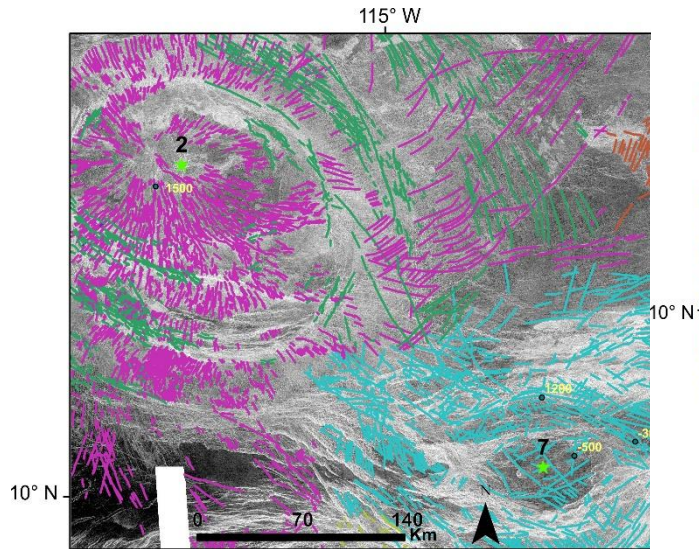


Fig.4: Detailed mapping of radiating and circumferential swarms associated with Gashan-Ki corona (no. 2) and unnamed corona no. 7.

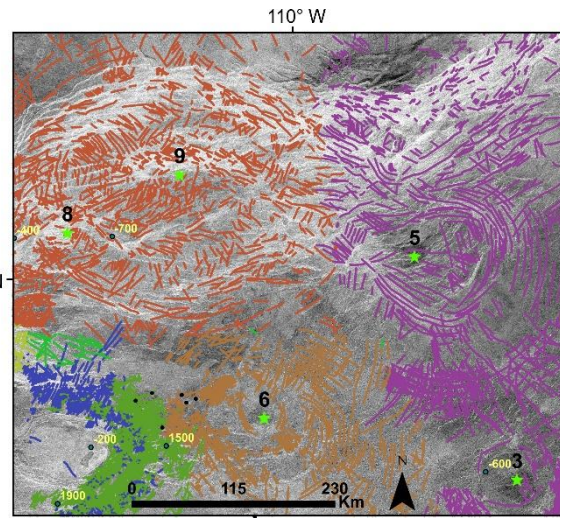


Fig.5: Detailed mapping of radiating and circumferential swarms associated with Prthivi corona (no. 9, and unnamed centre no. 5).

Wet melt ponding beneath thick lithosphere may explain continental flood basalt provinces

Alexei V. Ivanov¹, Gillian R. Foulger², Jordan J. J. Phethean³, Sergei A. Pisarevsky⁴

¹: Institute of the Earth's Crust, Siberian Branch of the Russian Academy of Sciences, 128 Lermontov Street, Irkutsk 664033, Russia

²: Department of Earth Sciences, Durham University, Durham DH1 3LE, U.K.

³: Department of Environmental Sciences, College of Science and Engineering, University of Derby, Derby DE22 1GB, U.K.

⁴ Earth Dynamics Research Group, School of Earth and Planetary Sciences, The Institute for Geoscience Research, Curtin University, GPO Box U1987, Perth, WA 6845, Australia

Continental flood basalt provinces comprise large volumes of magma emplaced on continental lithosphere, usually at a high rate. The combination of large volume and high rate is a geological conundrum. If purely thermal processes and a homogeneous source are involved, emplacement would be prolonged, with initial, major, and dwindling stages of practically continuous magmatism due to thermal inertia. An additional problem is that continents typically comprise thick, cold lithosphere that depresses or even prevents melting beneath it. For example, the present-day lithosphere of the Siberian Craton is everywhere thicker than 180 km (Dymshits et al., 2020; Kuskov et al., 2014; Priestly et al., 2018) and there is no evidence that it was significantly thinner at the time of emplacement of the Siberian Traps – one of the largest preserved continental flood basalt provinces on Earth (Ivanov, 2015). No reasonable mantle temperature can lead to significant melting of dry peridotite at depths of 180 km, due to high pressure, even where a mafic lithology (eclogite or garnet pyroxenite) is assumed in the melt source. Sobolev et al. (2011) suggested that initially low-volume volcanism might result from melting of mafic lithologies at sublithospheric depths, followed by lithospheric delamination and voluminous decompression melting at shallow depths. However, at the Siberian Traps there are no signs of such delamination, whilst other known delamination events (e.g. the North China Craton in the Late Mesozoic; Gao et al., 2009) were not followed by the formation of flood basalt provinces and only produced low-volumes of alkaline basalt volcanism. Ivanov and Litasov (2014) pointed out that the problem of melting suppression can be overcome if the source is rich in fluids, and suggested that fluids can be introduced beneath continents by stagnant subducted slabs in the mantle transition zone. Thicker and faster-subducting slabs can deliver more fluid to the mantle transition zone, including water in form of the high-pressure ice VII (“cubo-ice”) (Bina and Navrotsky, 2000), which has since been found as inclusions in diamonds (Tschauner et al., 2018). However, subduction is a slow and prolonged process compared to flood basalt volcanism. To reconcile these mismatch, we demonstrate here that a combination of the ideas expressed by Ivanov and Litasov (2014) (that melting can occur even at cratonic sublithospheric depths if sufficient water is present) and by Silver et al. (2006) (that melt ponding can occur at cratonic sublithospheric depths) are able to solve the conundrum of voluminous and sudden volcanism at regions of thick lithosphere. Moreover, we counter-intuitively propose thick lithosphere is a *prerequisite* to the formation of voluminous flood basalt provinces, because it allows the required ponding of melt, which is later quickly released through formation of cross-lithospheric faults. If the lithosphere is initially thin, any formed melt is extracted as soon as it is produced, leading only to low-volume prolonged volcanism.

Bina, C.R. and Navrotsky, A., 2000. Possible presence of high-pressure ice in cold subducting slabs. *Nature* 408, 844-847.

Dymshits, A.M., Sharygin, I.S., Malkovets, V.G., Yakovlev, I.V., Gibsher, A.A., Alifirova, T.A., Vorobei, S.S., Potapov, S.V., Garanin, V.K., 2020. *Thermal State, Thickness, and Composition of the Lithospheric Mantle beneath the Upper Muna Kimberlite Field (Siberian Craton) Constrained by Clinopyroxene Xenocrysts and Comparison with Daldyn and Mirny Fields. Minerals, 10, 549.*

Gao, S., Zhang, J.-F., Xu, W.-L., Liu, Y.-S., 2009. *Delamination and destruction of the North China Craton. Chinese Science Bulletin, 54, 3367-3378.*

Ivanov, A.V., 2015. *Why volatiles are required for cratonic flood basalt volcanism: Two examples from the Siberian craton: in The Interdisciplinary Earth: A Volume in Honor of Don L. Anderson, GSA Special Paper 514 & AGU Special Publication 71, 325-338.*

Ivanov A.V., Litasov K.D. *The deep water cycle and flood basalt volcanism. International Geology Review, 2014, v. 56, p. 1-14, doi: 10.1080/00206814.2013.817567.*

Kuskov, O.L., Kronrod, V.A., Prokof'ev, A.A., Pavlenkova, N.I., 2014. *Lithospheric mantle structure of the Siberian craton inferred from the superlong Meteorite and Rift seismic profiles. Russian Geology and Geophysics, 55, 892-906.*

Priestley, K., McKenzie, D., Ho, T., 2018. *A lithosphere-asthenosphere boundary – a global model derived from multimode surface-wave tomography and petrology: in Lithospheric Discontinuities, Geological Monograph 239, 111-123.*

Silver P.G., Behn M.D., Kelley K., Schmitz M., Savage B. *Understanding cratonic flood basalts. Earth and Planetary Science Letters, 2006, v. 245, p. 190-201, doi: 10.1016/j.epsl.2006.01.050.*

Sobolev, S.V., Sobolev, A.V., Kuzmin, D.V., Krivolutsкая, N.A., Petrunin, A.G., Arndt, N.T., Radko, V.A., Vasiliev, Y.R., 2011. *Linking mantle plumes, large igneous provinces and environmental catastrophes. Nature 477, 312-316.*

Tschauner, O., Huang, S., Greenberg, E., Pakapenka, V.B., Ma, C., Rossman, G.R., Shen, A.H., Zhang, D., Newville, M., Lanzirotti, A., Tait, K., 2018. *Ice-VII inclusions in diamonds: Evidence for aqueous fluid in Earth's deep mantle. Science, 359, 1136-1139*

Neoproterozoic plate mobilism: constraints from paleomagnetic results of Wyoming and Superior

Jikai Ding^{a, b}, Chris Rogers^c, Ulf Söderlund^{d, e}, David A.D. Evans^{a, f}, Zheng Gong^{a, f}, Richard E. Ernst^c, Kevin Chamberlain^g, Taylor Kilian^h

^a Department of Earth & Planetary Sciences, Yale University, New Haven, CT 06520, USA, Jikai.ding@yale.edu

^b State Key Laboratory of Biogeology and Environmental Geology, China University of Geosciences, Beijing 100083, China

^c Department of Earth Sciences, Carleton University, Ottawa, ON, Canada

^d Department of Geology, Lund University, Sölvegatan 12, SE-223 62 Lund, Sweden

^e Department of Geosciences, Swedish Museum of Natural History, Box 50 007, SE-104 05 Stockholm, Sweden

^f Department of Earth and Planetary Sciences, Harvard University, Cambridge, MA 02138, USA

^g Department of Geology & Geophysics, University of Wyoming, Laramie WY, USA

^h KoBold Metals, Berkeley, California 94704, USA

How far back in time plate tectonics has operated is one of the largest questions in Earth sciences. Existing estimates for the onset of plate tectonics range from the Hadean to Cambrian based on diverse constraints from geology, geochemistry, paleomagnetism and numerical models. One of the most robust arguments for plate tectonics is Paleomagnetism, which could tell us if two cratons have experienced relative horizontal motions in the geologic past (Evans and Pisarevsky, 2008). At present, the most reliable paleomagnetic data suggested the relative cratonic motion occurred during 2.7–2.17 Ga (Kilian, 2015). In this study, a new paleomagnetic pole was reported from the ca. 2480 Ma mafic dikes from the Wyoming craton. It will provide constraint on the assembly time of Wyoming and Superior, and constrain the oldest relative motion in earth's history at present.

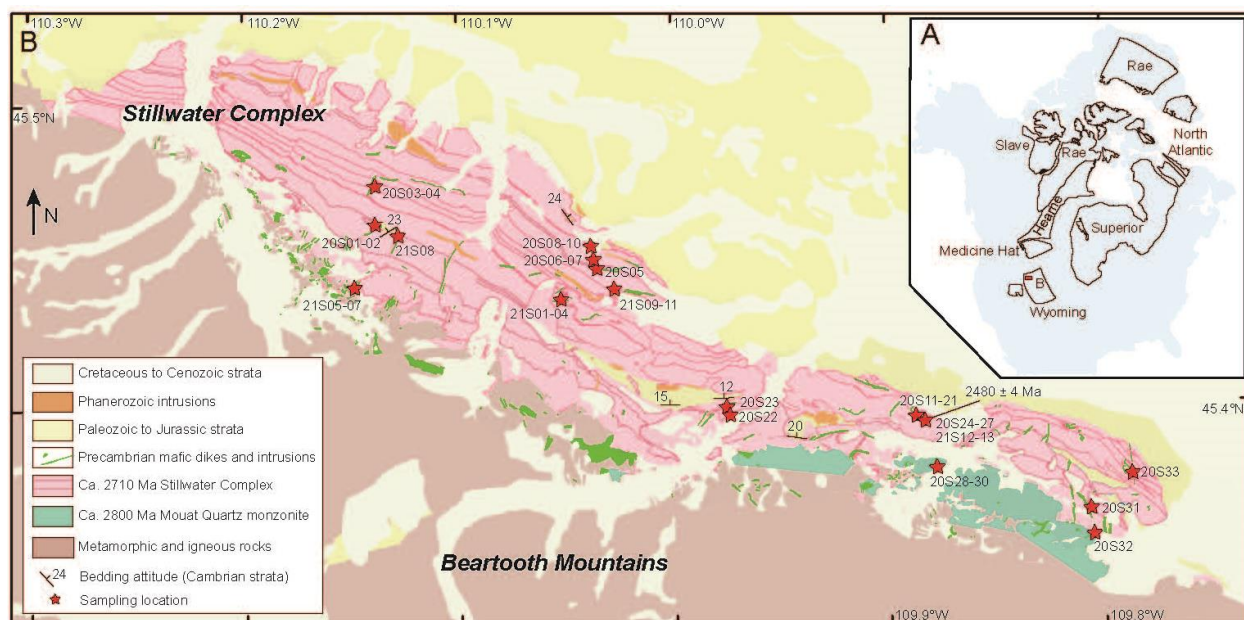


Figure 1. A: Simplified overview of the Archean provinces in North America. B: Simplified geologic map of the Stillwater complex and the distribution of the sampling locations.

The ca. 2480 Ma mafic dikes appear to be wide-spread in the Stillwater complex in the Wyoming craton (Fig. 1). The ca. 2.71 Ga Stillwater Complex is exposed within the Beartooth mountains of southern

Montana. After the emplacement of the Stillwater complex, ca. 2480 Ma mafic dikes intruded into the Stillwater complex and the basement. The dikes are NW-trending or NE-trending diabase or gabbro. In this study, a total of 46 sites were collected including 27 sites from dikes, as well as 17 sites from the host rocks of Stillwater complex and 2 sites from the granitic basement. After stepwise thermal demagnetization, 12 dikes hold a consistent high temperature component (HTC) which directs south-southeast and down with moderate inclination. Two tentatively positive baked-contact tests demonstrate that the HTC can be interpreted as primary in origin.

The pole was achieved by averaging 12 VGPs from 12 Elbow Creek mafic dikes. By matching the new pole with the poles from the ca. 2505 Ma Ptarmigan-Mistassini dikes and the ca. 2466-2446 Ma Matachewan dikes (Evans and Halls, 2010), while also matching the ca. 2160 Ma poles from the Rabbit Creek dikes and the Biscotasing dikes (Evans and Halls, 2010; Kilian et al., 2015), the aggregate dataset demonstrates Wyoming and Superior assembled before ca. 2500 Ma (Fig. 2). Our preferred reconstruction (Fig. 2) is based on broad alignment of paleo-magnetic poles as well as geological similarities such as Huronian and Snowy Pass Supergroup juxtaposition and consideration of mafic dike trends within and between the two cratons (Roscoe and Card, 1993). The ca. 2.71 Ga poles from the Wyoming craton and the Abitibi subprovince of Superior are substantially separated from each other (Fig. 2), suggesting Neoproterozoic relative lateral motion between cratons.

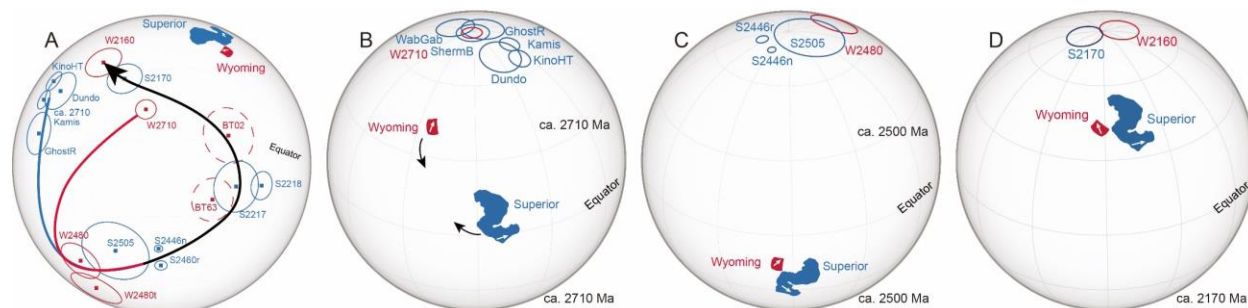


Figure 2. A: Comparison of the ca. 2710–2160 Ma paleomagnetic poles of the Wyoming and Superior (in present East Superior coordinates). B-D: Paleogeographic reconstructions for Superior and Wyoming at ca. 2710 (B), 2500 (C) and 2170 Ma (D).

References

- Evans, D.A.D., Pisarevsky, S.A. Plate tectonics on early Earth? Weighing the paleomagnetic evidence[J]. *When did plate tectonics begin on planet Earth*, 2008, 440: 249-263.
- Evans, D. A. D. and Halls, H. C., 2010. Restoring Proterozoic deformation within the Superior craton. *Precambrian Research*, v. 183, p. 474 – 489
- Kilian TM. *Precambrian paleomagnetism of mafic dike swarms and the Wyoming craton: implications for an Archean supercontinent*. Yale University, 2015.
- Roscoe, S.M. and Card, K. D. 1993. The reappearance of the Huronian in Wyoming: rifting and drifting of ancient continents. *Canadian Journal of Earth Sciences*, v. 30, p. 2475–2480.

Sturtian snowball Earth triggered by a widespread magmatic province and thoughts on a possible mid-Sturtian glacial retreat

Kai Lu¹; Ross N. Mitchell^{1,2}; Xian-Hua Li^{1,2}

¹: State Key Laboratory of Lithospheric Evolution, Institute of Geology and Geophysics, Chinese Academy of Sciences, Beijing 100029, China.

²: College of Earth and Planetary Sciences, University of Chinese Academy of Sciences, Beijing 100049, China

The ca. 717–661 Ma Sturtian glaciation represents the first Neoproterozoic snowball Earth. Here we report that Franklin-aged magmatism was present not only in Laurentia and Siberia, but also in South China, where the Hubei–Shaanxi Magmatic Province formed at 720 Ma, revealing widespread magmatic provinces immediately preceding initiation of the Sturtian snowball Earth. This widespread volcanism across supercontinent Rodinia, extending from tropical to temperate latitudes, started at ca. 720 Ma and lasted until the ca. 717 Ma Sturtian onset. The widely distributed, coeval volcanism could be related to a mantle superplume beneath Rodinia. Such rapid and widespread volcanism may have triggered the Sturtian glaciation (Lu et al., 2022). Then, after the Sturtian was underway, geological evidence from five continents suggests a possible mid-Sturtian glacial retreat, which happens to coincide with two asteroid impacts, the ca. 687 ± 5 Ma Jänisjärvi (Baltica) and 657 ± 43 Ma Strangways (Australia) impact craters. The coincidence between the impact and glacial retreat has inspired a “snowball impact” hypothesis that greenhouse warming caused by the impact-generated vaporization of sea ice could have driven temporary, localized glacial retreat (Lan et al., 2022). An impact during snowball Earth—penetrating a massively thick continental ice sheet—provides an opportunity to look for evidence of large scale vaporization of the ice sheet. Our preliminary NanoSIMS analysis of the water contents of impact melt rocks from the ca. 687 Ma Jänisjärvi impact crater demonstrates extremely high water contents (up to several tens of thousands ppm), indicating the existence of impact-generated hydrothermal systems and possible impact-generated glacial meltwater input. Such extremely high water contents for the impact melt rocks potentially support the snowball impact hypothesis. However, further investigations are required to confirm this.

References

- Lan, Z., Mitchell, R. N., Gernon, T. M., Nordsvan, A. R., 2022. Did an asteroid impact cause temporary warming during snowball Earth?. *Earth and Planetary Science Letters*, 581, 117407.
- Lu, K., Mitchell, R. N., Yang, C., Zhou, J. L., Wu, L. G., Wang, X. C., Li, X. H., 2022. Widespread magmatic provinces at the onset of the Sturtian snowball Earth. *Earth and Planetary Science Letters*, 594, 117736.

Availability of Synthetic Aperture Radar Data and Mapping of Tectonic Controls on the Distribution of Volcanoes and Volcanic Fields in Antarctica

K S Misra¹; Anshuman Misra²

¹: University of Petroleum and Energy Studies, Dehradun, India

²: Doon University, Dehradun, India

Availability of Synthetic Aperture Radar (SAR) data sets has illustrated an intricate relationship between tectonic controls on distribution of volcanoes and volcanic fields in Antarctic Continent. Parallel sets of lineament, form orthogonal pattern, similar to any other shield region in the world. These lineaments have propagated upward through the ice sheets are characterized by straight courses and parallelism among them (Misra and Misra, 2023). Abrupt termination of glacio-morphic features such as compacted snow dunes (Fig.1), consolidated snow sheets and modifications in the course of glaciers are also conspicuously seen.

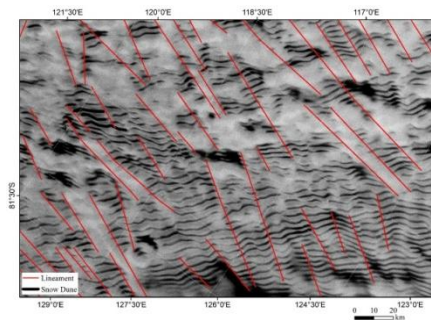


Fig.1 SAR imagery showing abrupt termination of compacted snow dunes along nearly parallel set of lineaments (after Misra and Misra, 2023).

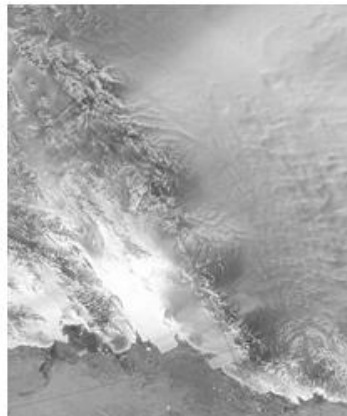


Fig.2 SAR imagery exhibits two rows of volcanoes aligned along particular basement tectonic trend forming alternate horst and grabens.

Rifting along the Trans-Antarctic Mountain Ranges and its continuation in Antarctic Peninsula is one of the longest rift systems with pronounced vertical movements and rampant volcanism. Several chains of dormant volcanoes, jutting out of ice sheets are identified in satellite data (Fig.2).

Unique mounds covering extensive regions, developed due to melting and freezing in ice sheets are mapped (Fig.3). Melting Of thick ice sheets covering extensive regions of continental dimensions, due to volcanic heat would have contributed to climatic changes due to return of water to oceans and increasing the water covered regions.



Fig.3 Satellite imagery exhibits melting and freezing of ice sheets around the volcanic vents as mounds.

Vertical movement is also conspicuously noticed along several sets of lineaments, forming major escarpments and sheltered valleys, presently occupied by the consolidated snow sheets. Volcanic field, identified east of Transantarctic Mountain Ranges, is vast and comprises huge calderas, craters and cones. Evidences to suggest prolonged volcanism, such as younging towards west and spasmodic by the presence of fresh parasitic cones within older craters are enumerated (Fig.4).

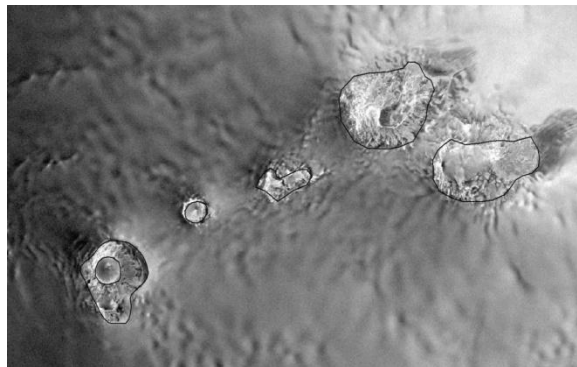


Fig.4 SAR imagery depicting volcanic Field east of Trans-Antarctic Ranges, encompassing several large craters, calderas along with parasitic cone within crater on the western side.

Furthermore, remnants of emanating lava channels from several volcanoes (Fig.5) are reported for the first time.

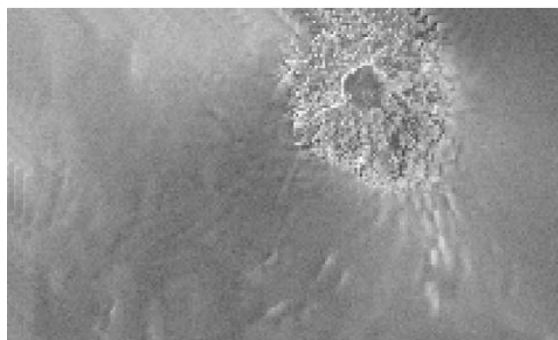


Fig.5 SAR imagery shows the remnants of two lava channels, emanating from a volcano towards the southern side in western Antarctica.

Reference

1. Misra, A., Misra, K. S., & Dobhal, D. P. (2023). Compacted Snow Dune Complexes in Antarctica and their Applicability as New Climate Change and Basement Tectonic Parameters. In *Climate Change and Environmental Impacts: Past, Present and Future Perspective* (pp. 215-228). Cham: Springer International Publishing.

Mafic dykes that are potentially related to the Kunene Igneous Complex

Martin B. Klausen¹, Philip R. Geldenhuys¹, Jayde Bromwich¹, David A.D. Evans², Ulf Söderlund³, Richard E. Ernst⁴, Richard E. Hanson⁵, Johanna Salminen⁶, I.F. Ricardo⁷, Ian Fieldhouse⁸

¹: Department of Earth Sciences, Stellenbosch University, RSA (klausen@sun.ac.za)

²: Yale University, USA

³: Lund University, Sweden

⁴: Department of Earth Sciences, Carleton University, Ottawa, Canada

⁵: Texas Christian University, USA

⁶: Department of Geography and Geosciences, University of Helsinki and Geological Survey of Finland (GTK)

⁷: Trindade University of São Paulo, Brazil

⁸: Sudbury, Canada

The arid region of south-western Angola exposes numerous crosscutting mafic dykes, in and around the Mesoproterozoic Kunene Igneous Complex (KIC), which is an Anorthosite-Charnockite-Mangerite-Granite (ACMG) complex that includes the World's largest known *massif* anorthosite (Bybee et al., 2019). Mafic dykes can on the basis of their trends be subdivided into (1) a >400 km-wide WNW-trending swarm (Fig. 1), (2) a NNW-trending swarm with Umkondo-aged dykes (Ernst et al., 2013) and (3) a coast-parallel Cretaceous swarm, related to the opening of the South Atlantic Ocean, close to a proto-Tristan da Cunha hot spot. The Angolan Shield host to these dyke swarms includes Neoproterozoic rocks, overprinted by Paleoproterozoic deformation and granitic plutonism (Jelsma et al., 2018). A cratonic peneplain covered by the ~1.8 Ga Chela Group was intruded over a protracted time period by the KIC, the mafic component of which is dated to 1.41-1.38 Ga (Lehmann et al., 2020). Since (1) WNW-trending dykes are crosscut by ~1.1 Ga Umkondo dykes yet do not crosscut the KIC, (2) one WNW-trending dyke near the municipal town of Virei has an unpublished baddeleyite U-Pb age of 1385 ± 5 Ma (Ernst et al., 2014), and (3) all dykes verge onto the KIC, a more intimate genetic relationship seems likely.

Most WNW-trending dykes are more or less metamorphosed by the Pan-African Kaoko orogen affecting the area from the SW (Fig. 1), with thicker and more inland dykes remaining more pristinely igneous. This overprint does not, however, appear to have affected even the most mobile large ion lithophile elements in geochemical analyses, forming the core of this study. Rare earth elements provide a first-order discrimination between high- and low- $(La/Sm)_N$ dykes (HLS & LLS, respectively), resembling E-MORB and N-MORB, respectively. Further incompatible element discriminations (e.g., Fig. 2) identify at least three sub-groups inside each of these two main groups, where more enriched and particularly high-(P, Ti) dykes bear slight resemblance with KIC's nelsonites and include the dated 1385 Ma dyke.

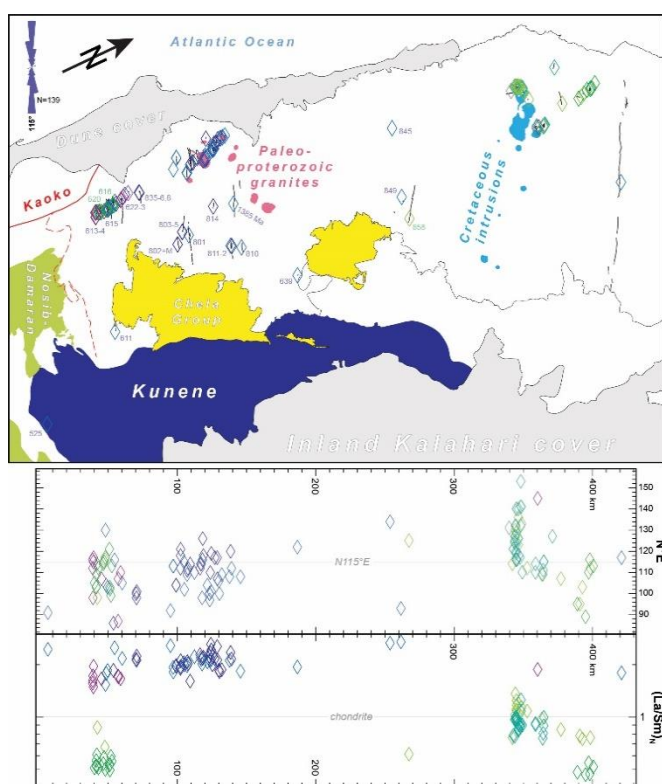


Figure 1: (a) Simplified geological map of south-western Angola, showing locations (diamonds) of sampled WNW-trending dykes, analysed for bulk rock geochemistry. (b) Dyke trends, also shown as a rose diagram inserted into (a). (c) $(La/Sm)_N$ -ratios provide a first-order discrimination between enriched “E-MORBs” (blueish) and depleted “N-MORBs” (greenish), which are further subdivided in Figure 2.

LLS-dykes cluster along both margins of the >400 km-wide swarm and are least related to the KIC. While Jerram et al. (2019) interpret the northern marginal LLS-subswarm as Cretaceous, this still leaves a southern marginal LLS-subswarm that shares the field relationships of the HLS-swarm and can thereby not be Cretaceous. Since few WNW-trending dykes crosscut the KIC and it is difficult to explain the emplacement of both HLS- and LLS-dykes that were derived from more fertile and depleted mantle sources, respectively, LLS-dykes could rather belong to a ~1.5 Ga Humpata LIP (Ernst et al., 2013).

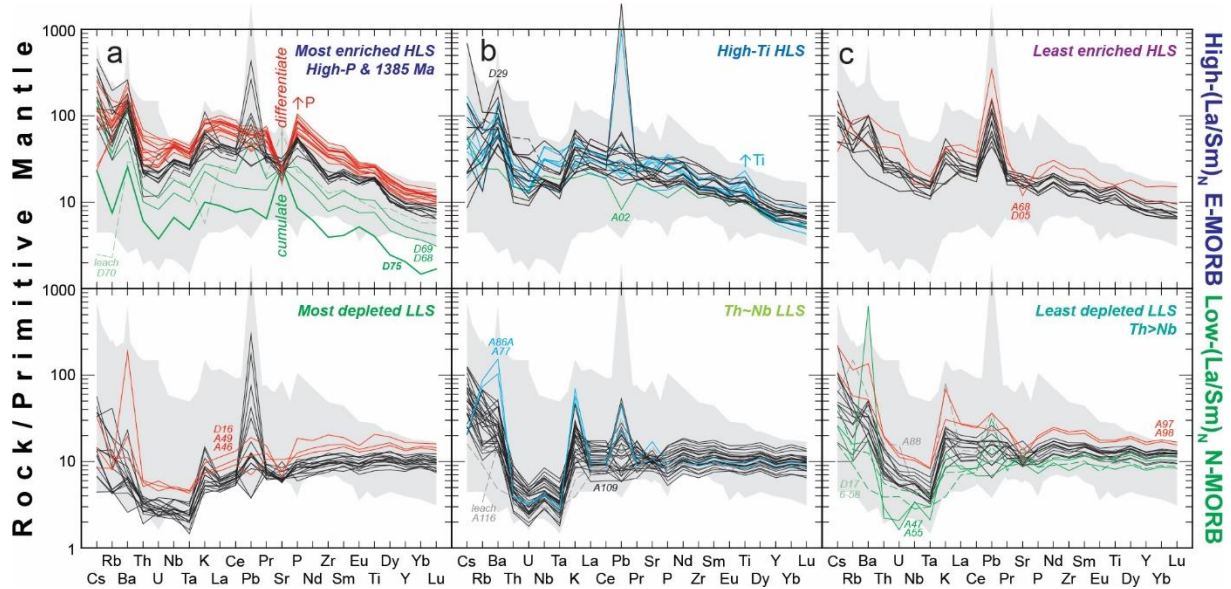


Figure 2: Geochemical subdivisions of first-order HLS (a-c) and LLS (d-f) groups, recognized from differing spider patterns, normalized against a primitive mantle (Lyubetskaya & Korenaga 2007). For each subgroup, black patterns are most representative while red and green patterns may be differentiates and cumulates of these, respectively. Cyan patterns represent further subdivisions. Grey backgrounds are for all SW Angola samples.

Assuming that WNW-trending dykes are coeval with the KIC, these could have been emplaced along a failed rift that radiated from a ~1385 Ma LIP center within the Nuna remnant reconstruction by Zhang et al. (2022). However, the protracted and pulsating magmatism during the Boring Billion's Nuna-to-Rodinia super-continental cycle, including that period's unique ACMG-complexes, is perhaps better accommodated within an accordion-type back-arc setting (Santosh & Groves, 2023). Inside such a setting, large, sub-crustal basic magma underplating could have generated WNW-trending HLS-dykes, buoyant plagioclase-rich mushes and high-T dry lower crust magmas over a longer time-period. The co-generation of more depleted LLS-dykes requires shallower partial melting of more depleted upper asthenosphere, possibly within a perplexing but prerequisite pair of marginal rifts along either side of a central KIC and its associated HLS dyke swarm.

Reference:

- Bybee et al. (2019) *Precamb. Res.* 332, 105393
 Ernst et al., 2013 *Precamb. Res.* 230, 103-118
 Ernst et al. (2014) *Unpublished LIPs-Industry Consortium Report A157* (www.supercontinent.org)
 Jelsma et al. (2018) In: Siegmund et al (eds) *Geology of Southwest Gondwana*, 217-239
 Jerram et al (2019) *Tectonophysics* 760, 252-266
 Lehmann et al. (2020) *Int. J. Earth Sci.* 109, 1463-1485
 Lyubetskaya & Korenaga (2007) *J. Geophys. Res.* 112, B03212
 Santosh & Groves (2023) *Earth-Sci. Rev.* 236, 104287
 Zhang et al. (2022) *EPSL* 597, 117815

The ancient Earth's crust hosted giant reservoirs with >380,000 km³ of magma

Rais Latypov¹, Sofya Chistyakova¹, Richard A. Hornsey², Gelu Costin³, and Mauritz van der Merwe⁴

¹School of Geosciences, University of the Witwatersrand, Johannesburg, South Africa; ²Richard Hornsey Consulting (Pty) Ltd, Paternoster, South Africa; ³Department of Earth Science, Rice University, Houston, TX, USA; ⁴Retired, Port Alfred, South Africa.

For over a century, the classic paradigm of volcanology and igneous petrology has been premised upon the existence of magma chambers, filled by crystal-free melt, forming 'big tanks'. Such magma chambers gradually lose heat and crystallize from all margins inwards and occasionally supply overlying volcanoes with magma that erupts onto the Earth's surface. This founding concept has been recently challenged on the basis of observations and evidence from various disciplines (Cashman et al. 2017). There are, however, some observations from magmatic complexes that conflict with this emerging paradigm. Here we present one well-constrained example from the Bushveld Complex in South Africa, indicating that its magma chamber appears to have contained, during one stage of its evolution, an enormous volume of resident melt that slowly crystallized from the base upwards to produce a continuous sequence of chemically stratified cumulate rocks (Latypov et al. 2022a). In the south-eastern part of the complex, the magmatic layering of the Main Zone continuously drapes across a ~4-km-high sloping step in the chamber floor. Such deposition of magmatic layering implies that the resident melt column was thicker than the stepped relief of the chamber floor. Prolonged internal differentiation within this thick magma column is further supported by evolutionary trends in crystallization sequence and mineral compositions through the sequence. The resident melt column in the Bushveld chamber during the formation of the Main Zone is estimated at >5-km in thickness and >380,000 km³ in volume (Latypov et al. 2022a). This volume is several orders of magnitude larger than the largest ignimbrite/tuff super-eruptions in Earth's history (e.g., Bishop tuff – 600 km³ and Youngest Toba eruption – up to 13,200 km³) and is only comparable to estimates of some of Earth's large igneous provinces, such as the Karoo (367,000 km³) and Afar (350,000 km³). This suggests that super-large, entirely molten, and long-lived magma chambers occur, at least occasionally, in the geological history of our planet. Therefore, the classical view of magma chambers as 'big magma tanks' remains a viable research concept for some of Earth's magmatic provinces (Latypov et al. 2022a, b).

Cashman, K. V., Sparks, R. S. J. and Blundy, J. D. Vertically extensive and unstable magmatic systems: a unified view of igneous processes. Science. 355, eaag3055 (2017).

Latypov, R. M., Chistyakova, S. Yu., Hornsey, R. A., Costin, G. and van der Merwe, M. A 5- km- thick reservoir with >380,000 km³ of magma within the ancient Earth's crust. Sci Rep. 12, 15651 (2022a).

Latypov, R. M., Chistyakova, S. Yu., Barnes, S., Godel, B., Delaney, G. W., Cleary, P. W., Radermacher, V., Campbell, I. and Jakata, K. Chromitite layers indicate the existence of large, long-lived, and entirely molten magma chambers. Scientific Reports 12:4092 (2022b).

Where is the western boundary of Bering plate?

Lebedev I.E.¹; Pasenko A.M.¹

¹: Institute of Physics of the Earth RAS (Moscow, Russia)

To date, two models of the formation of the so-called Bering Plate are actively discussed. The first one suggest extrusion of Alaska under the influence of the Pacific plate. An array of accumulated data in support of this theory is presented in (Redfield et al., 2007). According to this model, the eastern part of the Bering Plate is a collage of terranes extruded in a northwesterly direction parallel to the British Columbia margin. As a result of this movement, western part of potential Bering plate could experience counterclockwise rotation. Another model is presented in (Mackey et al., 1997), where seismic data also confirms the counterclockwise rotation of the rigid Bering Plate. However, these and similar models are primarily based on data collected to the east of the Bering Strait, while to the western part there is clearly insufficient data. This fact causes inconsistencies in the western boundary of the Bering Plate through the mainland Chukotka, Karyak, and Kamchatka (Mackey et al., 1997; Redfield et al., 2007). According to some models, boarder is drawn even under the basin of the Bering Strait (Chekhovich and Palandzhyan, 2021). In addition, the discrepancies are supported by the low seismicity of the mainland of the North-East of Russia, which does not allow to clearly draw a possible border today.

One of the methods that could estimate possible existence of the Bering Plate in the geological past is the paleomagnetic method. It does not allow us to reliably characterize potential movements within the first hundreds of kilometers. If we can establish the shift in large amplitudes, we can most likely approve the existence of small plates, such as the Bering Sea. To solve this goal, we need the most reliable and accurate paleomagnetic data based on the objects east of the Bering strait. Moreover, the age of the rocks should be younger than the completion of the formation of the South Anyui Suture (early Early Cretaceous), which was formed as a result of the closure of the Anyui Ocean. Also, it is desirable that the age of object as old as possible so that during this time the maximum displacement can accumulate and it becomes visible for paleomagnetic method. An ideal object for such a study is one of the largest Phanerozoic subduction-related igneous provinces: Cretaceous Okhotsk–Chukotka volcanic belt (OCVB). In addition, it is an excellent object for any paleomagnetic research, and its northern part overlaps the above-described boundary of the Bering Plate.

We sampled in detail two objects within the OCVB, which are located on opposite sides of the potential boundary of Bering plate, but located within the same elder Chukotka-Alaska microcontinent. The first one Kupol location is placed in Western Chukotka to the east of the large gold-silver deposit of the same name. The last U-Pb and Ar⁴⁰/Ar³⁹ isotope data allowed us to limit the age of our paleomagnetic sections to 88–84 Ma (Tikhomirov et al., 2021a). Paleomagnetic data for this location published in (Lhuillier et al., 2023 in press). The second location Valunistoe is placed in Central Chukotka in close to the gold-silver ore deposit of the same name. Our new isotope-geochronological data indicate a significantly younger age of formation of the studied volcanic rocks (76-71 Ma) than previously thought (Tikhomirov et al., 2021b). Kupol is located most likely to the west of the border with the Bering Sea Plate, and the Valunistoe is almost on the border according to (Mackey et al., 1997). For both locations, paleomagnetic poles were calculated, the primary remanence is verified by positive fold tests and electron microscopic studies.

The obtained paleomagnetic poles have a significant difference between them ($7.1^\circ \pm 6.0^\circ$). The obtained paleomagnetic data indicate the presence of clockwise rotation of central Chukotka (Valunistoye) relative to its western part (Kupol). This statement is also supported by the presence of a

similar rotation relative to neighboring large Eurasia, for which the APWP is well known (Torsvik et al., 2012). The observed displacement of Central Chukotka relative to its western part and Eurasia is similar to the expected rotation of the Bering Plate proposed by models (Redfield et al., 2007; Mackey et al., 1997). This may indicate that the Valunistoe location may belong to the Bering Plate, consequently its western boundary must lie somewhere to the west of this location. There are no large shear zones between the Kupol and Valunistoe on Chukotka which this displacement could occur. The only possible candidate for such a shear zone the Amguemo-Kanchalan fault zone, which lies in the immediate vicinity of the Valunistoe ore deposit. To date, the scales of this zone does not seem to be able to explain such a large movement, however, the degree of its study leaves much to be desired.

The research was supported by RSF Project №23-17-00112

Chekhovich, V.D., Palandzhyan, S.A., 2021. Geodynamics of the Active Margin of Northeast Asia in the Late Cretaceous–Paleogene. Geotecton. 55, 516–530. <https://doi.org/10.1134/S0016852121040051>

Mackey, K.G., Fujita, K., Gunbina, L.V., Kovalev, V.N., Imaev, V.S., Koz'min, B.M., Imaeva, L.P., 1997. Seismicity of the Bering Strait region: Evidence for a Bering block. Geol 25, 979. [https://doi.org/10.1130/0091-7613\(1997\)025<0979:SOTBSR>2.3.CO;2](https://doi.org/10.1130/0091-7613(1997)025<0979:SOTBSR>2.3.CO;2)

Redfield, T.F., Scholl, D.W., Fitzgerald, P.G., Beck, M.E., 2007. Escape tectonics and the extrusion of Alaska: Past, present, and future. Geol 35, 1039. <https://doi.org/10.1130/G23799A.1>

Tikhomirov, P.L., Lebedev, I.E., Lhuillier, F.J.L., Pavlov, V.E., 2021a. Stratigraphy of the Okhotsk–Chukotka Belt in the Headwaters of the Malyi Anyui River (the Vicinity of Kupol Deposit): U–Pb and 40Ar/39Ar Age Data. Dokl. Earth Sc. 501, 1059–1064. <https://doi.org/10.1134/S1028334X2112014X>

Tikhomirov, P.L., Lebedev, I.E., Pasenko, A.M., Lhuillier, F.J.L., Alekseev, D.V., Pavlov, V.E., 2021b. The “Upper Basalts” of the East Chukotka Segment of Okhotsk–Chukotka Belt: the Along Strike Migration of Volcanic Activity or the Overprint by Later Magmatic Event? Dokl. Earth Sc. 501, 1038–1042. <https://doi.org/10.1134/S1028334X21120151>

Torsvik, T.H., Van der Voo, R., Preeden, U., Mac Niocaill, C., Steinberger, B., Doubrovine, P.V., van Hinsbergen, D.J.J., Domeier, M., Gaina, C., Tohver, E., Meert, J.G., McCausland, P.J.A., Cocks, L.R.M., 2012. Phanerozoic polar wander, palaeogeography and dynamics. Earth-Science Reviews 114, 325–368. <https://doi.org/10.1016/j.earscirev.2012.06.007>

Global plate reconstruction since 2 billion years: The start of the supercontinent cycle, evolving mantle dynamics, and new constraints on absolute paleolongitude

Zheng-Xiang Li¹; Yebo Liu¹; Richard Ernst²

¹: Earth Dynamics Research Group, School of Earth and Planetary Sciences, The Institute for Geoscience Research, Curtin University, GPO Box U1987, Perth, WA 6845, Australia

²: Department of Earth Sciences, Carleton University, Ottawa, ON K1S 5B6, Canada

An advanced understanding of how tectonic plates have moved since deep time is essential for understanding how Earth's geodynamic system has evolved and interacted with the plate tectonic system, i.e., the longstanding question of what "drives" plate tectonics. In this work, we take advantage of the rapidly improving database and knowledge about the Precambrian world, and the conceptual breakthroughs both regarding the presence of a supercontinent cycle and possible dynamic coupling between the supercontinent cycle and mantle dynamics, to establish a full-plate global reconstruction back to 2000 Ma. We utilise a variety of global geotectonic databases to constrain our reconstruction, and use palaeomagnetically recorded true polar wander events and global plume records to help evaluate competing geodynamic models regarding the origin and evolution of first-order mantle structures, and provide new constraints on the absolute longitude of continents and supercontinents. After revising the configuration and life span of both supercontinents Nuna (1600–1300 Ma) and Rodinia (900–720 Ma), we present here a 2000–540 Ma animation featuring the rapid assembly of large cratons and supercratons (or megacontinents) between 2000 Ma and 1800 Ma after billion years of dominance by many small cratons, that kick started the ensuing Nuna and Rodinia supercontinent cycles and the emergence of hemisphere-scale (long-wavelength) degree-1/degree-2 mantle structures. We further use the geodynamically-defined type-1 and type-2 inertia interchange true polar wander (IITPW) events, which likely occurred during Nuna (type-1) and Rodinia (type-2) times as shown by the palaeomagnetic record, to argue that Nuna assembled at about the same longitude as the latest supercontinent Pangea (320–170 Ma), whereas Rodinia formed through introversion assembly over the legacy Nuna subduction girdle either ca. 90° to the west (our preferred model) or to the east before the migrated subduction girdle surround it generated its own degree-2 mantle structure. Our interpretation is broadly consistent with the global LIP record. Using TPW and LIP observations and geodynamic model predictions, we further argue that the Phanerozoic supercontinent Pangea assembled through extroversion on a legacy Rodinia subduction girdle with a geographic centre at around 0°E longitude before the formation of its own degree-2 mantle structure, the legacy of which is still present in present-day mantle.

Work published in:

Li, Z.-X., Liu, Y., Ernst, R. (2023). A dynamic 2000–540 Ma Earth history: From cratonic amalgamation to the age of supercontinent cycle. *Earth-Science Reviews* 238, 104336. (Open access at: <https://doi.org/10.1016/j.earscirev.2023.104336>).

A new reliable ~1885 Ma paleomagnetic pole from Svecofennian gabbros of central Finland with implications to the amalgamation of Nuna

Toni Luoto^{1,2,*}; Johanna Salminen^{1,2}, Satu Mertanen², Sten-Åke Elming³, Lauri J. Pesonen⁴

¹: Department of Geosciences and Geography, University of Helsinki, Finland

²: Geological Survey of Finland

³: Luleå University of Technology, Sweden

⁴: Department of Physics, University of Helsinki, Finland

*: Corresponding author, e-mail address: toni.luoto@gtk.fi; toni.luoto@helsinki.fi

Majority of the global high-quality paleomagnetic poles are derived from mafic intrusions, as they are often reliable recorders of ancient geomagnetic field and can be precisely dated radiometrically. However, as intrusions are episodic events by nature, significant gaps exist in the global high-quality paleomagnetic record. In Fennoscandia, the majority of the Paleoproterozoic paleomagnetic data are derived from gabbro intrusions formed during the Svecofennian orogeny, one of the global 2100–1800 Ma orogenies associated with the amalgamation of the supercontinent Nuna. These intrusions have been comprehensively dated with radiometric methods, yielding age clusters at ca. 1885 Ma, 1860 Ma, 1800 Ma, and 1780 Ma. Many of these Svecofennian gabbros have been targeted for paleomagnetic investigations, but only the 1786 Ma Hoting gabbro provides a key pole with a proven primary magnetization (Elming et al. 2009).

Partly simultaneously with the Svecofennian orogeny, global high-quality paleomagnetic record indicates large oscillatory movements for several cratons. Back-and-forth movements are particularly well observed in the ca. 2020–1870 Ma high-resolution paleomagnetic data from the Slave craton compiled by Gong & Evans (2022). These oscillations have been interpreted as inertial interchange true polar wander events, basin-scale or local-scale rotations, unstable geomagnetic field, or any combination of these (Gong & Evans 2022). Just in the aftermath of global oscillating paleomagnetic record, Djeutchou et al. (2021) provided high-resolution compilation of 1890–1830 Ma paleomagnetic poles for Kalahari craton from the Black Hills Dyke Swarm and coeval regional magmatic provinces. This data indicates a period of relatively stable position for Kalahari craton at 1880–1830 Ma. High-quality 1870–1790 Ma paleomagnetic poles of Fennoscandia are tightly clustered indicating that Fennoscandia has experienced similar period of minimal apparent drift.

In this work, we targeted ca. 1885 Ma Svecofennian gabbros in central Finland with an aim to provide a new reliable pole to fill a gap at ca. 1930–1870 Ma in the paleomagnetic record of Fennoscandia. Paleomagnetism of two of the target intrusions, 1883±8 Ma Ylivieska gabbro (Patchett & Kouvo 1986) and 1886±5 Ma (Marttila 1981) Kiuruvesi gabbrodiorite, has been investigated earlier (Pesonen & Stigzelius, 1972; Neuvonen, 1981), but the sampling scheme does not meet the present-day requirements for statistics.

Paleomagnetic data obtained in this study was combined with the data provided by Pesonen & Stigzelius (1972) and Neuvonen et al. (1981) to provide a new reliable paleomagnetic pole. New pole has a well-constrained rock age of 1886±5 Ma (Marttila 1981) and 1883±8 Ma (Patchett & Kouvo 1986). It is produced from adequate number of samples to meet the present-day statistical requirements, and the paleosecular variation is statistically averaged out. Rock magnetic methods were used to identify single domain magnetite as main magnetic carrier. Subvertical dykes have been reported to crosscut the Kiuruvesi gabbrodiabase, indicating that no significant tilting has occurred after the intrusion. New pole does not overlap Phanerozoic apparent polar wander path. However, due to the magnetic instability of the host rock and the lack of unaltered unmetamorphosed crosscutting

dykes in the area, new pole lacks the paleomagnetic field tests to prove the primary nature of magnetization. However, magnetization ages of the studied gabbro intrusions are likely close to their crystallization ages, based on the cooling rates of similar gabbro intrusions. As there are no reversed polarities in the data, new pole does not pass the reversal tests. Therefore, new pole satisfies five of seven reliability criteria of Meert et al. (2020). The new pole overlaps the cluster ca. 1870–1790 Ma high-quality poles of Fennoscandia, possibly extending the period of apparent minimum drift in Fennoscandia to 1885–1790 Ma. During this period, Fennoscandia was located at ca. 35–20 °N, which is further supported by paleoclimatic indicators, such as evaporites, lateritic paleosols and stromatolite-like structures in Finland and Sweden.

In our proposed 1885 Ma reconstruction Fennoscandia and the Superior craton are located at moderate northern latitudes with connection to Kalahari (Djeutchou et al. 2021). Joint Sarmatia-Volgo-Uralia and Siberia are reconstructed on the Equator (e.g., Elming et al. 2021). The Slave craton, already assembled together with Rae and Hearne at that point (Hoffman, 2014), is reconstructed on intermediate northern latitudes, with the Manikewan Ocean separating it from the Superior craton (Stauffer 1984). This reconstruction indicates that both Baltica and Laurentia were still assembling as a part of amalgamation of the Nuna supercontinent.

We also explored the global ca. 2100–1790 Ma high-quality paleomagnetic data covering both the period of large global oscillations and its aftermath. Our purpose was to investigate if the period of minimal apparent drift observed in Fennoscandia and Kalahari in the aftermath of oscillations was a global phenomenon. Data from other cratons is scarce, but three ca. 1880–1850 Ma paleomagnetic poles from Siberia at close proximity to each other supports minimal apparent drift being a global phenomenon.

Djeutchou, C., de Kock, M. O., Wabo, H., Gaitán, C. E., Söderlund, U., Gumsley, A. P., 2021. *Geology* 49, 1375–1380. doi: 10.1130/G48811.1.

Elming, S.-Å., Moakhar, M. O., Layer, P., Donadini, F., 2009. *Geophysical Journal International* 179, 59–78. doi: 10.1111/j.1365-246X.2009.04265.x.

Elming, S.-Å., Salminen, J., Pesonen, L. J., 2021. *Paleo-Mesoproterozoic Nuna supercycle*. In Pesonen, L. J., et al. (Eds.), *Ancient Supercontinents and the Paleogeography of Earth*, Elsevier, pp. 499–548.

Gong, Z., Evans, D. A. D., 2022. *Precambrian Research* 369, 106516. doi: 10.1016/j.precamres.2021.106516.

Hoffman, P.F., 2014. *Geoscience Canada* 41, 313–320. doi: 10.12789/geocanj.2014.41.049.

Marttila, E., 1981. *Kiuruveden kartta-alueen kallioperä. Summary: Pre-Quaternary rocks of the Kiuruvesi map-sheet area. Suomen geologinen kartta 1:100 000, Kallioperäkartan selitykset, 3323 Kiuruvesi.*

Meert, J. G., Pivarunas, A. F., Evans, D. A. D., Pisarevsky, S. A., Pesonen, L. J., Li, Z.-X., Elming, S.-Å., Miller, S. R., Zhang, S., Salminen, J. M., 2020. *Tectonophysics* 790, 228549. doi: 10.1016/j.tecto.2020.228549.

Neuvonen, K. J., Korsman, K., Kouvo, O., Paavola, J., 1981. *Bulletin of the Geological Society of Finland* 53, 109–133.

Patchett, J., Kouvo, O., 1986. *Contributions to Mineralogy and Petrology* 92, 1–12. doi: 10.1007/BF00373959.

Pesonen, L. J., Stigzelius, E., 1972. *Geological Survey of Finland Bulletin* 260, 1–27.

Stauffer, M. R., 1984. *Precambrian Research*, 25, 257–281.

1005-970 Ma Sette-Daban mafic magmatic event of the Siberian Craton: Remnant of a LIP?

Sergey V. Malyshev¹, Alexander D. Savelev¹, Andrei K. Khudoley¹, Richard E. Ernst², Kevin R. Chamberlain³

¹ Institute of Earth Sciences, St. Petersburg State University, St. Petersburg, Russia

² Department of Earth Sciences, Carleton University, Ottawa, Canada

³ Department of Geology and Geophysics, University of Wyoming, Laramie, United States

The Meso- and Neoproterozoic rock succession of the southeastern margin of the Siberian Craton is cut by numerous mafic sills and dykes during the latest Mesoproterozoic – early Neoproterozoic magmatic event, commonly known as “Sette-Daban event” [1,2]. Magmatic rocks are represented mainly by sills with few dykes. The highest concentration of sills was documented in late Mesoproterozoic succession (Ui Group) where they form a significant part of the succession with total thickness close to 1100-1200 m. The thickness of individual sills varies from 1 m to 170 m, although a sill as thick as 300 m was documented as well. The total volume of mafic magmatic rocks is highest in the western parts of Sette-Daban Ridge and decreases to the west, south and southeast along with thinning of the Ui Group. Mafic dykes of the Sette-Daban complex are less numerous and they typically have approximately E-W trend [3].

Three U-Pb baddeleyite ages of the mafic intrusions are 974 ± 7 , 1005 ± 4 and 971 ± 4 Ma ([4], this study) gives evidence to estimate the duration of the magmatic event as ca. 1005-970 Ma. In the modern structure, the Sette-Daban magmatic rocks occupy an area approximately 500 km in length and 70-100 km in width and its composition and duration satisfy the characteristics of a typical LIP.

The Sette-Daban mafic intrusions are classified as subalkalic mostly low-Ti dolerites, although high-Ti dolerites have been locally documented as well. Trace element abundances in dolerites vary from typical to E-MORB to OIB with arc-like signatures represented by high Th/Yb and low TiO_2/Yb ratios. All dolerite samples display moderately positive $\epsilon Nd(t)$ values varying from +3.3 to +7.7 and indicating the magmas were derived from a depleted mantle source. Three groups of mafic intrusions with distribution corresponding to the geographical areas are identified due to variations in their chemical compositions: (i) MORB-like dolerites and (ii) high-Ti OIB-like dolerites could be explained by different degrees of partial melting while (iii) arc-like signatures inherited from the heterogeneous metasomatically enriched source region. Units with arc-like chemistry and OIB chemistry are attributed to the different degrees of interaction of magma between the depleted asthenospheric mantle and metasomatically enriched regions within the SCLM that formed during ancient subduction events. The suggested tectonic environment is thinning of SCLM due to intra-continental rifting with the possible influence of wet-diapir upwelling or distal plume head.

[1] Khudoley, A.K., Rainbird, R.H., Stern, R.A., Kropachev, A.P., Heaman, L.M., Zanin, A.M., Podkovyrov, V.N., Belova, V.N., Sukhorukov, V.I., 2001. Sedimentary evolution of the Riphean-Vendian basin of southeastern Siberia. *Precambrian Res.* 111, 129–163.

[2] Savelev, A.D., Malyshev, S. V., Savatenkov, V.M., Ignatov, D.D., Kuzkina, A.D., 2020. Meso-Neoproterozoic Mafic Sills along the South-Eastern Margin of the Siberian Craton, SE Yakutia: Petrogenesis, Tectonic and Geochemical Features. *Minerals* 10, 805.

[3] Khudoley, A.K., Kropachev, A.P., Tkachenko, V.I., Rublev, A.G., Sergeev, S.A., Matukov, D.I., Lyahnitskaya, O.Y., 2007. Mesoproterozoic to Neoproterozoic Evolution of the Siberian Craton and Adjacent Microcontinents: An Overview with Constraints for a Laurentian Connection. *Proterozoic Geol. West. North Am. Sib.* 209–226

[4] Rainbird, R.H., Stern, R.A., Khudoley, A.K., Kropachev, A.P., Heaman, L.M., Sukhorukov, V.I., 1998. U-Pb geochronology of Riphean sandstone and gabbro from southeast Siberia and its bearing on the Laurentia-Siberia connection. *Earth Planet. Sci. Lett.* 164, 409–420.

Graben Systems of Sith and Khabuchi Coronae along Dali Chasma, Southwest of Atla Regio, Venus.

M.A. Mediany¹, H. El Bilali^{2,3}, R.E. Ernst^{2,3}, J.W. Head⁴, N. Youbi^{1,3}

¹Department of Geology, Faculty of Sciences-Semlalia, Cadi Ayyad University, Marrakesh, Morocco; acheraf17@gmail.com,

²Department of Earth Sciences, Carleton University, Ottawa, Ontario, Canada;

³Faculty of Geology and Geography, Tomsk State University, Tomsk, Russia

⁴Department of Earth, Environmental and Planetary Sciences, Brown University, Providence, Rhode Island, USA

The Dali-Diana Chasmata (rift zone) trends SW from Atla Regio (Fig. 1). This region is part of Quadrangle V-37 which has been mapped at 1:5,000,000 scale (Hansen and DeShon, 2003). The present detailed 1:500,000 scale study focuses on the magmatic component along Dali Chasma and specifically, the grabens associated with two important coronae along Dali Chasma, Sith (Si) and Khabuchi (K) coronae. This study builds on the previous mapping reported in (Mediany et al 2022). Detailed mapping of the graben sets associated with corona in rift systems (in this case Khabuchi and Sith coronae) will further elucidate the nature of the frequent association of coronae with rift systems (Hamilton and Stofan, 1996; Martin and Stofan, 2004). Detailed mapping of graben (32,000 lineaments to date) reveals a complex distribution of radiating, linear and circumferential graben sets, distinguished by color (in Fig 2). On the basis of criteria discussed in (Grosfils and Head, 1994; Buchan and Ernst, 2021) we provisionally interpret these graben systems as the surface expression of dyke swarms. We distinguish 12 different swarms, that allow us to identify at least 6 magmatic centres (3 for Khabuchi Corona and 2 for Sith Corona and a final one for an unidentified centre, as well as a circumferential system around Sith Corona) (Fig. 2A). To improve the visualization of these distributions and relationships, we produced generalized distributions of each graben sets (Fig. 2B). Two radiating swarms (shades of green lines) are centered on Khabuchi Corona. Two radiating systems are associated with the Sith (shades of blue lines), as well as the unnamed system in pink. The Khabuchi radiating swarm (green) has a maximum radius >400 km and transitions from radiating to a more linear SSW trend after about 100 km. Such relationships indicate the transition from a central radial stress to the regional stress field and may indicate the radius of an underlying upwelling diapir (Buchan and Ernst, 2021). Other graben sets associated with the Khabuchi centre generally have trends suggesting links to multiple radiating centres within the corona, a feature that has been noted for other coronae (Ernst et al., 2003). For Sith Corona, its radial system extends more than 500 km NE towards Atla Regio. A large circumferential system is identified around Sith Corona as well.

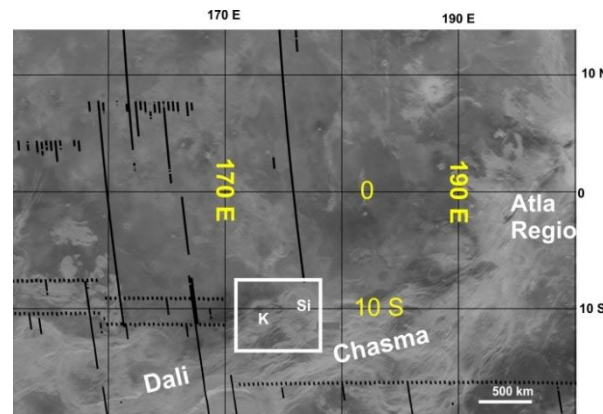


Figure 1 : Location map for study area along Dali Chasma.

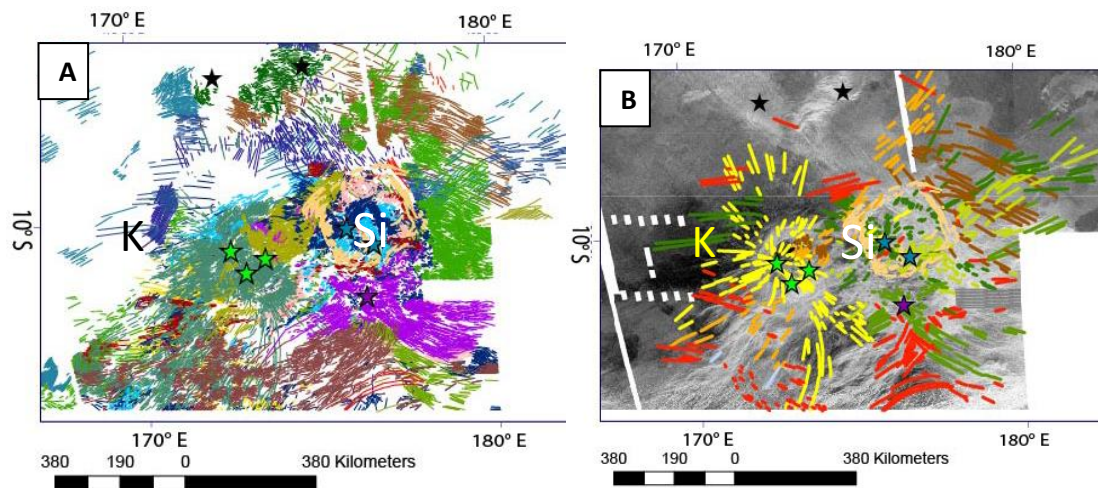


Figure 2 : (A) Detailed mapping of graben in the study area and coding by colour into sets based on geometry: linear, radiating or circumferential. (B) Generalized graben distributions distinguished by colour. Superimposed on Magellan SAR image

References:

- Buchan, K.L., Ernst, R.E., 2021. Plumbing systems of large igneous provinces (LIPs) on Earth and Venus: Investigating the role of giant circumferential and radiating dyke swarms, coronae and novae, and mid-crustal intrusive complexes. *Gondwana Res.* 100, 25–43.
- Cawood, P.A., Pisarevsky, S.A., 2017. Laurenti. Ernst, R.E., Desnoyers, D.W., Head, J.W., and Grosfils, E.B. (2003) Graben-fissure systems in Guinevere Planitia and Beta Regio (264-312°E, 24-60°N), Venus, and implications for regional stratigraphy and mantle plumes. *Icarus* 164: 282-316.
- Grosfils, E.B., and Head, J.W. (1994) The global distribution of giant radiating dike swarms on Venus: implications for the global stress state. *Geophys. Res. Lett.* 21, 701-704.
- Hamilton, V.E. and Stofan, E.R. (1996), *La géomorphologie et l'évolution d'Hécate Chasma, Vénus*, *Icarus*, 121, 171-194.
- Hansen, V.L., and DeShon, H.R. (2003), *Carte géologique du quadrilatère de Diana Chasma (V-37), Venus: US Geological Survey Geologic Investigations Series I-2752.*
- Martin, P., and Stofan, E.R. (2004), *Coronae of Parga Chasma, Venus*, *Lunar Planet. Sci.*, XXXV, Abstract 1576.
- Mediany, M.A., El Bilali, H., Ernst, R.E., Head, J.W., and Youbi, N. (2022), *Graben Systems Of Sith And Khabuchi Corona Along Dali Chasma, Southwest Of Atla Regio, Venus*, *LPSC abstr.* 1252.
- Mediany, M.A., El Bilali, H., Ernst, R.E., Head, J.W., and Youbi, N. (2023), *Graben Systems (Interpreted as Dyke Swarms) of Sith And Khabuchi Coronae Along Dali Chasma, Southwest of Atla Regio, Venus.*, *LPSC abstr.* 1397.

Evolving mantle convection from bottom up to top down

Ross N. Mitchell¹ ; Michael Brown²; Thomas M. Gernon³; Christopher J. Spencer⁴

¹: State Key Laboratory of Lithospheric Evolution, Institute of Geology and Geophysics, Chinese Academy of Sciences, Beijing 100029, China

²: Laboratory for Crustal Petrology, Department of Geology, University of Maryland, College Park, MD 20742, USA

³: School of Ocean and Earth Science, University of Southampton, Southampton SO22 4JR, UK

⁴: Department of Geological Sciences and Geological Engineering, Queen's University, Kingston, ON K7L 2N8, Canada

When it comes to convection, what goes up must come down. Or is it, what goes down must come up? The truth is, it depends. Although convection must be mass-balanced, there is no reason that it must be force-balanced: the positive and negative buoyancy forces driving convection up and down, respectively, do not necessarily need to be balanced. The balance, or imbalance, all depends on the top and bottom boundary layers. Thus, convection in Earth's mantle depends on the temperature differences across the core–mantle boundary (CMB) below and the lithosphere–asthenosphere boundary (LAB) above. Convective asymmetry predominated by positive buoyancy, or bottom-up convection, would be driven by plume ascent, whereas if it were predominated by negative buoyancy, or top-down convection, would be driven by plate subduction. Symmetric convection would balance plume ascent and plate subduction. Is mantle convection on Earth balanced, dominantly top-down or bottom-up, or time dependent? Symmetric convection—balanced vigor of down- and upwelling—is unlikely for Earth's mantle for various fundamental reasons such as internal heating, temperature-dependent viscosity, and sphericity (Bercovici et al., 2015). Naturally, then, there is debate over whether Earth's geodynamics is predominantly top down or bottom up. Evidence for both deep subduction and deep-rooted mantle plumes exists; however, the antiquity of the former and the prevalence of the latter are often questioned. We propose that convective asymmetry evolving over time—from bottom up to top down predominating, with balanced convection occurring in between—may reconcile these two criticisms. If the balance of mantle convection has shifted from being dominated by upwelling to downwelling through time, then there should be a progression in the conditions of mantle melting.

We identify changes in the abundances of komatiites, anorthosites, and kimberlites through time that support an evolution from bottom-up asymmetric, to symmetric, to top-down asymmetric geodynamics, respectively (Mitchell et al., 2022). To be clear, we are not proposing a petrogenic connection between these disparate rock types but rather an underlying connection between them as an evolving record of mantle heat. This sequence of rock types reflects high-temperature mantle melting or higher heat flow into the crust dominating, in turn, from komatiites, to anorthosites, to kimberlites through time. Notably, straddling the interval of symmetric convection characterized by anorthosite magmatism, the two transitions—the Palaeoproterozoic demise of bottom-up convection and the Neoproterozoic rise of top-down convection—each coincide with an indicator of the increasing predominance of subduction over time: the earliest occurrence of high-pressure and the beginning of common (or widespread) ultrahigh-pressure metamorphism (Brown et al., 2020), respectively (Fig. 1). We suggest that recognizing the transition in convective asymmetry provides a critical geological constraint for understanding how secular trends in mantle cooling and properties have evolved over time.

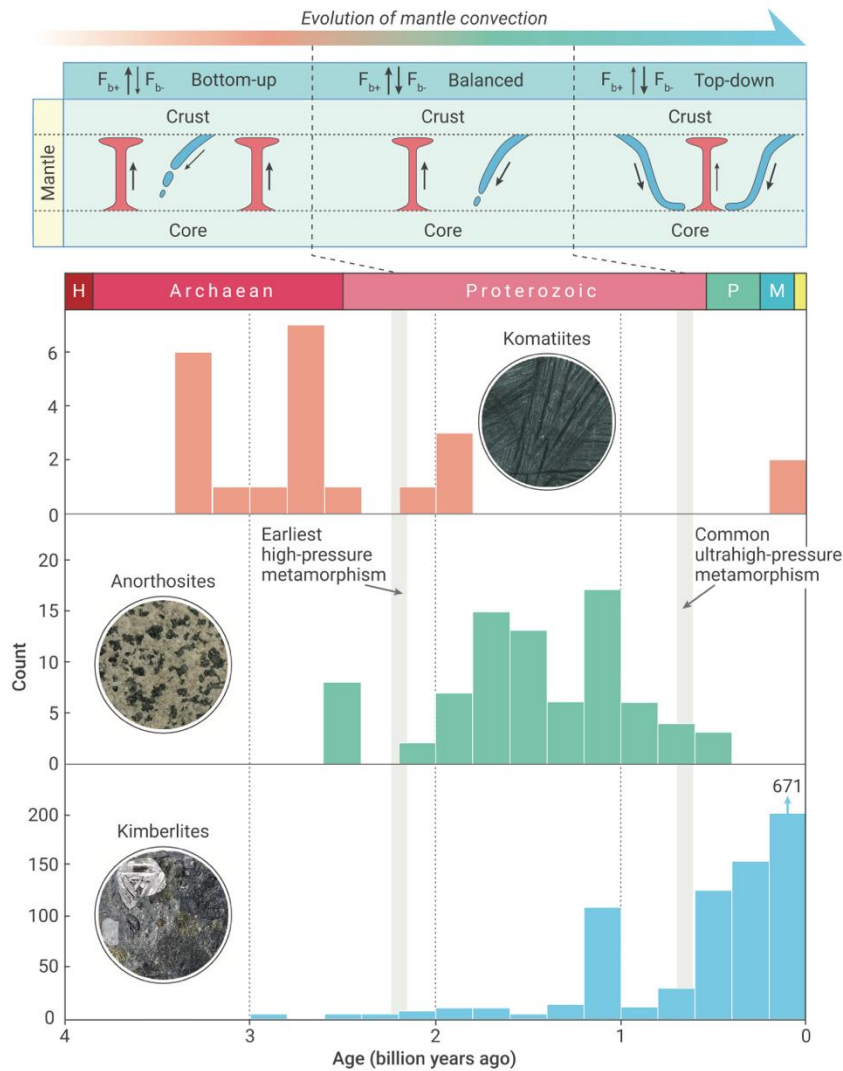


Figure 1. Evidence from changing mantle melts for the evolution of mantle convection over time (Mitchell et al., 2022). Histograms of komatiites (Barnes and Arndt, 2019), anorthosites (Ashwal and Bybee, 2017), and kimberlites (Tappe et al., 2018). Gray bars show ages of the earliest occurrences of high-pressure and ultrahigh-pressure metamorphism, which reflect the evolution of subduction over time (Brown et al., 2020). H, Hadean; P, Palaeozoic; M, Mesozoic; yellow, Cenozoic; F_{b+} , positive buoyancy force; F_{b-} , negative buoyancy force.

References

- Ashwal, L. D., and Bybee, G. M., 2017, Crustal evolution and the temporality of anorthosites: *Earth-Science Reviews*, v. 173, p. 307-330.
- Barnes, S. J., and Arndt, N. T., 2019, Chapter 6 - Distribution and Geochemistry of Komatiites and Basalts Through the Archean, *in* Van Kranendonk, M. J., Bennett, V. C., and Hoffmann, J. E., eds., *Earth's Oldest Rocks (Second Edition)*, Elsevier, p. 103-132.
- Bercovici, D., Tackley, P. J., and Ricard, Y., 2015, The Generation of Plate Tectonics from Mantle Convection, *in* D. Bercovici editor; G. Schubert, e. i. c., ed., *Treatise in Geophysics*, 2 ed., vol. 7, *Mantle Dynamics*: New York, Elsevier.
- Brown, M., Johnson, T., and Gardiner, N. J., 2020, Plate Tectonics and the Archean Earth: *Annual Review of Earth and Planetary Sciences*, v. 48, p. 12.11-12.30.
- Mitchell, R. N., Brown, M., Gernon, T. M., and Spencer, C. J., 2022, Evolving mantle convection from bottom up to top down: *The Innovation*, v. 3, no. 6.
- Tappe, S., Smart, K., Torsvik, T., Massuyeau, M., and de Wit, M., 2018, Geodynamics of kimberlites on a cooling Earth: Clues to plate tectonic evolution and deep volatile cycles: *Earth and Planetary Science Letters*, v. 484, p. 1-14.

Physical volcanology and geochemistry of the Triassic-Jurassic CAMP basaltic lava flows: Insights from the Middle Atlas and Midelt sequences (Morocco).

Abdelhak Moumou¹, Nasrddine Youbi², Hind El Hachimi³, José Madeira⁴, Andrea Marzoli⁵, Hervé Bertrand⁶, Mohamed Khalil Bensalah⁷, Línia Martins⁴, João Mata⁴, Fida Medina⁷, Moulay Ahmed Boumechdi² and Mohamed Ben Abbou⁸

¹Geology Department, Faculty of Sciences, Abdelmalek Essaadi University, 2117, Tetouan, Morocco. e-mail: moumou.abdelhak@gmail.com

²Geology Department, Faculty of Sciences-Semlalia, Cadi Ayyad University, Prince Moulay Abdellah Boulevard, P.O. Box 2390, Marrakech, Morocco, e-mail: youbi@uca.ac.ma

³Geology Department, Faculty of Sciences, Chouaib Doukkali University, 24000, El Jadida, Morocco. e-mail: elhachimi.h@ucd.ac.ma

⁴Instituto Dom Luiz, Faculdade de Ciências, Universidade de Lisboa, 1749-016 Lisboa, Portugal.

⁵Dipartimento di Geoscienze, Università di Padova, Italy.

⁶Laboratoire Sciences de la Terre, ENS de Lyon et UCBL, 46, Allée d'Italie, 69364 Lyon, France.

⁷Laboratory Geotol (URAC 46), Scientific Institute, University Mohammed V-Agdal, Rabat, Morocco.

⁸Geology Department, Faculty of Sciences Dhar Al Mahraz, Sidi Mohammed Ben Abdellah University, Fès, Morocco.

The Central Atlantic Magmatic Province (CAMP) is one of the largest Continental Flood Basalt (CFB) provinces in the world (Marzoli et al. 1999) covering an area in excess of 10 million km² on the supercontinent Pangaea at about 201 Ma. The morphology, internal architecture and geochemistry of the Central Atlantic Magmatic Province (CAMP) lava flows of Middle Atlas and Midelt sequences in Morocco are presented.

The field survey and correlation of several sections across the Middle Atlas volcanic pile and Midelt sequence, supported by whole-rock geochemistry, showed that it is composed of three formations (“lava flow fields”) that are the product of three successive but separate eruptions. These formations are similar to the lower, intermediate, and upper formations of the CAMP in the High Atlas, which suggests a synchronous inception of the volcanic activity in the two regions. The lower formation corresponds to a succession of 4 to 11 individual flows created by 1 to 2 eruptions; the intermediate formations, composed of 2-5 individual flows formed by 1-3 eruptions and the upper formation composed of 1 individual flow created by 1 eruption. These formations are separated by thin silty or sandy horizons or by paleosols that represent minor periods of volcanic inactivity. The CAMP flows of the Middle Atlas and Midelt can be grouped into ‘compound pahoehoe flows’ and ‘simple flows’. The largest lobes as well as several small lobes forming the compound pahoehoe flows are typically characterized by the threefold structure comprising a thin vesicular basal crust, a dense core, and a thick vesicular upper crust. The simple flows appear as single cooling units without multiple flow lobes.

The basalts from the three formations yield distinct geochemical compositions. The primary paragenesis is typical of continental tholeiites. Their major and trace element concentration and ratios match respectively the composition of the Lower, Intermediate and Upper Formations from the Central High Atlas (Bertrand et al., 1982; Aït Chayeb et al., 1998; Youbi et al., 2003; Marzoli et al. 2004; Deenen et al., 2010). The Recurrent Formation, which complete the volcanic sequence in the Central High Atlas, is absent in the Middle Atlas and Midelt sequences.

References

Aït Chayeb, E. H., Youbi, N. ; EL Boukhari, A. ; Bouabdelli, M. & Amrhar, M., 1998. Le volcanisme Permien et Mésozoïque inférieur du bassin d'Argana (Haut-Atlas occidental, Maroc): un magmatisme intraplaque associé à l'ouverture de l'Atlantique central. *Journal of African Earth Sciences*, 26, 4, 499-519.

Bertrand, H., Dostal, J., Dupuy, C., 1982. Geochemistry of early Mesozoic tholeiites from Morocco. *Earth and Planetary Science Letters*, 58, 225-239.

Deenen, M.H.L. 2010. *A new chronology for the late Triassic to early Jurassic. PhD thesis, Utrecht, Geologica Ultraiectina No. 323 Universiteit Utrecht, <http://igitur503.archive.library.uu.nl/dissertations/2010-0414-200155/UUindex.html>.*

El Hachimi, H. Youbi, N., Madeira, J., Marzoli, A., Mata, J., Bertrand, H., Bensalah, M.K., Boumehdi, M.A., Doblás, M., Medina, F., Ben abbou, M., and Martins, L., 2020. *Physical volcanology and emplacement mechanism of the Central Atlantic Magmatic Province (CAMP) lava flows from the Central High Atlas, Morocco. Comptes Rendus Géosciences, 352, 2, 135-153. <https://doi.org/10.5802/crgeos.7>*

Marzoli, A., Bertrand, H., Knight, K.B., Cirilli, S., Buratti, N., Vérati, C., Nomade, S., Renne, P.R., Youbi, N., Martini, R., Allenbach, K., Neuwerth, R., Rapaille, C., Zaninetti, L. & Bellieni, G., 2004. *Synchrony of the Central Atlantic magmatic province and the Triassic–Jurassic boundary climatic and biotic crisis. Geology, 32, 973-976.*

Marzoli, A., Bertrand, H., Knight, K.B., Cirilli, S., Buratti, N., Marzoli, A., Renne, P.R., Piccirillo, E.M., Ernesto, M., Bellieni, G. and De Min, A., 1999. *Extensive 200-million-year-old continental flood basalts of the Central Atlantic Magmatic Province. Science, 284, 616-618.*

Youbi, N., Martins, L.T., Munha, J.M., Ibouh, H., Madeira, J., Ait Chayeb, H. & El Boukhari, A. 2003. *The Late Triassic-Early Jurassic Volcanism of Morocco and Portugal in the Framework of the Central Atlantic Magmatic province: An Overview. In: J.G.M. W. E. Hames, P. R. Renne, C. Ruppel (eds), The Central Atlantic Magmatic Province: Insights from Fragments of Pangea. AGU Geophysical Monograph Series, 136, 179-207.*

Geological analysis of a caldera cluster (21.5 N, 201.5 E), located NE of Atla Regio, Venus.

Moutbir O.¹; El Bilali H.^{2,3}; Ernst R.E.^{2,3}; Head J.W.⁴; Youbi N.^{1,3}

¹: Department of Geology, Faculty of Sciences-Semlalia, Cadi Ayyad University, Marrakesh, Morocco, oussma.moutbir2@gmail.com,

²: Department of Earth Sciences, Carleton University, Ottawa, Ontario, Canada,

³ Faculty of Geology and Geography, Tomsk State University, Tomsk, Russia

⁴: Department of Earth, Environmental and Planetary Sciences, Brown University, Providence, Rhode Island, USA.

Introduction: On Venus, a typical caldera is defined as “circular to elongate in shape, surrounded by an annulus of closely spaced fractures along the topo-graphic rim, a floor from 1 to 3 km below the surrounding terrain, and evidence for associated surface volcanism” (Crumpler and Aubele, 2000; Head et al., 1992).

In this contribution we aim to explore the various stages of collapse in a caldera cluster (labeled C1) located in the northeastern region of the Atla Regio Quadrangle (V-26) (Fig. 1). We will accomplish this by analyzing the fracture systems and lava flows of the caldera cluster to gain insight into its geological evolution. The area also features three additional calderas (C2, C3, and C4) (Fig.2). While detailed mapping at 1:500,000 scale of the Atla Regio region is currently underway by (El Bilali et al., 2021 and 2022), the northern quadrangle V-14 (north of 25 N) has already been mapped at a scale of 1:5,000,000 by (Grosfils et al., 2011). Additionally, Studd et al. (2011) has conducted a detailed mapping of the Ulfrun Regio area to the east, focusing on graben systems.

Graben Systems: Four main graben system, interpreted to overlie dyke swarms (e.g. Buchan and Ernst, 2021), are present in the study area (Fig. 2). The ENE-WSW trending graben set (blue) covers almost the entirety of the study area and may have originated from Asintmah Corona (25.9°N, 208°E), which is situated 800 km to the ENE. Although the N-S trending grabens (yellow) and the trending NNE-SSW grabens (purple) must have originated from magmatic centers outside of the area, their specific sources have not been identified yet. Furthermore, a dense network of NW-SE trending wrinkle ridges is also present. The three main regional graben sets, interpreted as dyke swarms with ENE-WSW, N-S, and NNE-SSW trends, as well as the NW-SE wrinkle ridges, are older because they have been cross-cut by caldera structures and associated lava flows. The N-S graben set is older than the ENE-WSW graben set, associated with Asintmah Corona, because it has been cut by it. Furthermore, the wrinkle ridges are younger than the other two graben sets, as they clearly crosscut them.

Caldera and associated fractures: Four calderas are present in the study area (see Fig. 3a). Among them, three have experienced at least two stages of collapse, while the most complex one (C1) has undergone over 5 collapse stages (see Fig. 3b). Each collapse stage of a caldera is typically linked with annular structures and, sometimes, with lava flows. Circumferential fractures (also possibly overlying dykes) labeled as S1 and S2, which have a diameter of approximately 100 km, are part of the C1 caldera cluster or potentially an even older and larger corona that has been obscured by C1.

Flows Associated with Caldera Collapse: The distribution of lava flows in the study area indicates multiple phases of volcanic activity, resulting in a heterogeneous pattern. The northern side of the C1 caldera cluster, which is the most complex one, is covered by the down-slope distribution of a lava flow identified as fC1-a (Fig. 4). The source of this flow is the youngest caldera, C1a, which has an elliptical fracture system and a magma reservoir inferred below it. Therefore, fC1-a is the most recent lava flow in this region. The center of the C1a caldera is occupied by fC1-d and part of the fC1-c flow. The fC1-d is divided into separate lobes located in the northwest and southeast of C1, and it is covered by the fC1-c flow (Fig. 4). The fC1-c originates from the C1c caldera. Although it is possible that its flows may have been concealed by the younger flows, C1b is a small caldera without any apparent associated lava flows. In the western part of C1, a radar-bright flow (fC1-g) seems to originate either at a normal fault (part of the rift zone, as described below) or at the annular structures of a caldera stage. The lava flow fC1-g appears to be younger than fC1-d as its boundary has a lobate shape on fC1-d (Fig. 4). However, it is older than flow fC1-h, which is indicated by the boundary geometry and cross-cutting relationships (flow lobes are superimposed on the fC1-h flow; Fig 4). Although the

origin of fC1-h flow is not yet determined, we provisionally suggest that it originates from normal faults associated with a rift to the southwest of the Caldera complex C1. We are currently incorporating our detailed mapping and stratigraphic relationships into an updated synthesis of the geological and geodynamic history of the region.

References: Crumpler L.S. and Aubele J.C. (2000), in *Encyclopedia of Volcanoes*, Acad. Press. Head J.W. et al. (1992), *JGR*, 97, 13153-13197. El Bilali, H. et al. (2021) *LPSC Abstr.* 2529. El Bilali, H. et al. (2022) *LPSC Abstr.* 1256. Grosfils, E., et al. (2011) *USGS SIM* 3121. Studd, D. et al. (2011) *Icarus*, 215, 279-291. Buchan, K.L. and Ernst, R.E. (2021) *Gondwan. Res.*, 100, 25–43.

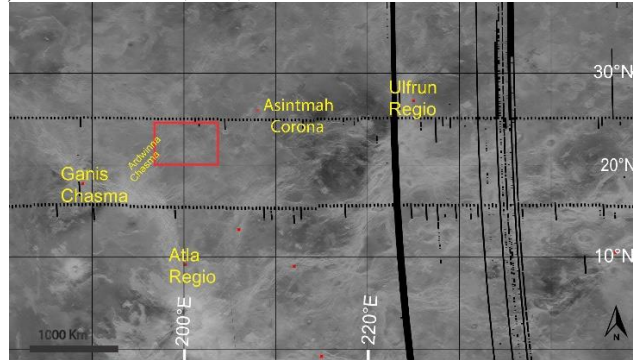


Figure 1. Regional setting with red box locating study area, on background SAR (synthetic aperture radar) of 1989-1994 Magellan mission.

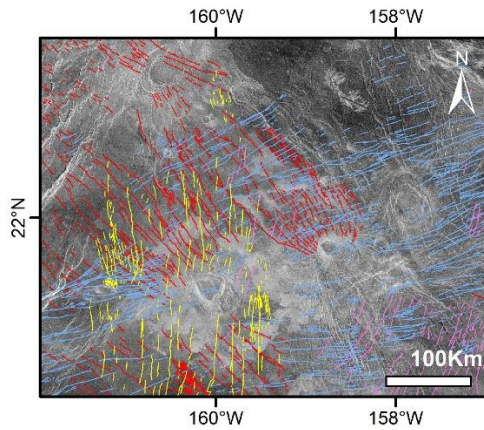


Figure 2. Distribution of linear graben sets in the study area: ENE-WSW trend (blue), N-S trend (yellow), NNE-SSW trend (purple) and NW-SE trending wrinkle ridges (red).

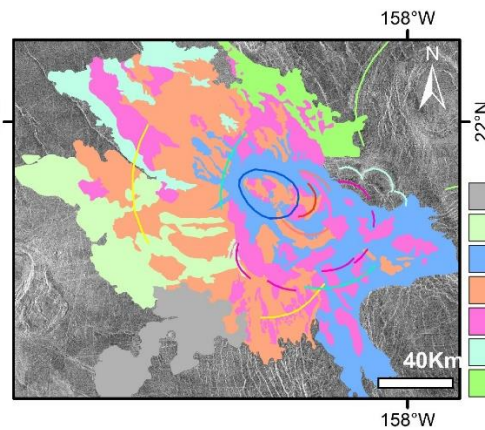


Figure 4. Distribution of mapped lava flows in C1 Caldera complex area superimposed on Magellan SAR image. (fC4 and fC1-x are not described in the text).

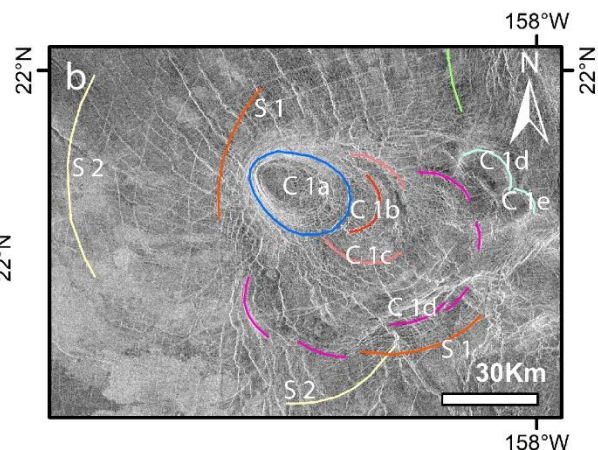
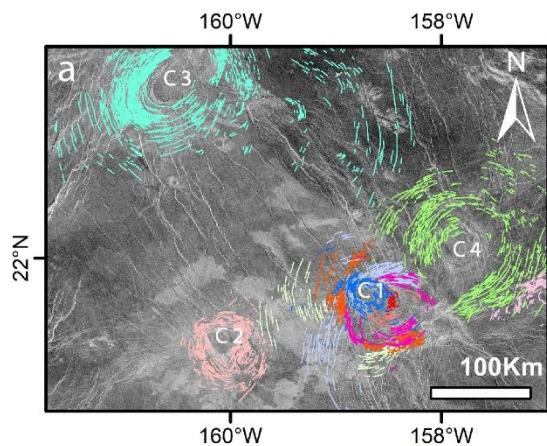


Figure 3. Circumferential graben systems, superimposed on Magellan SAR image. a) detailed linework of the broader study area; b) generalized linework related to different stages of the Caldera complex C1.

The Jebilet-Rehamna-Fourhal Large Igneous Province of 348-340 Ma (Meseta, Variscan Belt, Morocco): U-Pb geochronology, geochemistry, and links with coeval magmatism on other crustal blocks.

Moutbir O. ⁽¹⁾; Ait Lahna A. ⁽¹⁾; Youbi N. ^{(1), (2)}; Tassinari C.C.G. ⁽³⁾; Boumehdi M.A. ⁽¹⁾; Bensalah M.K. ⁽¹⁾; Ernst R.E. ^{(2), (4)}; El Bilali H. ^{(2), (4)}; I. Hadimi ⁽¹⁾

¹: Department of Geology., Faculty of Sciences-Semlalia, Cadi Ayyad University, Prince Moulay Abdellah Boulevard, P.O. Box 2390, Marrakech, Morocco, (oussama.moutbir2@gmail.com, aitlahna.abdelhak@gmail.com, youbi@uca.ac.ma).

²: Faculty of Geology and Geography, Tomsk State University, 36 Lenin Ave, Tomsk 634050, Russia,

³: Centro de Pesquisas Geocronológicas (CPGeo), Instituto de Geociências (IG), Universidade de São Paulo-USP, Caixa Postal 11348, CEP 05422-970, São Paulo (SP), Brazil,

⁴: Department of Earth Sciences, Carleton University, 1125 Colonel By Drive, Ottawa, Canada K1S 5B6.

The Mesetian Domain represents a part of the Moroccan Variscan belt. It's separated by the Middle Atlas folded belt into two structural domains: the Eastern and the Western Meseta. The latter comprise the basins of Jebilets, Rehamna and Fourhal (Central Hercynian Massif of Morocco) which show important similarities of tectono-sedimentary evolution during Early Carboniferous. Their deposits record large instabilities and disorganization with enormous thickness and lithological variations caused syn-sedimentary tectonic movements. Meanwhile, tilted block tectonics affect the basement of these basins, controlled by bordering transfer faults. These basins have recognized magmatic activities during the Carboniferous period similarly to other areas in Morocco. These magmatic rocks, of mantle origin and of tholeiitic to transitional affinity, constitute a magmatic province mainly of gabbroic intrusions, mafic sills and dykes, and basaltic lavas, associated to subordinate layered ultramafic intrusions and felsic volcanic/intrusive rocks. Based on U-Pb sensitive high-resolution ion microprobe (SHRIMP) and laser ablation-inductively coupled plasma-mass spectrometry (LA-ICP-MS) on zircon, 6 new ages are obtained from various rocks in this province, combined to the previously obtained U-Pb ages, we can state that the magmatism occurring between 349 and 340 Ma is coeval with the Eastern Meseta volcanism in northeastern Morocco. The opening of the Jebilet basin would be linked to an East-West and a North-South major accidents, as has been suggested in other basins of the western meseta: Sidi Bettache, Central Morocco, Rehamna and Guemassa. Considering the importance of these accidents, we can link the distension origin of the western Meseta magmatism to an opening (extension) in a pull-apart system according to strike-slip faults. The placement of these magmatic rocks shows a remarkable age similarity with the Tazekka-Debdou-Mekkam igneous rocks in eastern Meseta, the likely 345-340 Ma Southern Vosges magmatism and other equivalents such as 353-346 Ma St. Jean du Doigt bimodal layered intrusion (Brittany, France), in combination with the tectonic reconstruction of northwestern Gondwana ca. 350 Ma ago. These magmatic rocks may represent the erosional and/or deformational remnants of a large igneous province, which we call the Jebilets-Rehamna-Fourhal LIP.

Constraining the chronology of Ghaap Plateau dykes in the western proto-Kalahari Craton, South Africa

Rebeun Ngobeli¹, Hervé Wabo¹, Clarisa Vorster¹ and Michiel de Kock¹

¹: Paleoproterozoic Mineralization Research Group (PPM Research Group), Department of Geology, University of Johannesburg ; PO Box 524 Aucklandpark 2006 Johannesburg, South Africa.

In Large Igneous Provinces (LIPs), dyke swarms constitute the link between the melts generated at depths and volcanic end products erupted at the surface. The proto-Kalahari craton in Southern Africa (i.e., the conjoined Kaapvaal craton, Limpopo Metamorphic Complex, Zimbabwe Craton and surrounding Palaeoproterozoic orogenic belts, which later became part of the Kalahari craton) is host to numerous Precambrian dyke swarms that may relate to LIPs. Previous studies in the western part of the proto-Kalahari craton have identified five Precambrian dyke swarms thus far. These dyke swarms, in chronological order, are related to the ~2.4 Ga Ongeluk LIP (Kampmann et al., 2015, Gumsley et al., 2017), the ~1.93 Ga Hartley event (Alebouyeh Semami et al., 2016), the ~1.8 Ga intraplate magmatism (Ncube et al., 2023), the ~1.1 Ga Umkondo LIP (de Kock et al., 2014) and finally the ~0.792- 0.788 Ga Gannakouriep event (Rioux et al., 2010, Hanson et al., 2011). Despite the above-mentioned studies, several dykes associated with the Ghaap Plateau in the Griqualand West basin in the western part of the Proto-Kalahari craton still lack analytical information (geochronology, paleomagnetism, petrology). These dykes (hereby named the Ghaap Plateau dykes) are traceable as strong magnetic lineaments with some showing the same NE-trend as the ~1.93 Tsineng Dyke Swarm further to the west. In order to thoroughly investigate these Ghaap Plateau dykes, a total of 19 sites consisting of dykes with NW-trend (8), NE-trend (7), N-trend (1) and E-trend (1) were sampled either from surface outcrops or by percussion drilling where there was no suitable outcrop. Surface samples were further collected from 2 mafic sills. All of the sampled sites are considered for petrology, geochemistry and geochronology (baddeleyite U-Pb dating). Furthermore, paleomagnetic sampling was achieved at sites with suitable in-situ outcrops. Preliminary petrographic results reveal that samples are generally well-preserved dolerites mainly composed of plagioclase and clinopyroxene. Samples can be geochemically arranged into four groups. i.e., A, B, C and D. These groups display wide compositional ranges, different Mg#, and various levels of rare earth elements enrichments that suggest links to distinctly different parental magmas. When compared to existing geochemical data in the proto-Kalahari craton, Group A dykes (E-trend and ENE-trend) and Group B dyke (N-trend) show some geochemical resemblance to rocks of ~0.18 Ga Karoo and ~2.4 Ga Ongeluk Large Igneous Provinces (LIPs) respectively. Group C samples (NE and NW trends) share compositional similarities with ~1.11 Ga Umkondo-related units. This view is consistent with the paleomagnetic signature (north and shallow) revealed by one sill site of Group C. Group D dykes (NE and NW trends) are geochemically compatible with the ~1.93 Ga Hartley LIP and also the younger ~1.8 Ga Black Hills dykes. The paleomagnetic results of three Group D dykes reveal characteristic magnetizations (southeast and upward) that show resemblance to the ~1.93 Ga remanent directions, and also to the younger ~1.8 Ga remanent directions (Ncube et al., 2023; Alebouyeh Semami et al., 2016). The above dataset supports the interpretation that the Ghaap Plateau dykes are probably not related to a single magmatic event, but represent swarms of different generations. Our results need to be further constrained by baddeleyite U-Pb age dating and we are in the process of extracting baddeleyite grains from samples for this purpose.

References

- Alebouyeh Semani, F., de Kock, M., Söderlund, U., Gumsley, A., da Silva, R., Beukes, N., Armstrong, R., 2016. *New U–Pb geochronologic and paleomagnetic constraints on the late Paleoproterozoic Hartley magmatic event: evidence for a potential large igneous province in the Kaapvaal Craton during Kalahari assembly, South Africa. GFF 138, 166–185.*
- Gumsley, A.P., Chamberlain, K.R., Bleeker, W., Söderlund, U., de Kock, M.O., Larsson, E.R., Bekker, A., 2017. *Timing and tempo of the great oxidation event. Proceedings of the National Academy of Science USA, 114, 1811–1816.*
- Hanson, R.E., Rioux, M., Bowring, S.A., Gose, G.A., Bartholomew, L.T., Kilian, T.M., Evans D.A., Panzik, J.E., Hoffmann, K.H., Reid, D.L., 2011. *Constraints on Neoproterozoic intraplate magmatism in the Kalahari craton: geochronology and paleomagnetism of ~890–795 Ma extension-related igneous rocks in SW Namibia and adjacent parts of South Africa. In: Geological Society of America Abstracts with Programs, vol 5, p 371*
- Kampmann, T.C., Gumsley, A.P., de Kock, M.O., Söderlund, U., 2015. *U-Pb geochronology and paleomagnetism of the Westerberg Sill Suite, Kaapvaal Craton – support for a coherent Kaapvaal-Pilbara Block (Vaalbara) into the Paleoproterozoic? Precambrian Research, 269, 58–72.*
- Ncube, S., Wabo H., Owen-Smith, T.M., Gumsley A.P., Beukes, N.J., 2023. *The Pudukush gabbro in Griqualand West, South Africa: extending ca. 1.89 to 1.83 Ga intraplate magmatism across the proto-Kalahari Craton. South African Journal of Geology, 126, 75-92.*
- Olsson, J.R., Klausen, M., Hamilton, M., März, N., Söderlund, U., Roberts, R.J., 2016. *Baddeleyite U-Pb ages and geochemistry of the 1875–1835 Ma Black Hills Dyke Swarm across north-eastern South Africa: part of a trans-Kalahari Craton back-arc setting? GFF 138 (1), 183–202.*
- Rioux, M., Bowring, S.A., Dudás, F., Hanson, R.E., 2010. *Characterizing the U-Pb systematics of baddeleyite through chemical abrasion: application of multi-step digestion methods to baddeleyite geochronology. Contributions to Mineralogy and Petrology, 160, 777–801.*

GEOLOGICAL HISTORY OF ITOKI FLUCTUS (A LARGE LAVA FLOW SYSTEM) ON VENUS

K. Ouaskioud¹ ; H. El Bilali^{2,3} ; R.E. Ernst^{2,3} ; J.W. Head⁴ ; N. Youbi¹

¹: Department of Geology, Faculty of Sciences-Semlalia, Cadi Ayyad University, Marrakesh, Morocco; ouaskioudkhalid84@gmail.com;

²: Department of Earth Sciences, Carleton University, Ottawa, Ontario, Canada; hafidaelbilali@cunet.carleton.ca; richard.ernst@ernstgeosciences.com.

³: Faculty of Geology and Geography, Tomsk State University, Tomsk, Russia;

⁴: Department of Earth, Environmental and Planetary Sciences, Brown University, Providence, RI, USA.

Introduction: Flucti represent large basaltic lava flow fields on Venus. More than 200 extend over at least 50,000 km², and are interpreted to be analogous to terrestrial flood basalts associated with Large Igneous Provinces (LIPs) (Magee et al., 2001; Ernst, 2014). At the regional scale, these flucti have been classified and analyzed; however, detailed mapping is needed to identify their sources and potential link to other magmatic components of LIP-like events. We have selected Itoki Fluctus for the present detailed study.

Methodology: We used SAR and topography data from the NASA Magellan mission, and ArcGIS v 10.8.2 for mapping. Our strategy in mapping graben-fissure lineaments was based on an interpretation that they are mainly underlain by dykes and are grouped into swarms (radiating, circumferential, and linear (Buchan and Ernst et al., 2021; Ernst et al., 2022)). Normal faults associated with rift zones were also distinguished. The strategy in the mapping of lava flows was to draw boundaries based on differences in texture, morphology, and radar brightness.

Itoki Fluctus: Itoki Fluctus is the largest flow field mapped within the Taussig Quadrangle V39 (Brian et al., 2005). We undertook detailed (1:500,000 scale) mapping of Itoki Fluctus (located east of Atla Regio), which flows for 900 km from NW to SE of Taussig Quadrangle and whose source is uncertain; possibilities include Ledoux Patera (-9.2°N, 224.8°E) or Maram Corona (7.5°N, 221.5°E). Itoki Fluctus features three connected lava lakes, labeled Upper, Middle, and Lower (Fig.1).

Upper Lava Lake (Fig.2a): This lake is associated with a complex of secondary lakes in the south and is less than 50 km across.

Middle Lava Lake (Fig.2b): This lake is 50 km across and is sub-circular and surrounded by older host units exhibiting a partial circumscribing set of grabens (possibly the Upper Lava Lake as well), suggesting that the Middle Lava Lake fills a central depression associated with a magmatic feature, likely a corona exhibiting a central depression (possibly due to down-sag caldera collapse) (pink unit in Fig.2b). On the eastern side, another large volume of lava with low backscatter (orange unit) interpreted as younger pulse is juxtaposed with this lava lake.

Lower Lava Lake (Fig.2d): This lake is about 100 km across and covers about 2500 km² and is spatially associated with an E-W rift zone (see the distribution of white lines in Fig.3); basin formation is likely to have been influenced both by the rift zone and also possibly by central depressions associated with multiple coronae (collectively representing a nested caldera complex). An extremely unusual channelized flow system greater than 240 km in length connects the Middle and Lower lava lakes (Fig.2c).

Dyke Swarms of the Itoki Fluctus Region (Fig.3): Our mapping has yielded and characterized multiple graben-fissure sets mapped across the study area (4720 to date) (Fig.3). Each is interpreted to represent a regional dyke swarm, with cross-cutting relationships revealing relative ages. The NE trending swarm (in purple) is partially covered by the Lower Lava Lake. N-S-trending grabens (in yellow) are cross-cut by the Middle and Upper Lava lakes, and E-W extensional lineaments (belonging to the rift system mentioned above) are interpreted to be normal faults (in white).

Many circumferential systems (in addition to those described above for the Middle and Upper Lava Lakes) are present in the region, each defining a corona (Fig.3). A radiating swarm (green in Fig.3) belonging to Cherskaya Patera corona-nova is flooded and cross-cut by the Lower Lava Lake. Most of the interpreted dyke swarms do not cut Itoki Fluctus, indicating its relatively young age.

References

Brian, A.W. et al. (2005), *USGS Sci. Invest. Map 2813*.

Buchan, K.L. & Ernst, R.E. (2021) *Gond. Res.*, 100, 25–43.

Ernst, R.E. (2014), *Large Igneous Provinces*. Cambridge U. Press.

Ernst, R.E. et al. (2022) *LPSC abstr.* 1188.

Herrick, R.R. (1999) *GRL*, 26, 803–806.

Magee, K.P., & Head, J.W., (2001), *In: Geol. Soc. Amer. Spec. Pap.* 352, 81–101.

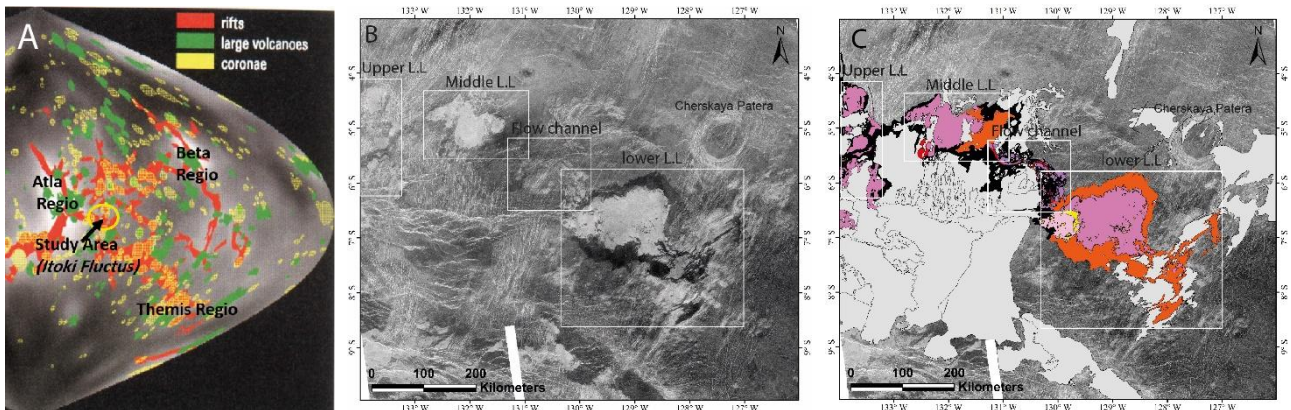


Figure 1. A). Global map (Herrick, 1999) showing the location of the study area. B). SAR Image of the study area, with white boxes corresponding to locations of detailed maps in Figure 2. C). Map highlighting Itoki Fluctus units (in colour), with the gray polygons showing other units mapped to date.

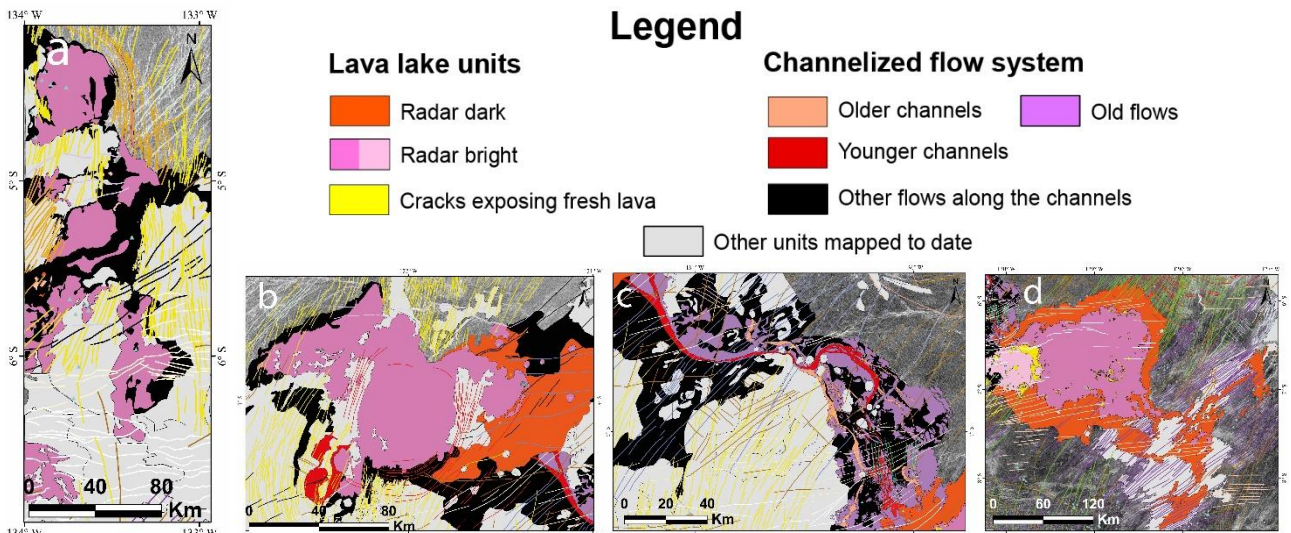


Figure 2. Detailed maps of the different parts of Itoki Fluctus. a: The Upper Lava Lake, b: the Middle Lava Lake, c: the channelized lava flow system, d: the Lower Lava Lake.

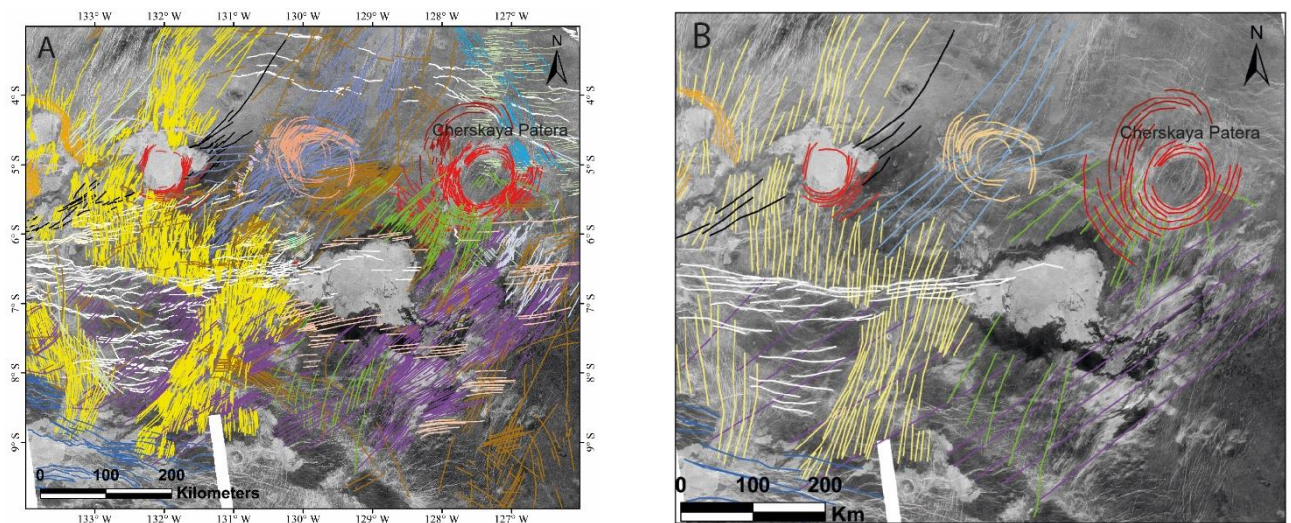


Figure 3. A): Detailed mapping of grabens (4720 mapped so far). B) Generalized map of the grabens, with each colour representing a different interpreted dyke swarm. The white lines represent normal faults associated with an E-W trending younger rift system.

High-precision U-Pb zircon geochronology of the Oued Dar'a Caldera supereruptions (Ouarzazate Supergroup, Saghro Massif, Anti-Atlas, Morocco).

Rachid Oukhro^{1*}, Jörn-Frederik Wotzlaw^{2,3}, Maria Ovtcharova⁴, Mohamed Achraf Mediany¹, Nasrddine Youbi^{1,4}

^{1*}: Department of Geology., Faculty of Sciences-Semlalia, Cadi Ayyad University, Marrakech, Morocco.

²: Institute of Geochemistry and Petrology, Department of Earth Sciences, ETH Zurich, Zurich, Switzerland.

³: Dipartimento di Scienze della Terra, Università degli Studi di Milano, Milan, Italy

⁴: Département des Sciences de la Terre, University of Geneva, Genève, Switzerland.

⁵: Faculty of Geology and Geography, Tomsk State University, 36 Lenin Ave, Tomsk, Russia.

We report for the first time a new high-precision TIMS U-Pb zircon ages of volcanic rocks from the Oued Dar'a caldera volcanic succession of the Ouarzazate Supergroup, in the NW edge of the Saghro Inlier, Anti Atlas Morocco. Oued Dar'a caldera is a large rectangular volcanic structure filled with a uniform section of crystal- to very crystal-rich, quartz-rich, biotite-bearing, moderately to densely welded, ash-flow tuff of rhyolite composition (Walsh et al., 2012). The caldera is northeast-striking along the dominant structural trend of the region and is ~11 km wide by 18 km long. It is bounded to the northwest and southeast by a major strike-slip fault system. The Oued Dar'a caldera was formed in a pull-apart graben created by a left step in a northeast-striking, left-lateral, strike-slip fault zone. SHRIMP U-Pb ages ranging from 574 ± 7 Ma (caldera fill) to 571 ± 5 Ma (outflow facies; Walsh et al., 2012) were previously obtained from rhyolitic volcanic rocks in the Lower Ouarzazate Supergroup, including ash-flow tuffs from the Oued Dar'a caldera. Three volcanic rocks yield crystallization ages from 564 ± 0.045 to 561.37 ± 0.14 , consistent with the upper Ouarzazate Group. suggest that the Caldera fill is ~10 million years younger than indicated by previous SHRIMP zircon ages. The miarolitic rhyolites, stratigraphically located at the top of the volcanic pile of the Ouarzazate Supergroup, are slightly younger than the caldera fill. They could be contemporaneous with the emplacement of the caldera. These new geochronology data suggest that an angular unconformity between the Lower and Upper Ouarzazate Supergroups must be older than 564 Ma. The LIP record of the Central Iapetus Magmatic Province (CIMP) of the West African Craton can be correlated with all these new ages.

References

Walsh, G.J., Benziene, J.N., Aleinikoff, F., Harrison, R.W., Yazidi, A., Burton, W.C., Quick, J.E., and Saadane, A., 2012, Neoproterozoic tectonic evolution of the Jebel Saghro and Bou Azzer–El Graara inliers, eastern and central Anti-Atlas, Morocco: *Precambrian Research*, v. 216–219, p. 23–62, <https://doi.org/10.1016/j.precamres.2012.06.010>.

Temporal calibration of mid-late Ediacaran life changes from carbonate successions of Amane-n'Tourhart and Tifernine in the Anti-Atlas (South of Morocco)

Jihane Ounar¹; Eliza Poggi²; James Pierce²; Achraf Mohamed Mediany¹; Rachid Oukhro¹; Mghazli Kamal¹; David Evans²; Justin Strauss³; Brenhin Keller³; Jörn-Frederik Wotzlaw^{4,5}; Maria Ovtcharova⁶; Andrey Bekker⁷; El Hassane Chellai¹, Nasrddine Youbi^{1,8}

¹ : Department of Geology, Cadi Ayyad University, Marrakech, P.O. Box 2390, Morocco

² : Department of Earth and Planetary Sciences, Yale University, New Haven, CT 06511, USA

³ Department of Earth Sciences, Dartmouth College, Hanover, NH, 03755, USA

⁴: Institute of Geochemistry and Petrology, Department of Earth Sciences, ETH Zurich, Zurich, Switzerland.

⁵: Dipartimento di Scienze della Terra, Università degli Studi di Milano, Milan, Italy

⁶: Department of Earth Sciences, University of Geneva, Genève, Switzerland.

⁷: Department of Earth & Planetary Sciences, University of California, Riverside CA 92521 USA

⁸: Faculty of Geology and Geography, Tomsk State University, 36 Lenin Ave, Tomsk, Russia

Ediacaran period (635-538Ma) is characterized by appearance and diversification of various microbiota and more importantly – appearance and diversification of complex multicellular metazoans (Ediacaran biota). It is generally regarded that Ediacaran life is dominated by deep and shallow marine biota, preserved in carbonate and siliciclastic successions worldwide. Very little is known though for the environmental conditions of the terrestrial counterparts of those marine successions. Only few locations in the world provide opportunity to study Ediacaran sections in lacustrine settings and one of them are the carbonate successions of Amane-n'Tourhart and Tifernine localities (Quarzazate Group) in the Anti-Atlas Mountains (South Morocco). It is extremely important to provide a comprehensive study of these sections and place them in the temporal and spatial framework of the Ediacaran period. The main aim of this project (PhD thesis of Jihane Ounar) is to develop a temporally calibrated record of the sedimentological, geochemical, paleontological and paleogeographic conditions during mid-late Ediacaran period in the terrestrial carbonate successions of Quarzazate Group in Anti-Atlas (South Morocco). This will be achieved via applying: i) lithostratigraphy and sequence stratigraphy in order to characterize the depositional environment and diagenetic processes; ii) chemostratigraphy using carbon, oxygen and strontium isotope variations associated with terrestrial carbonate successions and combine this with sedimentary geochemistry (trace and rare earth elements) in order to reconstruct the paleoenvironment conditions; iii) detailed characterization of microfossils and trace fossils in order to place them in the global record of Ediacaran biostratigraphy and iv) determine a precise age of the studied carbonate sections by bracketing each of the carbonate troughs with high precision U-Pb zircon ID-TIMS geochronology of the overlying and underlying volcanics and ash beds. Completion of this project will bring new insights into the spreading of life across diverse ecological niches, contribute to better correlations of Ediacaran successions worldwide and establish tectonostratigraphic and isotopic record of the mid-late Ediacaran in the Anti-Atlas margin of Gondwana supercontinent.

Evidence for a Lower Espinhaço Rift Sequence in the Guanhões basement inlier, MG-Brazil: insights from detrital zircon U-Pb and Lu-Hf isotopes analysis

Ricardo Pagung¹; Carlos Alberto Rosière¹; Armin Zeh²

¹ Universidade Federal de Minas Gerais, Instituto de Geociências, Av. Antônio Carlos, 6627, Belo Horizonte

² Karlsruher Institut für Technologie, Institut für Angewandte Geowissenschaften, Adenauerring 20b, 76131 Karlsruhe

The Espinhaço rift system's southern segment lies in the outer region of the Neoproterozoic Araçuaí Orogen, which delimitates the São Francisco craton's eastern border (Fig. 1a). Three basinal cycles developed in this rift system between the Statherian to Tonian (Chemale et al., 2012; Guadagnin et al., 2015). The bimodal Borrachudos Large Igneous Province (Borrachudos Suite), positioned toward east of the southern Espinhaço ranges into the Guanhões basement inlier (Fig. 1), fertilized the basal rift strata, known as the Lower Espinhaço Sequence, with younger (Statherian) zircon grains characterized by negative ϵ_{Hf} values (-4.1 to -17.6) (Magalhães et al., 2018). Results of new geological-structural mapping in combination with LA-ICP-MS U-Pb dating, and Lu-Hf isotope analyses of detrital zircons grains place new constraints on the occurrence of the Lower Espinhaço Sequence in the Guanhões basement inlier and define a new formal stratigraphic for the metasedimentary rocks and their temporal position in relation to the Rhyacian-Orosirian BIF-bearing Serra da Serpentina Group.

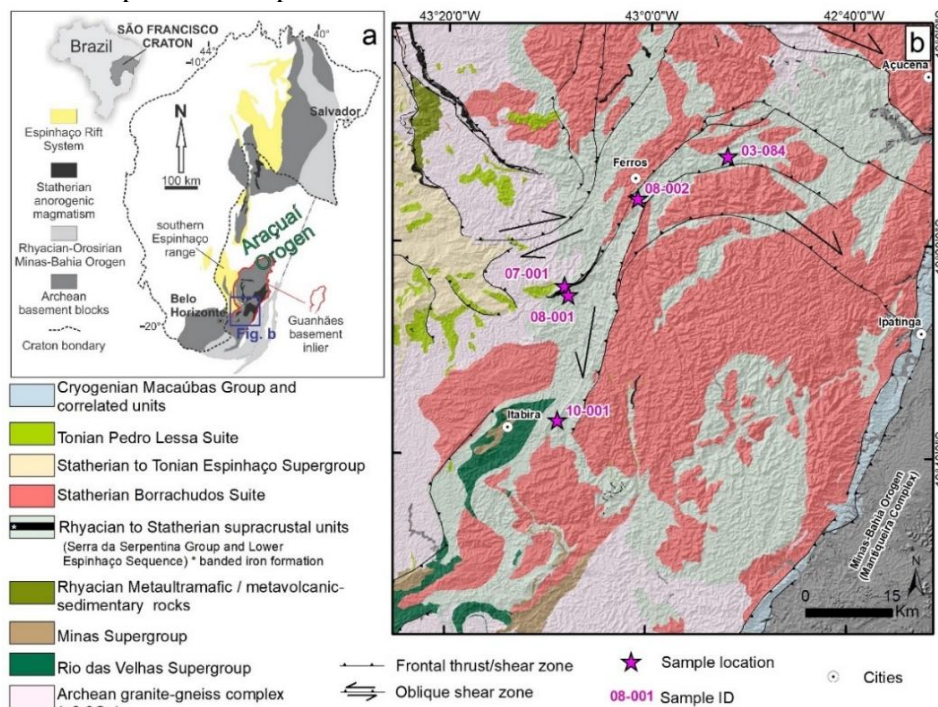


Figure 1: (a) Geotectonic context and (b) geological map of the study area

Zircon grains were recovered from five samples collected from the Lower Espinhaço Sequence (10-001, 03-084, 07-001, 08-001 and 08-002) using standard preparation methods. U-Pb dating was carried out at Karlsruhe Institute of Technology and Lu-Hf isotope analysis at Goethe University of Frankfurt, Germany. For this study only $^{207}\text{Pb}/^{206}\text{Pb}$ ages with a concordance level of 90-110% are discussed.

The sample 10-001 (Fig. 1b) is a poorly sorted, polymitic metaconglomerate with large boulders collected on the top of the Pedra Branca ridge (UTM 694142/7830393). Fifty-two detrital zircon analyses out of 88 yielded concordant ages. The majority of the grains yielded Archean ages between 2507 ± 9 Ma and 3311 ± 11 Ma (50%), and the rest either Siderian ages (ca. 2444 Ma; 6%), Rhyacian ages (2052 ± 15 to 2290 ± 15 Ma; 21%), Orosirian ages (1808 ± 25 to 2042 ± 20 Ma; 13%), and Statherian age (1740 ± 27 to 1768 ± 17 Ma; 10%). The Statherian zircon population revealed subchondritic ϵ_{Hf} values between -6.7 and -19.3.

The sample 03-084 (Fig. 1b) is a coarse-grained biotite-sillimanite quartzite collected at the Santo Antônio River valley (UTM 723789/7876154). Seventy out of 114 analyses yielded concordant ages. The oldest zircon grains gave Archean ages (2674 ± 10 Ma to 3356 ± 13 Ma; 20%). There is a large number of younger grains revealing Siderian (ca. 2406 Ma, 6%), Rhyacian (2055 ± 15 to 2299 ± 12 Ma; 67%), and Orosirian

ages (ca. 2038 Ma; 6%). One single grain reflects a Statherian age (1676 ± 12 Ma) and a subchondritic ϵ_{Hf_t} value of -14.7.

The sample 07-001 is a mylonitic kyanite quartzite, which was collected on the southeastern slope of the Morro Escuro ridge (UTM 695378/7853664) (Fig. 1b). This quartzite is interlayered to mono-polymictic, clast-supported and poorly sorted metaconglomerate with a large number of angular BIF-clasts. Sixty-two out of 101 zircon analyses yielded concordant ages between 1690 ± 17 and 1809 ± 48 Ma, with a sharp age peak at 1758 Ma. Hafnium isotope analyses gave negative ϵ_{Hf_t} values between -12.7 and -18.0. In combination, the data provide evidence that the detrital zircon grains were supplied solely from a Statherian basement, made up by reworked older crust.

Two samples, 08-001 and 08-002 (Fig. 1b), of highly weathered fine-grained sericite quartzite were sampled from the tectonic surface mapped as a basal detachment. The sample 08-001 was collected at the base of the Morro Escuro ridge (UTM 696058/7852065), and sample 08-002 near to the town of Ferros (UTM 708157/7868836). From the fifty-six zircon grains analyzed of sample 08-001, only three gave concordant ages: two Neoproterozoic (2635 ± 20 Ma and 2721 ± 11 Ma), and one Statherian age (1763 ± 15 Ma). The Statherian zircon yielded a subchondritic ϵ_{Hf_t} value of -14.3. Twenty U-Pb zircon analyses were accomplished for sample 08-002, but only two of them produced concordant ages (2865 ± 10 Ma and 1757 ± 25 Ma). The Statherian grain of the sample 08-002 yielded a negative ϵ_{Hf_t} value of -20.2.

The age spectra of the detrital zircon grains (Fig. 2) indicate that the detritus of the investigated metasedimentary rocks was delivered from different sources comprising Archean and Paleoproterozoic basement rocks. Furthermore, it reflects that all rocks were deposited during the Statherian, as indicated by the youngest detrital zircon grains found in all samples. Abundant input of Statherian detritus is well reflected by a pronounced age peak at ca. 1760 Ma, and a minor peak at ca. 1680 Ma (Fig. 2a). All Statherian zircon grains reveal highly subchondritic ϵ_{Hf_t} values between -12.7 and -20.2, except one grain with $\epsilon_{\text{Hf}_t} = -6.7$ (Fig. 2b). These data overlap with such previously obtained from magmatic rocks of the Borrachudos Suite (Magalhães et al., 2018), and indicating that the magmatic source in the hinterland resulted from reworking of older (Archean) continental crust, as reflected by Hf model ages between ca. 2.7 to 3.5 Ga. In summary, the new data demonstrate that the investigated rocks were deposited during the initial stage of the Espinhaço rifting at ca. 1750-1680 Ma. Nevertheless, detailed scale mapping and additional geochronological-isotope studies are necessary to delimitation all rift-related sedimentary units and their temporal-spatial relationships to the BIF-bearing sequences of the Serra da Sepentina Group.

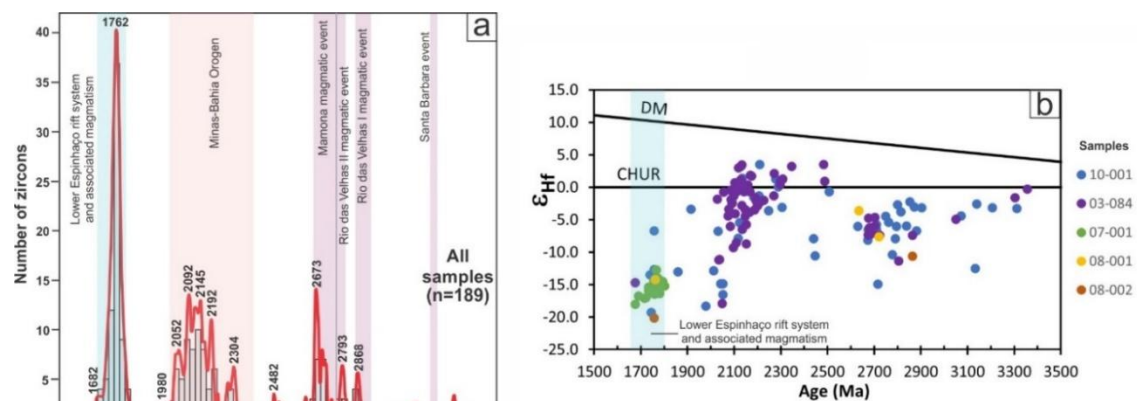


Figure 2: Results of zircon U-Pb dating and Lu-Hf isotope analyses of all investigated samples (only data with 90-110% concordance). (a) Histogram of detrital zircon ages, (b) ϵ_{Hf} vs. U-Pb age diagram

- Chemale, F., Dussin, I. A., Alkmin, F. F., Martins, M. S., Queiroga, G., Armstrong, R., & Santos, M. N. (2012). Unravelling a Proterozoic basin history through detrital zircon geochronology: The case of the Espinhaço Supergroup, Minas Gerais, Brazil. *Gondwana Research*, 22(1), 200–206.
- Guadagnin, F., Chemale, F., Magalhães, A. J. C., Santana, A., Dussin, I., & Takehara, L. (2015). Age constraints on crystal-tuff from the Espinhaço Supergroup - Insight into the Paleoproterozoic to Mesoproterozoic intracratonic basin cycles of the Congo-São Francisco Craton. *Gondwana Research*, 27(1), 363–376.
- Magalhães, J. R., Pedrosa-Soares, A., Dussin, I., Müntener, O., Pinheiro, M. A. P., da Silva, L. C., Knauer, L. G., Bouvier, A. S., & Baumgartner, L. (2018). First Lu-Hf, $\delta^{18}\text{O}$ and trace elements in zircon signatures from the Statherian Espinhaço anorogenic province (Eastern Brazil): Geotectonic implications of a silicic large igneous province. *Brazilian Journal of Geology*, 48(4), 735–759.

Large igneous provinces in North China craton and their links with global events: A review

Peng Peng^{1,2}

¹ Institute of Geology and Geophysics, Chinese Academy of Sciences, Beijing 100029, China

² University of Chinese Academy of Sciences, Beijing 101408, China, e-mail: pengpengwj@mail.iggcas.ac.cn

Precambrian Large igneous provinces (LIPs) are much eroded; however, vestiges including giant dike swarms, sill complexes, and other associated igneous units and erosions in sediments may have been preserved in crust or basins. The vestiges of five major Proterozoic LIP periods/peaks in the North China craton (Peng et al., 2022a,b, 2023; Fig. 1) and their possible connections and significances to major global events will be examined.

Period 1 (2.2-2.0 Ga) includes 6 sequential LIPs, i.e., the ca. 2.22 Ga Yejishan, ca. 2.14 Ga Hengling, ca. 2.12 Ga Haicheng, ca. 2.09 Ga Zanzhuang, and ca. 2.06 Ga Yixingzhai. They are featured by sill complexes, ring complexes, and bimodal magmatism.

Period 2 (2.0-1.9 Ga) includes the 1.92 Ga Xuwujia LIP with sill complexes and plutons, followed by the 1.9 Ga Halaqin volcanics. They are featured by high-Mg gabbro-noritic rocks, which occur along with contemporaneous metapelite with ultra-high temperature metamorphism.

Period 3 (1.8-1.6 Ga) includes 5 sequential LIPs with vestiges of mainly giant dike swarms, i.e., ca. 1.79 Ga Xiong'er, ca. 1.77 Ga Taihang, ca. 1.73 Ga Miyun-Beitai, ca. 1.69 Ga Laiwu, and ca. 1.63 Ga Taishan. These vestiges also have contemporaneous bimodal magmatism.

Period 4 (1.4-1.2 Ga) includes two major LIPs, i.e., the ca. 1.32 Ga Yanliao LIP dominated by sill complexes with minor diabase and carbonatite dikes, and ca. 1.23 Ga Licheng LIP dominated by dikes. The 1.32 Ga Yanliao LIP is concurrent with the world largest light rare earth element deposit, the Bayan Obo ore deposit.

Period 5 (1.0-0.8 Ga) includes 4 LIPs, i.e., the ca. 0.94 Ga Baengyoengdo sill complex, ca. 0.92 Ga Dashigou giant dike swarm and coeval sills, the ca. 0.9 Ga Sariwon sill complex, and the 0.83 Ga Qianlishan dike swarm with volcanics and sills.

These LIP periods are not only well-concurrent with global peaks but also connected with global tectonics. Period 1 follows the global magmatic quiescent, and intercepts the transition from supercratons to supercontinents; while Period 2 is likely associated with the ultrahigh temperature metamorphism and arc magmatism, and thus a ridge subduction or plume plus subduction tectonic process could be applied for them (Peng et al., 2023). Periods 3 to 5 are well-correlated with the evolution of the supercontinents, from Columbia to Rodinia. Among them, Period 3 is a peak with both plume activity and subduction. Based on a global reconstruction of continents and dike swarms, we presume that it indicates a hotspot track advected by the subduction system during the amalgamation of the continent to form Columbia (Peng et al., 2022a). Period 4 is probably happened during the breakup of supercontinent or the supercontinental transformation from the Columbia to the Rodinia with evidence from paleomagnetic datasets (Wang et al., 2020; Zhang et al., 2022); while Period 5 might be the earliest stage of breakup right at the time the supercontinent formed (Peng et al., 2022b; Hu et al., 2022).

LIPs may affect environments and life by the releasing of gases, nutrients, and/or toxic elements, and consuming of gases during weathering (Ernst and Youbi, 2017). Here Period 1 LIPs are concurrent with the late stages of the Great Oxidation Event (GOE) and especially the Lomagundi-Jatuli Event, and Period 2 LIPs emplaced at its aftermath. We propose that Period 1 LIPs may have helped sustaining the GOE by providing nutrients from its volcanics and tuffs; however Period 2 LIPs and the contemporaneous ultrahigh temperature metamorphism may have recycled organic carbon back into the atmosphere by transforming graphite into carbon dioxide, which consumed oxygen (Peng et al., 2023).

As for Period 3 LIPs, it may have contributed to a fast drafting of continents away and back to the tropic – a mechanism applied to explain the cause of the oldest Neoproterozoic negative carbonate carbon excursion by a temporaneous reduced bury of organic materials in subtropic zone during the drafting of continents (Zhang et al., 2021).

References:

- Ernst RE, Youbi N, 2017. How Large Igneous Provinces affect global climate, sometimes cause mass extinctions, and represent natural markers in the geological record. *Palaeogeography, Palaeoclimatology, Palaeoecology* 478, 30-52. <https://doi.org/10.1016/j.palaeo.2017.03.014>
- Hu, Y., Zhao, X., Peng, P., Yang, F., D'Agrella - Filho, M.S., Chen, W., Xu, M., 2022a. Paleomagnetic Constraints From 925 Ma Mafic Dykes in North China and Brazil: Implications for the Paleogeography of Rodinia. *Journal of Geophysical Research: Solid Earth* 127. <https://doi.org/10.1029/2022JB025079>
- Peng P, Liu X, Feng, L, Zhou X, Kuang H, Liu Y, Kang J, Wang X., Wang C, Dai K, Wang H, Li J, Miao P, Guo J, Zhai M, 2023. Rhyacian intermittent large igneous provinces sustained Great Oxidation Event: Evidence from North China craton. *Earth-Science Reviews* 238: 104352. <https://doi.org/10.1016/j.earscirev.2023.104352>
- Peng P, Xu HR, Wang C, Su XD, Sun FB, Wang XP, 2022b. Spatiotemporal evolution of large igneous provinces and their related rifts in North China craton: Role in craton breakup and destruction. *Geological Society, London, Special Publications*. SP518: SP518-2021-45. <https://doi.org/10.1144/SP518-2021-45>
- Peng P, Xu H, Mitchell RN, Teixeira W, Kirscher U, Qin Z, Oliveira EP, Girardi VAV, Wang C, Chemale F, 2022a. Earth's oldest hotspot track at ca.1.8 Ga advected by a global subduction system. *Earth and Planetary Science Letters* 585.117530. <https://doi.org/10.1016/j.epsl.2022.117530>
- Zhang Z, Peng P, Feng L, Gong Z, Mitchell RN, Li Y, 2021. Oldest-known Neoproterozoic carbon isotope excursion: Earlier onset of Neoproterozoic carbon cycle volatility. *Gondwana Research* 94, 1-11. <https://doi.org/10.1016/j.gr.2021.01.013>
- Wang, C., Peng, P., Li, Z.X., Pisarevsky, S., Denysyn, S., Liu, Y., Gamal El Dien, H., Su, X., 2020. The 1.24–1.21 Ga Licheng Large Igneous Province in the North China Craton: Implications for Paleogeographic Reconstruction. *Journal of Geophysical Research: Solid Earth* 125. <https://doi.org/10.1029/2019JB019005>
- Zhang, S.-H., Ernst, R.E., Munson, T.J., Pei, J., Hu, G., Liu, J.-M., Zhang, Q.-Q., Cai, Y.-H., Zhao, Y., 2022. Comparisons of the Paleo-Mesoproterozoic large igneous provinces and black shales in the North China and North Australian cratons. *Fundamental Research* 2, 84-100. <https://doi.org/10.1016/j.fmre.2021.10.009>

Helium and oxygen isotopes in the Hovsgol alkaline and subalkaline intrusions, northern Mongolia: evidence of the Paleozoic mantle-crustal magmatism

A.A. Petlina^a, V.V. Vrublevskii^a, E.N. Kozlov^b^aNational Research Tomsk State University, Tomsk, Russia^bGeological Institute of Kola Science Centre of Russian Academy of Sciences, Apatity, Russia

Small areas of alkaline and subalkaline magmatism occurred during the formation of the Central Asian orogenic belt in the Neoproterozoic, Paleozoic, and Mesozoic (Yashina, 1982; Doroshkevich et al., 2012; Vrublevskii, et al., 2018a, b, 2020; Vrublevskii, Gertner, 2021; Nikiforov, Yarmolyuk, 2019; Vorontsov et al., 2021). In such a tectonic setting, primary mantle magmas are often contaminated by crustal material. Isotope ratios for igneous rocks is a sensitive indicator of its influence (Pokrovsky, 2000). We studied the isotopic composition of helium and oxygen for some plutonic rocks in the Hovsgol lake area of northern Mongolia. They are derived from two Paleozoic magmatic series: alkali gabbro-foioidolite-nepheline syenite (430–390 Ma) and subalkaline gabbro-monzonite-alkali syenite (300–275 Ma) (Yashina, 1982). Isotopic analysis was performed on gas mass spectrometers at the Geological Institute KSC RAS (Apatity, MI-1201IG, for helium) and the Geological Institute SB RAS (Ulan-Ude, Finnigan MAT-253, for oxygen), respectively.

The ⁴He content trapped by fluid inclusions in the accessory magnetite ranges from 6.6×10^{-7} to 1.1×10^{-5} cm³/g. Compared to mantle reservoirs, most samples have a low isotope ratio from 0.26 to 0.59 *Ra* (Fig. 1a). The exception is subalkaline gabbro, in which the ³He/⁴He isotopic ratio is higher than the atmospheric value (AIR) and reaches 3.02 *Ra*. If we assume that the generation of mafic magma occurred with SCLM-type matter (6 *Ra*) or a less ³He-enriched (4–5 *Ra*) plume-like source (Gautheron and Moreira, 2002), then the calculated proportion of mantle helium (Kendrick et al., 2001) in the fluid could be ~50 or 60–70%, respectively. On the other hand, the mantle component in the evolution of fooidic and syenitic melts did not exceed 10–15%. Obviously, the ³He/⁴He ratios in the studied plutons reflect the significant participation of crustal helium in petrogenesis.

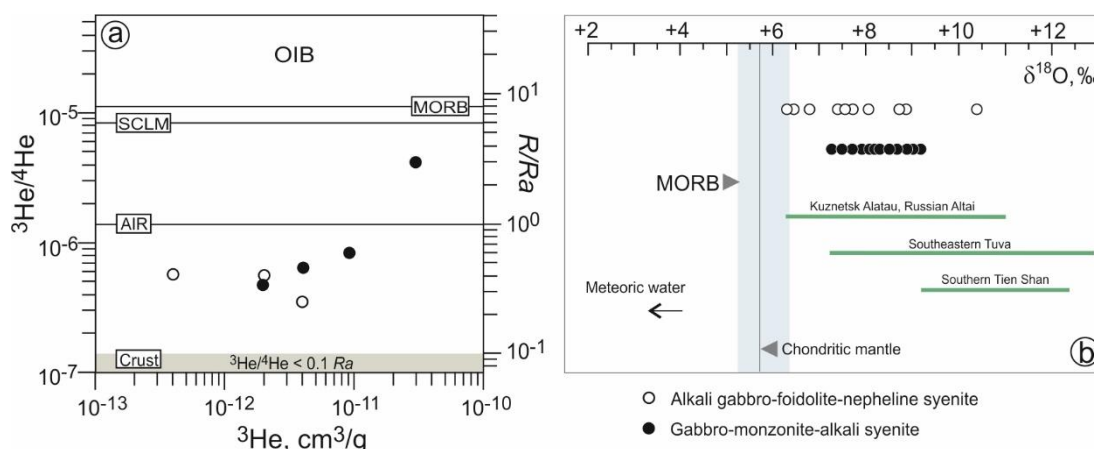


Fig. 1. Helium (a) and oxygen (b) isotope compositions of the Hovsgol alkaline and subalkaline igneous rocks. Deep helium reservoirs SCLM (Subcontinental lithospheric mantle), MORB (Mid-Ocean ridge basalts), and OIB (Ocean Island basalts), after (Gautheron, Moreira, 2002). AIR= atmospheric helium. $\delta^{18}\text{O}$ ratio in MORB (Harmon, Hoefs, 1995), and chondritic mantle, after Rollinson, 1993. Oxygen isotope data of intrusions of the Kuznetsk Alatau, Russian Altai, SE Tuva, and southern Tien Shan, after (Vrublevskii, et al., 2012, 2018a, b, 2020; Vrublevskii, Gertner, 2021).

Elevated $\delta^{18}\text{O}_{\text{SMOW}}$ values in the Hovsgol intrusions also indicate crustal contamination of deep melts. Despite the difference in silica (SiO_2 41–64 wt. %) and magnesium (MgO 0.2–5 wt. %) content in rocks, the $\delta^{18}\text{O}$ value varies up +6.3 to +10.5‰ (in average 8.1‰, $n=22$). This exceeds the $\delta^{18}\text{O}$ values of $5.7 \pm 0.2\%$ in mantle derivatives (Harmon, Hoefs, 1995). Other alkaline and subalkaline plutonic complexes of the Western Central Asian orogenic belt (Kuznetsk Alatau, Russian Altai, SE Tuva, and South Tien Shan Mountain regions) are characterized by a similar oxygen isotope composition (Fig. 1b). In spite of the spatial separation and age differences of these intrusions, the degree of their ¹⁸O enrichment is approximately the same. This may indicate the contamination already at the melt stage and the same type of mineral formation, as well as the similar amount and composition of the crustal component. According to a widespread geodynamic model, the formation of Early Paleozoic structures of the Central Asian orogenic belt took place

under the conditions of an active continental margin (Yarmolyuk et al., 2014.). Therefore, we assume that the primary magmas interacted with fragments of ancient accretionary-collisional complexes.

This study was supported by the Ministry of Science and Higher Education of the Russian Federation (State Assignment TSU, project no. 0721–2020–0041).

Gautheron, C., Moreira, M., 2002. Helium signature of the subcontinental lithospheric mantle. *Earth and Planetary Science Letters* 199, 39-47.

Harmon, R.S., Hoefs, J., 1995. Oxygen isotope heterogeneity of the mantle deduced from global ^{18}O systematics of basalts from different geotectonic settings. *Contributions to Mineralogy and Petrology* 120, 95–114.

Doroshkevich, A.G.; Ripp, G.S.; Izbrodin, I.A.; Savatenkov, V.M., 2012. Alkaline magmatism of the Vitim province, West Transbaikalia, Russia: Age, mineralogical, geochemical and isotope (O, C, D, Sr and Nd) data. *Lithos* 152, 157–172.

Kendrick, M.A., Burgess, R., Pattrick, R.A.D., Turner, G., 2001. Fluid inclusion noble gas and halogen evidence on the origin of Cu-porphry mineralizing fluids. *Geochimica et Cosmochimica Acta* 65, 2651–2668.

Nikiforov, A.V., Yarmolyuk, V.V., 2019. Late Mesozoic carbonatite provinces in Central Asia: Their compositions, sources, and genetic settings. *Gondwana Research* 69, 56–72.

Pokrovsky, B.G., 2000. Crustal contamination of mantle magmas: on evidence of isotope geochemistry. Moscow: Nauka, 2000, pp. 228 (In Russian).

Vorontsov, A., Yarmolyuk, V., Dril, S., Ernst, R., Perfilova, O., Grinev, O., Komaritsyna, T., 2021. Magmatism of the Devonian Altai-Sayan rift system: Geological and geochemical evidence for diverse plume-lithosphere interactions. *Gondwana Research* 89, 193–219.

Vrublevskii, V.V., Krupchatnikov, V.I., Izokh, A.E., Gertner, I.F., 2012. The alkaline and carbonatitic rocks of Gorny Altai (Edel'veis complex) as indicators of Early Paleozoic plume magmatism in the Central Asian Fold Belt. *Russian Geology and Geophysics* 53, 721–735.

Vrublevskii, V.V., Kotel'nikov, A.D., Izokh, A.E., 2018a. The age and petrologic and geochemical conditions of formation of the Kogtakh gabbro–monzonite complex in the Kuznetsk Alatau. *Russian Geology and Geophysics* 59, 718–744.

Vrublevskii, V.V., Morova, A.A., Bukharova, O.V., Konovalenko, S.I., 2018b. Mineralogy and geochemistry of Triassic carbonatites in the Matcha alkaline intrusive complex (Turkestan-Alai Ridge, Kyrgyz Southern Tien Shan), SW Central Asian Orogenic Belt. *Journal of Asian Earth Sciences* 153, 252–281.

Vrublevskii, V.V., Nikiforov, A.V., Sugorakova, A.M., Kozulina, T.V., 2020. Petrogenesis and tectonic setting of the Cambrian Kharly alkaline-carbonatite complex (Sangilen Plateau, Southern Siberia): Implications for the Early Paleozoic evolution of magmatism in the western Central Asian Orogenic Belt. *Journal of Asian Earth Sciences* 188:104163.

Vrublevskii, V.V., Gertner, I.F., 2021. Paleozoic alkali-mafic intrusions of the Kuznetsk Alatau, their sources and conditions for the formation of melts. *Petrology* 29(1), 31–63.

Yarmolyuk, V.V., Kuzmin, M.I., Ernst, R.E., 2014. Intraplate geodynamics and magmatism in the evolution of the Central Asian Orogenic belt. *Journal of Asian Earth Sciences* 93, 158–179.

Yashina, R.M., 1982. Alkaline magmatism in orogenic areas. Moscow: Nauka, pp. 1–274 (In Russian).

Congo-São Francisco in Paleoproterozoic-Mesoproterozoic supercontinent Nuna

Johanna Salminen¹; David A.D. Evans²; Ricardo, I.F. Trindade³; Richard Hanson⁴; Martin B. Klausen⁵; Philip R. Geldenhuys¹; Ulf Söderlund⁶; Richard E. Ernst⁷; Ian Housefield⁸

¹: Department of Geography and geosciences, University of Helsinki and Geological Survey of Finland

²: Yale University, USA

³: University of São Paulo, Brazil

⁴: Texas Christian University, USA

⁵: Stellenbosch University, South Africa

⁶: Lund University, Sweden

⁷: Carlton University, Canada

⁸: Sudbury, Canada

The location of Congo-São Francisco (C-SF) craton, one of the largest cratons in Proterozoic paleogeography, has been poorly constrained for the supercontinent Nuna interval (ca. 1.80–1.30 Ga). Previously, C-SF has been placed adjacent to Baltica and Siberia based mainly on ages of mafic magmatism in the interval 1.5–1.38 Ga (Ernst et al., 2013), and later this location was supported with the high quality 1.5 Ga Curaça paleomagnetic pole from São Francisco (Salminen et al., 2016). If the geologically based SAMBA (South AMERICA BAltica) model (Johansson, 2009) is adopted, C-SF was connected to Amazonia as well in Nuna, but in a way different to their relative position in Gondwana. Testing the kinematics of C-SF during the Nuna interval is hampered by the lack of paleomagnetic data. Only a small number of paleomagnetic data exist for C-SF, and the only good quality published pole for the Nuna interval is the 1.5 Ga Curaça pole. The motivation for the present study was to obtain paleomagnetic data from the 1.38 Ga Virei dyke swarm of the Congo craton and to examine the C-SF craton's placement within Nuna.

Tens of WNW-trending dykes, part of the >400 km-wide Virei swarm, were sampled. The dykes trend prominently towards the Mesoproterozoic Kunene Igneous Complex (KIC), and one thick dyke near Virei has been dated at 1.385 ± 0.005 Ga (baddeleyite, U-Pb) (Ernst et al., 2014). Based on the more pristine dated E-MORB Virei dyke, Klausen et al. (2023) proposed that all dykes were injected during a protracted KIC-event.

As part of a broader study on numerous dyke swarms exposed in the area, we identified 12 WNW trending dyke sites (i.e., separate cooling units) that preserve either an intermediate-steep NW-up (5 dykes) or intermediate -steep SE-down (7 dykes) characteristic remanent magnetization direction. Magnetization directions and virtual geomagnetic poles are scattered, which lowers the statistical quality of the paleomagnetic pole, and all the attempted baked contact tests were inconclusive. Other dyke swarms in the same region, however, have magnetizations that are systematically different according to age (Salminen et al., 2018), which satisfies the “consistency test” of Buchan (2014). In addition, the new Virei swarm magnetization is distinct from known overprint directions in the adjacent Kaoko orogen, which would have been the most likely source of remagnetization in the subsequent geologic history of the region.

If the new Virei 1.38 Ga pole is reliable then it can serve towards modeling the placement of C-SF both within Nuna and through its early stages of breakup. Including our new pole with quality-filtered poles from the other cratons during the Nuna interval, we propose a SW Congo–Siberia–North China connection at 1.7-1.5 Ga together with NENA (North Europe North America) and SAMBA configurations. In our proposed Nuna model at 1.5 Ga there is also a SE Congo – NW West Africa

connection. The proposed 1.5 Ga reconstruction conforms well with the global large igneous province records. The new 1.38 Ga Virei pole, however, requires a substantial transform motion and large-magnitude azimuthal rotation ($>90^\circ$) of C-SF between 1.5 and 1.38 Ga, in order to bring SW Congo ends up connected with NW West Africa. These motions could be related to the onset of the break-up of Nuna.

Buchan 2014. Precambrian Res. 244, 5-22.

Ernst et al. 2013. Precambrian Res. 230, 103–118.

Ernst et al. 2014. Unpublished LIPs-Industry Consortium Report A157 (www.supercontinent.org)

Johansson 2009. Precambrian Res. 175, 221–234.

Klausen et al. 2023. Potential Kunene-related mafic dyke swarms. GeoCongress 11-13 Jan, 2023.

Salminen et al. 2016. Precambrian Res. 286, 195–212.

Salminen et al. 2018. Geology, <https://doi.org/10.1130/G45294.1>

Timing of Neoproterozoic alkaline ultramafic carbonatitic massifs in Southern Siberia

Ekaterina Salnikova¹, Mariya Stifeeva¹, Alexander Kotov¹, Valentina Savelyeva²

¹: Institute of Precambrian Geology and Geochronology, RAS, Makarova Emb., 2, St. Petersburg 199034, Russia

²: Institute of the Earth's Crust, Siberian Branch of the RAS, Irkutsk 664033, Russia

Timing of duration magmatic activity within the large igneous provinces is an important problem related to geodynamics constrains. The Eastern Sayan province of alkaline-ultrabasic massifs with carbonatites (LIP) is traced for more than 200 km along the southern boundary of the Siberian craton. The Beloziminsky, Sredneziminsky, Bolshetagninsky, Zhidosky ultrabasic-alkaline massifs with carbonatites and the Monkresovsky and Yarma fields of dikes belong to this province. The unique Ziminskii rare-metal ore district (Nb, Ta, REE, U, Pb, Zn и P) is related to these massifs. One of the largest niobium deposits of this province is linked with the Belaya Zima massif which is the most well studied massif within this province. Formation of the massif on the boundary of the Siberian continent related to Angara-Taimyr rift structure formed during the last stages of the supercontinent Rodinia breakup.

Available geochronological data reported for the Belaya Zima massif: U-Pb zircon and garnet ages, Ar-Ar phlogopite age (Salnikova et al., 2019), Zhidoy massif - zircon U-Pb (Yarmolyuk et al., 2005) and Bolshetagninsky masif: Sm-Nd, Ar-Ar phlogopites ages indicating crystallization age in age span at 645 ± 6 Ma - 632 ± 2 Ma. Ar/Ar ages of aillikite and ultramafic bodies range from 645-622 Ma (Ashchepkov et al., 2020).

This contribution presents new U-Pb (ID-TIMS) geochronological and geochemical data for Ca-Fe-Ti garnets from four massifs of the Eastern Sayan magmatic province. Numerous recent studies have convincingly shown that Ca-Fe-Ti garnets are the prospective minerals offers unique opportunities for timing of magmatic events with a temporal resolution comparable to that of zircon dating. Andradite from the Sredneziminskii melteigites has a U-Pb age at 624 ± 5 Ma, andradite from the nepheline syenite and ijolites from the Bolshetagninsky massif yields the age at 632 ± 5 Ma. Therefore U-Pb ID-TIMS ages obtained in the present study for the various rocks demonstrate the advantages of Ca-Fe garnets to evaluate the main pulse of alkaline ultramafic magmatism in the Eastern Sayan province (624– 645 Ma).

The research was supported by grant No. 22-17-00211 from the Russian Science Foundation.

Ashchepkov I., Zhmodik S., Belyanin D., Kiseleva O., Medvedev N., Travin A., Yudin D., Karmanov N., Downes H. Aillikites and Alkali Ultramafic Lamprophyres of the Beloziminsky Alkaline Ultrabasic-Carbonatite Massif: Possible Origin and Relations with Ore Deposits // Minerals 2020. 10, 404.

Salnikova E.B., Chakhmouradian A.R., Stifeeva M.V., et al. Calcic garnets as a geochronological and petrogenetic tool applicable to a wide variety of rocks // Lithos, <https://doi.org/10.1016/j.lithos.2019.03.032>

Savelyeva, V.B., Danilova, Y.V., Letnikov, F.A. et al. Age and Melt Sources of Ultramafic Dykes and Rocks of the Bolshetagninskii Alkaline Carbonatite Massif (Urik-Iya Graben, SW Margin of the Siberian Craton). Dokl. Earth Sc. 2022. 505, 452–458.

Yarmolyuk V. V., Kovalenko V. I., Salnikova E. B., Nikiforov A. V., Kotov A. B., Vladykin N. V. Late riphean rifting and breakup of Laurasia: data on geochronological studies of ultramafic alkaline complexes in the southern framing of the Siberian craton // Dokl. Earth Sci. 2005. 404 (7), 986–991.

Proterozoic mafic complexes of the southeastern part of the Anabar Shield (Northeast Siberia)

Aleksandr D. Savelev^{1,2}, Andrey K. Khudoley¹

¹St Petersburg University, St Petersburg, 199034, Universitetskaya emb., 7–9, Russian Federation

²VSEGEI, St Petersburg, 199106, Sredny pr., 74, Russian Federation

In the northeast of the Siberian Platform, the Proterozoic basic magmatism is associated with outcrops of the crystalline basement. The largest of them, the Anabar shield (Fig. 1), consists of three terranes (Magan, Daldyn, and Khapchan) and three melange zones (Magan, Kotuykan, Billyakh). The rocks of the shield were affected by two stages of granulite metamorphism and are represented mainly by granites, gneisses, and schists (Parfenov & Kuzmin, 2001).

The Anabar shield hosts a number of major mafic dyke swarms of a variety of trends which patterns were initially sorted out by Okrugin et al. (1990) on the basis of trend, K-Ar dating and composition. Subsequent precise U-Pb dating mostly funded through the LIPs-Industry Project has revealed three Proterozoic swarms that represent three LIPs:

- NNW-trending dykes of the 1770 Ma Eastern Anabar portion of the 1750-1775 Ma Tipton LIP (Gladkochub et al. 2010; Ernst et al. 2016b; Gladkochub et al. 2022);
- E-W trending dykes (and sills) of the 1500 Ma Kuonamka LIP (Ernst et al. 2000; Ernst et al. 2016a);
- NW-trending dykes of the 1385 Ma Chieress swarm (Ernst et al. 2000);

In recently published maps and explanatory notes, a different view prevails, where dyke complexes were distinguished in accordance with their structural position, petrographic and geochemical features, and even K-Ar ages. However, their trend was not used as a key criterion. Following this approach, within the southeastern part of the Anabar Shield, six igneous complexes (mostly dykes) have been identified for the Proterozoic basic magmatism: Kendei (1700 Ma) NW-trending dykes, Kengedin (1500 Ma) EW-trending dykes, Tokur (1380 Ma) NW-trending dykes, Budiurkhai (1250 Ma) EW-trending dykes, Kotuykan (1100 Ma) NE-trending dykes and Chieress (950 Ma) NW-trending dykes (Gusev et al., 2016). But at the moment there is no reliable confirmation of the existence of separate Budiurkhai, Kotuykan, and Chieress complexes. U-Pb baddeleyite dating of mafic intrusions (Ernst et al., 2000; Ernst et al. 2016a) showed that they are older and should be attributed to the Tokur and Kengedin complexes.

Thus, we consider only 3 igneous complexes verified, which can be correlated with already known LIPs or dyke swarms: Kendei (Tipton LIP), Kengedin (Kuonamka LIP) and Tokur (Chieress swarm). In order to develop clearer criteria for determining the relationship of intrusions to a particular complex, we conducted studies on the geochemical database for the southeast of the Anabar shield dolerites. It includes both predecessor results and data from the current mapping project.

The rocks of the Kendei complex have high SiO₂ contents (> 54%), forming a group in the fields of basaltic andesites and trachyandesites on the TAS diagram. The Kengedin and Tokur complexes form a group in the fields of basalts and trachybasalts, while the Tokur dykes are more alkaline. At the same time, all samples fell into the field of tholeiitic basalts on the AFM diagram.

Chondrite-normalized REE patterns of Kendei, Kengedin and Tokur complexes dolerites demonstrate contrasting REE behaviors. All samples show an enrichment in light rare earth elements (LREE) over heavy rare earth elements (HREE), but Kendei and Tokur complexes are OIB-type intrusions, while the Kengedin complex is E-MORB-type intrusions.

The most significant differences between the complexes are shown in the (Sm/Yb)_n vs. (La/Sm)_n plot. The flat HREE profile (Sm/Yb)_n ratio (Fig. 1) is typical for Kengedin samples corresponding to melting at relatively low pressures within the spinel stability field (at <75 km depth). Tokur dolerites require significant amounts of garnet in their source to account for their high Sm/Yb ratios. This implies a deep (> 80 km) melting zone. Kendei samples are located in the transition zone between groups Kengedin and Tokur, but have a lower degree of melting.

Most of the intrusions of the Kendei and Kengedin complexes cut rocks of the Archean crystalline basement, while the intrusions of the Tokur complex are located within the Proterozoic carbonate-bearing sequences and carbonate rocks of the Mesoproterozoic sedimentary cover. In this case, the question is whether the difference between the Tokur and Kengedin complexes is due to their original composition, or whether the main influence on the formation of the groups was contamination of the crustal material.

Thus, the most reliable way to separate the complexes is to determine the trend of individual bodies, estimate the content of SiO₂ (Kendei), the distribution of REE elements (Kengedin), and also the position on (Sm/Yb)_n vs. (La/Sm)_n diagram. Note that the results obtained are preliminary and require additional confirmation by new isotope dating and a more detailed study of the geochemical features of the complexes. The data obtained give additional information to establish a connection with synchronous magmatic events in other cratons.

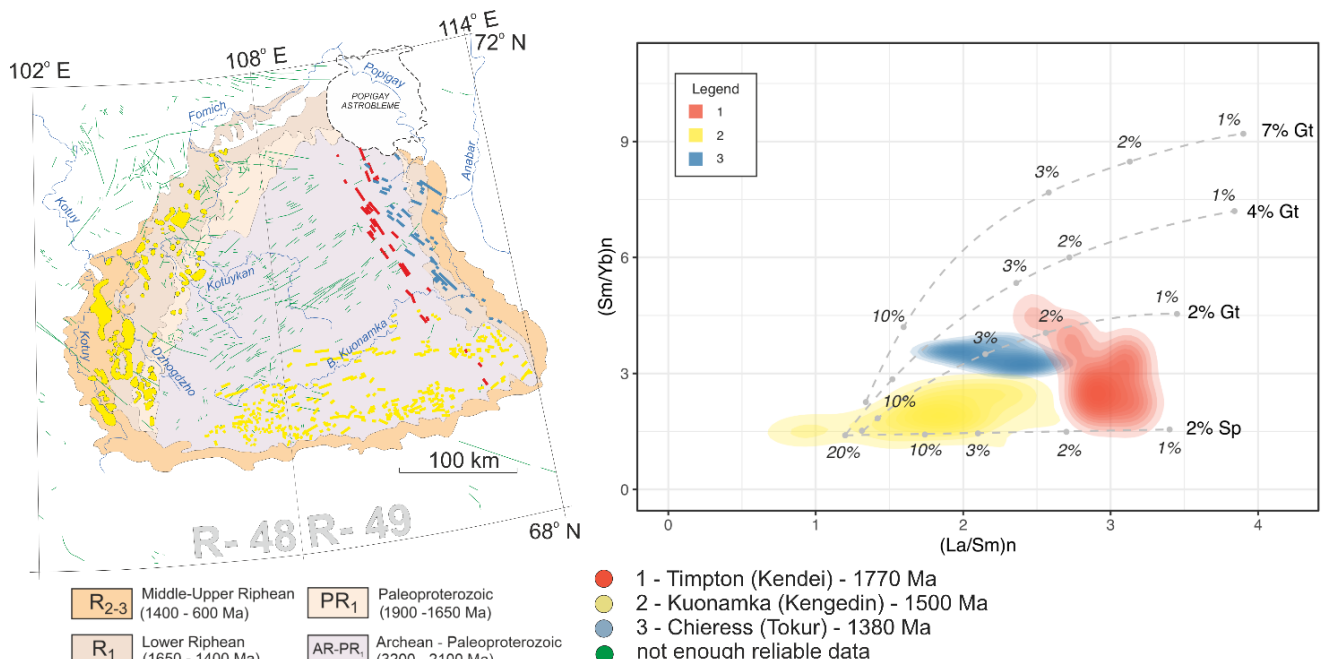


Fig. 1. Geological scheme of the Anabar Shield with marked dyke swarms (based on Ernst et al., 2016a) and (Sm/Yb)_n vs. (La/Sm)_n plot (Jourdan et al., 2007), modeling a lherzolithic mantle source.

Ernst, R.E., A.V. Okrugin, R.V. Veselovskiy, S.L. Kamo, M.A. Hamilton, V. Pavlov, U. Söderlund, K.R. Chamberlain, C. Rogers (2016a). The 1501 Ma Kuonamka Large Igneous Province of northern Siberia: U-Pb geochronology, geochemistry, and links with coeval magmatism on other crustal blocks. *Russian Geology and Geophysics*, v. 57, p. 653-671.

Ernst, R.E., Buchan, K.L., Hamilton, M.A., Okrugin, A.V., Tomshin, M.D. (2000) Integrated paleomagnetism and U-Pb geochronology of mafic dikes of the Eastern Anabar shield region, Siberia: implications for Mesoproterozoic paleolatitude of Siberia and comparison with Laurentia. *J. Geology*. v. 108, p. 381-401.

Ernst, R.E., Hamilton, M.A., Söderlund, U., Hanes, J.A., Gladkochub, D.P., Okrugin, A.V., Kolotilina, T., Mekhonoshin, A.S., Bleeker, W., LeCheminant, A.N., Buchan, K.L., Chamberlain, K.R., Didenko, A.N. (2016b). Long-lived connection between southern Siberia and northern Laurentia in the Proterozoic. *Nat. Geosci.* v. 9, p. 464-469.

Gladkochub, D.P., Donskaya, T.V., Pisarevsky, S.A., Ernst, R.E., Söderlund, U., Kotov, A.B., Kovach, V.P., Okrugin, A.V. 1.79-1.75 Ga mafic magmatism of the Siberian craton and late Paleoproterozoic paleogeography (2022) *Precambrian Research*, v. 370, 106557, <https://doi.org/10.1016/j.precamres.2022.106557>.

Gladkochub, D.P., Pisarevsky, S.A., Donskaya, T.V., et al. (2010). Proterozoic mafic magmatism in Siberian craton: an overview and implications for paleocontinental reconstruction. *Precambrian Research*, v. 183, p. 660-668.

Gusev, N.I., Pushkin, M.G., Kruglova, A.A., Sergeeva, L.Yu. etc. State geological map of the Russian Federation. Scale 1:1,000,000 (third generation). Sheet R-49 - Olenyok. Explanatory note. (2016) - St. Petersburg: Cartographic factory VSEGEI, 448 p. (In Russian)

Jourdan, F., Bertrand, H., Schärer, U., Blichert-Toft, J., Féraud, G., Kampunzu, A.B., 2007. Major and trace element and Sr, Nd, Hf, and Pb isotope compositions of the Karoo large igneous province, Botswana - Zimbabwe: Lithosphere vs Mantle Plume Contribution. *J. Petrol.* 48, 1043-1077. <https://doi.org/10.1093/petrology/egm010>

Okrugin, A.V., Oleinikov, B.V., Savvinov, V.T., Tomshin, M.D. (1990). Late Precambrian dike swarms of the Anabar Massif, Siberian Platform, USSR, in: Parker, A.J., Rickwood, P.C., Tucker, D.H. (Eds.), *Mafic Dikes and Emplacement Mechanisms*. Balkema, Rotterdam, p. 529-533.

Parfenov, L. M. and Kuzmin, M. I. (2001). *Tectonics, geodynamics and metallogeny of the territory of the Republic of Sakha (Yakutia)*. Moscow: MAIK "Nauka/Interperiodica" Publ. (In Russian)

GEOLOGY OF THE LATMIKAIK AND XCACAU CORONAE IN THE HENIE (V-58) QUADRANGLE, VENUS.

J. Shackman¹, K.J.E. Boggs¹, R.E. Ernst^{2,3}, E.M. Bethell⁴, H.G. Wehnes¹, E. Varg¹, C. Pendleton¹, W. Jans¹, J. Hall¹, R.C. Dietrich¹, L. Dham¹, J. Demorcy², B. Dear¹, M. Chowdhury¹, H.N. Bley¹, B. Beckie¹, and M. Becerra De Rosales¹.

¹ Department of Earth and Environmental Sciences, Mount Royal University, 4825 Mount Royal Gate SE, Calgary, Alberta, Canada T3E 6K6;

² Department of Earth Sciences, Carleton University, 1125 Colonel By Drive, Ottawa, Ontario, Canada K1S 5B6;

³ Faculty of Geology and Geography, Tomsk State University, 36 Lenin Avenue, Tomsk, Russia 634050;

⁴ Department of Earth and Environmental Sciences, University of Ottawa, 75 Laurier Avenue E, Ottawa, Ontario, Canada K1N 6N5.

Keywords: Planetary Science, Planetary Geology, Volcanology, Venus, Coronae, Henie (V-58) Quadrangle, Latmikaik Corona, Xcacau Corona.

Introduction: Latmikaik Corona (345 km x 650 km) and Xcacau Corona (120 km x 165km) are both elongated N-S and constrained by annulus material defined by dense swarms of radar bright, linear and curvilinear subparallel lineaments. Annulus material defines a topographic high around the edge of Latmikaik Corona with the core material slightly raised and defining an overall W-W shaped topographic profile. Xcacau Corona has a less well-defined annulus and a sunken core giving it a U-shaped profile. Tellervo Chasma extends between the two coronae (striking 050-230°). Six densely packed graben swarms (011-191°; 010-190°; 340-160°; 325-145°; 337-157°). One graben system (025-205°) extends the length of the chasma but does not appear to extend significantly past the margins of the chasma. One radiating graben system originates from an enigmatic feature at the southeastern corner of Xcacau Corona. Two further graben systems (331-151°; 015-195°) were mapped south of Xcacau Corona. A further five graben swarms cut across the southern end of Latmikaik Corona (022-202°; 027-207°; 055-235°; 353-173°; 005-185°). The W-W shaped profile of Latmikaik Corona suggests that this corona is in a regressive stage and the sunken U-shaped profile of Xcacau Corona also suggests a regressive stage. The densely packed graben are interpreted to be the surficial expression of underlying dyke swarms. The complex system of up to 14 swarms that cut across the coronae and Tellervo Chasma suggest a prolonged history of magmatism and extension, possibly related to the formation of these two coronae and more distal magmatic centers in response to underlying mantle plumes.

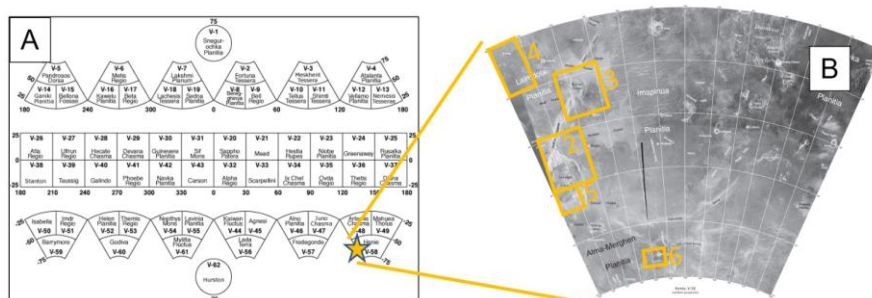


Figure 1: Study Area. The Henie (V-58) Quadrangle is located in southern Venus.

Methodology: Geological features traced out in ArcGIS (1:500,000) on files downloaded from the Planetary Data System for Magellan data. Mapped geological features categorized by defining characteristics such as orientation and trend.

Results: Both Coronae elongate N-S, constrained by annulus material (radar bright with dense swarms of subparallel lineaments; Figs. 2, 3) Latmikaik (Fig. 2) - 345 km wide, 650 km long Core – radar dull mottled, nearly devoid of fractures, radar bright flow material. Annulus forms a topography high around edge with core material raised giving an overall W-profile^[1] Xcacau (Fig. 3) - 120 km wide, 165 km long, and core sunken, less well-defined annulus Graben systems – at least three swarms (e.g. Table) cross Xcacau corona.

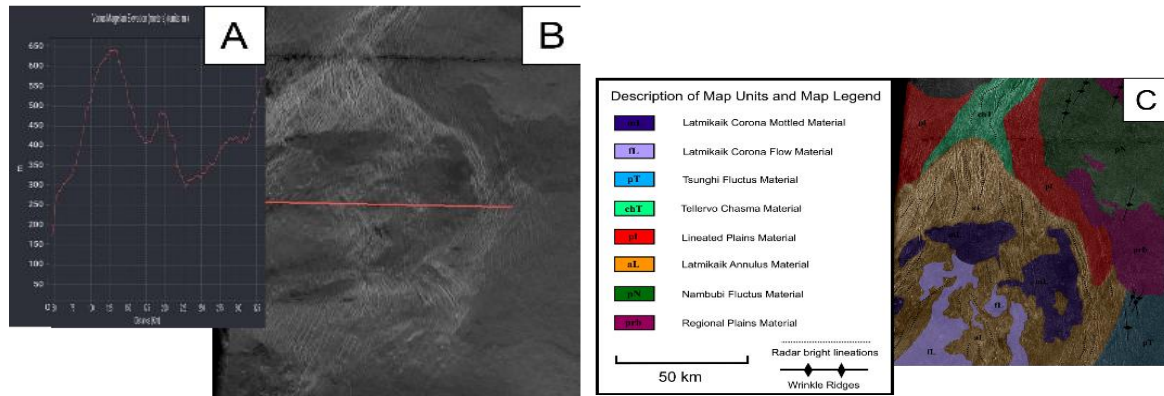


Figure 2: Morphology and Geology of the Latmikaik Corona. A topographic profile is presented on the left (“A”), the uninterpreted Magellan mission data in the middle (“B”) and the mapped geology on the right (“C”). This corona has a “W-W profile” suggestive of a regressive stage in corona development^[1], with the elevated portions defined by the intensely grooved annulus (brown in Fig. 1C).

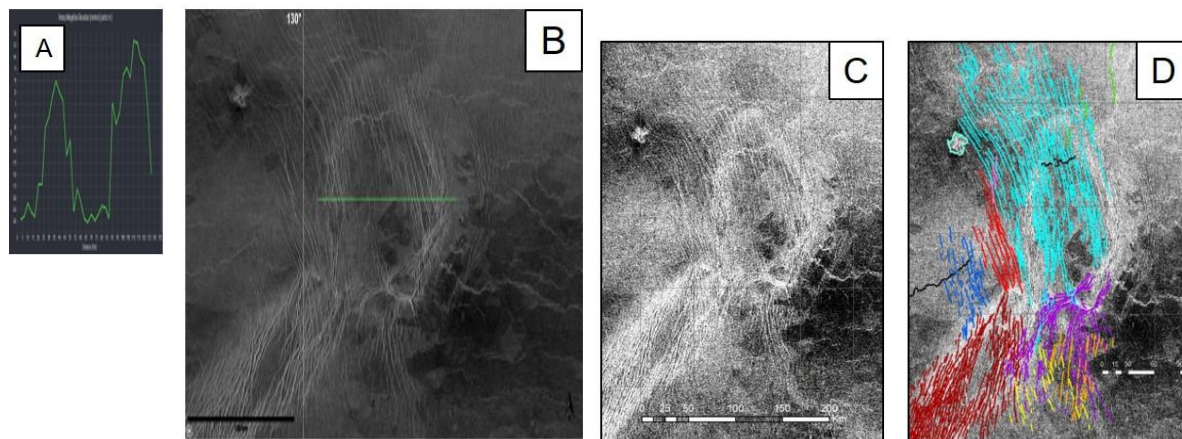


Figure 3: Morphology of the Xcacau Corona and associated Grabens. The topographic profile is presented on the left (“A”), and the uninterpreted Magellan mission data in the middle (“B”, “C”). The Xcacau Corona has a sunken core which is interpreted to represent a regressive stage. The mapped grabens in “D” are interpreted to represent underlying dyke swarms.

Discussion and Conclusions: Latmikaik Corona is considered regressive due to its W-W shaped profile. Xcacau Corona is considered regressive due to sunken U-shaped profile.^[1] Densely packed grabens – surficial expression of underlying dyke swarms. Complex system (up to 15) graben swarms - cut across the coronae and Tellervo Chasma suggest a prolonged history of extension.

Acknowledgements: Acknowledgements to the USGS Astropedia data source for supplying radar images of Venus collected by the Magellan spacecraft.

References: ^[1] Guseva, E. N., Ivanov, M. A. Structures of Coronae on Venus: Results of Topographic and Geologic Analysis. // Solar System Research. 2020, V. 54. N. 6. P. 529-536.

From Yanliao mafic sill swarms in the North China Craton to 1.4–1.3 Ga large-scale continental rifting in the Columbia (Nuna) supercontinent

Shuan-Hong Zhang¹; Richard E. Ernst^{2,3}; Yue Zhao¹; Jun-Ling Pei¹

¹: Institute of Geomechanics, Chinese Academy of Geological Sciences, MLR Key Laboratory of Paleomagnetism and Tectonic Reconstruction, Beijing 100081, China

²: Department of Earth Sciences, Carleton University, Ottawa, Ontario K1S 5B6, Canada.

³: Faculty of Geology and Geography, Tomsk State University, Tomsk 634050, Russia.

The Yanliao basin in the northern North China Craton (NCC) hosts the standard section for late Paleoproterozoic–Mesoproterozoic strata in China (Lu et al., 2008). Large volumes of dolerite sill swarms are common within the late Paleoproterozoic–Mesoproterozoic strata, especially the black shales of the Xiamaling Formation. SIMS U-Pb/Pb-Pb baddeleyite dating of 23 sill samples has yielded crystallization ages between 1330±4 Ma and 1305±11 Ma with a weighted mean age of 1323±2 Ma (Li et al., 2009; Zhang et al., 2012a, 2017a; Wang et al., 2014; Su et al., 2016; Zhu et al., 2020). The Yanliao dolerite sills are distributed over a region >600 km long and >200 km wide; they have an areal extent >120,000 km² and a cumulative thickness ranging from 50 m to >1800 m and constitute a large igneous province (LIP) (Zhang et al., 2017).

Comparisons with coeval LIPs in other continents combined with paleomagnetic results show that the Yanliao LIP in the NCC and the Derim Derim-Galiwinku LIP in the North Australian Craton (NAC) represent portions of the same LIP separated by continental breakup, suggesting a connection (or at least near neighbors) between the NCC and NAC during the early Mesoproterozoic period (Zhang et al., 2017; Bodorkos et al., 2021). A comparison of major mafic magmatic events and black shales in Paleo-Mesoproterozoic successions of the NCC and NAC shows that the northern–northeastern margin of the NCC was connected to the northern margin of the NAC from 1800 Ma to 1300 Ma during the late Paleoproterozoic to Mesoproterozoic (Zhang et al., 2022a). This long-lived connection lasted for at least 500 million years until separation of the NCC and NAC between ca. 1320 and ca. 1230–1220 Ma, likely associated with the ca. 1320 LIP event. The long-lived connection between the NCC and NAC from 1800 Ma to 1300 Ma during the late Paleoproterozoic to Mesoproterozoic is supported by paleomagnetic results obtained in these two cratons (Zhang et al., 2012b; Xu et al., 2014; Wang et al., 2019; Kirscher et al., 2021).

The 1.4–1.3 Ga LIPs (and smaller intraplate mafic magmatic events interpreted as LIP fragments/remnants) and REE-rich carbonatites are common in many cratons within the Columbia (Nuna) supercontinent (Ernst, 2014; Zhang et al., 2022b). Spatial and temporal distributions of the 1.4–1.3 Ga LIPs (and the interpreted LIP fragments/remnants) in the refined paleogeographic reconstruction map of Columbia supercontinent reveal a 1.4–1.3 Ga large-scale continental rift zone along western Laurentia, western-northern Siberia, southeastern Baltica, western-northern West Africa, southwestern Amazonia, southern-eastern Congo/São Francisco, eastern Kalahari, northern North China and northern North Australia. The 1.4–1.3 Ga continental rift system extends about 15,000 km across the Columbia supercontinent and is considered as the main indicator and a proximal reason for final breakup of the Columbia supercontinent. This newly identified huge continental rift zone system also controlled the distributions of Bayan Obo (zircon Th-Pb age of 1.33–1.30 Ga, Zhang et al., 2017b, 2022; Li et al., 2018), the world's first and largest REE-Nb deposit in northern North China and Mountain Pass, the world's second largest REE deposit in western Laurentia (monazite Th-Pb ages of carbonatite ranging from 1396±16 Ma to 1371±10 Ma, Poletti et al., 2016). These new observations more broadly suggest this rift zone as a favorable metallogenic belt for other carbonatite-related REE(-Nb) deposits, and other commodity types such as giant clastic-dominated

Zn-Pb-Ag deposits. Future work should focus on a more systematic comparison of the 1.4–1.3 Ga rift system with the entire Atlantic rift system, the mechanism and deep processes for formation of this huge rift system and global environmental effects of the 1.4–1.3 Ga large-scale rift system.

This research was financially supported by the National Natural Science Foundation of China (41920104004, 41725011, U2244213).

References:

- Bodorkos, S., Crowley, J.L., Claoué-Long, J.C., Anderson, J.R., Magee, C.W., Jr., 2021. Precise U-Pb baddeleyite dating of the Derim Derim Dolerite, McArthur Basin, Northern Territory: Old and new SHRIMP and ID-TIMS constraints. *Australian Journal of Earth Sciences*, 68, 36–50.
- Ernst, R.E., 2014. *Large Igneous Provinces*. Cambridge University Press, Cambridge. 653 p.
- Kirscher, U., Mitchell, R.N., Liu, Y., Nordsvan, A.R., Cox, G.M., Pisarevsky, S.A., Wang, C., Wu, L., Murphy, J.B., Li, Z.-X., 2021. Paleomagnetic constraints on the duration of the Australia-Laurentia connection in the core of the Nuna supercontinent. *Geology*, v. 49, 174–179.
- Li, H.K., Lu, S.N., Li, H.M., Sun, L.X., Xiang, Z.Q., Geng, J.Z., Zhou, H.Y., 2009. Zircon and baddeleyite U-Pb precision dating of basic rock sills intruding Xiamaling Formation, North China. *Geological Bulletin of China*, 28, 1396–1404 (in Chinese with English abstract).
- Li, Q., Liu, Y., Tang, G., Wang, K., Ling, X., 2018. Zircon Th–Pb dating by secondary ion mass spectrometry. *Journal of Analytical Atomic Spectrometry*, 33, 1536–1544.
- Lu, S.N., Zhao, G.C., Wang, H.C., Hao, G.J., 2008. Precambrian metamorphic basement and sedimentary cover of the North China Craton: A review. *Precambrian Research*, 160, 77–93.
- Poletti, J.E., Cottle, J.M., Hagen-Peter, G.A., Lackey, J.S., 2016. Petrochronological constraints on the origin of the Mountain Pass ultrapotassic and carbonatite intrusive suite, California. *Journal of Petrology* 57, 1555–1598.
- Su, L., Wang, T.G., Li, X.H., Song, S.G., Yang, S.W., Zhang, H.Y., Zhong, L.X., 2016. Petrogenesis and emplacement age of the gabbro-dolerite sills within the Mesoproterozoic Xiamaling Formation in Yanliao rifting zone. In: Sun, S., Wang, T.G. (eds.), *Meso-Neoproterozoic geology and oil and gas resources in eastern China*, Science Press, Beijing, p. 325–342.
- Wang, Q., Yang, H., Yang, D., Xu, W., 2014. Mid-Mesoproterozoic (~1.32 Ga) diabase swarms from the western Liaoning region in the northern margin of the North China Craton: Baddeleyite Pb–Pb geochronology, geochemistry and implications for the final breakup of the Columbia supercontinent. *Precambrian Research*, 254, 114–128.
- Wang, C., Li, Z.-X., Peng, P., Pisarevsky, S., Liu, Y., Kirscher, U., Nordsvan, A., 2019. Long-lived connection between the North China and North Australian cratons in supercontinent Nuna: paleomagnetic and geological constraints. *Science Bulletin*, 64, 873–876.
- Zhang, S.H., Zhao, Y., Santosh, M., 2012a. Mid-Mesoproterozoic bimodal magmatic rocks in the northern North China Craton: Implications for magmatism related to breakup of the Columbia supercontinent. *Precambrian Research*, 222–223, 339–367.
- Zhang, S., Li, Z., Evans, D.A.D., Wu, H., Li, H., Dong, J., 2012b. Pre-Rodinia supercontinent Nuna shaping up: A global synthesis with new paleomagnetic results from North China. *Earth and Planetary Science Letters*, 353–354, 145–155.
- Zhang, S.H., Zhao, Y., Li, X.H., Ernst, R.E., Yang, Z.Y., 2017a. The 1.33–1.30 Ga Yanliao large igneous province in the North China Craton: Implications for reconstruction of the Nuna (Columbia) supercontinent, and specifically with the North Australian Craton. *Earth and Planetary Science Letters*, 465, 112–125.
- Zhang, S.H., Zhao, Y., Liu, Y., 2017b. A precise zircon Th–Pb age of carbonatite sills from the world's largest Bayan Obo deposit: implications for timing and genesis of REE-Nb mineralization. *Precambrian Research* 291, 202–219.
- Zhang, S.H., Ernst, R.E., Munson, T.J., Pei, J.L., Hu, G.H., Liu, J.M., Zhang, Q.Q., Cai, Y.H., Zhao, Y., 2022. Comparisons of the Paleo-Mesoproterozoic large igneous provinces and black shales in the North China and North Australian cratons. *Fundamental Research*. 2(1), 84–100.
- Zhang, S.H., Ernst, R.E., Yang, Z.Y., Zhou, Z.Z., Pei, J.L., Zhao, Y., 2022b. Spatial distribution of 1.4–1.3 Ga LIPs and carbonatite-related REE deposits: evidence for large-scale continental rifting in the Columbia (Nuna) supercontinent. *Earth and Planetary Science Letters*. 597, 117815.
- Zhu, Y.-S., Yang, J.-H., Wang, H., Wu, F.-Y., 2020. Mesoproterozoic (~1.32 Ga) modification of lithospheric mantle beneath the North China craton caused by break-up of the Columbia supercontinent. *Precambrian Research*, 342, 105674.

Detrital zircon geochronology of the Volyn-Orsha sedimentary basin in Western Ukraine: a possible link to Amazonia

Leonid Shumlyansky^{1,2}, Andrey Bekker^{3,4}, Ion Francovschi^{5,6}, Simon A. Wilde¹

¹ School of Earth and Planetary Sciences, Curtin University, Perth, GPO Box U1987, WA 6845, Australia; Leonid.Shumlyansky@curtin.edu.au

² Institute of Geological Sciences, Polish Academy of Sciences (ING PAN), Research Centre in Kraków, Senacka 1, PL-31002 Kraków, Poland

³ Department of Earth & Planetary Sciences, University of California, Riverside, CA 92521, USA; andreyb@ucr.edu

⁴ Department of Geology, University of Johannesburg, Auckland Park 2006, South Africa

⁵ The University of Bucharest, Faculty of Geology and Geophysics, Bucharest, Romania; frankovski.ww@gmail.com

⁶ Institute of Geology and Seismology, Chişinău, Republic of Moldova

During the Mesoproterozoic and early Neoproterozoic, most parts of Baltica (also known as the East European platform) experienced a tectonically quiet regime that was accompanied by denudation. Orogenic processes in these times were manifested in the Transscandinavian igneous belt (ca. 1810-1650 Ma) and the Sveconorwegian orogenic belt (ca. 1140-960 Ma), located in the extreme NW part of Baltica. Despite the generally stable tectonic regime that dominated Baltica from the Mesoproterozoic to early Neoproterozoic, a series of intracratonic sedimentary basins developed. One of them, known as the Volyn-Middle Russia, extends from SW to NE across the whole of Baltica for a distance of over 2000 km, and includes the Volyn-Orsha basin and Middle Russian – Moscow – Valdai (Krestsy) aulacogen. At the SW margin of Baltica, the system is abruptly terminated by the Trans-European Suture Zone. The Pachelma aulacogen is another example of this system of sedimentary basins, and strikes nearly perpendicular to the Volyn-Middle Russia system.

It has been recognized that the Volyn-Middle Russia system of sedimentary basins and the Pachelma aulacogen broadly developed along the suture zones between the main crustal segments constituting Baltica, i.e., Sarmatia, Fennoscandia and Volgo-Uralia. Other important features of the Volyn-Orsha basin include its amagmatic nature, lack of well-defined rift boundaries, and low heat flow (Bogdanova et al., 1996).

The Volyn-Orsha basin is located in the SW part of Baltica. It is an elongated sedimentary depression that runs in a northeast direction with rather gentle bedding slopes towards the axial part. The size of the basin is about 625×250 km, and the maximum thickness is approximately 900 m. The Volyn-Orsha basin is divided into two sub-basins (Volyn and Orsha) by the Central-Belarussian saddle. Arcose sandstones prevail in the Volyn sub-basin, while the Orsha sub-basin is dominated by quartz sandstones.

The Polissya Group fills the Volyn sub-basin and comprises a continental, silty to sandy, red-bed sedimentary succession that was unconformably deposited on a Paleoproterozoic crystalline basement. The thickness of the group gradually increases from the basin margins towards the basin axis, where it reaches 900 m.

A sandstone sample was collected from drill-core #70 at a depth of 106.5 m. It represents the uppermost part of the Romeyki Formation, the lowermost unit of the Polissya Group. The analysed sample is a fine-grained, greenish-grey, bedded and poorly cemented quartz sandstone. Numerous zircon crystals were separated from this rock, which are predominantly 100 to 150 µm in size, colourless, and transparent. Grains are well to very well rounded and have an equant to short-prismatic shape. U–Pb zircon geochronology was performed at the University of California, Santa Barbara, using a Nu Plasma HR MC-ICP-MS and a Photon Machines Excite 193 excimer ArF laser-ablation system equipped with a HeLex sample cell.

In total, 103 zircon crystals were dated. Seventeen grains were more than 10 % discordant and were excluded from further consideration. Eighty-six grains yielded concordant ages, with most of them (74 grains, or 86 %) in the age interval between 1655 ± 3 and 1044 ± 16 Ma, with two well-defined peaks at ca. 1630 and 1230 Ma. The next group (7 zircons, 8 %) yielded ages between 2004 ± 9 and 1799 ± 9 Ma. Finally, 5 zircons had even older ages, extending back to 3260.3 ± 4.3 Ma (Fig. 1). The youngest dated grain yielded a date of 1044 ± 16 Ma, and the next three youngest grains formed a tight group with a weighted mean age of 1079 ± 8 Ma.

Paleoproterozoic, ca. 2000-1800 Ma zircons, in general, correspond to the time of formation of the crystalline basement that directly underlies the Volyn-Orsha basin. However, a closer examination of the zircon ages reveals significant difference with the ages of the potential local zircon sources. For instance, 1800-1740 Ma zircons are absent in the studied sample, whereas this age interval corresponds to the time of active intraplate magmatism in the Ukrainian Shield. Zircons with ages of 2150-2050 Ma are also absent in

the studied sample, whereas rocks of this age are widely distributed in the Ukrainian Shield. The studied sample contains a small number of ca. 2000 Ma zircons that could have been sourced from the Osnitsk-Mikashevychi igneous belt. Igneous and metamorphic zircons with dates between 1950 and 1800 Ma could have been derived from the Svecofennian orogen. Zircons with ca. 1650-1500 Ma dates could have been sourced from large anorthosite-mangerite-charnockite-granite complexes in SW Fennoscandia. Also, potential sources of the ca. 1500-1000 Ma zircons, which are the most abundant in the studied sample, are unknown in Sarmatia, but could have been derived from the Sveconorwegian belt. A small population of Archean zircons were likely derived from Archean complexes widely developed in the Ukrainian Shield.

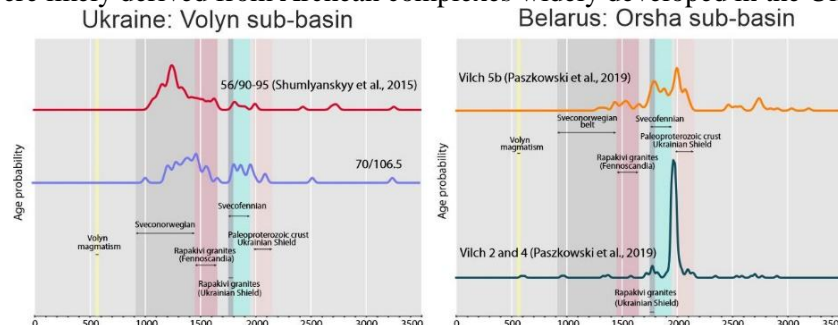


Figure 1. The detrital zircon age spectra (KDE plots) for the sediments filling the Volyn and Orsha sub-basins. Arrangement of the plots on the diagram broadly corresponds to their position in the sedimentary succession.

Many studies have suggested a strong link between Baltica and Amazonia during the Proterozoic. The western margin of Baltica (the Trans-European Suture Zone) was attached to Amazonia, suggesting that the Volyn-Orsha basin possibly continued farther westward towards Amazonia. Available geological data do not indicate any closure of the Volyn-Orsha basin towards the Trans-European Suture Zone; rather, it is sharply aborted by the zone. If this reconstruction is correct, then Amazonia might have been supplying detrital material to the basin, rather than the distally-located Sveconorwegian rocks.

Geochronological and isotope geochemical data regarding the Amazonia craton suggest that it could have been a suitable source of detrital material deposited in the Volyn sub-basin. Indeed, active magmatism in Amazonia started at ca. 2200 Ma and lasted until ca. 1250 Ma. It decreased in scale after 1250 Ma, but continued until ca. 950-900 Ma (see overview in Johansson et al., 2022).

The detrital zircon age distribution patterns in Neoproterozoic sedimentary samples collected from the stratigraphic units overlying the Volyn-Orsha basin (Paszowski et al., 2019) change drastically after the breakup of Rodinia. Samples of the Vilchitsy Group, which was deposited above the Belarus Group (equivalent of the Polissya Group in Belarus), demonstrate a wide spectrum of zircon dates with MDA of ca. 1000 Ma, similar to that observed in the Polissya Group. In contrast, all younger Ediacaran samples reveal a different pattern with a strong peak at ca. 1500 Ma and a small peak at ca. 1800 Ma, and lack younger ages except for ca. 570 Ma zircons related to the Volyn flood basalt province. Such a difference in the detrital zircon patterns indicates a dramatic change in the provenance. The most likely explanation is that after the Rodinia breakup, Amazonia sources were not anymore available and thus disappeared from the sedimentary record of Baltica.

Bogdanova, S.V.; Pashkevich, I.K.; Gorbatshev, R.; Orlyuk, M.I. Riphean rifting and major Palaeoproterozoic crustal boundaries in the basement of the East European Craton: geology and geophysics. *Tectonophys.* **1996**, *268*, 1-21. [https://doi.org/10.1016/S0040-1951\(96\)00232-6](https://doi.org/10.1016/S0040-1951(96)00232-6)

Johansson, Å.; Bingen, B.; Huhma, H.; Waight, T.; Vestergaard, R.; Soesoo, A.; Skirdlaite, G.; Krzeminska, E.; Shumlyanskyy, L.; Holland, M.E.; Holm-Denoma, C.; Teixeira, W.; Faleiros, F.; Ribeiro, B.; Jacobs, J.; Wang, C.C.; Thomas, R.; Macey, P.; Kirkland, C.; Hartnady, M.; Eglington, B.; Puetz, S.; Condie, K.C. A geochronological review of magmatism along the external margin of Columbia and in the Grenville-age orogens forming the core of Rodinia. *Precam. Res.* **2022**, *371*, 106463. <https://doi.org/10.1016/j.precamres.2021.106463>

Paszowski, M.; Budzyn, B.; Mazur, S.; Slama, J.; Shumlyanskyy, L.; Środoń, J.; Dhuime, B.; Kedzior, A.; Liivamagi, S.; Piszczowska, A. Detrital zircon U–Pb and Hf constraints on provenance and timing of deposition of the Mesoproterozoic to Cambrian sedimentary cover of the East European Craton, Belarus. *Precam. Res.* **2019**, *331*, 1–19. <https://doi.org/10.1016/j.precamres.2019.105352>

Shumlyanskyy, L.; Hawkesworth, C.; Dhuime, B.; Billström, K.; Claesson, S.; Storey, C. $^{207}\text{Pb}/^{206}\text{Pb}$ ages and Hf isotope composition of zircons from sedimentary rocks of the Ukrainian shield: crustal growth of the south-western part of East European craton from Archaean to Neoproterozoic. *Precam. Res.* **2015**, *260*, 39–54. <https://doi.org/10.1016/j.precamres.2015.01.007>

Do the ambient and/or magmatic stress regimes control the emplacement of a radiating dyke swarm?: a case study from the mafic dyke swarms of the eastern Dharwar Craton

Srinjoy Datta; Amiya K. Samal; Sayandeep Banerjee; Rajesh K. Srivastava

Department of Geology, Banaras Hindu University, Varanasi, 221005

Mafic dyke swarms act as the plumbing system for Large Igneous Provinces, transporting magma from the deeper magma chambers to the crustal depth. They can either be emplaced via primary hydraulic fracturing, wherein the magmatic overpressures would control the dyking or may infiltrate into pre-existing fractures and inhomogeneities, employing them as potential pathways of magma transport. In the former case, the primary magmatic stress regime would regulate the emplacement, whereas, in the latter, there will be a significant impact of the ambient stress field of the country rock in dyking. These situations, however, are two absolute requirements rather than end members for dyke emplacement. In nature, both of these above circumstances tend to coexist most of the time. This makes the study of dyke emplacement systematics and magma flow dynamics fascinating. The emplacement of parallel dykes is attributed to rifting and regional stress regimes (Hou, 2012; Ernst et al., 2014). The small radiating dyke swarms that are generally found close to a volcanic edifice are related to the local magmatic stress regime. Whereas the dynamics of the mantle plume have been linked to the giant radiating dyke swarms. The magmatic stress regime generally governs the emplacement close to the plume centre and regional stress regime is crucial at farther distances from the plume centre (Hou et al., 2010; Ernst, 2014). In spite of several established models on this topic, the interrelationship of the magmatic stress regime and the pre-existing ambient stress regime in the emplacement of giant radiating dyke swarms is not fully understood. As magnetic minerals generally mimic the magma flow, when coupled with petrofabric analyses and field observations, anisotropy of magnetic susceptibility (AMS) analyses present a powerful and effective tool to constrain the magma flow dynamics within the dyke fractures. We can better comprehend the interactions between the magmatic and ambient stress fields in a dyking event by comparing this to the pre-existing stress field.

The eastern Dharwar Craton has exposures of nine Paleoproterozoic mafic dyke swarms that span from ca. 2.37 Ga to ca. 1.79 Ga. They cover the entirety of the craton, and some of them display spectacular radiating geometry. Herein we have included two classical radiating dyke swarms, i.e. the ca. 2.21 Ga NW- WNW trending Anantapur Kunigal dyke swarm and the N-, NW- and NE- trending ca. 2.08 Ga Devarabanda dyke swarm in our quest to understand the interrelationship between the magmatic and ambient stress regimes in their emplacement. We conducted detailed analyses of magnetic anisotropy in the oriented dolerite samples from the dyke margins, followed by petrofabric analyses (shape preferred orientation) to understand the nature of the magma flow dynamics. Further, the AMS of host granites was studied to quantify the pre-existing stress regimes under which the dykes were emplaced. To delineate the regional crustal inhomogeneities and compare them with the dyke geometries for determining their influence (if any) on the emplacement of the dyke swarms, we also included in-depth fracture analysis, field observations, and satellite imagery. Our results suggest the ca. 2.21 Ga dyke swarm has lateral dyke emplacement in a setting where the natural magmatic stress field is complemented by the ambient stress field. Whereas the ca. 2.08 Ga dyke swarm displays a spatial variation in its emplacement mechanism between its three subswarms, which is again based on the combined influence of the magmatic and the ambient stress regime. It is established that magma generally takes up the most viable path for its emplacement. From our multiproxy approach, we suggest a combined control of both ambient and magmatic stress fields in the dyke emplacement for both the studied cases; however, the nature of their interrelationship guides the magma flow dynamics. We propose that the geometry of the dyke swarm would be usually governed by the regional stress field and that the magma would follow the available crustal inhomogeneities that have favourable geometry with respect to the location of the plume centre. In these situations, the magmatic stress regime would only play a little part in the emplacement of the dyke. On the other hand, the primary magmatic stress field would take control of the dyke emplacement by forming primary dyke fractures

with favourable geometry, provided there is sufficient magma input, even when the available inhomogeneities do not have a favourable geometry for magma transport, even at great distances from the plume centre. Based on these observations, we further present two emplacement models for both the studied dyke swarms that are comprehensive and can be used as a template for the emplacement mechanism of dyke swarms exposed in the other related cratons.

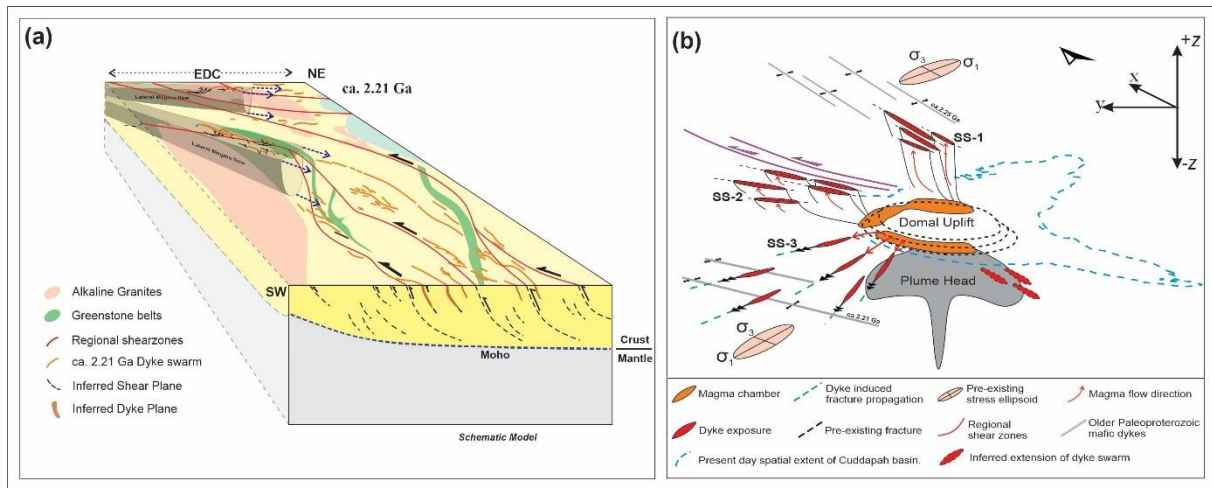


Figure 1: (a) Schematic emplacement models of ca. 2.21 Ga Anantapur- Kunigal dyke swarm, vertical section after Chadwick et al., (2007). (b) Schematic emplacement model of ca. 2.08 Ga Devarabanda dyke swarm.

References

- Chadwick, B., Vasudev, V. N., Hegde, G. V., & Nutman, A. P. (2007). Structure and SHRIMP U/Pb zircon ages of granites adjacent to the Chitradurga schist belt: Implications for Neoarchaean convergence in the Dharwar craton, southern India. *Journal of the Geological Society of India*, 69.
- Ernst, R. E. (2014). *Large igneous provinces*. Cambridge University Press.
- Kumar, A., Parashuramulu, V., & Nagaraju, E. (2015). A 2082 Ma radiating dyke swarm in the Eastern Dharwar Craton, southern India and its implications to Cuddapah basin formation. *Precambrian Research*, 266, 490-505.
- Hou, G., Kusky, T. M., Wang, C., & Wang, Y. (2010). Mechanics of the giant radiating Mackenzie dyke swarm: a paleostress field modeling. *Journal of Geophysical Research: Solid Earth*, 115(B2).
- Hou, G. (2012). Mechanism for three types of mafic dyke swarms. *Geoscience Frontiers*, 3(2), 217-223.
- Samal, A. K., Rai, A. K., & Srivastava, R. K. (2021). Multiple mantle melting events for two overlapping ca. 2.21-2.18 Ga mafic dyke swarms in the Dharwar craton, India. *International Geology Review*, 63(17), 2166-2191.

The extent of distinct Precambrian mafic dyke swarms and sills in the Indian Shield: current scenario and implications

Rajesh K. Srivastava, Amiya K. Samal and Gulab C. Gautam

Department of Geology, Banaras Hindu University, Varanasi 221005, India

A number of distinct mafic dyke swarms (MDSs) and mafic sills (MSs) are emplaced within the Indian Shield, spanning in age between ca. 2.8 Ga and 1.4 Ga (e.g., Samal et al. 2019, 2021; Söderlund et al. 2019; Srivastava et al. 2020, 2022). Although MDSs and MSs are reported from all the cratons of the Indian Shield, however these are more spectacular and studied in detail from the Dharwar, Bastar, Singhbhum and Bundelkhand cratons; Aravalli craton is poorly constrained (Fig. 1).

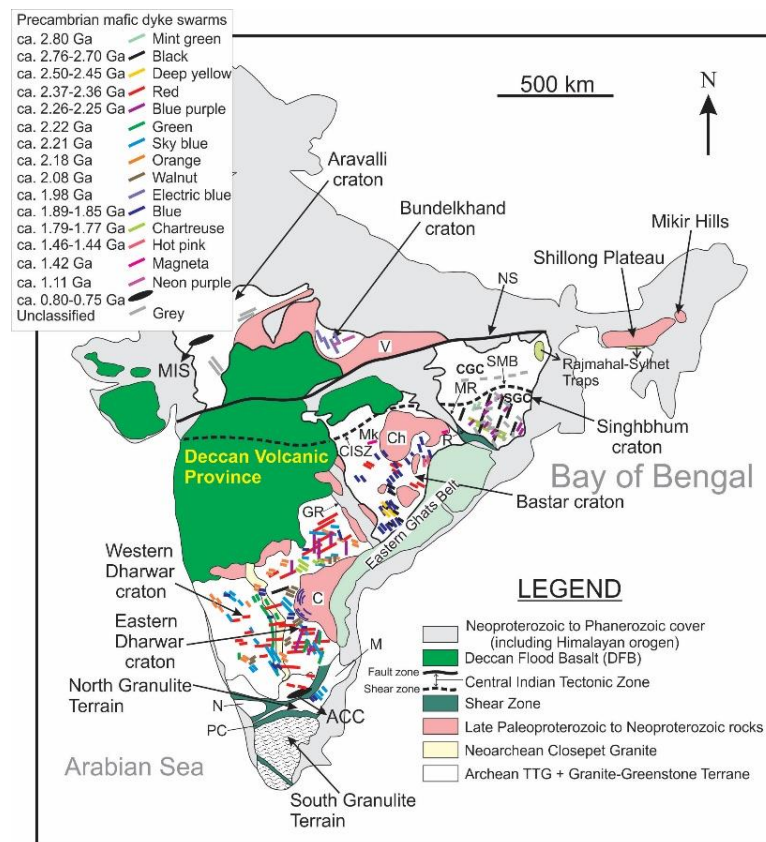


Figure 1: Generalized geological map of the Indian Shield showing distinct Precambrian mafic dyke swarms (MDSs) (after Samal et al. 2019).

Most of these MDSs are precisely dated and connected to different large igneous province events. The Dharwar craton is intruded by 10 distinct MDSs/MSs; these include – (i) Ca. 2.37-2.36 Ga NE- to ESE-trending Bangalore–Karimnagar swarm, (ii) Ca. 2.26-2.25 Ga N- to NNE-trending Ippaguda-Dhiburahalli swarm, (iii) Ca. 2.22 Ga N- to NNW-trending Kandlamadugu swarm, (iv) Ca. 2.21 Ga NW- to WNW-trending Anantapur–Kunigal swarm, (v) Ca. 2.18 Ga NW- to WNW-trending Mahbubnagar–Dandeli swarm, (vi) Ca. 2.08 Ga N-, NW-, and NE-trending Devarabanda swarm, (vii) Ca. 1.96 Ga ENE-trending Mundagiri dyke, (viii) Ca. 1.89–1.88 Ga E- to ENE-trending Hampi swarm (this also includes ca. 1.89-1.88 Ga Pulivendla sills emplaced in the Cuddapah basin), (ix) Ca. 1.85 Ga NW-trending Dharmapuri swarm, and (x) Ca. 1.79 Ga NW-trending Pebbair swarm.

The Bastar craton is transected by 9 distinct MDSs; these are – (i) Ca. 2.7 Ga WNW–to NW–trending Sukma swarm, (ii) Ca. 2.5–2.4 Ga NW–trending Dantewara swarm, (iii) Ca. 2.37 Ga NW–trending Bhanuprtappur swarm, (iv) Ca. 2.25 Ga ENE–trending Chhura swarm, (v) Ca. 1.89–1.88 Ga NW–, NNW– to N–trending Bastanar swarm, (vi) Ca. 1.85 NNW– to NW–trending Sonakhan swarm, (vii) Ca. 1.78 Ga NW–trending Geedam swarm, (viii) Ca. 1.46–1.44 Ga N– to NNE–trending Lakhna swarm, and (ix) Ca. 1.42 Ga ENE–trending Bandalimal swarm, emplaced within the Chhattisgarh basin. Similarly, the Singhbhum also comprises 7 distinct MDSs/MSs, however only four are precisely dated, and the rest three are identified on the basis of cross-cutting relationships with dated dykes. The seven swarms of the Singhbhum craton are – (i) Ca. 2.80 Ga NE–trending Keshargaria swarm, (ii) Ca. 2.76–2.75 Ga NNE– to NE–trending Ghatgaon swarm, (iii) Ca. 2.26 Ga NE– to ENE–trending Kaptipada swarm, (iv) Ca. 1.77 Ga WNW–trending Pipilia swarm, (v) Early-Paleoproterozoic E– to ENE–trending Keonjhar swarm, (vi) Middle-Paleoproterozoic NW– to NNW–trending Bhagamunda swarm, and (vii) Late-Paleoproterozoic N– to NNE–trending Barigaon swarm. The Bundelkhand craton has two distinct MDSs – (i) NW–trending ca. 1.98 Ga Jhansi swarm and (ii) ENE–trending ca. 1.11 Ga Mahoba swarm. The Paleoproterozoic basins, neighboring the Bundelkhand craton, also have evidence of intrusions of mafic sills – (i) Ca. 1.98–1.97 Ga mafic sills in the Bijawar basin and (ii) Ca. 1.73 Ga mafic sills in the Gwalior basin.

Based on these distinct mafic intrusion records in the Indian Shield, >10 Precambrian large igneous province (LIP) events are identified. The identified LIPs are – (i) Ca. 2.80–2.75 Ga Ghatgaon LIP, (ii) Ca. 2.50–2.47 Ga Dantewara LIP, (iii) ca. 2.37–2.236 Ga Bangalore LIP, (iv) Ca. 2.26–2.25 Ga Ippaguda LIP, (v) Ca. 2.22 Ga Kandalamadugu LIP, (vi) Ca. 2.21–2.18 Ga Anantapur LIP, (v) Ca. 2.08 Ga Devarabanda LIP, (vi) Ca. 1.98–1.97 Ga Jhansi LIP, (vii) Ca. 1.89–1.85 Ga Bastanar LIP, (viii) Ca. 1.79–1.77 Ga Pipilia LIP, (ix) Ca. 1.73 Ga Gwalior LIP, (x) Ca. 1.46–1.42 Ga Lakhna LIP, and (xi) Ca. 1.12–1.05 Ga Mahoba LIP. The overlapping LIP events in the Dharwar, Bastar and Singhbhum cratons also facilitated to identify a megacraton DHABASI in the Indian Shield. The identified LIP events of the Indian Shield are supposed to be an integral part of most of the known supercontinents, such as Kenorland/Superia, Columbia/Nuna, Rodinia, Gondwana/Pannotia, and Pangea, in Earth's evolution. Many of these mafic-ultramafic units of LIPs are supposed to be potential targets for mineralization of the Cu-Ni-Co-platinum group elements (PGEs), Fe-Ti-V and Cr – both as oxides and sulphides (Samal et al. 2021).

Samal, A.K., Srivastava, R.K., Ernst, R.E. and Söderlund, U. (2019) Neoproterozoic mafic dyke swarms of the Indian Shield mapped using Google Earth™ images and ArcGIS™, and links with Large Igneous Provinces. In: Srivastava, R.K., Ernst, R.E., Peng, P. (Eds.), *Dyke Swarms of the World – A modern perspective*, Springer Nature Singapore Pte Ltd., 335–390.

Samal, A.K., Srivastava, R.K. and Ernst, R.E. (2021) An appraisal of mineral systems associated with Precambrian Large Igneous Provinces of the Indian Shield. *Ore Geology Reviews*, 131: 104009; <https://doi.org/10.1016/j.oregeorev.2021.104009>

Söderlund, U., Bleeker, W., Demirel, K., Srivastava, R.K., Hamilton, M., Nilsson, M., Pesonen, L.J., Samal, A.K., Jayananda, M., Ernst, R.E. and Srinivas, M. (2019) Emplacement ages of Paleoproterozoic mafic dyke swarms in eastern Dharwar craton, India: Implications for paleoreconstructions and support for a ~30° change in dyke trends from south to north. *Precambrian Research*, 329: 26–43

Srivastava, R.K., Samal, A.K., Ernst, R.E., Söderlund, U. and Ravi Shankar (2020). Spatial and temporal distribution of large igneous provinces in the Indian shield – highlights of recent researches. *Proceedings of the Indian National Science Academy*, 86: 313–330.

Srivastava, R.K., Ernst, R.E., Söderlund, U., Samal, A.K., Pandey, O.P. and Gautam, G.C. (2022). Existence of the Dharwar-Bastar-Singhbhum (DHABASI) megacraton since 3.35 Ga: constraints from the Precambrian large igneous province record. *Geological Society, London, Special Publication*, 518, 175–198; DOI: <https://doi.org/10.1144/SP518-2021-53>

2.00 Ga mafic sills in the Onega basin, Fennoscandian Shield: implications Pechenga-Onega LIP and age restrictions for Paleoproterozoic Shunga event

Stepanova A.V.¹; Salnikova E.B.²; Samsonov A.V.³; Sukhanova M.A.²; Ustinova V.V.¹; Larionova Yu.O.³; Prave, T.⁴; Kirsimäe, K.⁵; Lepland A.⁶

¹ Institute of geology, Karelian Research Centre RAS, Petrozavodsk, Karelia, Russia

² Institute of Precambrian geology and geochronology RAS, Saint-Petersburg, Russia.

³ Institute of Geology of Ore Deposits, Petrography, Mineralogy and Geochemistry RAS, Moscow, Russia

⁴ Department of Earth and Environmental Sciences, University of St Andrews, St Andrews, KY16 9AL, Scotland, UK

⁵ Department of Geology, University of Tartu, 50411 Tartu, Estonia

⁶ Geological Survey of Norway, Postboks 6315 Sluppen, 7491 Trondheim, Norway

The Pechenga-Onega LIP in the Eastern Fennoscandian Shield comprise a series of voluminous pulses of mafic magmatism of age 2.00-1.94 Ga (Puchtel et al., 1999, Lubnina et al., 2016, 2018). Despite general similarity in age and composition of mafic rocks in Pechenga and Onega segments of this LIP, no mafic rocks with age older than 1.98 Ga have been previously recognized in the Onega segment of Pechenga-Onega LIP.

Newly discovered 2.00 Ga mafic sills were studied in the north-eastern part of the Zaonega peninsula in the central part of the Onega Basin (Melezhik et al., 2013). Studied mafic sills cut organic-rich mudstones (shungites) of the Zaonega Fm. Sills are up to 50 m thick and comprise metadolerites of high-Fe-Ti tholeiitic series affinity rocks. The evolved varieties comprise two types of gabbro-pegmatites: small schlieren enriched in TiO₂ (up to 3.5 wt.%) and Fe₂O₃ (up to 25 wt.%) and relatively large pegmatite lenses and granophyre rocks enriched in SiO₂ (up to 57 wt.%), which represent residual melts formed after magnetite crystallization. Dolerites are slightly enriched in LREE and have flat HREE distribution patterns. εNd values in dolerites are +0.4 – +0.6 suggesting contamination of melts by Archean basement granitoids or host sediments.

Several sills in the Lebeschina, Tolvuya, and Shunga localities were sampled. Baddeleyite was extracted from medium-grained dolerites, high Fe-Ti gabbro-pegmatites and high-Si gabbro-pegmatites. The U-Pb age of baddeleyite vary insignificantly, given an age of 2000±5 Ma for all studied samples. This new baddeleyite age data for mafic sills in the Onega Basin define the minimum age for the organic-rich sediments of the Zaonega Fm, and consequently give age restrictions for the Shunga event (Melezhik et al., 1999).

New U-Pb ID-TIMS baddeleyite data for Fe-Ti tholeiitic mafic sills indicate that mafic magmatism in the Onega segment of the Pechenga-Onega LIP starts at least at 2.00 Ga and includes several pulses of low-Mg high-Fe-Ti tholeiitic magmatism with age of 2.00, 1.98, 1.97 Ga (Lubnina et al., 2016, 2018), and high-Mg OIB-type mafic rocks of age 1.96 Ga (Puchtel et al., 1999).

Lubnina N. V., Pisarevsky S. A., Stepanova A. V., Bogdanova S. V., Sokolov S. J. Fennoscandia before Nuna/Columbia: Paleomagnetism of 1.98–1.96 Ga mafic rocks of the Karelian craton and paleogeographic implications // Precambrian Res. 2017. V. 292. P. 1-12

Lubnina N. V., Stepanova A. V., Ernst R. E., Nilsson M., Söderlund U. New U–Pb baddeleyite age, and AMS and paleomagnetic data for dolerites in the Lake Onega region belonging to the 1.98–1.95 Ga regional Pechenga–Onega Large Igneous Province // GFF. 2016. V. 138. P. 54–78.

Melezhik V. A., Fallick A. E., Filippov M. M., Larsen O. Karelian shungite-an indication of 2.0-Ga-old metamorphosed oil-shale and generation of petroleum: Geology, lithology and geochemistry. Earth Science Reviews, 1999. V. 47 P. 1–40

Melezhik V. A., Medvedev P. V., Svetov S. A. 4.3 The Onega Basin // Reading the Archive of Earth's Oxygenation, Volume 1: The Palaeoproterozoic of Fennoscandia as Context for the Fennoscandian Arctic Russia - Drilling Early Earth Project Frontiers in Earth Sciences. / ed. V. A. Melezhik, A. R. Prave, A. E. Fallick, L. R. Kump, H. Strauss, A. Lepland, E. J. Hanski. Berlin, Heidelberg: Springer Berlin Heidelberg, 2013. P. 387–490.

Puchtel I. S., Arndt N. T., Hofmann A. W., Haase K. M., Kröner A., Kulikov V. S., Kulikova V. V., Garbe-Schönberg C.-D., Nemchin A. A. Petrology of mafic lavas within the Onega plateau, central Karelia: evidence for 2.0 Ga plume-related continental crustal growth in the Baltic Shield // Contrib. to Mineral. Petrol. 1998. V. 130. № 2. P. 134- 153

Puchtel I. S., Brüggemann G. E., Hofmann A. W. Precise Re–Os mineral isochron and Pb–Nd–Os isotope systematics of a mafic–ultramafic sill in the 2.0 Ga Onega plateau (Baltic Shield) // Earth Planet. Sci. Lett. 1999. V. 170. № 4. P. 447–461.

Timing of Paleoproterozoic carbonatitic magmatism by U-Pb ID-TIMS dating of calcic garnets

M.V. Stifeeva¹, Yu.V. Plotkina¹, E.B. Salnikova¹, A.B. Kotov¹, K.A. Savko²

¹Institute of Precambrian Geology and Geochronology RAS, 199034 Makarova emb. 2, St.Petersburg, Russia

²Voronezh State University, 394018 Universitetskaya Square 1, Voronezh, Russia

Early Precambrian alkaline-carbonatitic complexes often underwent by large-scale accretionary and collisional reworking, strongly transforming primary igneous associations, thus complicating geochronological and petrogenetic reconstructions.

We provide U–Pb geochronological data on Ca-Fe garnet, zircon and titanite from two metamorphosed Paleoproterozoic alkaline–carbonatite complex from the the Kursk block of Sarmatia and the Aldan shield.

The Dubravinsky alkaline-carbonatite complex is located within the Kursk-Besedino domain, which, together with the Azov block, forms the Paleoarchean core of eastern Sarmatia (Azov-Kursk domain) (Bogdanova et al., 2016; Savko et al., 2021). The Dubravinsky massif consists of clinopyroxenites, carbonatites (together with silicocarbonatites and phoscorites) and syenites (including alkaline granites).

Zircons in silicocarbonatite have short-prismatic or dipyrmidal habit typical for many carbonatite rocks. Zircon crystals are euhedral and subhedral, semitransparent and transparent, of gray color, sometimes square in shape or with smoothed, almost rounded tips, 50–80 µm in size. In CL images most crystals show a zonal structure - lighter inhomogeneous centres with a very dark high-uranium regions occupying up to 50% area, and dark gray rims 10–15 µm as wide. The U-Pb isotope system in carbonatitic zircons is disturbed, which suggests influence of superimposed events.

The ages of titanite 2071 ± 11 Ma and andradite 2075 ± 12 Ma from the alkaline pyroxenite, as well as of titanite from carbonatite 2080 ± 13 Ma (Albekov et al., 2017) The closing temperatures of the U–Pb titanite isotope system in the range of 650–700 °C (Frost et al., 2000, Wu et al., 2010) are close to the peak temperatures of metamorphism (~ 650 °C), precluding choosing one of interpretations. However, for calcium garnet with a grain size of 100 µm from the alkaline rocks and carbonatites, the closing temperature is 750–800 °C (Yang et al., 2018). This suggests that the U-Pb age of andradite from the alkaline pyroxenites of the Dubravinsky massif corresponds to the age of its crystallization from the melt.

U–Pb (ID-TIMS) garnet and U–Th–Pb (LA-ICP-MS) zircon geochronological studies were performed for the carbonatites veins from the Late Archaean Ukduška alkaline-carbonatitic massif, Aldan shield. Zircons extracted from carbonatite are subeuhedral crystals with prismatic habits. Zircon crystals are usually fractured, opaque, and dark cherry colored. Their structure is characterized by the brown-color zoned cores and two generations of rims. The U–Th–Pb (LA-ICP-MS) studies were carried out in the core and rims of zircon grains. The average ages (207Pb/206Pb) of the cores are 2708 ± 14 Ma (MSWD = 0.36), the first-generation rims are 2645 ± 17 Ma, and, finally, the second-generation rims are 1865 ± 16 Ma (MSWD = 0.36). U-Pb age of andradite from the Ukduška carbonatite is at 1881 ± 8 Ma (MSWD = 0.70).

Hence, two formation stages of Early Precambrian carbonatites can be distinguished in the southeastern part of the Chara–Olyokma geoblock. The first of them includes the formation of carbonatites related to the Late Archean alkali potassic and ultrapotassic magmatism with an age of 2719 ± 14 Ma (Tabuns et al., 2004). The second stage carbonatites form dikes and veins developed in the Early Proterozoic (1881 ± 8 Ma).

Therefore U-Pb ID-TIMS ages obtained for Ca-Fe garnets demonstrate the advantages that these minerals offer to geochronological study of Precambrian carbonatites affected by metamorphic alteration.

The investigations were supported by RSF (grant № 22-17-00211).

Albekov, A.Yu., Chernyshov, N.M., Ryborak, M.V., Kuznetsov, V.S., Salnikova, E.B., Kholin, V.M., 2017. U-Pb isotopic age of apatite-bearing carbonatites in the Kursk Block, Voronezh Crystalline Massif. *Dokl. Earth Sci.*, 473, 271–272.

Bogdanova, S.V., Gorbatshev, R., Garetsky, R.G., 2016. EUROPE/East European Craton. Reference Module in Earth Systems and Environmental Sciences, Elsevier. <https://doi.org/10.1016/B978-0-12-409548-9.10020-X>.

Frost, B.R., Chamberlain, K.R., Schumacher, J.C., 2000. Spinel (titanite): phase relations and role as a geochronometer. *Chemical Geology* 172, 131–148.

Savko K.A., Samsonov A.V., Larionov A.N., Chervyakovskaya M.V., Korish E.H., Larionova Yu.O., Bazikov N.S., Tsybulyaev S.V. *A buried Paleoproterozoic core of the Eastern Sarmatia, Kursk block: U-Pb, Lu-Hf and Sm-Nd isotope mapping and paleotectonic application// Precambrian Research 353. 2021. 106021*

Tabuns E.V., Sal'nikova E.B., Kovach V.P., Kotov A.B., Yakovleva S.Z., Fedoseenko A.M., Tolkachov M.D., Plotkina Yu.V., Kovalenko V.I. *Late Archean initial potassic magmatism of the Aldan shield (Ukduska massif): evidence from U-Pb single zircon dating. 2004. Doklady Earth Sciences. 398, 7, 943-946.*

Wu, F.Y., Yang, Y.H., Marks, M.A.W., Liu, Z.C., Zhou, Q., Ge, W.C., Yang, J.S., Zhao, Z.F., Mitchell, R.H., Markl, G., 2010. *In situ U-Pb, Sr, Nd, and Hf isotopic analysis of eudialyte by LA-(MC)-ICP-MS. Chemical Geology 273, 8-34.*

Yang Y.H., Wu F.Y., Yang J.H., Mitchell R.H., Zhao Z.F., Xie L.W., Huang C., Ma Q., Yang M. and Zhao H. 2018. *U-Pb age determination of schorlomite garnet by laser ablation inductively coupled plasma Mass spectrometry. Journal of Analytical Atomic Spectrometry, 33, 231-239.*

A mantle plume origin for the Scandinavian Dyke Complex: a “piercing point” for 615 Ma plate reconstruction of Baltica?

**Christian Tegner¹, Torgeir B. Andersen², Hans Jørgen Kjøll², Eric L. Brown¹, Graham Hagen-Peter^{1,3},
Fernando Corfu², Sverre Planke², and Trond H. Torsvik²**

¹: Department of Geoscience, Aarhus University, Denmark Adress: (Times New Roman, 10, single-spaced.)

²: Department of Geosciences, University of Oslo, Norway

³: Vrije Universiteit Amsterdam, Netherlands

The origin of Large Igneous Provinces (LIPs) associated with continental breakup and the reconstruction of continents older than c. 320 million years (pre-Pangea) are contentious research problems. Here we study the petrology of a 615 - 590 Myr dolerite dyke complex that intruded rift-basins of the magma-rich margin of Baltica and now is exposed in the Scandinavian Caledonides. These dykes are part of the Central Iapetus Magmatic Province (CIMP), a LIP emplaced in Baltica and Laurentia during opening of the Iapetus Ocean within the Caledonian Wilson Cycle. The >1000 km long dyke complex displays lateral geochemical zonation from enriched to depleted basaltic compositions from south to north. Geochemical modelling of major and trace elements shows these compositions are best explained by melting hot mantle 75-250°C above ambient mantle. Although the trace element modelling solutions are non-unique, the best explanation involves melting a laterally zoned mantle plume with enriched and depleted peridotite lithologies, similar to present-day Iceland and to the North Atlantic Igneous Province. The origin of CIMP appears to have involved several mantle plumes. This is best explained if rifting and breakup magmatism coincided with plume generation zones at the margins of a Large Low Shear-wave Velocity Province (LLSVP) at the core mantle boundary. If the LLSVPs are quasi-stationary back in time as suggested in recent geodynamic models, the CIMP provides a guide for reconstructing the paleogeography of Baltica and Laurentia 615 million years ago to the LLSVP now positioned under the Pacific Ocean. Our results provide a stimulus for using LIPs as piercing points for plate reconstructions (Tegner et al., 2019).

*Tegner, C., Andersen, T.B., Kjøll, H.J., Brown, E.L., Hagen-Peter, G., Corfu, F., Planke, S., and Torsvik, T.H. (2019). A mantle plume origin for the Scandinavian Dyke Complex: a “piercing point” for 615 Ma plate reconstruction of Baltica? *Geochemistry, Geophysics, Geosystems* 20, 1075-1094. doi:10.1029/2018GC007941*

Wrinkle Ridges, Henie Quadrangle (V-58), Southern Venus

E. Varga¹, K.J.E. Boggs¹, C. Pendleton¹, J. Shackman¹, H.N. Bley¹, J. Demorcy², L. Dhimi¹, M. Chowdhury¹, B. Dear¹, Herrington, S.¹, H.G. Wehnes¹, R.E. Ernst^{2,3}, H. El Bilali^{2,3} and, E.M. Bethell⁴,

¹Department of Earth and Environmental Sciences, Mount Royal University, 4825 Mount Royal Gate se, Calgary, Alberta, Canada T3E 6K6;

²Department of Earth Sciences, Carleton University, 1125 Colonel By Drive, Ottawa, Ontario, Canada K1S 5B6;

³Faculty of Geology and Geography, Tomsk State University, 36 Lenin Avenue, Tomsk, Russia 634050;

⁴Department of Earth and Environmental Sciences, University of Ottawa, 75 Laurier Avenue E, Ottawa, Ontario, Canada K1N 6N5.

Introduction: Wrinkle ridges (WR) are long sinuous features (e.g. Fig. 2) thought to form under compression due to asymmetry observed in topographic cross sections across WRs on Mars and the Moon (Hanmer, 2023). Venusian WRs are unique due to uniform spacing, and lack of observed master faults (Bilotti and Suppe, 1999). Only one study (Bethel et al 2023) has used stereographic projections to produce topographic cross-sections across WRs. More work is needed to confirm whether Venusian WRs form in compression, how much compression could be represented by these WRs, if and why Venusian WRs don't have master faults. Here we are characterizing the WRs across the Henie Quadrangle starting with the study area in (outlined in orange in Fig. 1).

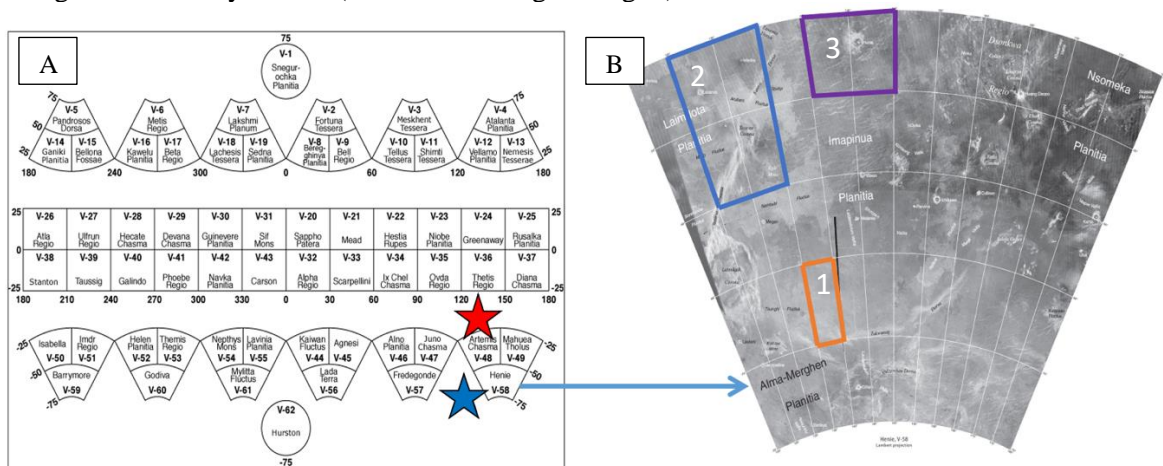


Figure 1. A) Henie Quadrangle (V-58; blue star) in southern Venus. B) Study area (orange box #1) for this poster. Purple box #2, has 11 wrinkle ridges over 320 km (Shackman et al, 2023). Blue box #3, as 14 wrinkle ridges over 500km (Herrington et al, 2023). The red star is the Artemis Quadrangle named after Artemis which is proposed to be one of the largest tectonomagmatic features in the Solar System (Hansen et al 2010), and a possible source for the strain that formed the northeastern WR's (yellow box Fig 2).

Methodology: Radar image files are from the Planetary Data System (NASA Magellan mission; images obtained 1990-94). Geological features were traced out using ArcGIS (at 1:500 000). Only the right-look radar data was available in the study area, which prevents the creation of stereographic imaging for topographic cross-sections.

Results: There are two distinct populations of WRs (in the northeast and southeast; Fig. 2). The twelve northern WRs (275°-095° to 240°-060°) have an average length of 30km; the western WRs are spaced at 20-30km, and the eastern WRs are spaced at 10-15km. The two southeastern WRs (330°-120°) are 86 and 115km long, separated by ~54km. In the transition area between these two WR groupings are (398) extensional grabens with lengths from 5 to 20km and an average spacing of 20km. There are no observed master faults in either the WRs or graben populations. The northern WRs from the study area are parallel to WRs further north in the Henie Quadrangle. There are seven episodes of lava flows across the study area. The relationships between the WRs, lava flows and grabens are summarized in Table 1.

Discussion and Conclusions: In this study area (Fig. 2), WRs cut across lava flows #1 through #4 (but not across #7 to #9) suggesting that they are younger than these lava flows, but older than lava flows #7 through #9. The orientation of the northern WRs in the study area, parallel to WRs in the northern Henie Quadrangle suggest that the formation of the Artemis tectonomagmatic (Hansen et al 2010) feature may have created the compressional strain that formed these WRs. (See Varga et al. (2023) poster for more information about the extent of the influence of the Artemis

feature across the Henie Quadrangle). These WRs and grabens are uniformly spaced with no evidence of master faults, possibly due to the hot surface temperatures on Venus. Areas 2 and 3 (Figure. 1) show similar spacing of wrinkle ridges, suggesting Artemis wrinkle ridges will be similar in spacing.

Table 1. Relative Order of Geological Events in Study Area.

Order	Relative Order of Geological Events in Study Area [Numbered boxes in Fig.2 A]
1-2 Oldest Lava Flows	Lava flows (green & blue) appear to be intergrown. All other geological features cut across these suggesting they are the oldest features in the study area
3 Lava Fluctus	Fluctus (orange); flow from west (green arrow). The northern edge appears to have flowed over lava flows #1/2 suggesting that the fluctus is younger
4 Lava Flow	Lava flow (purple) from the east (blue arrow). Western lobe flowed over the fluctus suggesting that this is younger
5-6 Wrinkle Ridges	WRs (green, red) cut across lava flows 1-4 suggesting that the WRs are younger. The relative order between the two WRs is indeterminate because they don't connect.
7 Lava Flow	Lava flow (light green) is not cut by WRs suggesting that this lava flow is younger
8-9 Lava Flow	Lava flows (yellow, pink) appear to flow along WRs. Lobes cut across lava flows 1-7 suggesting that these are the youngest lava flows. Relative order between these two lavas flows is indeterminate.
10 Youngest Grabens	Grabens (blue); cut across all geological features in study area, suggesting that the grabens are the youngest geological features

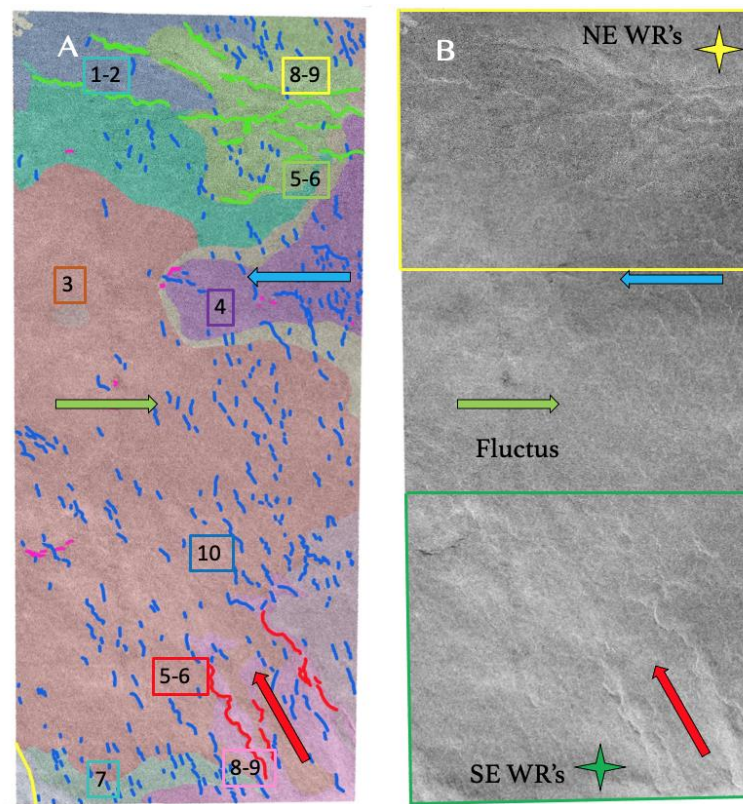


Figure 2. A) Mapped study area (orange box in Fig. 1). The northeastern WRs are green and the southeastern are red. A lava channel is yellow (see Demorcy et al. 2023 abstract/poster for more information about canali). The orange polygon is a fluctus, six further lava flows (other colours) are further described in Table 1. **B)** Non-interpreted radar image of study area. Arrows indicate direction of lava flow around SE wrinkle ridges.

Future Work: The MRU Venus geological mapping team next steps include: i) Complete the mapping of the Henie Quadrangle, ii) Examine all the WRs in order to identify other possible sources of compression for WRs not associated with the Artemis feature (e.g. southeastern WRs in this study area), iii) Determine where the origin of the 7 lava flows, two groups of WRs, and grabens in the study area fit with the formation of the Artemis feature, and iv) Identify regions with more than one look of radar images, in order to create stereographic topographic cross-sections across WRs to further test if compression formed these WRs.

References:

- Bethell, E.M., Ernst, R.E., and Samson, C., 2022, *Analysis of Venusian Wrinkle Ridge Morphometry Using Stereo-Derived Topography: A Case Study From Southern Eistla Regio*: *Journal Of Geophysical Research: Planets*, v. 127, doi:<https://doi.org/10.1029/2021je006879>.
- Bilotti, F., and Suppe, J., 1999, *The Global Distribution of Wrinkle Ridges on Venus*: *Icarus*, v. 139, p. 137–157, doi:<https://doi.org/10.1006/icar.1999.6092>.
- Hanmer, S., 2023, *Basic structural geology of Venus: A review of the gaps and how to bridge them*: *Earth-Science Reviews*, v. 237, p. 104331, doi:<https://doi.org/10.1016/j.earscirev.2023.104331>.
- Hansen, V.L., Olive, A., 2010, *Artemis, Venus: the largest tectonomagmatic feature in the Solar System?* // *Geology*, 2010, V. 38: P. 467–470

Origin of clinopyroxene megacrysts from basanite pipes in the Minusa trough, Southern Siberia

V.V. Vrublevskii, F. Kazenova, A.P. Korneva, A.D. Kotel'nikov, I.O. Kremer, P.A. Tishin
National Research Tomsk State University, Tomsk, Russia

The Late Cretaceous (~80 Ma) basanite pipes and dikes are localized in the Minusa paleorift between the Early Paleozoic orogens of Kuznetsk Alatau, East Sayan and West Sayan in southern Siberia. They cut the Devonian and Carboniferous clastic sediments around the Kop'yevo dome within the North Minusa basin and contain xenoliths of mantle peridotites (Malkovets et al., 2003). Basanites are characterized by low silica content (42–49 wt. % SiO₂) and variable alkalis (3.5–6.5 wt. % Na₂O+K₂O; Na₂O/K₂O 1.5–5.2). High MgO (6–12 wt. %) and compatible elements contents (~100–390 ppm Cr, 90–180 ppm Ni, 140–170 ppm V, 40–60 ppm Co) may indicate an undifferentiated parent melt. However, the content and ratios of HFSE (70–115 ppm Nb, 140–250 ppm Zr, 6.5–9.4 ppm Th, 200–300 ppm REE; (La/Yb)_{Ch} 17–37, Zr/Nb 1.8–2.4) and LILE (15–30 ppm Rb, 450–650 ppm Ba, 900–1350 ppm Sr) in rocks reflect enriched OIB-like magma source (Vrublevskii et al., 2022).

In addition to peridotite xenoliths, basanites include clinopyroxene megacrysts, which are thought to be trapped fragments of mantle pyroxenites. This association is widespread in the Kongar pipe. Some prismatic crystals can reach 2–4 cm in size and have a blocky microstructure (Fig. 1). Major and trace element contents in minerals were determined by the electron microprobe analysis on Ultim Max 40 EDS and by the LA-ICP-MS on Agilent 7900 spectrometer with an Analyte Excite laser ablation system, respectively, at the National Research Tomsk State University (Fig. 2).

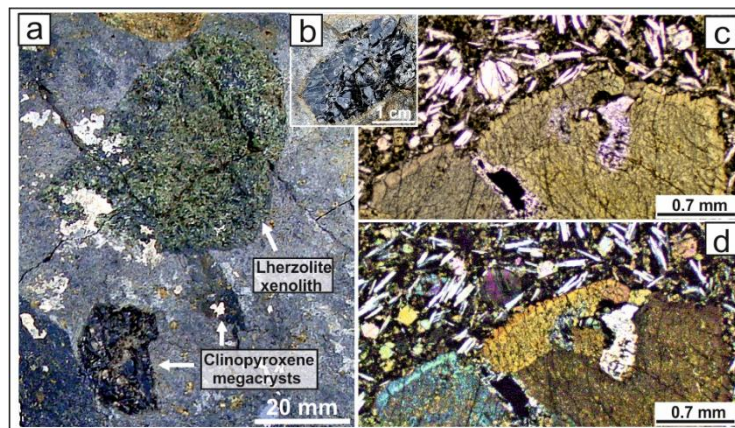


Fig. 1. Habit (a, b) and microstructure (c, d) of clinopyroxene megacrysts (c: plane-polarized light image; d: cross-polarized light image)

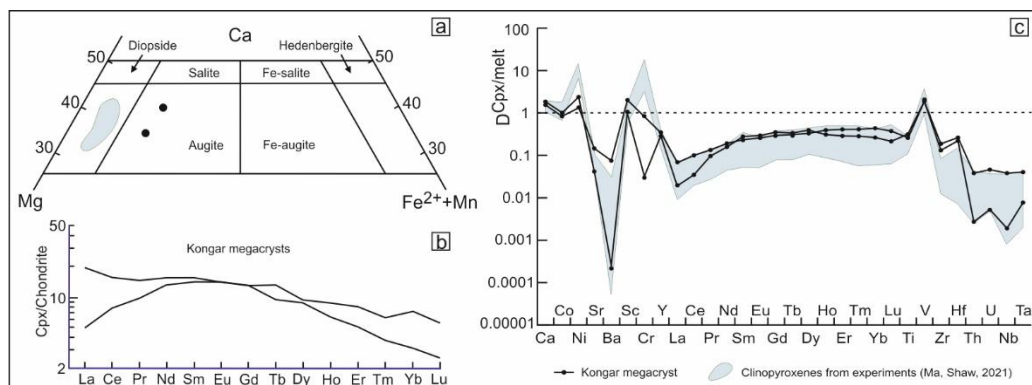


Fig. 2. Chemistry of clinopyroxene megacrysts. a: Relationships of Mg, Ca and (Fe²⁺+Mn); b: Chondrite-normalized REE patterns; c: Trace element partition coefficients between clinopyroxene and host basanite compared with experimental data (shaded area, after Ma, Shaw, 2021)

The chemical composition of clinopyroxene (47–48 wt. % SiO₂, 0.9–1.2 wt. % TiO₂, 9.5 wt. % Al₂O₃, 15–16 wt. % CaO, 13–15 wt. % MgO, 8–9 wt. % FeO, 1.6 wt. % Na₂O) corresponds to low-Ti augite Wo_{35–40} En_{45–50} Fs_{15–16} (Fig. 2a). The mineral has a higher Fe/Mg-ratio compared to clinopyroxenes obtained in

experiments on the interaction of basanite melt with peridotites (Ma, Shaw, 2021). Concentrations of rare earths (ΣREE 23–35 ppm, La/Yb_{Ch} 1.6–2.7; Fig. 2b) and some other trace elements (65–140 ppm Sr, 0.2–7 ppm Nb, 26–38 ppm Zr, 9–13 ppm Y) are comparable to their contents in clinopyroxenes from xenoliths of lithospheric mantle lherzolite (Xu et al., 2008, 2022). Among the compatible elements, the exception is low chromium (14–270 ppm Cr, 170–209 ppm Ni, 290–350 ppm V, 50–55 ppm Co, 25–40 ppm Sc).

The presence of different peridotite xenoliths or fragments of pyroxene xenocrysts is considered as a sign of alkaline mafic melt transport through mantle substrates. Reservoirs in the enriched lithospheric mantle (SCLM) are assumed to be the most probable sources of continental basaltic magmatism in the Mesozoic–Cenozoic (Furman, 1995; Hunt et al., 2012; Jung et al., 2012). Typically, the generation of melts occurs with the participation of sublithospheric mantle plumes (Ernst, 2014). Geochemical features of Minusa basanites and included lherzolite xenoliths suggest possible magma generation during 1–2 % decompression melting of garnet-spinel peridotites SCLM-type, which experienced earlier impact by sublithospheric plume (Vrublevskii et al., 2022).

Variations of clinopyroxene/whole rock ratios for trace elements in studied basanites except for chromium are like their distribution in the experimental "clinopyroxene/basanite melt" system at 1250°C and 1 GPa (Ma, Shaw, 2021) (Fig. 2c). Close crystallization temperatures (T=1300–1200°C) are fixed by melt inclusions in phenocrysts of olivine and clinopyroxene from the Minusa basanites (Golovin et al., 2000; Timina et al., 2006). Probably, the equilibration of the pyroxene phase with the melt is reflected in the blocky microstructure of large crystals. Its formation could be related to the initial segregation of the nuclear crystallites, which later formed a common border (see Fig. 1c). We assume that the studied clinopyroxenes, despite their close association with deep-level xenoliths, could have crystallized directly from the basanite melt and are not trapped alien mantle material.

This study was supported by the Russian Science Foundation, project no. 22–27–00362.

Ernst, R.E., 2014. Large Igneous Provinces. Cambridge: Cambridge University Press, pp. 630.

Furman, T., 1995. Melting of metasomatized subcontinental lithosphere: undersaturated mafic lavas from Rungwe, Tanzania. Contributions to Mineralogy and Petrology 122, 97–115.

Golovin, A.V., Sharygin, V.V., Malkovets, V.G., 2000. Evolution of melt during crystallization of the Bele pipe basanites. Russian Geology and Geophysics 41, 1710–1731.

Hunt, A.C., Parkinson, I.J., Harris, N.B.W., Barry, T.L., Rogers, N.W., Yondon, M., 2012. Cenozoic volcanism on the Hangai Dome, Central Mongolia: geochemical evidence for changing melt sources and implications for mechanisms of melting. Journal of Petrology 3, 1913–1942.

Jung, S., Vieten, K., Romer, R.L., Mezger, K., Hoernes, S., Satir, M., 2012. Petrogenesis of Tertiary alkaline magmas in the Siebengebirge, Germany. Journal of Petrology 53, 2381–2409.

Ma, S., Shaw, C.S.J., 2021. An experimental study of trace element partitioning between peridotite minerals and alkaline basaltic melts at 1250°C and 1 GPa: Crystal and melt composition impacts on partition coefficients. Journal of Petrology 62 (11), 1–27.

Malkovets, V.G., Litasov, Yu.D., Travin, A.V., Litasov, K.D., Taylor, L.A., 2003. Volcanic pipes as clues to upper mantle petrogenesis: Mesozoic Ar–Ar dating of the Minusinsk basalts, South Siberia. International Geology Review 45, 133–142.

Timina, T.Yu., Sharygin, V.V., Golovin, A.V., 2006. Melt evolution during the crystallization of basanites of the Tergesh pipe, Northern Minusinsk depression. Geochemistry International 44, 752–770.

Vrublevskii, V.V., Kotel'nikov, A.D., Tishin, P.A., Izokh, A.E., Kazenova, F., Kremer, I.O., 2022. Geochemical evidence for multi-depth magma generation for Permian–Triassic dolerite and Late Cretaceous basanite of the Minusa paleorift, Siberia. Doklady of Earth Sciences 506 (2), 729–733.

Xu, Y-G., Blusztajn, J., Ma, J-L., Suzuki, K., Liu, J-F., Hart, S.R., 2008. Late Archean to Early Proterozoic lithospheric mantle beneath the western North China craton: Sr–Nd–Os isotopes of peridotite xenoliths from Yangyuan and Fansi. Lithos 102, 25–42.

Xu, Y., Zhang, H-F., Lin, A-B., 2022. Widespread refertilization of cratonic lithospheric mantle related to circum-craton plate subduction: evidence from peridotite xenoliths from the central North China Craton. Contributions to Mineralogy and Petrology 177:67.

POLYMETALLIC VEIN AND REPLACEMENT MINERALIZATION IN THE JBEL HAÏMER AREA, JEBILET MASSIF, VARISCAN BELT, MOROCCO

Amina Wafik¹, Amal El Arbaoui², Lhou Maacha³,

¹ DLGR laboratory, Department of Geology, Faculty of Sciences Semlalia, Cadi Ayyad University, Bd. Prince My Abdellah, B.P. 2390, 40000 Marrakech, Morocco

² Institute of Mines of Marrakech, Department of Geology, Rue Machaar El Haram Quartier Issil, Marrakech 40000, Morocco

³ Managem Group, 52 Tween Center, Casablanca 40000, Morocco

The Jbel Haïmer mineralization in the Jebilet Massif is related to a system of NNE-trending gold-sulfide-bearing iron oxide-chlorite-quartz veins, stockworks and breccias. The host rocks are low grade metamorphosed sandy shales and black shales with cordierite spots.

Structural analysis of strike and dip data of the mineralized structures establishes the importance of the brittle shear zone and the associated subsidiary structures in the style and distribution of the Jbel Haïmer copper-gold-bearing veins. Occurrence of the orebodies within and next to the shear/fault zone is evident by the orientation of the mineralized veins consistent with the principal finite strain axes. Ore mineralogy comprises abundant iron oxides/hydroxides and variable amounts of chalcopyrite, pyrite, pyrrhotite, sphalerite, galena, and electrum.

The geochemical data of the mineralized veins reveal the presence of significant amounts of Cu, Au and Ag content. The EPMA data of the massive iron oxides from the mineralized veins reveal a high Zn and Cu contents and very low Ti, V and Cr contents. Hydrothermal alteration includes silicification, sericitization, chloritization, and sulfidation of the host rocks. Chlorite geothermometry indicates hydrothermal alteration conditions of ~365 - 395 °C.

Ore microscopy and SEM investigations reveal that thin Cu-Au veinlets are late-paragenetic compared to the iron oxide masses and veins. The Jbel Haïmer mineralization was probably wedged between leucogranite (300 Ma) and microdiorite (~240 Ma) magmatism in the area, prior to the waning of regional deformation (D₃).

The glacial deposits during Ediacaran-Cambrian transition in the southern North China Craton and the global correlation

Xiaoshuai Chen¹; Hongwei Kuang^{1*}; Yongqing Liu^{1*}; Nan Peng¹; Yuchong Wang^{1,2}; Kening Qi^{1,3}

¹: Institute of Geology, Chinese Academy of Geological Sciences, Beijing 100037, China

²: College of Geosciences and Surveying Engineering, China University of Mining and Technology, Beijing 100083, China

³: School of Resources and Environmental Engineering, Hefei University of Technology, Hefei, 230009, China

The Ediacaran-Cambrian transition is recognized as a warm period. However, glaciation have been reported from many paleocontinents around the world, especially the Luoquan glaciation in northern China. The type of glacier is still unclear, and there're still doubts about the differences and similarities between the Luoquan glaciation and other Ediacaran glaciations, which restricts the global comparison of the characteristics of glaciations. Research of the sedimentary characteristics and succession of 8 sections of the Luoquan and Dongpo formations in western Henan, southern North China Craton shows obvious sedimentary environment evolution of subglacial-periglacial-glaciomarine-shallow marine from north to south, namely, from the subglacial lodgement to the periglacial outwash fan and permafrost, then to the proximal glaciomarine grounding-line fan and iceberg rainout to the distal glaciomarine ice-rafted deposits, and finally to the normal shallow sea. The spatial evolution of the sedimentary environment indicating that the Luoquan glaciation in the southern North China Craton was a large ice sheet that extends from land to the ocean, and was not completely frozen, instead, there existed partially melting and temporary open water conditions. Further comparison shows although the period and the global characteristics have not yet been determined, the global Ediacaran glaciations, for example Bou Azzer glaciation in Anti-atlas, Morocco (Vernhet et al., 2012; Letsch et al., 2018), and Gaskiers glaciation in Newfoundland (Gravenor, 1980; Eyles and Eyles, 1989), etc., also have the dynamic evolution characteristics from continental glaciers to marine glaciers, which is similar to the evolution mechanism of glaciers during the snowball Earth, and also do not belong to the hard snowball Earth pattern of completely ice-covered. Detrital zircons from Ediacaran glaciations in northern China are predominantly older than 800 Ma and do not record information of Pan-African Orogeny. In contrast, the detrital zircons from Ediacaran glaciations in West Africa, Avalonia, Iran, and Cadomia have peaks of 500-600 Ma and are products of Pan-African events. Thus, the Ediacaran glaciations in northern China developed after the final breakup of the Rodinia and synchronized with the evolution of the assembly of the Gondwana.

Eyles, N., and Eyles, C.H., 1989. *Glacially - influenced deep - marine sedimentation of the Late Precambrian Gaskiers Formation, Newfoundland, Canada. Sedimentology*, 36(4): 601-620.

Gravenor, C. P., 1980. *Heavy minerals and sedimentological studies on the glaciogenic Late Precambrian Gaskiers Formation of Newfoundland. Canadian Journal of Earth Sciences*, 17(10): 1331-1341.

Letsch, D., Large, S. J., Buechi, M. W., Winkler, W., and von Quadt, A., 2018. *Ediacaran glaciations of the West African Craton-evidence from Morocco. Precambrian research*, 310, 17-38.

Vernhet, E., Youbi, N., Chellai, E. H., Villeneuve, M., and El Archi, A., 2012. *The Bou-Azzer glaciation: evidence for an Ediacaran glaciation on the west African craton (anti-atlas, Morocco). Precambrian Research*, 196: 106-112.

Acknowledgements

This study was financially supported by the National Natural Science Foundation of China (42072135, U19B6003 and 41472082), National Key Research and Development Program of China (2022YFF0800302; 2016YFC0601001), China Geological Survey program (DD20221649; DD20190005), Peking International Innovation and Resource Cooperation Program “The Precambrian last glaciation and the evolution of palaeoenvironment and life on Earth” (Z201100008320007). We express our gratitude to Profs. Xingliao Zhang and Jincheng Feng from the Department of Natural Resources of Henan province; Prof. Shiyan Wang from Henan Institute of Geological Survey; Prof. Yuansheng Geng from Institute of Geology, CAGS; Prof. Daniel Le Heron from the University of Vienna, Dr. Thomas Vandyk from Royal Holloway University of London; Prof. Deshun Zheng and Dr. Biyun Zhang from Henan Polytechnic University for their great help and cooperation.

Toward an understanding of paleogeographic evolution of the West African Craton in Proterozoic time: Insights from mafic dikes in the Anti-Atlas Belt, Morocco

Zheng Gong^{1,2,*}, David Evans¹, Nasrddine Youbi³, Kevin Chamberlain⁴, Bin Wen¹,
Xianqing Jing¹, Jikai Ding¹, Abdelhak Ait Lahna³, Malika Ait Malek³,
Rachid Oukhro³, Achraf Mohamed Mediany³, Jihane Ounar³

¹ Department of Earth and Planetary Sciences, Yale University, New Haven, CT 06511, USA
² Department of Earth and Planetary Sciences, Harvard University, Cambridge, MA 02138, USA
³ Department of Geology, Cadi Ayyad University, Marrakech, P.O. Box 2390, Morocco
⁴ Department of Geology and Geophysics, University of Wyoming, Laramie, WY 82071, USA

* Email: zheng_gong@fas.harvard.edu

Holistic paleogeographic reconstruction models are being developed to understand the Earth's tectonic evolution in deep time. However, when it comes to Proterozoic time, robust constraints become scarce, resulting in large spatial and temporal gaps in reconstruction models. Mafic Dikes can provide direct paleogeographic constraints in three aspects: (1) their ages allow global correlations; (2) their strikes often point to the location of common plume centers shared by neighboring cratons; (3) their paleomagnetic directions tell paleolatitude and paleoazimuth of the craton. Over the past five years, we utilized mafic dikes in the Anti-Atlas Belt (AAB) of Morocco to address the poorly-understood paleogeographic evolution of the West African Craton (WAC) in Proterozoic time. An integrated paleomagnetic and geochronological study was conducted on ~150 dikes with various ages in 8 inliers of the AAB (Figure 1). Although remagnetization was found in a subset of dikes, primary paleomagnetic directions can be successfully isolated from some dikes with support from positive field tests. We summarized the paleomagnetic directions into four groups. Group-1 directions are southeast pointing with very shallow inclinations; they are not correlated with ages or strikes of dikes, lie atop the Permo-Carboniferous reference direction of Africa, and likely indicate a remagnetization during the Hercynian orogeny. Group-2 directions, obtained from NE-trending dikes, are mainly north-and-moderate-down, Group-3 directions have very steep inclinations, and Group-4 directions are mainly southeast-down. Group 2-4 directions are all dual-polarity and seem not affected by the extensive Hercynian event. However, determining the ages of Group 2-4 directions is not so easy. For example, a dike from Group-2 was dated to be ~1380 Ma. But preliminary U-Pb data from another dike within this group yields a Tonian age, casting doubt on the common assumption that parallel dikes are coeval. Group-3 directions were identified from several dikes across the AAB among which two parallel dikes are ~1690 Ma. Without a baked-contact test, it is still too early to conclude that Group-3 directions are of Paleoproterozoic age because similar steep directions have also been obtained from Tonian and Ediacaran rocks in the WAC. Group-4 directions come from EW-trending dikes dated at ~2040 Ma, but the directions are not so different from Group-1 Hercynian overprints which require careful means of distinguishing them. Selecting only reliable paleomagnetic directions, we have attempted to reconstruct the paleogeography of the WAC in several Proterozoic intervals and constrained its position within supercontinents Nuna and Rodinia; but the whole Proterozoic paleogeographic evolution of the WAC is still at its embryonic stage given lingering degrees of freedom in the paleomagnetic dataset. Future work should also consider petrological and geochemical analyses, which provide additional constraints to differentiate the dike generations and understand the origins of their remanent magnetizations.

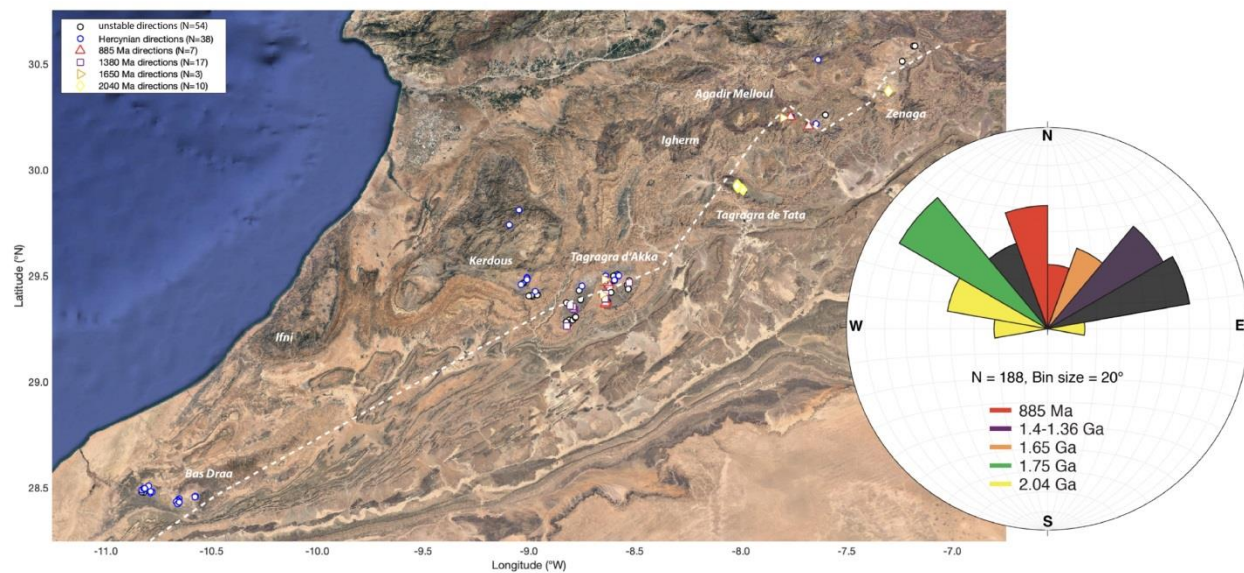


Figure 1 Left: Google Earth Map shows the location of dike samples relative to a prominent remagnetization front (white dashed curve). Colors represent 4 different paleomagnetic directional groups. Right: Rose diagram shows the strike orientations of dikes and their ages. Note that dike ages cannot be estimated solely by strike orientations.

JCM_2023
IDC8-LIPS8-Rodinia 2023
Marrakesh Morocco
Posters

Tectonic reactivation and ore-forming fault systems from the West African Craton northern margin

Ayoub AABI¹; **Lahssen BAIDDER**²; **Abdellah NAIT BBA**³; **Younes HEJJA**⁴

¹: Mohammed-V University, Ecole Normale Supérieure, Department of geology, Rabat, Morocco.

²: Hassan II University, Faculty of Sciences Ain Chock, Department of Geology, Casablanca, Morocco.

³: Mohammed I University, Faculty of Sciences, Department of Geology, Oujda, Morocco.

⁴: Managem, Twin Center, Tour A, Angle Bd Zerktouni-Abdelkarim Khattabi, Casablanca, Morocco

Abstract

The Moroccan Anti-Atlas (AA), of the West African Craton (WAC) margin, represents an important repository of mineral concentrations and the legacy of a complex geodynamic history inherited from several orogenic cycles, i.e. Pan-African, Variscan and Alpine. Located in the northern part of the AA, the Saghro massif is considered an ideal area to decrypt the tectonic reactivation process and its relationship with ore-deposit emplacement in the northern fringe of the WAC. The NE to ENE major faults are predominantly active from Precambrian onward, while most of the NW-SE rooted faults are not or partially remobilized. This structural configuration has significantly contributed to the current topographic features of the Saghro massif. The thick-skinned Variscan tectonics characterize the tectonic style of the paleozoic cover of the massif, whereas the thin-skinned deformation can be seen in the Ouarzazate foreland 'atlasique' basin. The most important polymetallic mineralized structures can be only seen within the Neoproterozoic basement, suggesting a late-Pan-African tectono-metallogenic control, while barite veins are concentrated in both Precambrian and Paleozoic outcrops.

Keywords: Structural configuration, Deformation style, mineralized structure, Saghro massif, West African Craton.

The Gabgaba gold deposit from the Arabian-Nubian Shield (Sudan): An example of a shear zone-related gold mineralization

Hassan Ait ben mouh^{a, b, *}, Ayoub Aabi^c, Abdellah Nait-Bba^d, Outhounjite Mohamed^b Ennaciri Aomar^b Younes Hejja^b, Lahssen Baidder^a, Lhou Maacha^b

^a Geosciences Laboratory, Department of Geology, Faculty of Sciences Ain Chock, Hassan II University, BP 5366 Maarif, Casablanca, Morocco

^b Managem, Twin Center, Tour A, Angle Bd Zerktouni-Abdelkarim Khattabi, Casablanca, Morocco

^c Department of geology, Ecole Normale Supérieure, Mohammed V University, BP 5118, 10000 Rabat, Morocco

^d Mineral Deposits, Hydrogeology & Environment Laboratory, Department of Geology, Faculty of Sciences, Mohammed I University, 60000, Oujda, Morocco

Kerfal Shear Zone (KSZ) of the Neoproterozoic Arabian-Nubian Shield (Sudan) constitutes an important world-class gold corridor due to its exceptional geological features, diverse deposit types, and the presence of significant gold resources. The Gabgaba gold deposit, in the central part of the KSZ, is hosted within magmatic formations, having been formed during the Pan-African orogeny. The main aim of this work focuses on studying the interplay between magmatic processes, hydrothermal activity, and structural controls in gold mineralization. For this purpose, a structural mapping and micro-tectonic analysis combined with a petrological study of the mineralized facies was undertaken.

A detailed geological map of the deposit together with a 60 km E-W cross-section has been established. The Gabgaba deposit consists basically of a vein-type deposit controlled by a set of submeridian felsic dykes locally associated with several quartz veins and hosted within a metamorphosed volcani-clastic and granitoid complex. The mineralization is commonly associated with sulfides such as pyrite, arsenopyrite, chalcopyrite and galena, while the related hydrothermalism is widespread with characteristic minerals (e.g. sericite, chlorite). Post-Pan African tectonic deformation occurs as folding and shearing that deforms the major part of the gold-bearing structures of the KSZ.

Petrography and petrogenesis of swarm dykes of central Urumieh-Dokhtar Magmatic Arc (the Kahak area, Qom province), Iran

Ashraf Torkian^{1*}; Nasrddine Youbi²

^{1*}: *Department of Geology, Faculty of Science, Bu- Ali Sina University, Hamedan, Iran*
a-torkian@basu.ac.ir

²: *Faculty of Sciences-Semlalia, Cadi Ayyad University, Marrakesh, Morocco*

Introduction:

The geology of Iran is important because it has the characteristics of continent-continent collision (Morley et al., 2009). The ongoing collision between the Arabian and Eurasian plates produced the Zagros Orogen (e.g., Stöcklin, 1968). The Zagros Orogen extends from the Turkish–Iranian border in the NW to the Makran area in the SE and it is subdivided into three parts: the Urumieh-Dokhtar Magmatic Arc (UDMA), the Sanandaj-Sirjan Zone (SaSZ), and the Zagros Fold and Thrust Belt (ZFTB) (e.g., Stöcklin, 1968; Berberian and King, 1981; Alavi, 1994; Agard et al., 2005; Mirnejad et al., 2019; Lustrino et al., 2021; Salehi et al., 2023; Shirmaohammadi et al., 2023). There has been considerable debate about the relationships between magmatism and the time of final collision of Arabian and Eurasia plates.

The UDMA is considered to have formed from a voluminous, and distinctly linear, Andean-style magmatic arc system (Dewey et al. 1973) that formed on the active SW margin of the Iranian plate during the Cenozoic (Arvin et al. 2007). Omrani et al. (2008) subdivided the UDMA volcanic rocks into an older Eocene suite and a younger upper Miocene to Plio-Quaternary suite. The Middle Eocene was thought to include the peak of magmatic activity in the region (Berberian and King 1981; Ghasemi and Talbot 2006). The Miocene igneous rocks of the UDMA were considered to mark the continental collision between Arabia and Eurasia (Berberian and King 1981; Ballato et al. 2011; Mohajjel and Fergusson 2014; Lustrino et al., 2021). The Kahak dykes is located in the central part of the northeastern margin of the UDMA. The geologic importance of this belt (UDMA) to the geotectonic evolution is well known and that petrology was first studied in this area further warrants a more detailed analysis of this region. Therefore this paper focuses on further describing the petrology and geochemistry attributes of the Kahak dykes to interpret the key magmatic processes involved in its genesis. Before this, swarm dykes from the Sanandaj- Sirjan zone have been studied (Torkian 2011; Torkian 2018).

2. Regional geology

The based on the Kahak geological map (Kahak 1:100000 sheet, Ghalamghash and Babakhani 1996) the Kermejgan area is a part of the western margin of central Iran and a part of Urmia-Dakhtar magmatic belt (Fig. 1). The rock units include upper Eocene andesite-basalt rocks, tuff and tuffite with interlayers of sandstone and limestones and intermediate to basic lavas (including andesite, megaporphyric basalts and gray rhyolitic tuff) (Fig. 1). These rock units are intruded by the granitoid mass bodies (Eocene –oligocene). In the study area, most previous studies (Beharifar 2011, Ghorbani and Bezenjani 2011, Moradi et al. 2021) have focused on understanding the formation of the intrusive (gd-g)(granitoid) and volcanic lava flows (E⁵) (basaltic-andesitic rocks) but the swarm dykes (diabasic-doleritic rocks) have not been studied in detail and they are not well understood. Baharifar investigated the garnets of rhyolites in the south of Dastgard city (50 km east of the study area). He proved that garnets have igneous nature and originated from a peraluminous magma. Also Ghorbani and Bezenjani (2011) studied the adakitic rocks in the central part of Urmia-Dokhtar belt (Tafresh city, 70 km west of Kahak).

U-Pb dating zircon yields early to middle Eocene (ca. 53 to 38 Ma) and Miocene (ca. 23 to 20 Ma) for the dioritic rocks in Naragh and gabbroic rocks in the Kerogan areas, respectively, which is located in SE-Kahak city (Moradi et al., 2021). The Kahak swarm dykes cut lava flows and this mass and they will refer as KSD (Kahak swarm dykes) in these paper.

The dykes are composed of diabase and dolerite. They generally have a NW-SE trend and plutonic mass have almost a N-S and NW-SE trend. KSD are cut across the volcanic and intrusive rocks and that the age of these unit is younger than the basaltic lava flows and granitoids.

3. Results

3.1. Petrography

Kahak swarm doleritic dyke unit: The doleritic dykes are mainly hosted in mafic to intermediate volcanic and granitoid rocks (Fig. 3). They typically are medium to fine grained, with intergranular/insertal texture. The

dykes are composed mainly of plagioclase (65-60%), clinopyroxene (10-5%) and amphibole (5-3%). Minor amounts of quartz (7-4%), biotite (~5%), and Fe-Ti oxides (8-6%) and very rare sphene, may be present. The groundmass is dominated by of subhedral laths of microcrystals of plagioclase, and quartz. Pyroxenes are also found as small interstitial grain (0.8–1.0 mm) or in groups of several grains (1.0–2.0 mm). Amphibole is usually subhedral and occasionally forms inclusions in plagioclase clusters and pyroxene oikocrysts. Pyroxene is partly altered, replacement minerals include biotite, chlorite and amphibole. In some

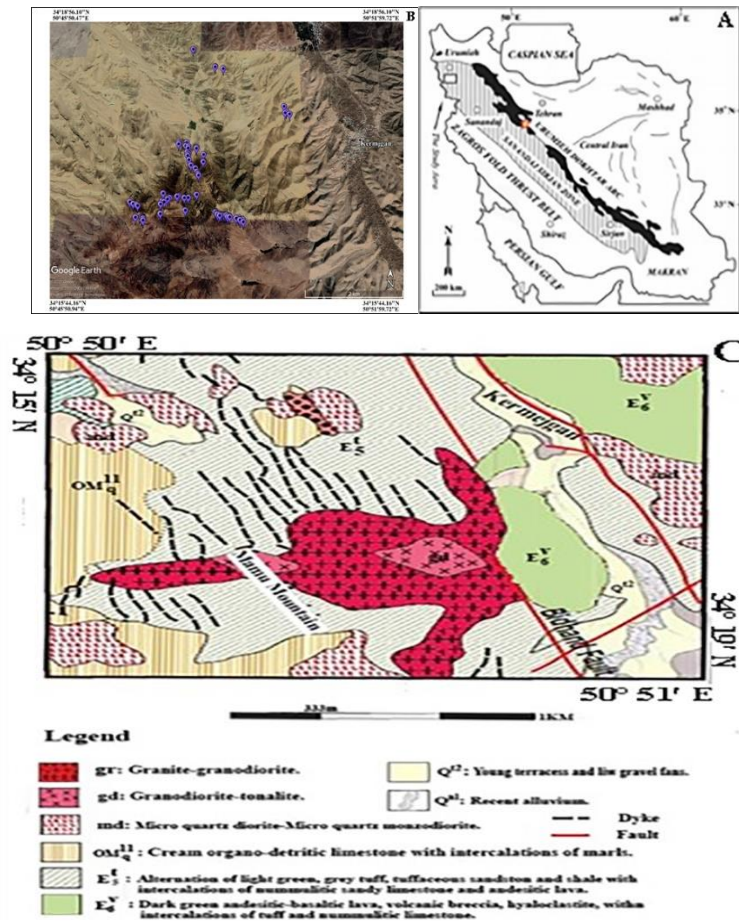


Fig. 1. A) Simplified geological map of Iran (modified after Aghanabati 2004) showing major tectonomagmatic units; B) The study area in the satellite image and location of sampling; C) The simplified geological map of S-Kahak region (after from Ghalamghash et al., 1998).

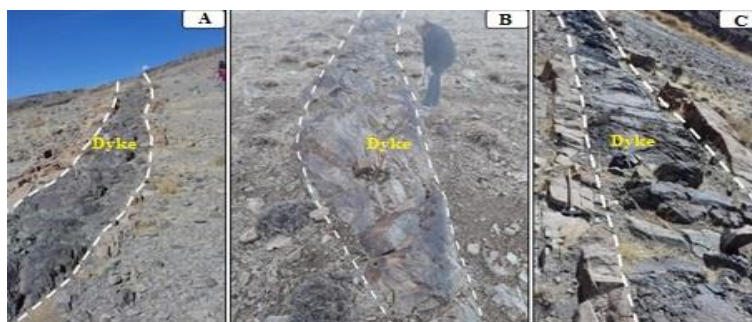


Fig. 2. Showing field relationship of mafic dykes intruding into A) host granitoid and B & C) volcanic rocks at the Kermejan area.

dolerites, plagioclase and sometimes augite form glomeroporphyritic clusters. The groundmass contains fresh glass or cryptocrystalline minerals, feathery augite and skeletal plagioclase and Ti-magnetite. Some plagioclase crystals are locally cut by sericite-filled cracks.

Host rocks of dykes:

Mafic rocks: The host mafic units have been defined as basaltic-andesitic rocks (Fig. 3). They crop out as numerous lavas flows. They are black or dark grey in color, porphyritic and melanocratic. They contain abundant plagioclase (55-45%), clinopyroxene (30-20%), opaque minerals and scarce microcrysts of biotite and amphibole in some samples. Sometimes these minerals have been altered to biotite and chlorite minerals. The plagioclases are generally zoned and euhedral to subhedral in shape, and are present as large clinopyroxene phenocrysts in some samples. The clinopyroxene crystals are smaller and have been patchy altered. Small sanidine and biotite microcrysts can be found in the groundmass of some andesitic samples.

Felsic rocks: Intrusive activity is represented by the association of granites, tonalites, and granodiorites. The age of emplacement of granodiorites and monzogranites must be less than 23 Ma (Moradi et al, 2021). In the Kahak area, host (granitoid) rocks with felsic compositions, such as tonalite, granite and granodiorite are visible. These rocks are composed of plagioclase, K-feldspar, quartz, biotite and zircon (Fig. 3). Under the microscope massive granitoids show hypidoimorphic granular texture and zoning and perthite are their dominant characteristics. Micrographic and myrmekitic texture are also found.

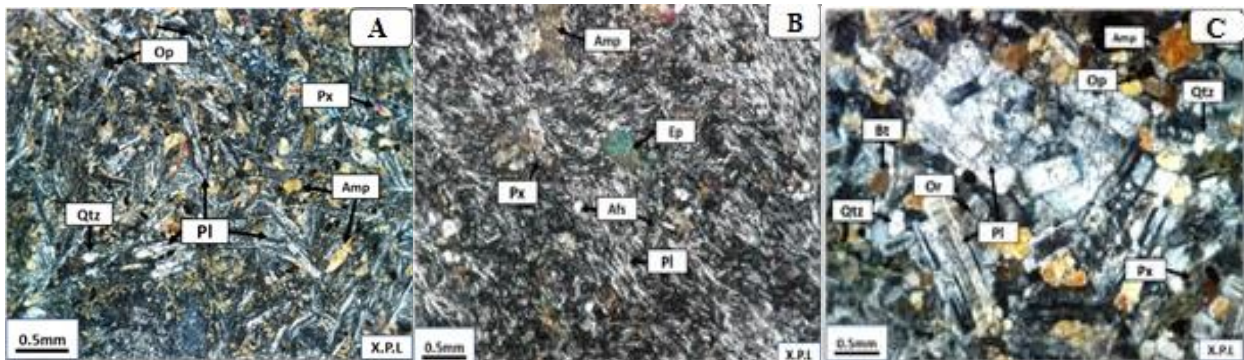


Fig. 3. Photomicrographs of A) dolerite dyke with intersertal texture; B) host volcanic rock with microlithic porphyritic texture; C) host granitoid rocks with granular-porphyroidal texture. Qtz: Quartz, Pl: Plagioclase, Or: Orthoclase, Amp: Amphibole, Px: Pyroxene, Bt: Biotite, Ep: Epidote, Op: Fe-Ti oxides.

3.2. Whole- rock geochemistry and tectonic setting

After petrographic study of collected rock samples, 20 (11 dykes and 9 host rocks) samples were selected for geochemical analyses. Whole-rock major and trace element analyses were performed by X-ray fluorescence and ICP-OES techniques in the Zarazma Co. (Iran).

SiO₂ and K₂O contents reach the highest concentrations in the host granitoid samples, while those of the KSD contain the highest contents of Al₂O₃, FeO, TiO₂, CaO and MgO. The Mg# contents are the highest for the dykes compared to the host samples. For the KSD, CaO, Al₂O₃, and TiO₂ increase as SiO₂ crease, whereas there are positive correlations between SiO₂ and V, Co and Sr. Based on the TAS nomenclature diagram (Le Bas et al., 1986), the dykes mostly consists of basaltic-andesite, and the granitoid pluton mostly consists of granodiorite-granite to tonalite and all of the studied samples plot in the subalkaline field and show a compositional trend from intermediate to acidic.

Primitive mantle normalized value (normalizing values of Sun and McDonough 1989) of trace-element abundances for doleritic swarm dykes show enrichment of large-ion lithophile elements (LILE) with respect to the high field strength elements (HFSE, including Zr, Nb and Ti) and enrichment of the light rare earth elements (LREE) with respect to the heavy rare earth elements (HREE). Depletion in Nb relatively to LILE and other characteristics, such as low TiO₂, and high Ba/ La for most of the doleritic dykes suggest affinities with other convergent plate boundary arc magmas around the world (Wilson, 1989). The typical geochemical signature of modern subduction environments reflects a mantle source enriched in large ion lithophile elements Cs, K, Rb, Sr, Ba, Th, Pb and often also in light REE (e.g., La and Ce), and relative depletion of high field strength elements Nb, Ta, Zr, and Ti (Pearce, 1982; Pearce and Cann, 1993). The Kahak doleritic dykes have negative Nb anomaly, consistent with derivation from an enriched mantle source. Tectonic discrimination diagrams

based on relative abundances of HFSE, i.e., Zr/Y–Ti/Y (Pearce and Gale, 1977) support geological evidence indicating the samples studied here originated in a continental volcanic arc setting.

Acknowledgments

This research was financially supported by the Bu-Ali Sina University (Iran) {T 1402G}. The first author expresses her gratitude to the Ministry of Science and Technology of Iran and the Vice-Chancellor for Research and Technology of the Bu-Ali Sina University.

References

1. Agard P, Omrani J, Jolivet L, Mouthereau F. Convergence history across Zagros (Iran): constraints from collisional and earlier deformation. *International journal of earth sciences*. 2005;94:401-19.
2. Aghanabati A. *Geology of Iran*. Geological survey of Iran; 2004.
3. Alavi M. Tectonics of the Zagros orogenic belt of Iran: new data and interpretations. *Tectonophysics*. 1994 Jan 30;229(3-4):211-38.
4. Arvin M, Pan Y, Dargahi S, Malekizadeh A, Babaei A. Petrochemistry of the Siah-Kuh granitoid stock southwest of Kerman, Iran: Implications for initiation of Neotethys subduction. *Journal of Asian Earth Sciences*. 2007; 30(3-4):474-89.
5. Baharifar AA, Mineralogy and origin of garnet in acidic volcanic rocks of Dastgerd area, Qom, Iranian Petrology. 11(4), 2011.
6. Ballato P, Uba CE, Landgraf A, Strecker MR, Sudo M, Stockli DF, Friedrich A, Tabatabaei SH. Arabia-Eurasia continental collision: Insights from late Tertiary foreland-basin evolution in the Alborz Mountains, northern Iran. *Bulletin*. 2011, 123(1-2):106-31.
7. Berberian M, King GC. Towards a paleogeography and tectonic evolution of Iran. *Canadian journal of earth sciences*. 1981;18(2):210-65.
8. Dewey JF, PITMAN III WC, Ryan WB, Bonnin J. Plate tectonics and the evolution of the Alpine system. *Geological society of America bulletin*. 1973;84(10):3137-80.
9. Ghalamghash G, Babakhani A, Geological map of Kahak: sheet 6158, Ministry of Mines and Metals. Geological Survey of Iran, Tehran, 1996
10. Ghasemi A, Talbot CJ. A new tectonic scenario for the Sanandaj–Sirjan Zone (Iran). *Journal of Asian Earth Sciences*. 2006; 26(6):683-93.
11. Ghorbani MR, Bezenjani RN. Slab partial melts from the metasomatizing agent to adakite, Tafresh Eocene volcanic rocks, Iran. *Island Arc*. 2011; 20(2):188-202.
12. Le Bas MJ. A chemical classification of volcanic rocks based on the total alkali-silica system. *J. Petrol*. 1986, 27: 247-57.
13. Lustrino M, Salari G, Rahimzadeh B, Fedele L, Masoudi F, Agostini S. Quaternary melanephelinites and melilitites from Nowbaran (NW Urumieh-Dokhtar Magmatic Arc, Iran): origin of ultrabasic-ultracalcic melts in a post-collisional setting. *Journal of Petrology*. 2021; 62(9):egab058.
14. Mirnejad H, Raeisi D, McFarlane C, Sheibi M. Tafresh intrusive rocks within the urumieh-dokhtar magmatic arc: Appraisal of neo-tethys subduction. *Geological Journal*. 2019; 54(3):1745-55.
15. Mohajjel M, Fergusson CL. Jurassic to Cenozoic tectonics of the Zagros Orogen in northwestern Iran. *International Geology Review*. 2014; 56(3):263-87.
16. Moradi S, Ghorbani MR, Jiang SY, Christiansen EH. Mafic to intermediate composition intrusions from the Kahak area, central Urumieh-Dokhtar arc of Iran: transition from Eocene to Miocene intra-arc extensional magmatism. *Mineralogy and Petrology*. 2021, 115:445-66.
17. Omrani J, Agard P, Whitechurch H, Benoit M, Prouteau G, Jolivet L. Arc-magmatism and subduction history beneath the Zagros Mountains, Iran: a new report of adakites and geodynamic consequences. *Lithos*. 2008; 106(3-4):380-98.
18. Pearce JA, Cann JR. Tectonic setting of basic volcanic rocks determined using trace element analyses. *Earth and planetary science letters*. 1973;19(2):290-300.
19. Pearce JA, Gale GH. Identification of ore-deposition environment from trace-element geochemistry of associated igneous host rocks. Geological Society, London, Special Publications. 1977;7(1):14-24.
20. Salehi N, Torkian A, Furman T, le Roux P. Petrogenesis and geochemical characteristics of Plio-Quaternary alkali basalts from the Qorveh–Bijar volcanic belt, Kurdistan Province, NW Iran. *Geological Magazine*. 2023, 17:1-7.
21. Shirmohammadi M, Sepahi AA, Santos JF, Maanijou M, Torkian A, Vahidpour H. Geochemistry and Sr–Nd isotopic characteristics of ferroan-magnesian metaluminous granites of the NW Sanandaj–Sirjan zone, Iran: granite formation in a compressional–extensional setting during Late Jurassic time. *Geological Magazine*. 2023:1-25.
22. Stoecklin J. Structural history and tectonics of Iran: a review. *AAPG bulletin*. 1968; 52(7):1229-58.

23. Torkian A. The Parishan pluton in Qorveh area, an example for magma mingling process, southeastern Sanandaj, Iran. *Dyke Swarms: Keys for Geodynamic Interpretation: Keys for Geodynamic Interpretation*. 2011:331-43.
24. Torkian A. Petrology and Tectonic Setting of Dyke Swarms Emplaced in the Upper Jurassic Qorveh Granitoid Complex (Majidabad. *Dyke Swarms of the World: A Modern Perspective*. 2018:439.
25. Wilson M, editor. *Igneous petrogenesis*. Dordrecht: Springer Netherlands; 1989.

Bibliographical synthesis and preliminary data on the VMS mineralizations of the Laachach -Koudiat Aïcha- Jbel Hadid axis, Central Jebilet, western Meseta, Morocco

ATYQ Touriya¹ MOUGUINA El Mostafa¹ OUADJOU Abdelmalek² ADMOU Safouane² EL MOSTADI Abdelfettah³ AGHZER Mohcine³

¹ Laboratory "Dynamics of the Lithosphere and Genesis of Resources "DLGR". Department of Geology. Faculty of Sciences Semlalia M.B.2390. Cadi Ayyad University. 40000 Marrakesh, Morocco.² CMG. Managem Group, Morocco. ³ Laboratory of Marine Geosciences and Soil Sciences (LGMSS) Department of Geology, Faculty of Sciences, Chouaïb Doukkali University, El Jadida, Morocco.⁴ Laboratory of Geodynamics and Geomatics (LGG), Department of Geology, Faculty of Sciences, Chouaïb Doukkali University, El Jadida, Morocco.

The Jebilet Variscan massif extends 170 km E–W and 7 to 40 km N–S and is subdivided into three domains: Western, Central and Eastern Jebilet. The Jebilet series was formed in an intra-continental rift basin, where marine sediments deposited in an anoxic environment during the Late Devonian and Early Carboniferous. Central Jebilet is dominated by the Carboniferous Sarhlef metasedimentary series (Upper Visean–Namurian: presence of *Posidonomya becheri* Bornn).

The Central Jebilet sulphide subprovince underwent synchronous hydrothermal activity over the entire block. This activity is manifested by Volcanogenic Massif Sulfide (VMS) deposits, such as: Draa Sfar, Kettara, Ben Slimane, Jbel Hadid, Koudiat Aïcha, Laachach, etc. These VMS are distributed along three axes subparallel to the meridian direction:

- Eastern axis comprising Draa Sfar to the south and Nzalet El Harmel to the north;
- Median axis, with the deposits of Kettara, Ben Slimane and Kerkoz;
- Western axis, with Bouhane, Laachach, Koudiat Aïcha and Jebel Hadid indices.

The western axis is the subject of our study, where the VMS mineralization is pyrrhotite predominantly and contains also minerals of the base metals such as sphalerite, galena, chalcopyrite, arsenopyrite and some traces of stannite. These VMS are hosted in the volcano-sedimentary formation intruded by a bimodal volcanism with basic dominance materialized by gabbroic rocks having a tholeiitic magmatic affinity of the Central Jebilet Hercynian massif , Western Meseta.

The Central Jebilet massif was structured during the Hercynian orogeny by a complex polyphase Hercynian and late-Hercynian deformation which results in the succession of a major Hercynian deformation (D1) synchronous with anchi- to epizonal regional metamorphism followed by a ductile shear phase deformation (D2) flexible (D3) and brittle (D4) deformation phases.

As perspective, we propose to realize a detailed geological study to understand the link between mineralization and host rocks. This study will be based on geological mapping, petrography, metallogeny, geochemistry and 3D modelling.

Spatial analysis of fractures to predict probable ore deposits (Middle Morocco)

Abderrahim Ayad

Department of Earth Sciences, Abdelmalek Essaadi University, Tangier, Morocco

Abstract

Fractures are the main conduits for hydrothermal fluid flow in bedrock and represent an important factor in the genesis of hydrothermal ore deposits. Hydrothermal fluids are able to transport and dissolve their minerals in rocks fractures, and fill openings in rocks with native metals such as gold and silver. In this work, we analyze the spatial distribution of fractures in middle Morocco to predict and discover the most favorable targets for probable polymetallic ore deposits in this area. The analysis is performed on Landsat MSS images using the fractal dimension method (D) [1] [2], and a fractal contour map covering the study area was created. Then, areas of known polymetallic mines were projected vertically onto the fractal contour map for checking any distribution conformity (Fig.1). The resulting combined map represents a numerical final index which acts as the answer for this study. Based on the results of this study, it is found that the high fractal dimension coincide broadly with the major known polymetallic mines, implying larger permeability of rocks in these areas which are favorable for the focusing of ore-forming fluid and formation of hydrothermal deposits. This result requires to be confirmed by field exploration work to provide a straightforward response to the mineral occurrence.

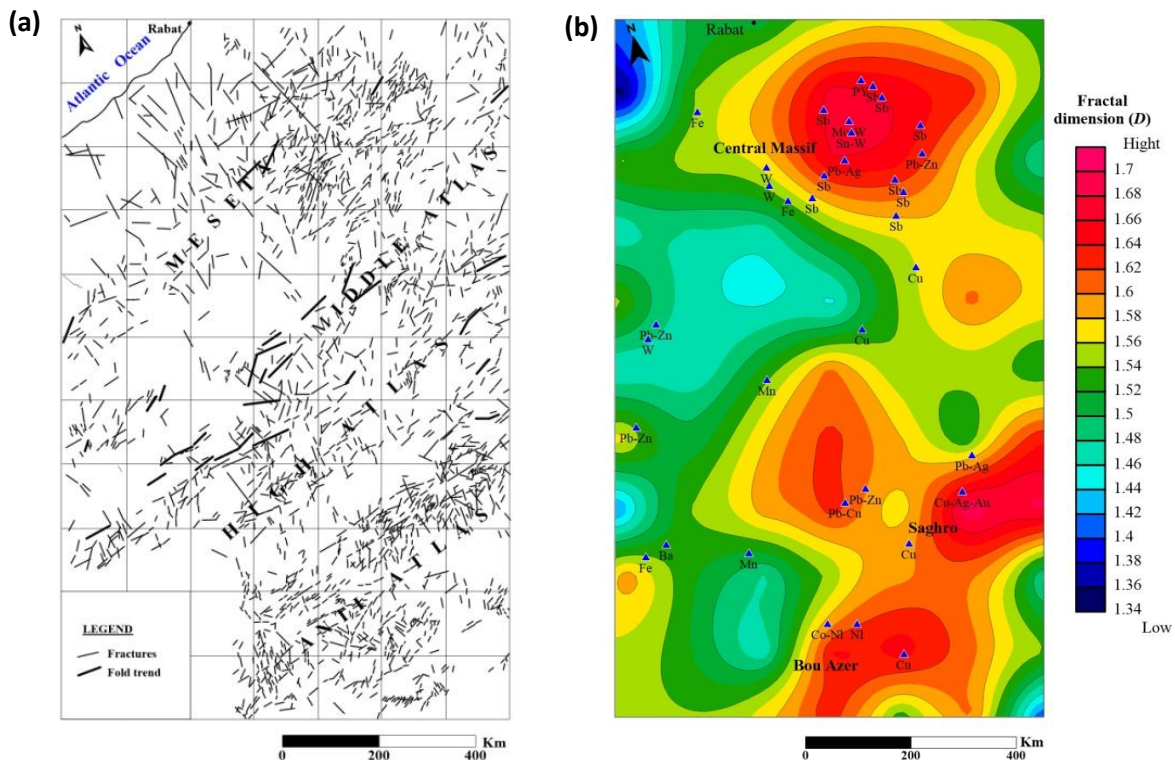


Fig.1: (a) Spatial distribution of fractures, (b) Major known polymetallic deposits superimposed on the contour fractal map.

References:

- [1] Bensaid, M., Mahmood, A., (1987). *The use of Landsat imagery in structural studies of Middle Morocco. Adv Space Res* 7(3):87–94.
- [2] Mandelbrot, B., (1983). *The fractal Geometry of Nature. American Journal of Physics. Vol.51, N°3, 468 pages.*

The lower Anti-Atlas Supergroup of the Zenaga and Siroua inliers, Anti-Atlas, Morocco: Evolution of the state-of-knowledge.

Barzouk, A.¹; Ait Lahna, A.¹; Gärtner, A.²; Linnemann, U.²; Nasrddine Youbi^{1,3}; El Moume, W.¹; Boumeahdi, M.A.^{1,4}; Bensalah M.K.^{1,4}; Chellai, E.H.¹; Bekker, A.^{5,6}

¹: *Department of Geology, Faculty of Sciences-Semlalia, Cadi Ayyad University, Prince Moulay Abdellah Boulevard, P.O. Box 2390, Marrakech, Morocco.*

²: *Senckenberg Naturhistorische Sammlungen Dresden, Museum für Mineralogie und Geologie, Sektion Geochronologie, GeoPlasma Lab, Königsbrücker Landstraße 159, 01109 Dresden, Germany.*

³: *Faculty of Geology and Geography, Tomsk State University, 36 Lenin Ave, Tomsk 634050, Russia.*

⁴: *Instituto Dom Luiz (IDL), Faculdade de Ciências, Universidade de Lisboa, Campo Grande, 1749-016, Lisboa, Portugal*

⁵: *Department of Earth and Planetary Sciences, University of California, Riverside, CA, 92521, USA*

⁶: *Department of Geology, University of Johannesburg, Auckland Park 2006, South Africa*

The lower Anti-Atlas Supergroup of the Anti-Atlas Belt (Lkest-Taghdout Group sensu Thomas et al., 2004) is one of the most important Proterozoic lithostratigraphic units on the northern part in the West African Craton (WAC, Anti-Atlas Belt, Morocco). This yet poorly dated supergroup consists essentially of basalts, quartzites, and stromatolitic/oolitic carbonates, intruded by dolerite dyke swarms and sill complexes. A reassessment of the published age and stratigraphic constraints suggests a revised stratigraphic framework for the lower Anti-Atlas Supergroup (Figure 1). Five major unconformity-bounded lithostratigraphic packages are distinguished: the two lower units of Paleoproterozoic age are named the Tasserda-Taghatine Group (ca. 2030-1706 Ma) and the Oumoula (aka Mimount) Formation (ca. 1745–1650 Ma); the third unit of Paleoproterozoic to Neoproterozoic age (ca. 1650 to >883 Ma) is the Tizi n’Taghatine Group; the fourth and fifth units of Neoproterozoic age are the ca. 883 Ma Tachdamt and the ca. 700 Ma Bleida formations (Ait Lahna et al., 2020). Here, we present additional constraints on the ca. 1640 Ma and 885 Ma magmatic events in the Zenaga and Siroua inliers. Igneous zircon grains from tuff layers (~porcelanite) approximately in the middle part of the Ifrane-n-Tagahtine Formation (aka Taghdout Formation) of the Zenaga Inlier yielded an U-Pb concordia zircon age at 1634 ± 13 Ma when combining the most concordant grains of the youngest age population. The same sample has an upper intercept at 1632.3 ± 7.7 [± 9.5] Ma when additionally including more discordant analyses (Laser Ablation Inductively Coupled Plasma Mass Spectrometry – LA-ICP-MS –, method). Zircon analyses of a basaltic lava flow near the base of the equivalent of the Tachdamt Formation in the Siroua Inlier yielded zircon ages with an upper intercept age at 590 ± 24 Ma and an older population at 831 ± 31 [± 32] Ma. The lower Anti-Atlas Supergroup records Paleoproterozoic and Neoproterozoic protracted and episodic deposition in basins developed in association with extension and emplacement of Large Igneous Provinces (LIPs) on the northern margin of the West African craton (WAC). Considering this protracted and episodic subsidence, likely linked to far-distant tectonic stresses and emplacement of mantle plumes, could have similarly taken place in other parts of the WAC, we explore here correlation with another Paleoproterozoic to Neoproterozoic basin on the WAC, the Taoudeni basin, located approximately 500 km to the south of the Anti-Atlas Belt.

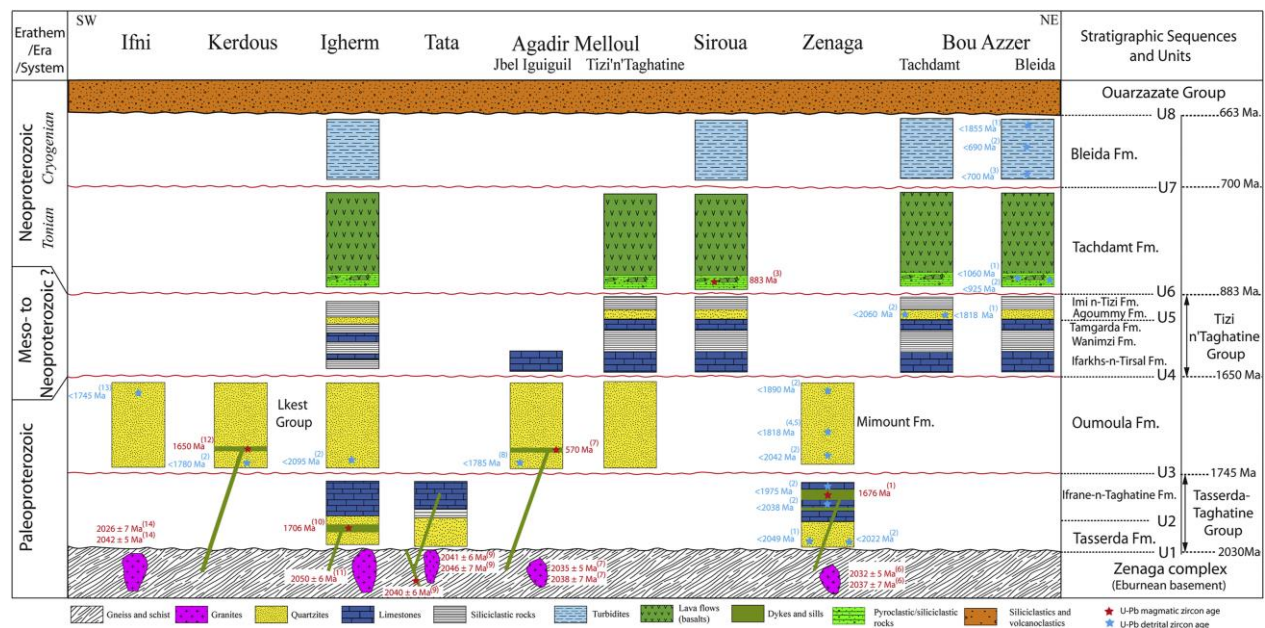


Figure 1. A tentative correlation scheme of the lower Anti-Atlas Supergroup and its stratigraphic equivalents in the Anti-Atlas inliers (after Ait Lahna et al., 2020). U1 to U8 are unconformities. U–Pb geochronology data are from Ait Lahna et al. (2020) and references therein.

References

Ait Lahna, A.; Youbi, N.; Gaeta Tassinari, C.C.; Stipp Basei, M.A.; Ernst, R.E.; Chaib, L.; Barzouk, A.; Mata, J.; Gärtner, A.; Admou, H.; Boumehdi, M.A.; Söderlund, U.; Bensalah, M.K.; Bodinier, J.L.; Maacha, L.; Bekker, A., 2020. Revised stratigraphic framework for the lower Anti-Atlas supergroup based on U–Pb geochronology of magmatic and detrital zircons (Zenaga and Bou Azzer-El Graara inliers, Anti-Atlas Belt, Morocco). *Journal of African Earth Sciences*, 171, November 2020, 103946

Thomas, R.J.; Fekkak, A.; Ennih, N.; Errami, E.; Loughlin, S.C.; Gresse, P.G.; Chevallier, L.P.; Liégeois, J.-P., 2004. A new lithostratigraphic framework for the Anti-Atlas Orogen, Morocco. *Journal of African Earth Sciences*, 39, 217–226.

MAFIC DYKE SWARMS OF THE WEST AFRICAN CRATON NORTHERN MARGIN (MOROCCAN SAHARA AND ANTI-ATLAS) REMOTE SENSING STUDY RESULTS

Ben-Daoud¹ M., Ibouh H². and Nasrddine Youbi N.^{1,3}.

¹ Department of earth sciences, Faculty of Sciences-Semlalia, Cadi Ayyad University, BP. 2390, Marrakech, 40000, Morocco.

² Georesources, Geoenvironment and Civil Engineering (L3G) Laboratory, Faculty of Sciences and Techniques Cadi Ayyad University, A. Al Khattabi Bd, P.O. Box 549, 40 000 Marrakesh, Morocco

³ Faculty of Geology and Geography., Tomsk State University, 634050 Tomsk, Russia

The Archean part of the Reguibat Rise of the West African Craton is characterized by the presence of extensive mafic dyke swarms with different chemical compositions, trends and ages. The spatial and temporal distribution and emplacement mechanism of mafic dyke swarms are closely related to the local and regional tectonic stress field and crustal evolution. Accurate mapping of these dykes and their grouping into swarms is fundamental to dyke research.

This work focuses on the use of remote sensing data (Landsat 8 OLI), Google Earth imagery and field measurements to map and identify the geometry, morphology and location of previously poorly known dyke swarms exposed on the Reguibat Rise. The spatial distribution and structural attributes of the dyke are obtained based on the statistics study of 3641 extracted mafic dykes. This study reveal that the dykes are organized in a structural patterns with a dominant of NE SW set trending, and a minor system trending N-S, these dykes show a variety of attributes (length, thickness, and aspect ratio), and magma chamber overpressures. Based on the estimated coefficients of determination, the result shows that dyke thicknesses are best fitted by negative exponent distributions while the Length distribution follows power law curve. The analysis of chronological relationship dyke swarms shows that from oldest to youngest: NW-SE trending, E-W trending, NE-SE trending, and N-S trending. The methodological approach used in this study, which aims to map the dikes and determine their temporal distribution, is effective and proven.

TECTONIC IMPACT ON THE FORMATION OF COPPER DEPOSITS IN THE BOU AZZER INLIER, CENTRAL ANTI-ATLAS, MOROCCO.

Ben massoude M. ¹, Wafik A. ¹, Admou H. ¹, Bajjdi A. ², , Karfal A. ² Maacha L. ³

¹ DLGR Laboratory, URAC 43, Faculty of Sciences Semlalia, Cadi Ayyad University, Marrakech, Morocco.

² CTT Mine de Bou Azzer Managem Group, Twin Center, Casablanca, Morocco

³ Managem Group, Twin Center, Casablanca, Morocco.

The Ingujjem-Ait Ahmane massif constitutes a section of the harzburgitic mantle of the Neoproterozoic Bou Azzer ophiolite. It consists of a fragmented ophiolitic sequence comprising all the ultrabasic, basic, and volcano-sedimentary components.

Our research has revealed an abnormal enrichment of copper in both primary and secondary sulfides. In addition to chromiferous magmatic mineralization, Ni-Co-Fe-As, and gold, numerous copper occurrences are present. The massif has undergone hydrothermal alteration, with the effects becoming more pronounced as one approaches the most deformed zones. The different phases of the copper mineralization process have been linked to the temporal evolution of the same multiphase hydrothermal system, which operated during a multiphase tectonic regime accompanied by several stages of serpentinization.

Tectonic, magmatic, metamorphic, and hydrothermal processes have contributed to the formation of copper mineralizations frequently observed in the mafic and ultramafic rocks of the Bou Azzer ophiolitic complex, which have been associated with an ancient abyssal hydrothermal system known as a black smoker. As the deformation and carbonation of the serpentinites intensify, the copper mineralization transitions from disseminated distribution to veinlet distribution. The remobilization and reconcentration of the mineralization are accompanied by a transition from serpentinites to deformed and carbonated serpentinites.

Pangea rifting as the main ore-forming processes for the genesis of the Merguechoum fluorite-barite mineralization, Eastern Meseta, Moroccan

Mohammed Cherai¹, Larbi Rddad², Fouad Talbi¹, Benjamin F. Walter^{3,4}, Mohamed Idbaroud⁵

¹: *Laboratoire de Géosciences, Géo-environnement et Prospection Minière et Hydrique, Faculté des Sciences, 60000 Oujda, BP 717, Maroc. cheraibg@gmail.com*

²: *Earth and Planetary Science Division, Physical Science Department, Kingsborough Community College of the City University Of New York (CUNY), 2001 Oriental Boulevard, Brooklyn, NY 11235–2398, USA.*

³: *Karlsruhe Institute of Technology (KIT), Chair of Economic Geology and Geochemistry, Adenauerring 20b, 76131 Karlsruhe, Germany*

⁴: *Laboratory for Environmental and Raw Material Analyses (LERA), Adenauerring 20b, 76131 Karlsruhe, Germany*

⁵: *Department of Geology, Cadi Ayyad University, B.P. 2390, Marrakech 40000, Morocco*

Abstract

The Merguechoum fluorite-barite mineralization, located in the Eastern Meseta of Morocco, is hosted in Late Hercynian granite. The fluorite-barite ore emplacement was structurally controlled as the mineralization occurs along NE-SW-trending meter-sized veins and as dissemination mineralization within the host granite. The REY data indicate that the basinal brines are involved in the genesis of the ore with a contribution of meteoric waters. It is likely that fluid mixing between the metal-rich basinal brines and diluted, cooler, sulfate-rich meteoric fluids occurred, triggering the precipitation of fluorite and barite. The O-S isotopes data of barite reveal that the dissolved sulfates (SO_4^{2-}) were derived from Permian-Triassic sulfates and/or coeval pore-seawater sulfates. Geologic, REY, and isotope data point to the ore genesis during the Permian-Triassic extensional tectonic activity in relation to the Pangea rifting. This extensional tectonic environment is likely the driving force that mobilized a large amount of the ore-forming basinal brines along the available faults and fractures to the loci of ore deposition.

Keywords: Fluorite-barite ore, REY, O-S isotopes, Late Hercynian granite, Pangea rifting, Merguechoum, Eastern Meseta of Moroccan.

CARBONATITES OF THE MOROCCAN SAHARA (TWIHINATE AND GLEIBAT LAHFOUDA COMPLEXES): ASSESSEMENT AND ALTERATION MAPPING BY REMOTE SENSING

Diallo Mamadou¹; Ibouh Hassan². and Nasrddine Youbi^{1,3}

¹ Department of earth sciences, Faculty of Sciences-Semlalia, Cadi Ayyad University, BP. 2390, Marrakech, 40000, Morocco.

² Georessources, Geoenvironment and Civil Engineering (L3G) Laboratory, Faculty of Sciences and Techniques Cadi Ayyad University, A. Al Khattabi Bd, P.O. Box 549, 40 000 Marrakesh, Morocco

³ Faculty of Geology and Geography., Tomsk State University, 634050 Tomsk, Russia

Carbonatites are special mantle-derived igneous rocks, consisting mostly of carbonate minerals that occur mainly in continental rifts and are usually associated minerals deposits (e.g., Berger et al., 2009). Many carbonatites are linked both spatially and temporally with large igneous provinces (LIPs), which produce significant amounts of energy and metals that can either drive or contribute to a variety of metallogenic systems including Rare Metals (Li, Be, Ti, Zr, Nb, Ta, Th and U), REE and other ore deposits. LIPs have played important roles in the breakup and dispersal of supercontinents Pangea and Rodinia. These associated LIPs and carbonatites have been considered as different evolutionary 'pathways' in a single magmatic process/system (Ernst, 2014)

Carbonatites, which are significant hosts of economically important rare-earth elements (REE), are challenging to locate as they may crop out as small bodies with indistinct field characteristics. A mapping approach was developed using Landsat 8-OLI and Advanced Spaceborne Thermal Emission and Reflection Radiometer (ASTER) data to map geological units of Twihinate and Gleibat Lahfouda complexes area, situated in the Southernmost part of Morocco. The combination of color composition (CC), principal component analysis (PCA), minimum noise fraction (MNF), spectral angle mapper classification (SAM) and band ratio (BR) highlighted the lithological facies and rapidly delineate carbonatites and hydrothermally alteration outcrops. The SAM digital map displays a "good" result for both area (Twihinate and Gleibat Lahfouda), with a respectively calculated kappa coefficient of 0.9306 and 0.6022, and an overall accuracy of about 95.37% and 67.12%. Our results therefore suggest that it is possible to map and assess carbonatite distribution from medium spatial resolution (Landsat 8 OLI) images for exploration purposes, but the technique suffers from accuracy issues that may negatively impact its usage for quantitative assessment of resource potential.

References

Berger, V., Singer, D., Orris, G., Brassinnes, S., Balaganskaya, E., DemaiFFE, D., 2009. Carbonatites of the world, explored deposits of Nb and REE; database and grade and tonnage models. US Geological Survey Open File Report 2009-1139, 76–92.

Ernst, R. E. (2014). Large igneous provinces. Cambridge University Press.

Subduction of the Mesoarchaeon spreading ridge by the example of the Gridino eclogitized mafic dyke swarm, the Belomorian Eclogite Province, eastern Fennoscandian Shield

Dokukina K.¹

¹: GIN RAS, Moscow, Russia, ksdokukina@gmail.com

Summarizing evidences, such as ophiolites, supra-subduction metasomatized mantle rocks, derivatives of continental arc and slab window magmatism, eclogite, in the Belomorian province of Fennoscandia shield, we suggest that the modern style of subduction and plate tectonics began already in Mezoarchaeon time. 2.9-2.8 Ga ago. A model of Mesoarchaeon spreading ridge subduction and related magmatism and metamorphism in the Kola active continental margin is presented here.

The Archean Karelia and Kola paleocontinents that consist predominantly of granite-greenstone terranes together with the Belomorian accretionary–collisional orogen are the main tectonic units in the eastern Fennoscandian Shield. The Belomorian tectonic province is a NW-trending segment of the Archean nucleus of the Fennoscandian Shield and is distinguished by repeated episodes of intense deformation and high- to moderate-pressure metamorphism during the Archean and Paleoproterozoic. The Keret tectonic nappe at the southern margin of the Kola continent contains 3.00–2.70 Ga tonalite-trondhjemite-granodiorite (TTG) gneisses and greenstones and is separated from the Belomorian accretionary–collisional orogen by the Central Belomorian greenstone belt, which is composed of an older mafic–ultramafic sequence ≥ 2.85 Ga. The belt is interpreted as an ancient suture zone. The Belomorian eclogite province (BEP) contains eclogite bodies that are hosted in TTG gneisses of the Keret Unit of the Kola active continental margin (Mints et al., 2014). There are two eclogite associations: (1) the subduction-type Salma association and (2) the Gridino dyke swarm. Protoliths of the Salma eclogites represent a sequence oceanic layered gabbros and basalt flows that contain layers, lenses, and interpillow sediments formed at ~ 2.9 Ga in a slow-spreading ridge. The subduction began in a time span 2.9-2.87 Ga, and eclogite-facies events occurred between ca.2.87 and ca.2.78 Ga.

The Gridino dykes represent typical fissure intrusions and underwent metamorphism to eclogite facies. Injection of a mafic magma into an active continental margin, recorded by the Gridino dyke swarm, is attributed to subduction of a mid-ocean ridge, commencing at 2.87 Ga. The dykes represent typical fissure intrusions and underwent metamorphism to eclogite, granulite and amphibolite facies. The dykes divide into two compositions (Fe-Ti gabbro and Mg-Cr gabbro) which represent alternating episodes of arc and slab window magmatism. The Fe-Ti gabbros have high Ti and low abundances of fluid-mobile and other LIL elements compared to HFSE and plot in the MORB and within-plate oceanic basalt fields. The Fe-Ti gabbros formed from low-degree of partial melting from a depleted mantle source. This petrogenesis is consistent with slab window model in which magmas were derived by decompression melting of suboceanic mantle that upwelled into the opening beneath continental margin following spreading ridge subduction. The Mg-Cr gabbros have low Ti along with high abundances of fluid-mobile elements and other LILE compared to HFSE and plot in arc basalt fields that imply melting of subduction-modified hydrous subcontinental mantle.

This study has been carried out following the plans of the scientific research of the Geological Institute of RAS (project no FMMG-2023-0007)

Mints M.V., Dokukina K.A., Konilov A.N. (2014). The Meso-Neoarchaeon Belomorian eclogite province: Tectonic position and geodynamic evolution. Gondwana Research, 25, 561–584.

Assessing reprocessing potential of abandoned zinc-lead tailings ponds

Ayoub El Aallaoui¹, Mustapha El Ghorfi^{1,2}, Abdellatif Elghali², Yassine Taha², Hamza Zine², Mostafa Benzaazoua², Rachid Hakkou^{2,3} and Hassan Ibouh¹

¹ Laboratory of Geo resources, Geo environment and civil engineering (L3G), Faculty of Sciences and Techniques Gueliz, Cadi Ayyad University, A. Elkhattabi Bd, BO 549, 40000 Marrakesh, Morocco

² Geology and sustainable Mining Institute (GSMI), Mohammad VI Polytechnic University (UM6P), Lot 660. Hay Moulay Rachid, 43150, Ben Guerir, Morocco

³ Laboratory of Innovative Materials, Energy and Sustainable Development (IMED-Lab), Faculty of Sciences and Techniques, Cadi Ayyad University, A. Elkhattabi Bd, BO 549, 40000 Marrakesh, Morocco.

Touissit-Boubeker mine (TBM) in Morocco, operated by Touissit Mining Company (CMT), holds valuable minerals and metals. Abandoned in 2001, it left untreated tailings. This study aims to estimate resources and evaluate reprocessing potential (Pb, Zn, Ag) of TBM tailings. 3D Modeling focused on tailings ponds drilling using reverse circulation drilling (RCD) sampling. Physicochemical characterization involved X-ray fluorescence (XRF), Total sulfur and carbon (C/S), inductively coupled plasma optical emission spectrometry (ICP-OES), and inductively coupled plasma mass spectrometry (ICP-MS). Mineralogy was studied using optical microscopy (OM), X-ray diffraction (XRD), electron probe microanalyzer (EPMA), and laser ablation inductively coupled plasma mass spectrometry (LA-ICP-MS). Quantitative Evaluation of Minerals by Scanning electron microscope (QEMSCAN) was used to quantitatively evaluate minerals and chemical element deportments. The 3D model indicates a total TBM tailings tonnage of 23,1 Mt. Chemical analysis revealed substantial Zn (370 Kt), Pb (140 Kt), Ag (160 thousand Kg) concentrations approaching 2% of Zn, Pb grades are around 1.5%, and Ag grades (~14 ppm). Tailings consist mainly of fine particles (<63mm), offering valorization potential with low treatment costs. The study highlights sustainable rehabilitation of these mine waste materials while mitigating their environmental impact.

TBM is situated along the Moroccan-Algerian border, approximately 30 km to the south of Oujda city, operated by CMT, is considered as a Mississippi Valley type deposit used for extracting Zn and Pb sulfides (Bouabdellah et al., 2015, 2012; Dupuy.J & Touray, 1986; Marcoux et al., 2021). The geological context features a schistose Paleozoic basement with Mesozoic cover and rhyodacitic intrusions, constrained between collapse zones. (Fig.1B). The mine left significant quantities of concentrated tailings in surface facilities (T11-T17) (Fig.1A) (Bruneel, 2016). Prior to closure, TBM produced 75 Mt of ore, yielding 350 Kt of Pb metal and 175 Kt of Zn metal. Pb and Zn concentrations varied in different zones. Tailings are a by-product of the concentration treatment process, known for their fine texture. 118 samples were collected from T12 and T17 impoundments by drilling, dried, crushed, grinded to a granulometry less than 250 μ m size for further analysis.

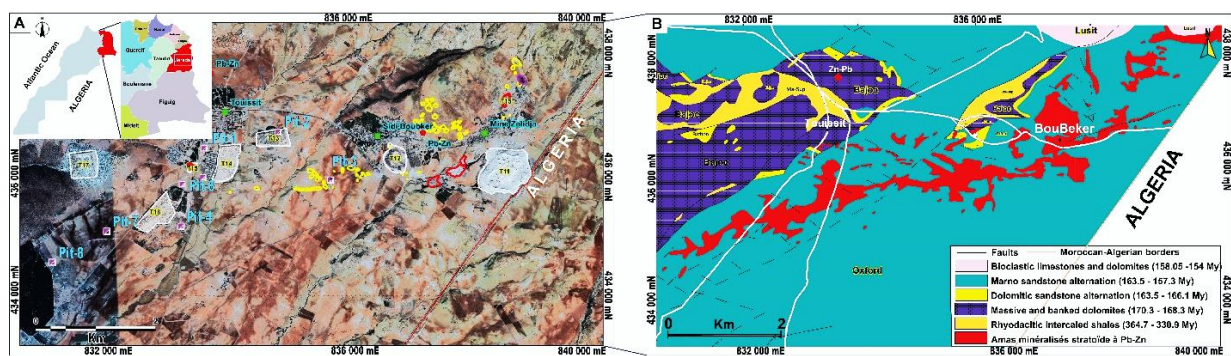


Figure 1. A: Geographical situation of the studied zone; B: Geological situation of TBM district simplified from (Owodenko, 1976; Samson, 1973).

TBM tailings analysis highlights advantages of physical and size-based chemistry assessments, reducing the need for additional crushing. Microscopic examination reveals elevated zinc concentration in fractions $<50 \mu\text{m}$ due to smithsonite hardness. Sulfide release is low for granulometry $>200 \mu\text{m}$ but increases at $100 \mu\text{m}$. Carbonates neutralize acidity, rendering tailings environmentally inert. IDW interpolation method is used for mineral resource estimation, and the accompanying images (Fig.2) depict the final block model of T12 mineral resources. 3D modeling estimates 3.7 Mt of ore in T12 and T17 with 1.5 g/cm^3 density. Core of each tailing exhibits high Zn, Pb grades, indicating potential for optimized extraction or alternative materials. TBM tailings can be reprocessed via open pit mining, achieving 1.5-2% Zn grades through flotation enrichment. Distribution includes 370 Kt Zn, 140 Kt Pb, and 160 thousand kg of Ag. Notably, T17 tailings pond contains significant Ag grades (approximately 14 ppm) for reprocessing.

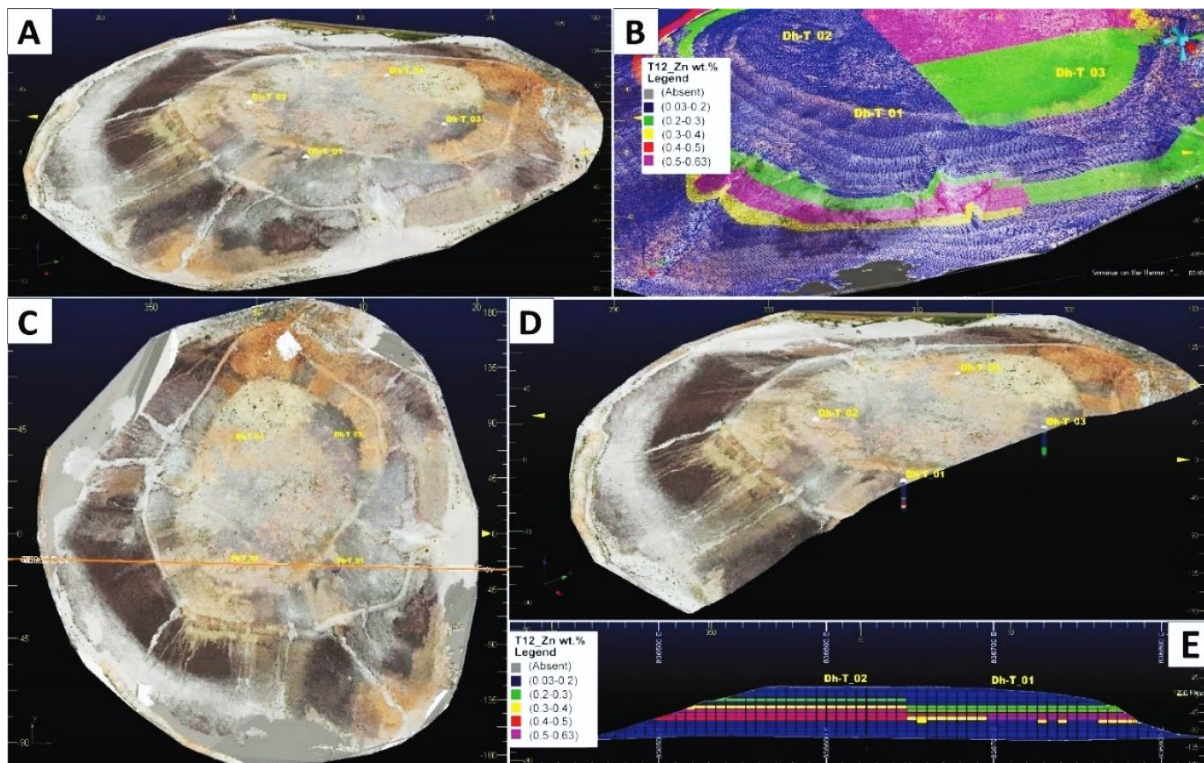


Figure 2. A: T12 Topo-Photogrammetric Model; B: Zinc Resources Model; C: Planar View; D and E: Cross Section with Drillholes (Dh-T_01, Dh-T_02, Dh-T_03, Dh-T_04) in yellow.

References:

- Bouabdellah, M., Sangster, D.F., Leach, D.L., Brown, A.C., Johnson, C.A., Emsbo, P., 2012. Genesis of the Touissit-Bou Beker Mississippi valley-type district (Morocco-Algeria) and its relationship to the Africa-Europe collision. *Econ. Geol.* 107, 117–146. <https://doi.org/10.2113/econgeo.107.1.117>
- Bouabdellah, Niedermann, Velasco, 2015. The Touissit-Bou Beker Mississippi Valley-type district of northeastern Morocco: Relationships to the Messinian salinity crisis, late Neogene-Quaternary alkaline magmatism, and buoyancy-driven fluid convection. *Econ. Geol.* 110, 1455–1484. <https://doi.org/10.2113/econgeo.110.6.1455>
- Bruneel, O., 2016. Implication des microorganismes dans les biotransformations et processus de transfert des métaux et métalloïdes dans les environnements contaminés par les mines 1–130.
- Dupuy, J. & Touray, 1986. Chronique de la recherche minière ; Le gîte plombifère de couverture d'Oued Mekta (district de Touissit -Bou Beker, Pays des Horsts, Maroc oriental). *Chron. Rech. Min.* 485, 17-32.
- Marcoux, É., Jébrak, M., Marcoux, É., Jébrak, M., Bulletin, M., Société, D., 2021. Plombotectonique des gisements du Maroc To cite this version : HAL Id : insu-03272522 0–27. <https://doi.org/10.1051/bsgf/2021019/5335510/bsgf>
- Owodenko, B., 1976. Le bassin houiller de Jerada (Maroc oriental). *Essai de synthèse et de paléogéographie. Notes Mém. Serv. Géol. Maroc*, 207 bis 148 p.
- Samson, P., 1973. Un gisement plombo-zincifère en milieu récifal : Touissit (Maroc oriental). *Notes Mém. Serv.*

Integration of aeromagnetic data in characterizing dike swarms and understanding their geological relationship with carbonatite bodies intruded in the Ouled Dlim massif (West African Craton, South Morocco)

Oualid El Amraoui¹ ; Mustapha Boujamaoui¹ ; Abdellah Nait Bba² ; Ibtissam Rezouki¹ ; Hassane Sahbi¹ ; Mohamed Ben-Daoud³ ; Mamadou Diallo³ ; Nasrddine Youbi³ ; My Ahmed Boumechdi³

¹: Moulay Ismail University, Faculty of Sciences, Earth Sciences Department, P.O. Box 11201, Meknes, 50000, Morocco

²: Mohamed Premier University, Faculty of Sciences, Earth Sciences Department, P.O. Box 717, Oujda, 60000, Morocco

³: Cadi Ayyad University, Faculty of Sciences-Semlalia, Geology Department, P.O.Box 2390, Marrakesh, 40000, Morocco

Aeromagnetic airborne represent an effective technique in mapping dike swarms and exploration for carbonatite bodies. Dikes are typically identified as elongated and narrow features with positive magnetic intensity, and carbonatite bodies can produce, in major cases, positive and circular shape magnetic anomalies. In this study, the aeromagnetic survey was conducted over the western margin of the peri-cratonic Ouled Dlim massif located in the southernmost part of Morocco (Fig. 1). It was analyzed and interpreted using several edge detection techniques, where the main results are illustrated as a ternary image that combines results from three main filters (Fig. 2).

The map reveals three dike groups concealed underneath the recent cover of the Tarfaya-Laayoune-Dakhla basin (Fig. 2). The first dike group (DG1) trend mainly NW-SE and coincide perfectly with the Aghracha Iron deposit. It demonstrates the lenticular shape of the mineralization and confirm its prolongation northwestward under recent sediments. The second dike group (DG2) displays a curved shape which is, from a plan view, following the curvature of the Ouled Dlim units. Hence, these dikes were intruded in Ouled Dlim massif prior to the last tectonic event responsible of its current structuration. The third dike group (DG3) is the widest and most representative in the study area. It consists of several dikes trending mainly NNE-SSW intruded in the Silurian-Devonian and the western Archean units of Ouled Dlim. Regarding their orientation and proximity to the Central Atlantic rifting axis (Fig. 2), they are likely related to the Central Atlantic Magmatic Province (CAMP). Additionally, they are associated with a large and highly magnetic body to their southern end, which is probably a sill related to the same magmatic event.

Being associated to large igneous provinces during Atlantic Ocean opening, Twihinat (TC), Lamlaga (LmC) and Lahjayra (LhC) calcio-carbonatites were successfully detected via our data as circular bodies aligned in a NNE-SSW atlantic direction. Also, they are intruding Ouled Dlim massif at the intersection of dikes, particularly Twihinat and Lamlaga bodies, or nearby a dike structure as for Lahjayra body (Fig. 2). This confirms the relationship between dikes of the CAMP (DG3) and these carbonatite bodies. Accordingly, these identified dikes have probably induced a structural weakness of hosting rocks, which has favored intense hydrothermal activity during emplacement of carbonatite magma in the Cretaceous.

Additionally, although they are reported to have identical geochemical and mineralogical composition and formed within the same geodynamic history, they depict distinct magnetic anomalies (Fig. 2). This may be linked to different weathering process or due to magnetic contrast with hosting terranes, as TC and LmC that show positive intensities are intruded in Silurian-Devonian unit, whilst LhC with negative anomaly is intruding the western Archean unit (Fig. 1). Eventually, regarding our findings we were able to identify a potential carbonatite circular body located farther to the North (Fig. 2), which is aligned in a NNE-SSW with mapped carbonatites, presenting a positive anomaly and linked to a CAMP dike intruding to its West.

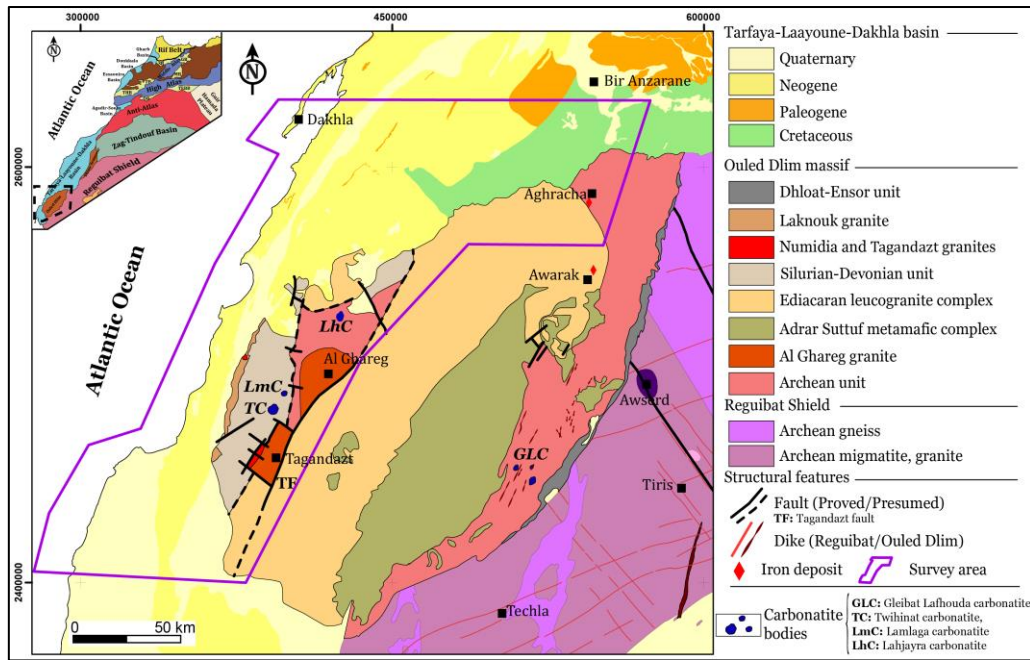


Fig.1- Geological map of the Ouled Dlim massif, illustrating the localization of the aeromagnetic survey area.

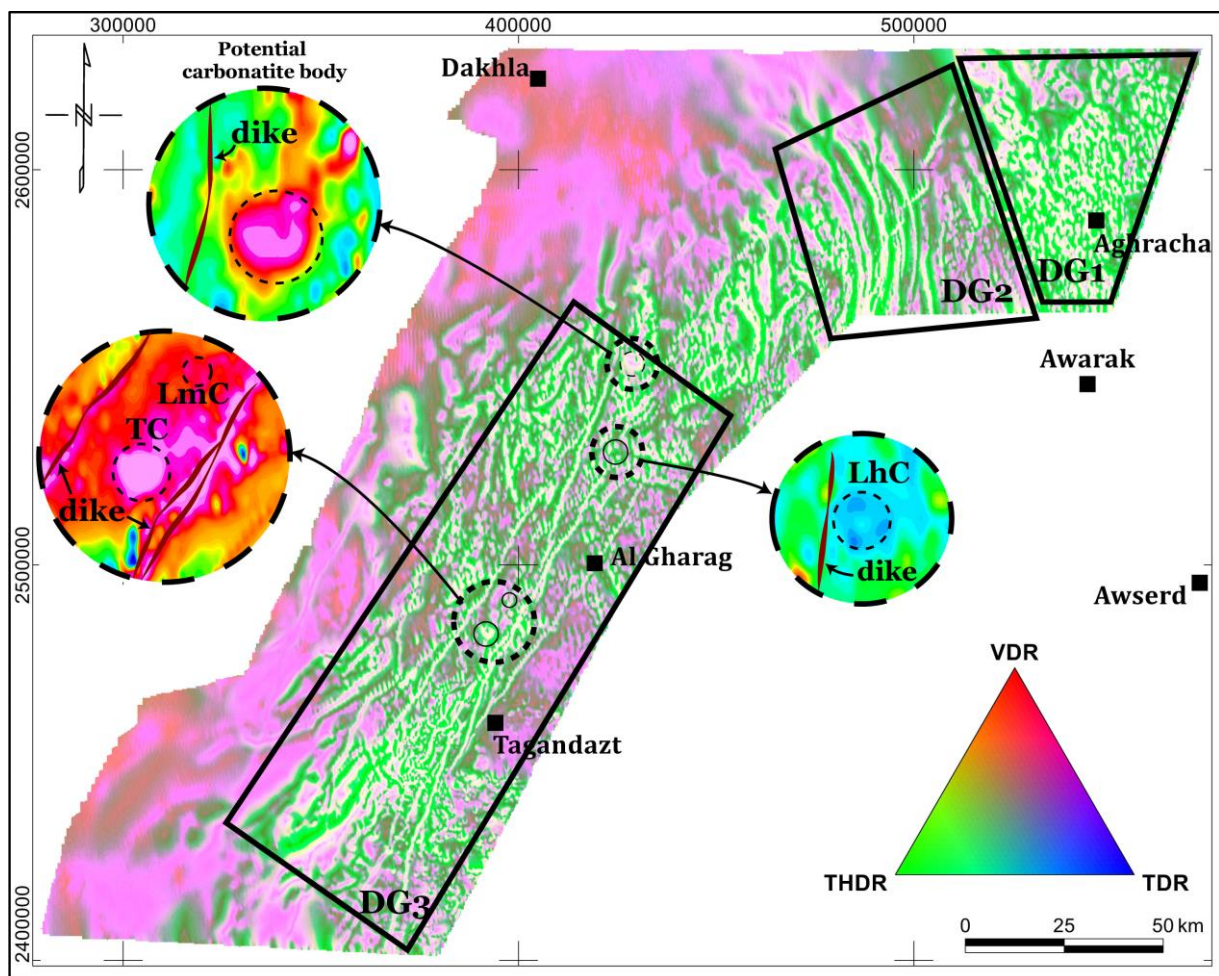


Fig. 2- Ternary image combining results from vertical derivative (VDR) total horizontal derivative (THDR) and tilt-angle derivative (TDR) maps of the study area. Black polygons represent dike groups (DGs). Black dashed large circles delineate carbonatite areas with small circles inside that represent carbonatite bodies. Their zoomed image displays their magnetic signal in the Reduced to pole map (Acronyms are indicated in Fig.1).

Geological and hydrothermal mapping using multispectral images in the prospecting mining in the Tighardine Ore deposit (Western High Atlas, Morocco): preliminary results

El Bakhouch N.¹, Ibouh H.¹, Touil A.¹, Chafiki D.¹ and ¹ Erragragui M.¹

¹Lab.. L3G, Depart. of earth sciences, FSTG, University Cadi Ayyad, Marrakech, Morocco

The Tighardine polymetallic deposit (Cu, Pb, Zn, Ag) is located on the southern flank of Tighardine mountain in the western High Atlas and at about 70 km SSW of Marrakech City.

The focus of this study is the use of remote sensing complements structural mapping and identifies hydrothermal alteration zones that may host mineralizations representing extensions of the exploitable mineralized horizon or corresponding to new prospects.

The formations composing the study area consist of an upper Neoproterozoic basement represented by the Wirgane granodiorite dated at 625 ± 5 Ma (Eddif et al., 2007), overlain in unconformity by a volcanic and volcano-detritic series of upper Ediacaran age (600 ± 3 Ma, Boukerrou et al., 2018). This basement sequence is unconformably overlain by a Cambrian schal-sandstone series, followed by Ordovician sandstones and quartzites, and then the Visean shale and sandstone. To the east and southeast of the mine, Triassic red sandstones directly overlie the granodiorite.

To achieve our objective, we used: (1) principal component analysis (PCA), (2) minimum noise fraction (MNF), (3) band ratios to map hydrothermal zones, and (4) application of N0°, N45°, N90°, and N135° directional filters with 5×5 and 7×7 matrices to achieve good lineament discrimination.

The analysis of lineament maps and statistical data obtained from satellite imagery allows us to distinguish three fault families (N10° to N50° (75.44%), N70° to N110° (34.47%), and N140° to 180° (3.33%)) using Landsat 8 OLI imagery, and (N10° to N60° (56.19%), N70° to N110° (21.80%), and N130° to N160° (21.70%)) using ASTER imagery.

Band ratios and principal component analysis show that phyllic and argillic hydrothermal alteration zones are generally developed along NE-SW-oriented faults and overlap with mineralized zones.

Reference:

- Boukerrou, S., Nalini, H., Moreira, H., Maacha, L., Zouhair, M., Outhounjite, M., Ouirouane, S., Hibti, M., Touil, A. (2018). Geochronology and geochemistry of Ediacaran volcanic rocks of the Tighardine ore deposit formation (western High Atlas, Morocco). *Arabian Journal of Geosciences*, 11(2). <https://doi.org/10.1007/s12517-017-3375-4>
- Eddif, A., Gasquet, D., Hoepffner, C., & Levresse, G. (2007). Age of the Wirgane granodiorite intrusions (Western High-Atlas, Morocco): New U–Pb constraints. *Journal of African Earth Sciences*, 47(4–5), 227–231. <https://doi.org/10.1016/J.JAFREARSCI.2007.02.003>

Microbially induced sedimentary structures from the Ediacaran of Anti-Atlas, Morocco: a record of marine and continental biosphere

Jamal El Kabouri¹, Ezzoura Errami^{1,2}, Bruno Becker-Kerber³, Nasser Ennih¹, Youbi Nasrddine^{4,5}

¹:Faculté des Sciences, Université Chouaïb Doukkali, EGGPG, B.P. 20, 24000, El Jadida, Morocco

²:Faculté Polydisciplinaire de Safi, Université Cadi Ayyad, Got, B.P. 4162, 46 000, Safi, Morocco

³: Brazilian Synchrotron Light Laboratory (LNLS), Brazilian Center for Research in Energy and Materials (CNPEM), 13083-970, Campinas, Sao Paulo, Brazil

⁴:Department of Geology, Faculty of Sciences Semlalia, Cadi Ayyad University, Prince Moulay Abdellah Boulevard, P.O. Box 2390, Marrakech, Morocco

⁵: Faculty of Geology and Geography, Tomsk State University, 36 Lenin Ave, Tomsk 634050, Russia.

The Neoproterozoic Era records the most important geological evolution in the history of the Earth. This era marks a change in the geodynamic and biosphere of the Earth marked by the second increase in oxygen dissolved in the ocean (Neoproterozoic Oxygenation Event), repeated glacial periods and the appearance of the first multicellular life and the development of the supercontinent Gondwanaland. In particular, the Ediacaran period shows the first appearance of abundant macroorganisms (Ediacaran biota) in an environment dominated by microbial substrates. In the West African craton, this assemblage of macro and microorganisms is still poorly recorded and its understanding is therefore crucial to create a complete snapshot of the Ediacaran ecosystem.

The Eastern Anti-Atlas of Morocco hosts an early Ediacaran turbiditic series (Saghro Group) (630-600 Ma) unconformably overlain by thick late Ediacaran (580-550 Ma) terrestrial volcano-clastic formations (Ouarzazate Supergroup), with thin and geographically limited paralic shallow marine sedimentary rocks.

This contribution highlights for the first time a large variety of structures related to the former presence of extensive microbial mats developed in marine, fluvial, and lacustrine environments during the Ediacaran in the Eastern Anti-Atlas. These microbially induced sedimentary structures (MISS) are largely found in well-laminated fine to coarse-grained sandstone and sandy-carbonate. They also cover vast bedding planes and occur in almost all sedimentary successions. MISS types include: gas domes structures, wrinkle structures, reticulated microbial mats, erosional remnants, flipped-over edges mats and roll-ups, drag folded bed surfaces, multidirectional linear ridges, sand cracks and biolaminated deposits. Based on morphology and petrographic macro and microfabrics, these microbial structures are very similar to modern photosynthetic cyanobacteria mats.

Together with previously reported stromatolites, these newly reported microbial structures could have played an important ecological role in stabilizing siliciclastic sediments and sustaining local oxygen oases. In particular, the close association of Ediacaran biota with the MISS in the Izelf Formation provides an example of interaction between macro-organism and microbial mats. The latter could provide nutrients and create local oxygen oases necessary for the establishment of more complex macro-organisms in Ediacaran times.

DYKE SWARM HISTORY OF SE THAUKHUD LINEA REGION, VENUS.

Z. El Kamel¹, H. El Bilali^{2,3}, R.E. Ernst^{2,3}, N. Youbi¹

¹Department of Geology, Faculty of Sciences-Semlalia, Cadi Ayyad University, Marrakesh, Morocco;

²Department of Earth Sciences, Carleton University, Ottawa, Ontario, Canada;

³Faculty of Geology and Geography, Tomsk State University, Tomsk, Russia;

Introduction: Lineae are elongated regional features on Venus that are associated with extensional lineaments that occur together in narrow elongated topographic highs. Lineae have also been termed fracture belts, densely lineated material, and more recently, groove belts (see summary of nomenclature in Ivanov et al. (2011) and Ivanov et al. 2015). Many interpretations emphasize an extensional origin (Ivanov et al. 2015), although a recent interpretation suggest they can also represent deformation belts (exhibiting both extensional and compressional features) between small crustal blocks (Byrne et al. 2021) Magmatic centres can occur along linea and the relationship between linea and their associated magmatic centres can be determined through detailed mapping (e.g Oukhro et al. 2023) which also provide insights into the origin of lineae.

Research Goals: The area selected for study (Fig. 1) is the Thaukhud Linea region (Brian et al 2005) along Parga Chasmata which is along the boundary between Imdr Regio Quadrangle V-51 and Taussig Quadrangle (V-39). Multiple corona-like magmatic centres, all unnamed, are present. The focus of this report is detailed mapping (1:500,000 scale) of graben-fissure lineaments, interpreted as dyke swarms according to the criteria in Grosfils et al. (1994) and Ernst et al. (2003). These dyke swarms are linked to the magmatic centres along Thaukhud Linea and can provide insight into the relationship between these magmatic centres and the linea.

Methodology: Mapping is carried out using the Synthetic Aperture Radar (SAR) of the 1990-1994 NASA Magellan mission, ArcGIS 10.8.2, and JMARS (Christensen et al. 2009) used for reconnaissance viewing and creating topographic profiles.

Graben Systems (Dyke Swarms): Several thousand extensional lineaments (mainly grabens and fissures) were mapped (Fig. 2) and they have been generalized and grouped into multiple systems (and interpreted to overlie dyke swarms) based on trend and geometry (radiating, circumferential and linear) (Fig. 3).

Magmatic Centres: Four main unnamed magmatic centres are linked to the dyke swarms (Fig. 3).

Centre 1: The radiating swarm is dense to the NE and SE of the centre, and partially, to totally, flooded by younger flows to the SW and the E. The circumferential swarm is partially flooded by younger flows. The mapped circumferential dykes indicate a radius of about 180 km. Centre 1 is located at about 850 km SSE of Nodi Corona and 550 km SE of Samsing Corona.

Centre 2: This centre exhibits clear radiating and circumferential dykes. The radius of the circumferential swarm is about 95 km, making it smaller than Centre 1. Two small rift arms appear to diverge at this centre and thus this centre is possibly the locus of triple junction rifting (Graff et al. 2018). This centre is located about 450 km NNE of Centre 1.

Centre 3: This centre shows both radiating and circumferential dykes. Radiating dykes appear to be masked by rift faults both north and south of the centre. Circumferential dykes are dense and show a radius of about 160 km. This centre is also the locus of a local triple junction rifting with two rift arms to the SE and SW (cf Graff et al. 2018). This centre is closest to Centre 2 (200 km) and 260 km SSE of Nodi Corona.

Centre 4: This cryptic centre is located at 600 km ENE of centre 1 and about 650 SE of Centre 2. Only radiating dykes were mapped. Circumferential dykes are not recognized, possibly due to flooding by younger lava flows.

Future work: Mapping of graben systems will be completed and then lava flows and the lineaments of Thaukhud Linea will be mapped in detail (1:500,000 scale. This will be followed by integration of information on graben-fissure systems (dyke swarms), lava flows and linea lineaments, in order to provide a geological history for the area and insights into the nature of Thaukhud Linea.

References:

- Brian, A.W et al. (2005) USGS SIM 2813.
Byrne, P.K. et al. (2021) PNAS, 118, e2025919118.
Christensen, P. R. et al. (2009) AGU Fall Meeting, Abstract #IN22A-06.
Ernst, R.E. et al. (2003) Icarus, 164, 282–316.
Graff, J.R. et al. (2018) Icarus, 306, 122-138.
Grosfils, E.B., Head, J.W. (1994) GRL, 21, 701–704.
Ivanov, M.A., Head, J.W. Space Sci., 2011, V. 59, P.1559-1600.
Ivanov, M.A., Head, J.W (2015), 113-114, 10–32.
Oukhro, R et al. (2023) LPSC abstr.

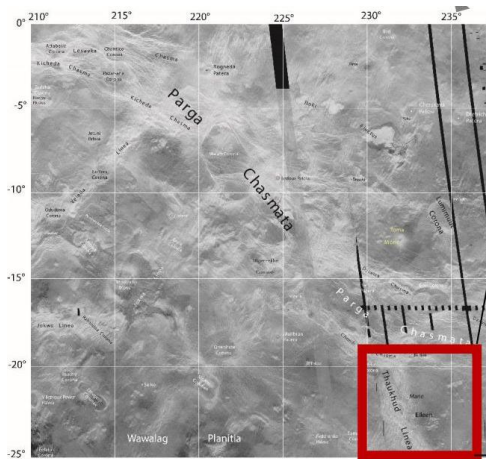


Figure 1: Study area (red box) on annotated SAR (synthetic aperture radar) image from the 1989-1994 Magellan mission.

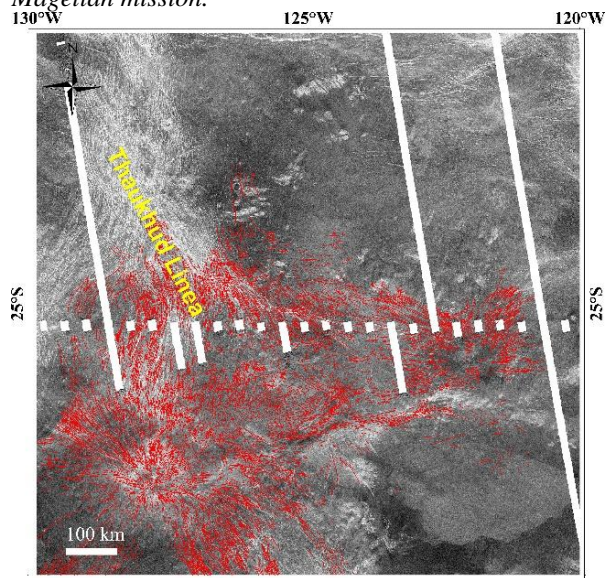


Figure 2: Detailed mapping of graben-fissure lineaments (several thousand to date).

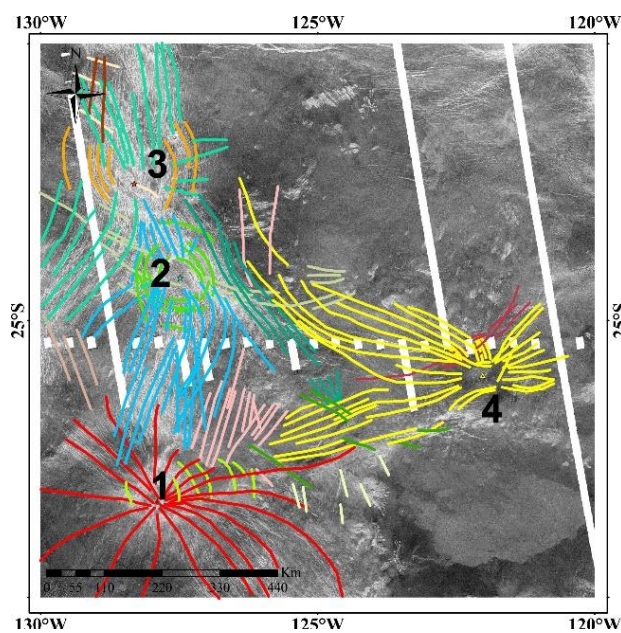


Figure 3: Generalized distribution of graben systems (colour coded to represent different radiating, circumferential and linear swarms) and their unnamed magmatic centres, labelled (1-4).

THE CONTRIBUTION OF SENTINEL-2 AND LANDSAT-8 SATELLITE IMAGES TO THE GEOLOGICAL MAPPING OF THE MAFIC COMPLEX OF ADRAR SOUTTOUF (OULAD DLIM MASSIF, SOUTHERNMOST MOROCCO)

El Houcine El Haous^{1*}, Abdelilah Fekkak¹, Youssef Houali², Faouziya Haissen³, Abdellatif Jouhari¹, Ilyasse Berrada⁴

¹ Geodynamics and Variscan Geosciences Laboratory, Chouaib Doukkali University, El Jadida, Morocco.

² Marine Geosciences and Soil Sciences Laboratory, Chouaib Doukkali University, El Jadida, Morocco.

³ LGAGE, Département de géologie, Faculté des sciences Ben M'sik, Hassan II University, Casablanca, Morocco.

⁴ Laboratoire de Recherche en Sciences et Techniques (LRST), Ecole Supérieure de l'Éducation et de la Formation, Ibn Zohr University, Agadir, Morocco.

* Corresponding author's Email: elhaouselhoucine@gmail.com

Abstract

The geological mapping in desertic areas can be confronted with numerous constraints such as silting and difficulty of access. Recently, several methods of spatial remote sensing have been used to facilitate this task; this discipline can allow us to extract relevant information on the geological structures and the facies identification in the studied region as for example the mafic complex of Adrar Souttoug (Massif of Oulad Dlim). Different processing techniques such as color combinations, band ratios and principal components were applied on Landsat-8 and Sentinel-2 satellite images in order to prepare maps for our study area and the updating of pre-existing data which contributed to the setup of a GIS database of the area. The results obtained show a strong discrimination of different lithological units. Field trips were carried out to validate these results and showed a great correlation between the maps generated and the field observations. A litho structural map of the Adrar Souttoug area was created on the basis of the results obtained in this work.

Keywords: Remote sensing, geology, mafic complex, Adrar Souttoug, Oulad Dlim massif.

The Ougnat dyke swarms (Eastern Atlas, Morocco): U-Pb geochronology, geochemistry, and geodynamic significance

El Moume W.^{1,2}; Gärtner, A.³; Linnemann, U.³; Youbi, N.^{1,4}; Ikenne, M.²; Garrido, C. J.⁵; Marchesi, C.⁵; Alpiste, M.J.R.⁵; Ait Lahna, A.¹; Boumehdi, M.A.^{1,6}; Bensalah, M.K.^{1,6}

¹: Department of Geology, Faculty of Sciences-Semlalia, Cadi Ayyad University, Prince Moulay Abdellah Boulevard, P.O. Box 2390, Marrakech, Morocco.

²: Department of Geology, Faculty of Sciences, Ibnou Zohr University, P.O. Box 28/S, Agadir, Morocco.

³: Senckenberg Naturhistorische Sammlungen Dresden, Museum für Mineralogie und Geologie, Sektion Geochronologie, GeoPlasma Lab, Königsbrücker Landstraße 159, 01109 Dresden, Germany.

⁴: Faculty of Geology and Geography, Tomsk State University, 36 Lenin Ave, Tomsk 634050, Russia.

⁵: Instituto Andaluz de Ciencias de la Tierra (IACT), CSIC-UGR), Av. Palmeras, 4, 18100 Armilla, Granada, Spain.

⁶: Instituto Dom Luiz (IDL), Faculdade de Ciências, Universidade de Lisboa, Campo Grande, 1749-016, Lisboa, Portugal

The Ougnat inlier is located in the easternmost portion of the pan-African Anti-Atlas Belt, Morocco, which itself is attached to the northern margin of the West African Craton (WAC). Numerous mafic and felsic dyke swarms and sill complexes cross-cut the Precambrian basement including the Saghro Group and the Ouarzazate Supergroup. The latter is composed of volcanic successions with andesitic lava flows, ignimbrite flow units and associated sedimentary rocks. The Ouarzazate Supergroup is subdivided into three Formations: Tamerzaga Formation, Isilif-Ouinou Oufroukh Formation, and Aoujane Aïssa Formation. The studied dykes and sills show diverse geochemical compositions: gabbro, micro-gabbro, micro-diorite, dolerite, basalt, andesite, and rhyolite including ignimbrite. They display four main trends N-S, N60°E, N30°E (60 % of all the Ougnat dyke swarms), and, rarely E-W. These dykes can be traced from a few meters to several kilometers in the field. None of the mafic/felsic dyke swarms cut through the Aoujane Aïssa Formation and overlying sequences of the Paleozoic cover. N-S trending dykes of the Ougnat dyke swarms were dated by U-Pb on zircon and apatite. Additionally, ages of detrital zircon grains extracted from a sandstone from the upper part of the volcanic pile were obtained applying the LA-ICP-MS (Laser Ablation Inductively Coupled Plasma Mass Spectrometry) method. The dykes yield 577 ± 9 Ma (mafic) and 597 ± 27 Ma, 581 ± 3 Ma (felsic). The youngest detrital zircon grains of this sandstone are ca. 572 Ma old. Therefore, the age of the volcanic pile is bracketed between ca. 572 Ma and ca. 540 Ma (age of the Ediacaran-Cambrian Transition). The mafic and felsic dyke swarms of Ougnat show geochemical characteristics of high-K calc-alkaline and continental tholeiitic magma and are interpreted as feeder dykes of the Ouarzazate Supergroup that belong to the so-called Central Iapetus Magmatic Province (i.e., CIMV). They were formed during the fragmentation of Rodinia (Pannotia) leading to the opening of the Central Iapetus Ocean.

THE CAMBRIAN ALKALINE COMPLEX OF JBEL BOHO : AN INTEGRATED MULTIDISCIPLINARY APPROACH TO STUDY AND VALORIZE RARE EARTHS AT THE SCALE OF THE BOU AZZER-EL GRAARA INLIER (CENTRAL ANTI-ATLAS, MOROCCO)

Fadil M.¹, Ibouh H² ; and Youbi¹ N.

1 Dynamics of the Lithosphere and Genesis of Resources Laboratory "DLGR". Earth Science Department. Faculty of Sciences Semlalia, BO .2390. Cadi Ayyad University, 40000 Marrakesh, Morocco

2 L3G, FSTM, Cadi Ayyad University, Marrakech, Morocco.

Located southeast of the Bou Azzer cobalt mine and the northern part of the West African craton, the Jbel Boho volcanic complex represents the witness of an intraplate magmatic activity of alkaline nature set up during the infracambrian period in the Bou Azzer El-Graara inlier (Central Anti-Atlas, Morocco).

This volcanic complex is marked by its lithological diversity from its core to its periphery including a volcanic suite composed by basanites, trachyandesites, trachytes and rhyolites. This complex is intruded later by a pluton of syenitic nature. The volcanic suite and the pluton are intersected by microsyenitic and andesitic dykes with a general direction N10° to N20° with a subvertical dip (70° to 90°) to the east to west, and rhyolitic dykes of direction (NE-SW), and posterior carbonate veins.

Previous work undertaken on this alkaline complex (Benaouda, 2015; Benaouda et al. 2017a and b) and exploration work conducted by the Managem Group (unpublished report) have highlighted the presence of rare earth element (REE) mineral potential associated with alkaline rocks namely rhyolites and syenites. The heavy rare earth elements are very abundant in the less acidic formations (trachytes, trachyandesites). The light REEs remain in the last supersaturated magmatic fluids enriching the acidic volcanic rocks of rhyolitic nature (rhyolitic dykes).

Within the framework of an evaluation of the mineralogical and economic potential of REE mineralization, this study is based on a multidisciplinary approach combining geological, petrographic, geochemical, geophysical studies and processing of high-resolution satellite imagery.

A set of treatments is applied on multispectral satellite images type Aster and Landsat 8 OLI for the study area of Jbel Boho. They include, Minimum Noise Fraction (MNF), Principal Component Analysis (PCA), Optimized Index Factor (OIF).

The satellite images Aster and Landsat 8 OLI allow to highlight the discrimination between the different formations at the level of Jbel Boho sector, and the ratios of bands that indicate the hydrothermal indices in this area.

The SPOT-5 satellite image allows to highlight the dykes that are located in the upper part of the syenite, as well as the structural part that has a general direction of Northeast and Southwest.

This processing model has allowed the realization of a lithological, mineralogical mapping indicating the hydrothermal showings in the Jbel Boho area as well as fracture maps through directional filters (1/10000).

The validity of the model is tested by comparison with what is found in the literature and the geological maps of Alougoum and Ait Ahmane (1/50000).

References :

- Benaouda, R., 2015. *Magmatic Evolution and REE Mineralization in the Early Cambrian Jbel Boho Complex in the Bou Azzer Inlier (Anti-Atlas/Morocco)*. (Ph.D. Thesis. Dissertation). Christian-Albrechts Universität, Kiel.
- Benaouda, R., Devey, C. W., Badra, L., & Ennaciri, A. (2017a). Light rare-earth element mineralization in hydrothermal veins related to the Jbel Boho alkaline igneous complex, AntiAtlas/Morocco: The role of fluid-carbonate interactions in the deposition of synchysite-(Ce). *Journal of Geochemical Exploration*, 177, 28–44. doi:10.1016/j.gexplo.2017.02.002
- Benaouda, R., Holzheid, A., Schenk, V., Badra, L., & Ennaciri, A. (2017b). Magmatic evolution of the Jbel Boho alkaline complex in the Bou Azzer inlier (Anti-Atlas/Morocco) and its relation to REE mineralization. *Journal of African Earth Sciences*, 129, 202–223. doi:10.1016/j.jafrearsci.2017.01

Moroccan Variscan Belts, a Legacy to Classical Wilson Cycle

Aboubaker Farah ¹; André Michard ²; Christian Hoepffner ³; Youssef Driouch ⁴; Yvette D. Kuiper⁵;
Hassan Ouanaimi ⁵; Abderrahmane Soulaïmani ⁶; Omar Saddiqi ¹.

¹ Geosciences Laboratory, Faculty of Sciences Ain Chock, Hassan II University of Casablanca, Morocco.

² Em. Prof. Paris-Saclay University (Orsay), 10 rue des Jeûneurs, 75002 Paris, France.

³ Em. Prof. Mohammed V University of Rabat, Morocco.

⁴ Department of Geology, Faculty of Sciences, Med. Ben Abdallah University of Fez. Morocco.

⁵ Department of Geology and Geological Engineering, Colorado School of Mines, USA

⁶ Em. Prof. Department of Geology, Ecole Normale Supérieure, Cadi Ayyad University of Marrakech, Morocco.

⁷ Department of Geology, Faculty of Sciences Semlalia, Cadi Ayyad University of Marrakech, Morocco.

The concept of cyclic opening and closure of ocean basins over millions of years along the same crustal scar was introduced by J.T. Wilson (1966) based on the example of the Atlantic Ocean and its continental borders. At that time, the only Variscan orogen cited south of Europe along the Atlantic coasts of Africa was the Mauritanides of Mauritania (Sougy, 1962). In complement to the Yvette D. Kuiper presentation about the Appalachian terrains on this event “Joint IDC-8, LIPs-8, & Rodinia 2023” in Marrakech, here we report on the recent achievements in the Moroccan Meseta Orogen, which together with the Mauritanides records the Variscan orogeny. The western Meseta orogen is only affected by Variscan Late Carboniferous-Permian events, mild in the Coastal Block, while the eastern Meseta was also affected by Eo-Variscan Late Devonian-Early Carboniferous events. The along-strike change from the Mauritanides to the Meseta orogen is interpreted by the transition from a head-on collision south of the South Meseta transform Fault (SMF, precursor of the South Atlas Fault, SAF) to a dextral, transpressional collision north of the SMF. The Meseta Coastal Block was probably displaced from the south-westernmost Anti-Atlas during this process. The Wilson Cycle concept was mostly operating in that the Atlantic Ocean opened where the prior Rheic Ocean had closed. Possible exceptions are the Sehoul Block of northern Meseta, which may have separated from NW-Africa and re-amalgamated to it during the Variscan orogeny, and the Silurian-Devonian Sector of the Moroccan Mauritanides (Oulad Dlim Massif), which may have existed as a separate (exotic?) crustal block prior to the Variscan orogeny. An early Ediacaran-Cambrian Wilson cycle nested in the overall cycle occurred along the margin of NW-Africa, where Cadomian terranes rifted off Africa, then some were transferred to Europe and some accreted back to NW-Africa. This early cycle likely deeply influenced the subsequent rifting process.

References:

Sougy, J., 1962. West African fold belt. *Geol. Soc. Amer. Bull.*, 73, 871-876. [https://doi.org/10.1130/0016-7606\(1962\)73\[871:WAFB\]2.0.CO;2](https://doi.org/10.1130/0016-7606(1962)73[871:WAFB]2.0.CO;2)

Wilson, J.T., 1966. Did the Atlantic close and then re-open? *Nature*, 211, 676-681, <https://doi.org/10.1038/211676a0>.

DETAILED CARTOGRAPHY OF DYKE SWARMS OF NINMAH CORONA AREA- VENUS.

A. Hasanaine¹, H. El Bilali^{2,3}, R.E. Ernst^{2,3}, N. Youbi¹.

¹Department of Geology, Faculty of Sciences-Semlalia, Cadi Ayyad University, Marrakesh, Morocco; hasanaine.abde@gmail.com,

²Department of Earth Sciences, Carleton University, Ottawa, Ontario, Canada; hafidaelbilali@cunet.carleton.ca ; richard.ernst@ernstgeosciences.com,

³Faculty of Geology and Geography, Tomsk State University, Tomsk, Russia.

Introduction: Coronae are common tectonomagmatic features on Venus. They typically have a quasi-circular/elliptical annulus of graben (or occasionally compressional ridges) with diameters ranging from 60 to 2600 km (mean ~300 km) (e.g. [1]). Recent studies suggest that a terrestrial analogue of corona can be circumferential swarms associated with mantle plumes or diapirs [2]. Detailed mapping of coronae is required to further test this hypothesis.

Ninmah Corona: In this research we investigate graben-fissure systems associated with a cluster of four large corona in Eastern Eistla Regio: Didilia, Pavlova, Ninmah, and Isong [3].

This abstract focusses on mapping results from Ninmah corona which is 700 km in diameter. Previous study of Ninmah corona (and the other corona) includes the 1:5,000,000 scale quadrangle map V-21 [3]. On this map abundant extensional lineaments (“fractures”) are mapped, but are not distinguished by trend or distribution (Fig. 1). In our research we apply the dyke swarm context to mapping of graben-fissure-fractures (e.g. [2]) and group them into separate radiating, circumferential and linear dyke swarms.

Methods: Our approach begins with detailed 1:500,000 scale mapping of grabens-fissures-fractures, which are then grouped into radiating, circumferential and linear dyke swarms. Radiating and circumferential swarms can be directly associated with magmatic centres. Linear swarms are linked to distal magmatic centres outside the study area, where possible.

Geological mapping is being carried out using full-resolution (75m/pixel) Magellan SAR images and its altimetry data in ArcGIS ArcMap v. 10.8. JMARS [4] is also used for reconnaissance.

Graben Sets (Dyke Swarms): We have mapped 16,000 extensional lineaments (mainly grabens and fissures) (Fig. 2) and these have been generalized and grouped into multiple systems (swarms) based on trend and geometry (radiating, circumferential and linear) (Fig. 3).

Ninmah corona: This corona (labelled N in figures 2 and 3) has a prominent radiating dyke swarm (coloured red) which extends 580 km to the west and 520 km to the east.

At least two circumferential swarms are identified to be associated with Ninmah: light blue lines partially circumscribe Ninmah, and yellow lines prominently and fully circumscribe centre 1, which is offset by 160 km to the north from the Ninmah centre

Pavlova Corona: The yellow dykes in the western part of the study area converge to Pavlova corona.

Didilia Corona: The NW linear green swarm trends toward Didilia corona (labelled D).

Isong Corona: Radiating swarm 4 converges to the south, to Isong corona (Fig. 3)

Centres 2 and 3: Two adjacent, and partially overlapping, circumferential swarms are located in the southeastern part of the map area. These coronae have diameters of 160 km and 120 km, respectively.

Linear Swarms: There are additional linear swarms which have not yet been linked with any magmatic centres.

References: [1] Buchan K.L., Ernst R.E. (2021) *Gond. Res.* 100, 25–43. [2] Campbell, B.A., Clark, D.A. (2006). USGS Sci. Invest. Map 2897. [3] Christensen, P. R. et al. (2009) AGU Fall Meeting, Abstract #IN22A-06. [4] Gülcher et al. (2020) *Nat. Geosci.*, 13, 547–554.

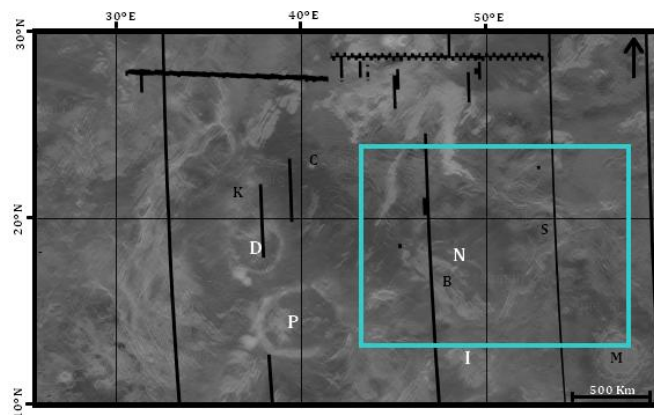


Figure 1. Location of study area in Eastern Eistla Regio. Named Coronae: N= Ninmah, P = Pavlova, D = Didilia, I= Isong, and named impact craters: K = Karo, M = Mead, S = Sheila, B = Bradstreet. G = Gautier, C = Corinna, V = Huarei. Background Magellan SAR image from JMARS [4].

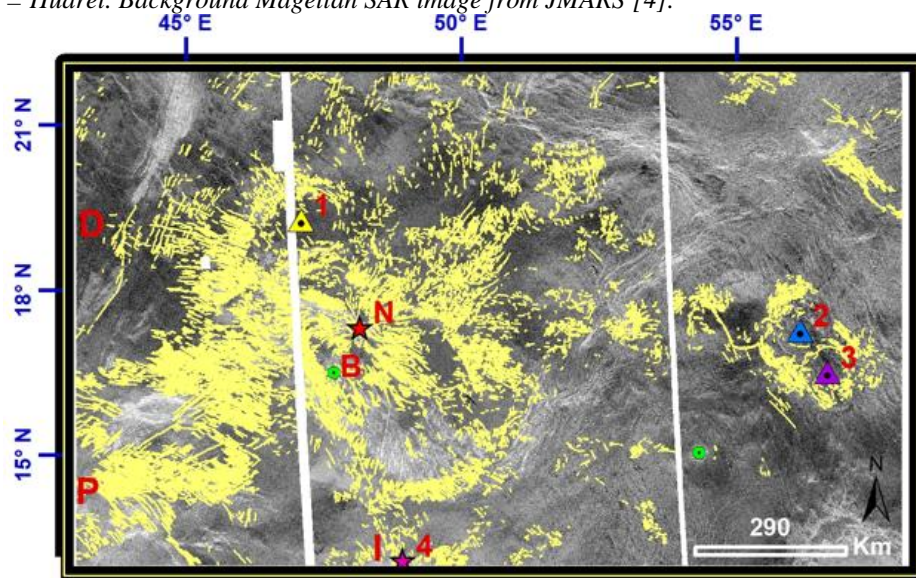


Figure 2. Detailed mapping of grabens. Stars locate inferred the radiating centres and triangles determine the circumferential centres, and are likely associated with coronae. Green dots located impacts.

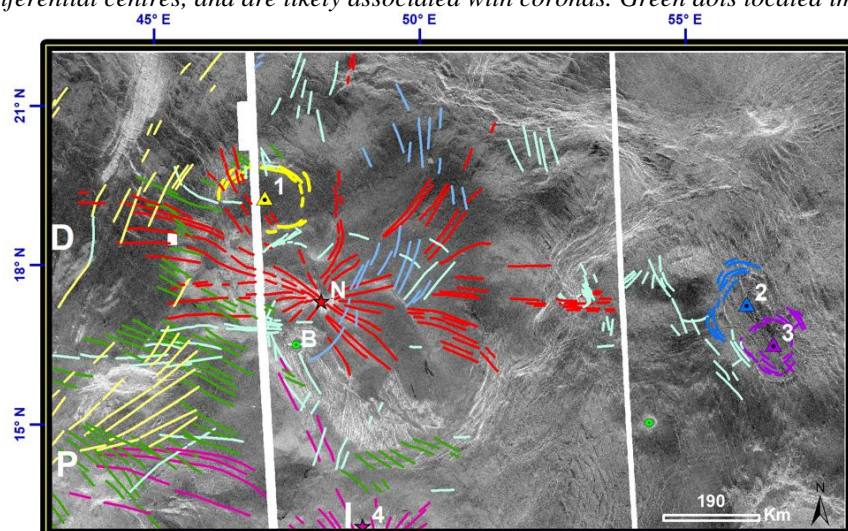


Figure 3. Generalized distribution of grabens grouped into distinct sets distinguished by colour. Labels are linked to the discussion in the text.

The Ait Dawd Cu-Ni vein deposit (western High Atlas district, Morocco): insights from mineralogical investigations

Said Ilmen ^{1,✉}, Bouchra Baidada ², Zaineb Hajjar ³, Abdelkhalek Alansari ⁴, Abdel-Ali Kharis ¹, Amal El Arbaoui ⁴, Amine Bajddi ⁵, Azizi Moussaid ⁶, Mohamed Bhilisse^{2,7}, Mohammed El Azmi⁵, M'hamed El Janati ³

¹ CAG2M, Polydisciplinary Faculty of Ouarzazate, Ibn Zohr University, Avenue Moulay Ettahar Ben Abdulkarim, BP. 638, 45000 Ouarzazate, Morocco

² Ecole Nationale de Technologie, Fkih Bensalah, Moulay Slimane University, Beni-Mellal, Morocco

³ Geoscience, Water and Environment Laboratory, Faculty of Sciences, Mohammed V University in Rabat, Avenue Ibn Batouta, Rabat 10100, Morocco;

⁴ Department of Geology, Faculty of Sciences-Semlalia, Cadi Ayyad University, Marrakech, Morocco

⁵ Managem Group, Twin Center Casablanca, Morocco

⁶ Department of Geology, Faculty of Sciences, Moulay Ismail University, Meknes, Morocco

⁷ Aya Gold and Silver, Zgounder, Taliwine, Morocco

The Ait Dawd Cu-Ni-Au vein deposit is hosted within the Cambrian-Ordovician formations of the Erdouz terranes from the western High Atlas (Morocco). These formations are folded during the Variscan orogeny and the schistosity is striking NNE to NE and strongly dipping to the east (40° to 70). Based on the petrographic observations, SEM, and EPMA investigations, the primary mineral assemblage is composed of chalcopyrite, pyrite, arsenopyrite, galena and sphalerite, tetrahedrite, freibergite, native gold and native bismuth. Argentio-pentlandite and cobaltite-gersdorffite serie are intimately associated or enclosed within chalcopyrite. Native gold is free in a quartz gangue or associated with chalcopyrite. The secondary minerals are composed of malachite, azurite, covellite, anglesite and iron oxides. The gangue minerals are consisting of quartz, calcite, dolomite, ankerite and chlorite. The studied hydrothermal alterations are formed mainly by silicification, chloritization, sericitization and carbonatation. The presence of disseminated cobaltite-gersdorffite and argentio-pentlandite in this area is in favor of the magmatic source of the ore fluids responsible of the deposition of several mineralizations. Several pending questions should be emphasized on the genetic model and the role-played by the Permian magmatism in the genesis and the mineral exploration of the entire mineralization within the western High Atlas mining district.

New sulpharsenide-arsenide and sulphide paragenesis from the Carbonate-amphibole-rich vein of the tholeiitic Gour Essafra sill (Variscan Belt, Central Jebilet of Morocco)

Abdelmajid Jarni ⁽¹⁾, El Mostafa Mouguina ⁽¹⁾, Mohammed Jaffal ^(3,4), El Mostafa Aarab ⁽²⁾,

¹ DLGR Laboratory (DLGR, URAC-43); Cadi Ayyad University, Semlalia Faculty of Sciences, Prince Moulay Abdellah Boulevard, PO Box 2390, mouguina@uca.ac.ma

E-mail (Corresponding author): abdelmajid.jarni@ced.uca.ac.ma ; mouguina@uca.ac.ma

² (3Geo-Lab,) Laboratory, Cadi Ayyad University, Semlalia Faculty of Sciences, Marrakech, Morocco; E-mail: aarab@uca.ac.ma

³ Georesources, Geoenvironment and Civil Engineering Laboratory, Faculty of Sciences and Techniques, Cadi Ayyad University, 40000 Marrakech, Morocco; Email: m.jaffal@uca.ma

⁴ Geology and Sustainable Mining Institute (GSMI), Mohammed VI Polytechnic University, 43150 Benguerir, Morocco

In the literature, sulpharsenide-arsenide and sulphide minerals showed wide range of composition in different chemical systems such as Co-Ni-Fe, Ni-As-S, Fe-Co-Ni-As-S, Fe-As-S, Ni-Fe-S, Co-Ni-S, Co-Fe-S, Fe-Ni-Co-S and Fe-Ni-As-S. These sulpharsenide-arsenide and sulphide minerals are used usually as indicator of metasomatic fluid temperature ranging from 550 to 650°C, from 400 to 1100°C and at low temperature reaching 100°C. In addition, Ni-rich arsenide and sulpharsenide of Co and Fe are found in various geological settings. These minerals exhibit complex paragenetic and compositional relations, and are commonly associated with Au-rich Ni-Cu sulphide deposit with or without Platinum Group Element.

In the Variscan Belt of the Central Jebilet, corresponding to an intracontinental rift basin, rich in sulphide mineralization, sulpharsenide-arsenide and sulphide minerals were observed in the Ca-amphibole-rich veins developed within plagioclase wehrlite and clinopyroxenite of the tholeiitic mafic-ultramafic Gour Essafra sill. Result of electron-probe microanalysis (EPMA), Wave-length Dispersive Spectrometers (WDS) and Energy Dispersive Spectrometer (EDS) performed on ore-minerals reveals a considerable variation in content of Arsenic (up to 54 Wt. %), Nickel (up to 44 Wt. %), Cobalt (up to 25 Wt. %), sulphur (up to 43 Wt. %), copper (up to 35 Wt. %) and iron (up to 62 Wt. %). Structural formulas determined by atoms per formula unit (apfu) method indicate in order of content, pyrrhotite, nickeline, cobaltite, chalcopyrite, pentlandite gersdorffite and pyrite.

In this paper, we report new Ni-Co-As-S-Cu-Fe minerals explained by nickeline, gersdorffite and cobaltite, pyrrhotite, pentlandite, chalcopyrite and pyrite hosted in the Ca-amphibole-rich veins. This mineral assemblage is discussed for the first time and constitutes a new founding in the Variscan belt of the Central Jebilet Massif of Morocco.

Carbon, Oxygen, and Sulfur isotopic constraints on fluid sources and evolution at the Amensif distal Skarn Zn–Cu (Pb-Ag-Au) deposit, western High Atlas, Morocco

Abdessamad Jinari ^a, El Mostafa Mougouina ^a, Larbi Rddad ^b, Mohamed Idbaroud ^a, Abdelmalek Ouadjou ^c

^a *Laboratory DLGR, Department of Geology, Faculty of Sciences Semlalia M.B.2390, Cadi Ayyad University, 40000 Marrakesh, Morocco.*

^b *Earth and Planetary Division, Department of Physical Sciences, Kingsborough Community College of the City University of New York, USA.*

^c *Groupe MANAGEM, Twin Center, Tour A, Angle Boulevard Zerktouni et Massira Khadra, BP 5199, Casablanca, Morocco.*

Amensif Zn–Cu (Pb-Ag-Au) skarn deposit is located in the northern part of the western High Atlas of Morocco. This deposit hosts 1 Mt of Zn-Cu-Pb metal reserves at 3% Zn, 2% Cu, and 1% Pb. The ore bodies are hosted in the Lower Cambrian carbonates and are structurally controlled. The mineralogy consists of andradite-quartz-epidote-dolomite-calcite-sphalerite-chalcopyrite-pyrite-galena, with minor crystals of barite. The $\delta^{13}\text{C}_{\text{PDB}}$ and $\delta^{18}\text{O}_{\text{SMOW}}$ values of the pre-ore stage and ore stage I dolomite samples range from -10.2 to -2.6‰ and 17.4 to 26.8‰, respectively. The lower $\delta^{18}\text{O}$ value of these dolomites suggests an isotopic exchange between the ore-forming fluids and the carbonate host rock, while the negative $\delta^{13}\text{C}_{\text{PDB}}$ values indicate the interaction between these metalliferous fluids and black shales. The $\delta^{34}\text{S}$ values of sphalerite, chalcopyrite, and pyrite range from 6.4 to 14.4‰. These S isotopic values reveal that sulfur of sulfides has a mixed origin of magmatic sulfur and lower Cambrian carbonate-derived sulfur, in nearly equal proportions. Isotopic and mineralogical data suggest that the hydrothermal-magmatic fluids exsolved from a hidden Permian magma or the nearby Azegour magma, flowing through available faults and fractures. During their ascent to the loci of deposition, these ore-forming fluids interacted with the Lower Cambrian carbonates and black shales, triggering the precipitation of sulfide ores. Additionally, mineralogical data also suggest that these hydrothermal-magmatic fluids mixed with an external fluid of unidentified origin, which also contributed to ore precipitation.

The role of the Mesozoic magmatic rocks in geo-tourism development: Case study from central High Atlas mountains

Kchikach N¹, Ibouh H.², Benali A.¹, and Kchikach A.²

¹*Cadi Ayyad University, Geomorphology, Environment and Society Laboratory, Marrakech, Morocco*

²*Laboratory of Geo resources, Geo environment and civil engineering (L3G), Faculty of Sciences and Techniques Gueliz, Cadi Ayyad University, A. Elkhatabi Bd, BO 549, 40000 Marrakesh, Morocco*

This work is a popularization of scientific geological information for the benefit of tourists who are passionate by mountains and their formation. In this work we take as the case study, the central High Atlas of Morocco.

The central High Atlas is a mountain chain oriented N70 that divides Morocco into two large parts: northern Morocco and the south, including the Moroccan Sahara. It is a so-called intracontinental mountain range, i.e. formed within a continent, as most mountain ranges are formed at the edge of tectonic plates by subduction, like the Andes in America (a tectonic plate that plunges beneath a continental plate), or by collision (two continents colliding head-on), like the Himalaya mountains in India.

The geological history of the Central High Atlas deserves to be simplified for tourists. Its formation began as a sedimentation basin at the same time as the Atlantic Ocean opening. In geology, this phenomenon is known as a "rift", i.e. a collapse of the continental crust and the formation of a large depression accompanied by a thinning of the continental crust. This thinning can reach its maximum and lead to a phenomenon known as "continental break-up", with a tearing of the crust and the upwelling of mantle rocks in the form of basalt. This phenomenon took place during the Triassic (a geological period that corresponds to around 200 million years ago). This rupture is expressed by the upwelling of basalts in the form of green flows that can be seen today in several regions of the High Atlas. These basalts are known by their "geodes". These later correspond to air bubbles trapped in the basalt and invaded by late basaltic magma fluids. These fluids can deposit clear and self-morphing quartz crystals. Mineral and fossil sellers, ca, sometimes, traffic in these crystals, by coloring them mauve or red to attract the tourists attention.

Another magmatic phenomenon in the central High Atlas dates back to the Upper Jurassic (around - 145 million years ago) and is responsible for the establishment of subvolcanic intrusions of the same age. These intrusions are located in anticline wrinkles and present a multitude of magmatic rocks ranging from troctolic rock (dark magmatic rock), diorites (light-colored mottled magmatic rock) and syenitic rocks (light to beige rock). The latter are rocks that offer the possibility of concentrations of crystals such as apatite. Apatite is phosphorus-rich minerals. These minerals are the main source of magmatic phosphates. For info 12% of the world's phosphate production is in the form of this magmatic mineral. The most important example of this type of phosphate deposit is located in Russia (Kola Peninsula).

So, in conclusion, of this all the information cited above, can give an example of the really link between, mountains and all the geological aspect on the surface earth to vulgarized scientific, information scientist and to our industry and to all what use every in our live. This can be in our opinion a great motivation for a geotourism and all the Moroccan mountains.

SEBT BRIKIINE MASSIF: AN EXAMPLE OF ACID-BASIC INTERACTION FROM HERCYNIAN GRANITOIDS (SOUTHERN REHAMNA, MOROCCO)

Kholaiq Mariame¹, El Hachimi Hind¹, Ezzouhairi Hassan ¹, Rahimi Abdelmejid ¹, Dias Rui ^{2,3}, Saber Najib⁴

1 Geodynamics and Geomatics Laboratory, Faculty of Sciences, Chouaib Doukkali University, P.B20, 24000, El Jadida, Morocco. e-mail: kholaiq.mariame@gmail.com

2 Earth Sciences Institute (ICT), Pole of the University of Évora, Rua Romão Ramalho, n° 59, 7000-671 Évora, Portugal;

3 Dep. Geociências, Escola de Ciências e Tecnologia, Univ. Évora (ECTUE), Largo dos Colegiais, 2-Apartado 94, 7002-554 Évora, Portugal

4 Ecole Supérieure de Technologie - Sidi Bennour(ESTSB), Chouaib Doukkali University,, P.B20, 24000, El Jadida, Morocco.

The Hercynian massif of Sebt Brikiine extends on area of about 250 km² and is essentially composed of porphyroid granite, most often leucocrate. It has a more or less circular shape and constitutes a topographic depression west of Benguerir.

It is a calco-alkaline granite (rich in biotite) with a monzonitic tendency, locally containing basic enclaves. Thus, the various petrographic facies are organized in two main units of unequal importance and whose mixture gave hybrid rocks. It is about the basic unit recognizable in the outcrop by its melanocratic aspect and outcropping in mafic micrograined enclaves and the acidic unit occupying more than 95% of the volume of the massif.

Field observations, petrographic and mineralogical analysis have shown that the basic unit, formed essentially by enclaves, contain feldspar phenocrysts and some quartz ocelles surrounded sometimes by discontinuous biotite border. Therefore, the links between enclaves and host rocks and the presence of hybrid rocks militate in favor of a synchronous setting of an acidic liquid and another basic liquid relatively solidified and fragmented to the centimetric scale. This would testify to a simultaneous intervention of the two liquids of different origins (crustal and mantle) in the genesis of this pluton and whose contact of the two liquids is probably realized in the deep parts of the crust.

The results of this study allowed considering, for the first time, the Hercynian granitic massif of Sebt Brikiine as an acid-base association resulting from an unfinished magmatic mixture process.

Where is the western boundary of Bering plate?

Lebedev I.E.¹; Pasenko A.M.¹

¹: Institute of Physics of the Earth RAS (Moscow, Russia)

To date, two models of the formation of the so-called Bering Plate are actively discussed. The first one suggest extrusion of Alaska under the influence of the Pacific plate. An array of accumulated data in support of this theory is presented in (Redfield et al., 2007). According to this model, the eastern part of the Bering Plate is a collage of terranes extruded in a northwesterly direction parallel to the British Columbia margin. As a result of this movement, western part of potential Bering plate could experience counterclockwise rotation. Another model is presented in (Mackey et al., 1997), where seismic data also confirms the counterclockwise rotation of the rigid Bering Plate. However, these and similar models are primarily based on data collected to the east of the Bering Strait, while to the western part there is clearly insufficient data. This fact causes inconsistencies in the western boundary of the Bering Plate through the mainland Chukotka, Karyak, and Kamchatka (Mackey et al., 1997; Redfield et al., 2007). According to some models, boarder is drawn even under the basin of the Bering Strait (Chekhovich and Palandzhyan, 2021). In addition, the discrepancies are supported by the low seismicity of the mainland of the North-East of Russia, which does not allow to clearly draw a possible border today.

One of the methods that could estimate possible existence of the Bering Plate in the geological past is the paleomagnetic method. It does not allow us to reliably characterize potential movements within the first hundreds of kilometers. If we can establish the shift in large amplitudes, we can most likely approve the existence of small plates, such as the Bering Sea. To solve this goal, we need the most reliable and accurate paleomagnetic data based on the objects east of the Bering strait. Moreover, the age of the rocks should be younger than the completion of the formation of the South Anyui Suture (early Early Cretaceous), which was formed as a result of the closure of the Anyui Ocean. Also, it is desirable that the age of object as old as possible so that during this time the maximum displacement can accumulate and it becomes visible for paleomagnetic method. An ideal object for such a study is one of the largest Phanerozoic subduction-related igneous provinces: Cretaceous Okhotsk–Chukotka volcanic belt (OCVB). In addition, it is an excellent object for any paleomagnetic research, and its northern part overlaps the above-described boundary of the Bering Plate.

We sampled in detail two objects within the OCVB, which are located on opposite sides of the potential boundary of Bering plate, but located within the same elder Chukotka-Alaska microcontinent. The first one Kupol location is placed in Western Chukotka to the east of the large gold-silver deposit of the same name. The last U-Pb and Ar⁴⁰/Ar³⁹ isotope data allowed us to limit the age of our paleomagnetic sections to 88–84 Ma (Tikhomirov et al., 2021a). Paleomagnetic data for this location published in (Lhuillier et al., 2023 in press). The second location Valunistoe is placed in Central Chukotka in close to the gold-silver ore deposit of the same name. Our new isotope-geochronological data indicate a significantly younger age of formation of the studied volcanic rocks (76-71 Ma) than previously thought (Tikhomirov et al., 2021b). Kupol is located most likely to the west of the border with the Bering Sea Plate, and the Valunistoe is almost on the border according to (Mackey et al., 1997). For both locations, paleomagnetic poles were calculated, the primary remanence is verified by positive fold tests and electron microscopic studies.

The obtained paleomagnetic poles have a significant difference between them ($7.1^\circ \pm 6.0^\circ$). The obtained paleomagnetic data indicate the presence of clockwise rotation of central Chukotka (Valunistoye) relative to its western part (Kupol). This statement is also supported by the presence of a

similar rotation relative to neighboring large Eurasia, for which the APWP is well known (Torsvik et al., 2012). The observed displacement of Central Chukotka relative to its western part and Eurasia is similar to the expected rotation of the Bering Plate proposed by models (Redfield et al., 2007; Mackey et al., 1997). This may indicate that the Valunistoe location may belong to the Bering Plate, consequently its western boundary must lie somewhere to the west of this location. There are no large shear zones between the Kupol and Valunistoe on Chukotka which this displacement could occur. The only possible candidate for such a shear zone the Amguemo-Kanchalan fault zone, which lies in the immediate vicinity of the Valunistoe ore deposit. To date, the scales of this zone does not seem to be able to explain such a large movement, however, the degree of its study leaves much to be desired.

The research was supported by RSF Project №23-17-00112

Chekhovich, V.D., Palandzhyan, S.A., 2021. Geodynamics of the Active Margin of Northeast Asia in the Late Cretaceous–Paleogene. Geotecton. 55, 516–530. <https://doi.org/10.1134/S0016852121040051>

Mackey, K.G., Fujita, K., Gunbina, L.V., Kovalev, V.N., Imaev, V.S., Koz'min, B.M., Imaeva, L.P., 1997. Seismicity of the Bering Strait region: Evidence for a Bering block. Geol 25, 979. [https://doi.org/10.1130/0091-7613\(1997\)025<0979:SOTBSR>2.3.CO;2](https://doi.org/10.1130/0091-7613(1997)025<0979:SOTBSR>2.3.CO;2)

Redfield, T.F., Scholl, D.W., Fitzgerald, P.G., Beck, M.E., 2007. Escape tectonics and the extrusion of Alaska: Past, present, and future. Geol 35, 1039. <https://doi.org/10.1130/G23799A.1>

Tikhomirov, P.L., Lebedev, I.E., Lhuillier, F.J.L., Pavlov, V.E., 2021a. Stratigraphy of the Okhotsk–Chukotka Belt in the Headwaters of the Malyi Anyui River (the Vicinity of Kupol Deposit): U–Pb and 40Ar/39Ar Age Data. Dokl. Earth Sc. 501, 1059–1064. <https://doi.org/10.1134/S1028334X2112014X>

Tikhomirov, P.L., Lebedev, I.E., Pasenko, A.M., Lhuillier, F.J.L., Alekseev, D.V., Pavlov, V.E., 2021b. The “Upper Basalts” of the East Chukotka Segment of Okhotsk–Chukotka Belt: the Along Strike Migration of Volcanic Activity or the Overprint by Later Magmatic Event? Dokl. Earth Sc. 501, 1038–1042. <https://doi.org/10.1134/S1028334X21120151>

Torsvik, T.H., Van der Voo, R., Preeden, U., Mac Niocaill, C., Steinberger, B., Doubrovine, P.V., van Hinsbergen, D.J.J., Domeier, M., Gaina, C., Tohver, E., Meert, J.G., McCausland, P.J.A., Cocks, L.R.M., 2012. Phanerozoic polar wander, palaeogeography and dynamics. Earth-Science Reviews 114, 325–368. <https://doi.org/10.1016/j.earscirev.2012.06.007>

The Tidili Zone, a pan-African collision junction marked by the interaction of a complex tectonic force system.

Lerhris I.E.^{1*}, Admou H.¹, Alansari A.¹, Ibouh H.², Chaib L.¹, Admou S.³

¹ Faculty of Sciences Semlalia, Prince My Abdellah Avenue, P.O. Box 2390, 40000, Marrakech, Morocco.

² Faculty of Science and Technology, P.O. Box 549, Av. Abdelkarim Elkhattabi, Gueliz Marrakech.

³ Managem Mining Company (SA), Twin Center, Casablanca, Morocco

The Tidili region is located between the central-western High Atlas to the north and the Precambrian suture of the Anti-Atlas in the south. From a geological perspective, this region is caught between two distinct domains: The Pan-African and Paleozoic domain to the north, represented by the Ouzellarh promontory of the High Atlas, and the Proterozoic domain of the Pan-African Siroua massif to the south.

The area under study represents a significant junction and collision point between these two domains, it is a dynamic space where the boundaries of these two domains intersect and interact, and It is characterized by several criteria:

- It forms a depression and basins where a set of sedimentary and magmatic formations have been deposited and established.
- The geometry of the magmatic bodies, especially the granite, exhibits crescent-shaped structures, attesting to a collision zone.
- The study area is characterized by a complex system of Pan-African, Paleozoic, and Atlasic faults and tectonic structures.
- This zone contains a set of magmatic markers that are the consequence of Pan-African subduction-collision processes in the Siroua massif.

The Ouzellarh promontory to the north (in the High Atlas) is a continuation of the granitic complex of Askaoun and Ida Ouilloun to the south of Siroua. It would form the northern margin of the Anti-Atlas, bordered to the south by a major fault line within the Anti-Atlas. This fault delineates two distinct structural domains during the Pan-African orogeny: a stable southwest zone (Eburnian Anti-Atlas) corresponding to the West African craton, and a mobile Anti-Atlas zone to the north.

Structural studies reveal brittle deformation characterized by four families of faults oriented in the N-S, E-W, NE-SW, and NNW-SSE directions, affecting all formations in the study area. The current structural configuration of this domain is the result of the combined effects of the Pan-African, Hercynian, and Alpine orogenic cycles. During the Cambrian period, a relaxation phase occurred while the region was buried under deep Paleozoic sedimentary basins.

The Tidili region, situated between the South Atlas fault and the major Anti-Atlas fault, suggests that it has been influenced by the intersection and branching of these two important structural lineaments, the Anti-Atlas lineament to the south and the Paleozoic and Atlas lineament to the north.

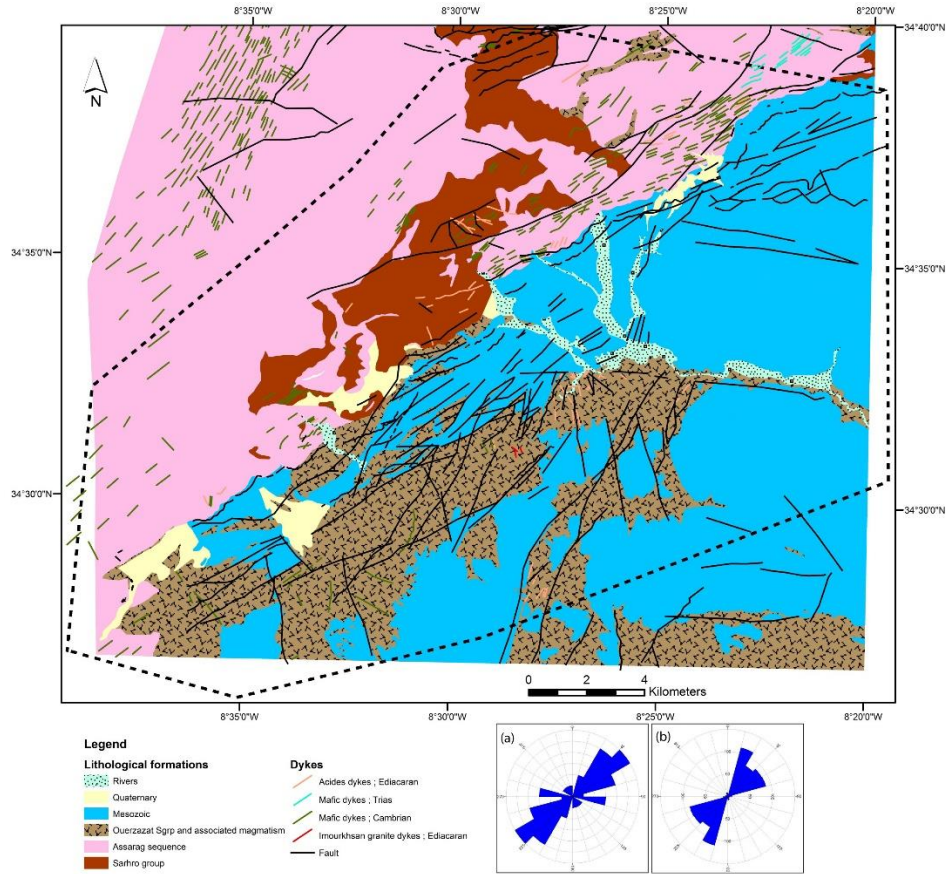


Figure 1: simple map of the area showing major geological groups and intrusions. (a) directional rosette of geological fractures. (b) rosette of intracambrian dyke swarm directions.

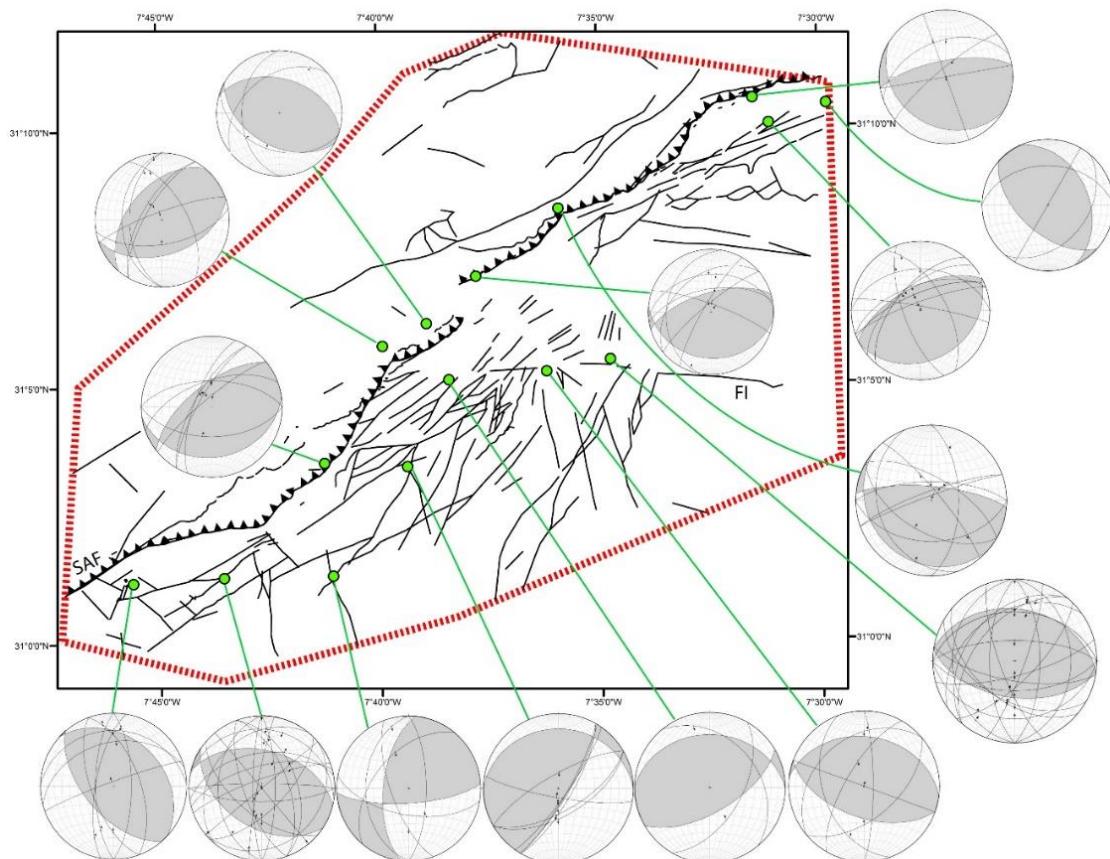


Figure 2: Fault map featuring stereograms of focal mechanism representations.

CONTRIBUTION TO THE PETROGEOCHEMICAL, STRUCTURAL AND METALLOGENIC STUDY OF COBALT MINERALISATION IN THE BOU AZZER EST-AGHBAR MINING DISTRICT (BOU AZZER-EL GRAARA BUTTONHOLE, CENTRAL ANTI-ATLAS, MOROCCO)

Lmahfoudi Yassine^{1,2,*}, Ouali Houssa¹, Ilmen Said³, Hajjar Zaineb⁴, El-Massoudy Ali², Sapor Laurent², Zouhair Mohamed², Maacha Lhou²,

¹ *Department of Geology, Faculty of Sciences, Moulay Ismail University, Meknes, Morocco*
y.lmahfoudi@managemgroup.com:

² *Managem Group, Twin Center, 20 100 Casablanca, Morocco*

³ *Polydisciplinarity Faculty of Ouarzazate, Ibn Zohr University, Avenue Moulay Ettahar Ben Abdulkarim, BP. 638, 45000 Ouarzazate, Morocco*

⁴ *Geoscience, Water and Environment Laboratory, Faculty of Sciences, Mohammed V University in Rabat, Avenue Ibn Batouta, Rabat 10100, Morocco*

The studied area is located between the Bou Azzer East and Aghbar deposits. It is a vast area of about 7 km in the ENE-WSW direction and 2 km in N-S direction. In this barren area outcrop volcano-sedimentary rocks attributed to the Ouarzazate group composed by volcanic rocks (rhyolite, dacite, ignimbrite ...) interstratified with chaotic breccia and polygenic conglomerates, overlain by the Adoudou formation through an angular unconformity. The whole is intersected by a N-S, NE-SW and E-W swarm of quartz and quartz-carbonate veins with iron oxides and/or manganese. These faults are similar to those mineralised in neighbouring deposits.

This area is marked by the absence at outcrop of serpentinite, which are considered to be the source of cobalt mineralisation. The drill hole made in the studied area intersected quartz diorite intrusions and serpentinite. Therefore, since drilling hole company realized by the geological survey of the CTT Bou Azzer Mine and geophysical data, the continuity of the serpentine massif at depth under the Ediacarian cover has been highlighted as well, the presence of Co-Fe arseniferous mineralisation for the first time in this area. The main objectives of this work is identify drill target positions for multi-commodity mineralization, carry out a detailed study of newly discovered cobalt mineralisation and characterise the conditions of its genesis and associated hydrothermal alteration

Geochemistry, Magma Characteristics, and New Age Dating: A case study of volcanic rocks from the Amensif-Tnirt district, Western High Atlas, Morocco

Loudaoued I.^{1,2}, Touil A.², Aysal N.³, Aissa M.¹, Ouadjou A.⁴

¹ Laboratory of Mineral and Energy Resources Studies, Faculty of Sciences, Moulay Ismail University, M.B. 11201, Zitoune, Meknes 50070, Morocco, loudaoued@gmail.com, mohamedaiassa@gmail.com).

² Lab. L3G, Faculty of Sciences and Techniques Gueliz, B.P. 549, 40010, Marrakech, Morocco a.touil@uca.ma

³ İstanbul University-Cerrahpasa, Department of geological engineering, Büyükçekmece, İstanbul, Türkiye aysal@iuc.edu.tr, iyilmaz@iuc.edu.tr).

⁴ MANAGEM group, Twin Center, Tour A, Angle Zerktouni boulevard and Massira Khadra, BP 5199, Casablanca, Morocco, a.ouadjou@managemgroup.com

The Western High Atlas Mountains include mafic, intermediate and felsic volcanic-subvolcanic intrusive rocks, representing a result of magmatism related to “Cambrian rift” during the Lower Cambrian and hercynian event.

The lithostratigraphy of the Amensif-Tnirt area consists of two units of Lower Cambrian age, the lower-unit mainly pelitic with intercalation of volcanic and volcano-carbonate in Tnirt and only volcano-carbonate rocks in Amensif area; the upper unit in both areas predominantly consists of a monotonous shale-sandstone formation, all of which unconformably overlie the lower unit.

The studied magmatic rocks in the Amensif-Tnirt area are divided into three main groups: microgabbros (SiO₂ 48.31 to 53.06 wt.%), andesites to dacites (SiO₂ 59.16 to 67.38 wt.%), and rhyolites (SiO₂ 76.39 to 79.65 wt.%). The mafic rocks correspond to microgabbros with high iron and titanium contents, varying between (10.98-12.42 wt.%) and (1.98-2.12 wt.%), respectively, and they exhibit FeO/MgO (1.65 to 1.90), La/Yb (9.09 to 11.60) and Nb/Zr (0.03 to 0.04) ratios, indicating an intracontinental tholeiite signature. The Nb/Yb and Zr/Y ratios ranging between 0.36 to 0.52 and 12.76 to 13.69, respectively suggest their derivation from an enriched mantle source during the opening of the Rheic ocean along the NW edge of Gondwana. The mafic rocks may be interpreted as the mixtures of melts derived from two contrasting mantle sources: (1) a garnet-bearing clinopyroxenitic ultramafic source and (2) an ultramafic source composed of spinel and peridotite. Petrographic and geochemical data indicate that mafic magmatism in the Amensif-Tnirt region may be the equivalent of the first Cambrian volcanic episode recorded in the Western High Atlas.

The intermediate and felsic rocks correspond to andesite-dacite and rhyolite with TiO₂ contents and FeO/MgO ratios ranging from 0.09 to 1.36 wt.% and 1.32 to 4.69, respectively. These values suggest their calc-alkaline affinities setting up during a compressive context. The youngest ²⁰⁶Pb/²³⁸U ages for intermediate rocks are 290.29 ± 4.68 and 291.27 ± 4.31 Ma, while the youngest felsic rocks yield a concordia age at 272.83 ± 0.73 Ma (MSWD = 0.25). Intermediate rocks are chronologically correlated to the Permian volcanic activities recorded in Central Morocco (Tiddas, Khenifra, Chougrane...) whereas felsic activity is correlated to the Permian Azegour granite from the Western High Atlas.

Maram Corona, Venus: Tectonic History and Influence of Parga Chasmata Faulting

K. Mghazli¹, H. El Bilali^{2,3}, R.E. Ernst^{2,3}, K.L. Buchan⁴, N. Youbi¹

¹Department of Geology, Faculty of Sciences-Semlalia, Cadi Ayyad University, Marrakesh, Morocco; mghazli.k@gmail.com.

²Department of Earth Sciences, Carleton University, Ottawa, Ontario, Canada; hafidaelbilali@cunet.carleton.ca; richard.ernst@ernstgeosciences.com, ³Faculty of Geology and Geography, Tomsk State University, Tomsk, Russia
a. ⁴273 Fifth Ave., Ottawa, Canada.

Introduction: The spatial association between coronae and chasmata (rift zones) has been extensively discussed, but genetic relationships remain less clear (Hamilton & Stofan 1996; Graff et al., 2018)

Maram Corona: We selected a study area along Parga Chasmata about 2000 km SE from the centre of Atla Regio which had previous quadrangle ---scale (1:5,000,000) mapping (Brian et al., 2005). We focus on the large Maram corona. In our previous LPSC 2022 abstract (Mghazli et al., 2022) we focused on the graben-fissure systems of Maram corona and vicinity, and their interpretation as dyke swarms. In the present contribution we consider topographic evidence for major faulting affecting Maram corona. In this abstract, we build on the observation in (Brian et al., 2005) that Maram corona was affected by rift tectonics of Parga Chasmata.

Stages of Faulting Affecting Maram Corona:

Numerous fault scarps are evident from the topography (see (Brian et al., 2005), and these can be mostly interpreted as normal faults associated with the rift-zone. A preliminary history of the tectonics affecting Maram corona is offered below in 6 stages.

- **Stage 1:** The NW trending fault north of Maram corona was active prior to corona formation since this fault seems truncated by the Stage 3 faults along the northern margin of Maram corona.
- **Stage 2:** An important observation is that the plateau of the corona is flooded by lava flows, which did not flow off the northern edge despite its current higher elevation. Also, as noted by (Brian et al., 2005), the floor of Maram corona is tilted southward, and yet the flows on the plateau do not seem to have preferentially flowed south. Therefore, the plateau of Maram corona must have been flat at the time of lava flooding and was subsequently tectonically tilted (see Stage 3).
- **Stage 3:** During this stage, Maram corona (and its plateau) was tilted at an angle of 0.5 degrees to the south (consistent with the interpretation of (Brian et al., 2005). It is assumed that this was associated with normal faulting.
- **Stage 4:** Major NNW trending faults parallel the east and west sides of Maram, and in particular the fault on the east side can be traced in the topography to the SSE for about 1000 km. These faults are associated with dip slip movement,
- **Stage 5:** On the eastern side of Maram, additional faulting has caused a triangular wedge of extension (see direction of arrows).
- **Stage 6:** This is the final stage where the uplifted plateau seems to break along a WNW- ESE fault.

References:

- Brian, A. W., Stofan, E. R., & Guest, J. (2005). *Geologic Map of the Taussig Quadrangle (V-39)*
- Graff, J. R., Ernst, R. E., & Samson, C. (2018). *Evidence for triple-junction rifting focussed on local magmatic centres along Parga Chasma, Venus. Icarus, 306, 122-138.*
- Hamilton, V. E., & Stofan, E. R. (1996). *The geomorphology and evolution of Hecate Chasma, Venus. Icarus, 121(1), 171-194. Venus. US Department of the Interior, US Geological Survey.*
- Mghazli, K., El Bilali, H., Ernst, R., & Youbi, N. (2022). *Dyke Swarms of the Maram Corona Area, Parga Chasmata, SE of Atla Regio, Venus. LPI Contributions, 2678, 1971.*

Paleobiogeographic aspects thought Moroccan Lower–Middle Cambrian small shelly fossils from the High Atlas, Morocco.

K. Mghazli¹, N. Lazreq¹, G. Geyer², Ed Landing³, Moulay Ahmed Boumehdi¹, N. Youbi¹

¹ Department of Geology, Faculty of Sciences Semlalia, Cadi Ayyad University Marrakech, Morocco

² Institut für Geographie und Geologie, Bayerische Julius-Maximilians-Universität Würzburg, German ³ New York state Museum, 222 Madison Avenue, Albany, NY, U.S.A

The Brèche à *Micmacca* Member at section Le IX in the Lemdad syncline, located in the southern part of the High Atlas in Morocco, contains a diverse range of helcionelloid molluscs, probable polychaetes, and sclerites from other metazoan groups. This collection, consisting of over 3,000 specimens, complements previously described faunal assemblages from the same interval.

The newly discovered material comprises 21 species belonging to 13 genera. Among these species, there are 15 helcionelloid species (or forms), one presumed orthothecid hyolith, and five species of pseudopelagielliform organisms. These findings provide insights into the relatively limited changes in biodiversity observed during the *Morocconus notabilis* and *Ornamentaspis frequens* trilobite biozones in the Souss Basin.

Notably, the discovery of *Eotebenna* cf. *papilio* Runnegar and Jell 1976 represents the first occurrence of this genus in Africa and the West Gondwana region. The study also proposes the existence of new species including *Dorispira? lemdadensis* n. sp., *Yochelcionella longituba* n. sp., and *Yochelcionella gracilituba* n. sp. (Mghazli et al., 2023).

The assemblages contain forms that show similarities to contemporaneous faunas found in the Siberian Platform, North China, Australia, and Laurentia (SNAL). These findings contribute to interregional and continental biostratigraphic correlation and enhance our understanding of paleogeographic connections

Reference:

Mghazli, K., Lazreq, N., Geyer, G., Landing, E., Boumehdi, M. A., & Youbi, N. (2023). Cambrian microfossils from the High Atlas, Morocco: Taxonomic, biostratigraphic, palaeobiogeographic, and depositional significance of the Brèche à *Micmacca* limestone beds. *Journal of African Earth Sciences*, 197, 104751.

The Great Ahmeyim Dyke and its satellite mafic dykes. Remote sensing, geophysics, geochemistry and geodynamic implications in the framework of the Tasiast-Tijirit Terrane (Rgueibat Shield, Northern Mauritania)

Moussa Hamath Ba^{a b}, Khalidou Lo^a, Nassreddine Youbi^{b d}, Mohammed Jaffal^c Hassan Ibouh^c.

^a Department of Geology, Faculty of Sciences and Technologies, University of Nouakchott Al Aasriya, Mauritania; moussabah85@gmail.com

^b Department of Geology, Faculty of Sciences-Semlalia, Cadi Ayyad University, Prince Moulay Abdellah Boulevard, P.O. Box 2390, Marrakech, 40 000, Morocco

^c Department of Geology, Georessources, Geoenvironment and Civil Engineering (L3G) Laboratory, Faculty of Sciences and Techniques, Cadi Ayyad University, Abdelkarim Al Khattabi Boulevard, P.O. Box 549, Marrakech, 40000, Morocco

^d Departamento de Geologia, Faculdade de Ciências and Instituto Dom Luís, Universidade de Lisboa, Edifício C6, Campo Grande, 1749-016, Lisboa, Portugal

Located in the North-West of the Rgueibat shield (or Reguibat shield), which is known for its great lithological and structural diversity, the Archean Terrane of Tasiast-Tijirit is crossed by several generations of mafic dykes (with different ages, trends, thicknesses and chemical compositions), crosscutting both the granite-gneisses and the supracrustal rocks. These dykes, usually result from periods of extension associated with ascent of large volumes of mantle melts, and are considered vestiges of the Large Igneous Provinces (LIPs) of the Precambrian. They are an essential tool to better retrace the geological events that affected the Archean basement.

The aim of this work is to characterize the petrogenesis and geodynamic evolution of mafic dykes, based on petrology, geochemical, geophysical and remote sensing studies.

The approach uses processed Landsat 8 and Google EarthTM satellite images, as well as field observations, allowing mapping of the distribution of the mafic dykes of the Archean of the Rgueibat shield. The geometric and statistical analysis resulting from this study globally shows four major trends (each interpreted to represent a different swarm): NE-SW to NNE-SSW, NW-SE to WNW-ESE, E-W to ENE-WSW and N-S. The chronological model that has been established, assumes that the trend dykes NE-SW to NNE-SSW form the most important generation.

The joint analysis of high resolution airborne geophysical data of magnetism and gamma-ray spectrometry produced a detailed map, in which the various magnetic data treatments allowed accurate mapping of the mafic dyke swarms, especially those hidden by sand dunes and younger sedimentary rocks. The use of gamma-ray spectrometry data has also resulted in the delineation of potassium-enriched areas that may correspond to potassic alteration that may be associated with hydrothermal activity and ore deposition.

Petrographic study of these mafic dykes indicates that they are mainly composed of gabbros, gabbrodiorites, gabbronorites, dolerites and gabbro-dolerites. These lithologies have homogeneous mineral paragenesis. Primary mineralogy is represented by plagioclase, hornblende, quartz, apatite, ilmenite, olivine and biotite. Secondary paragenesis is dominated by chlorite, actinolite, sericite, albite, sphene and opaque oxides, mainly from the processes of alteration of primary minerals.

Geochemically, these rocks have basaltic to andesitic compositions of a sub-alkaline nature. Different geotectonic discrimination diagrams of trace elements and Rare Earths Element (REEs) reveal basaltic suites of continental LIP that originate from a source of mafic magma that was enriched in light rare earths (LREE), probably from a contamination by lithospheric mantle that had been metasomatized by earlier subduction processes.

Petrogenesis of the Bakoudou TTGs and high-K biotite granites, southern Gabon

Nazaire Nzaou Mabika¹, Amina Wafik¹, Abdellah Boushaba², Ali Saquaque³, Lhou Maacha³, Gharrabi Mohamed³, Benyounes Maamar³

¹ Cadi Ayyad University, Marrakech, Morocco

² Sidi Mohamed Ben Abdellah University, Fes, Morocco

³ Université du Québec à Chicoutimi, Chicoutimi, Canada

⁴ Managem Mining Company (SA), Casablanca, Morocco

The Precambrian basement of western Central Africa is represented by the Congo Craton, which covers the Gabon-Democratic Republic of Congo border and extends to the Cameroon-Gabon border (Nédélec et al., 1990). This basement is composed of Archean cratons welded together by Meso- and Paleoproterozoic belts (De Wit and Linol, 2015) and is mainly represented on the Gabonese territory by the Chaillu Massif and the North Gabon Massif (Thiéblemont et al., 2009). The Chaillu Massif was affected by the Eburnian orogeny, which was responsible for the emplacement of the Paleoproterozoic Booue, Lastrouville, Okondja and Franceville basins (Pambo et al., 2006). These basins are discordant on the Archean Chaillu Massif (Thiéblemont et al., 2009).

Primary gold mineralization is rare, and the main representative is the Bakoudou gold deposit (Bouton et al., 2009; Thiéblemont et al., 2009). It is located in southeastern Gabon, in Haut-Ogooué Province, more precisely on the edge of the Chaillu Massif, approximately 100 km southwest of the Franceville basin (Bouton et al., 2009; Thiéblemont et al., 2009). The gold mineralization occurs as quartz veins hosted in the gray granitoids of the Chaillu Massif (Thiéblemont et al., 2009)

These granitoids of the Bakoudou deposit are subdivided into two main groups: TTGs and porphyritic biotite granites (Nzaou Mabika et al., 2020). The TTGs show geochemical characteristics similar to those of other TTGs worldwide, such as high Al₂O₃ (13.49–18.93 wt%) and Na₂O (3.27–4.66 wt%) and low K₂O (1.01–1.98 wt%), with low K/Na (0.15–0.32) ratios. Their Mg# (Mg/(Mg + Fe)*100) values vary from 34.81 to 50.76, with low to moderate Nb/Ta and Zr/Sm ratios (7.03–23.43 and 19.13–75.25, respectively). They are characterized by moderate (La/Yb)_N (6.70–41.71) and Sr/Y (20.80–72.13) ratios similar to those of adakites, negative Nb, Ta and Ti anomalies and LREE-enriched and HREE-depleted patterns, without significant Eu anomalies (Eu/Eu* = 0.93–1.11, average = 1.00). These geochemical characteristics suggest that the TTG rocks were formed by partial melting of hydrous basaltic crust, such as garnet-rich amphibolite (Nzaou Mabika et al., 2020). The porphyritic biotite granites show high-K calc-alkaline affinity. They are characterized by high SiO₂ (71.01–74.86 wt%) and K₂O (3.29–4.92 wt%) but relatively low MgO (0.38–0.92 wt%), with Mg# values varying between 31.78 and 40.27. The rocks show low to moderate Sr/Y (13.75–26.66) ratios and LREE-enriched and HREE-depleted patterns, with negative Eu anomalies (Eu/Eu* = 0.36–0.58, average = 0.47). These geochemical features indicate that the porphyritic biotite granites originated from partial melting of TTG lithologies (Nzaou Mabika et al., 2020).

References

- Bouton, P., Thiéblemont, D., Gouin, J., Cocherie, A., Guerrot, C., Tegye, M., Préat, A., Simo Ndounze, S., Moussavou, M., 2009. Notice explicative de la carte géologique de la République du Gabon à 1/200 000, feuille Franceville-Boumango. DGMG 1, 1–79.
- De Wit, M.J., Linol, B., 2015. Precambrian Basement of the Congo Basin and its Flanking Terrains. *Geology and Resource Potential of the Congo Basin*. pp. 19–37.
- Nédélec, A., Nsifa, E.N., Martin, H., 1990. Major and trace element geochemistry of the Archaean Ntem plutonic complex (South Cameroon): petrogenesis and crustal evolution. *Precambrian Res.* 47, 35–50.
- Nzaou Mabika, N., Gaboury, D., Wafik, A., Boushaba, A., Moukadiri, A., El Arbaoui, A., Saquaque, A., Gharrabi, M., Maamar, B., & Maacha, L., 2020. Petrogenesis of the Bakoudou TTGs and high-K biotite granites and associated gold mineralization, southern Gabon: An Archean example of a porphyry–epithermal transitional gold system. *Journal of African Earth Sciences*, 168, 103843.
- Pambo, F., Guiraud, M., Quesne, D., Gauthier-Lafaye, F., Azzibrouck, G., Lang, J., 2006. The Proterozoic Franceville Basin (S.E. Gabon): an example of interaction between marine sedimentation and extensional faulting. *Afr. Geosci. Rev.* 13, 77–106.
- Thiéblemont, D., Castaing, C., Billa, M., Bouton, P., Préat, A., 2009. Notice explicative de la Carte géologique et des Ressources minérales de la République Gabonaise à 1/ 1000000: Editions DGMG - Ministère des Mines, du Pétrole, des Hydrocarbures. pp. 384p Libreville.

THE IRON FORMATIONS OF THE SKOURAZ SEDIMENTARY AND VOLCANO-SEDIMENTARY COMPLEX, BOU AZZER INLIER, CENTRAL ANTI-ATLAS, MOROCCO.

Nahla Ntarmouchant¹, Amina Wafik¹, Hassan Admou¹

¹ DLGR Laboratory, URAC 43, Faculty of Sciences Semlalia, Cadi Ayyad University, Marrakech, Morocco

This work focuses on the iron formations of the Skouraz sedimentary and volcano-sedimentary complex, which is a NW-SE-oriented transition zone located between the Bou Azzer Pan-African ophiolite belt to the north and the Assif n'Bougamane-Takroumt plutonic-metamorphic arc to the south. The iron formations (the subject of this study) are predominantly dark outcrops associated with grayish facies of gneiss and mica schist. These iron ore deposits are very dense rocks that outcrop in two main forms:

-They appear as highly folded and deformed rocks, rich in metallic oligist, at the site of a fresh fracture. The oligist schist formations consist of rhythmically interbedded bands, alternating with basalts and volcano-sedimentary tuffs, and are often associated with thrust zones. A few meters northeast of these thrust fronts, these formations exhibit asymmetric (dissymmetric) folds, characterized by the alternation of carbonate (light), siliceous (white), and oligist schist (dark) layers, indicating a southwest vergence. The deformation intensity amplifies in the close proximity of the thrust fronts, leading to ductile deformation of the iron formation. This process gives rise to a intricate folding pattern that incorporates silica veins, carbonate deposits, layers of oligist schist, mica schist, and gneiss. The lithostratigraphic arrangement observed within this iron formation resembles that of the Um Nar BIFs in the central eastern desert of Egypt (A.K. El-Shazly a, K.I. Khalil, 2014).

-They appear as metric-scale mineralized veins, non-folded, with a N135 direction, intruding fractures within the basalts/diorites and metasedimentary formations. These undeformed veins are located far from the thrust fronts. They exhibit a milky white silica gangue associated with reddish carbonates (possibly a second gangue) rich in iron, which disappears towards the apex, giving way to massive oligist deposits. These fractures show a late sinistral strike-slip movement.

This transitional zone, located between two different geodynamic contexts, is therefore a key point in understanding the emplacement mode of these iron formations. Indeed, these formations are not only indicators of paleoclimate but also reveal the geodynamic contexts with which they are associated (Bekker 2020, 2010; Klein 2005).

The occurrence of boninite as product of subduction during the Rhyacian collage of Minas Accretionary Orogen in the southern of São Francisco Craton, Brazil

Eduardo Luís Carneiro de Oliveira¹, Carlos Alberto Rosière¹, Armin Zeh²

¹: Programa de Pós-graduação em Geologia e Centro de Pesquisas Manoel Teixeira da Costa, Instituto de Geociências, Universidade Federal de Minas Gerais (CPMTC-IGC-UFMG), Campus Pampulha, Av. Antônio Carlos 6627, CEP 31270-901 Belo Horizonte, MG, Brazil

²: Karlsruher Institut für Technologie (KIT) Institut für Angewandte Geowissenschaften – Mineralogie und Petrologie. Adenauerring 20b, Geb. 50.40 - 76131 Karlsruhe

In the southern limit of São Francisco Craton, the accretionary terrane of the Mineiro Belt comprises successive amalgamation of volcanic and continental arcs (Teixeira et al., 2015 and references therein). During the collage with the Minas Block amid the Minas-Bahia orogen (Bruno et al., 2021), a voluminous sanukitoid plutonic suite (Alto Maranhão) crystallized at 2.130Ma. These rocks have the magma composition of high-Mg andesites in modern subduction zones, that is interpreted as the product of partial melting from a mantle wedge, metasomatized to different degrees by slab-derived melts (Seixas et al., 2013). Systematic sampling, whole rock geochemistry (Table 1) and combined U-Pb and Lu-Hf LA-MC-ICP-MS dating (Figure 1 and Figure 2) of igneous bodies interlayered with metasedimentary rocks at the NE border of the Mineiro Belt revealed the occurrence of volcanic rocks of the boninite series (Pearce and Reagan, 2019). Boninite is a rare magnesium high, silica high, and low titanium rock, formed in early stage of subduction from a metasomatized mantle in a collisional arc environmental. The enrichment in incompatible elements, together with negative ϵ_{Hf} and Archean T_{DM} ages reveal the influence of Archean continental crust during the emplacement of the melt. Comparing the chemistry data of the sampled volcanic rocks with the sequence defined by Teixeira et al. (2015), it was possible to identify a continuous variation in the geochemical signature from a magnesium high, silica high, and low titanium boninite to a silica-high magnesium basalt and basalt-andesite. Two magmatic ages in this volcanic sequence were obtained, showing ages of $2.149.8 \pm 5.9\text{Ma}$ for the boninite and $2.151.8 \pm 9.4\text{Ma}$ for the basalt, which is consistent with the early stage of Alto Maranhão suite.

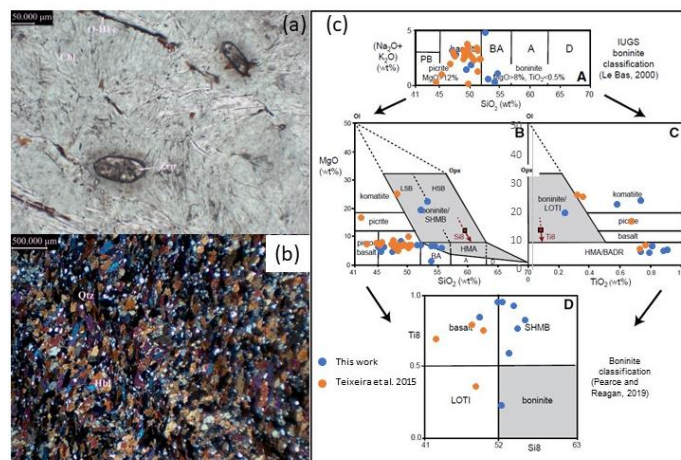


Figure 1: (a) boninite exemplified as chloritite with magmatic zircons; (b) quartz-hornblende-plagioclase sub-alkaline metabasalt. (c) diagram of boninite classification modified from Le Bas (2000) and Pearce and Reagan (2019)

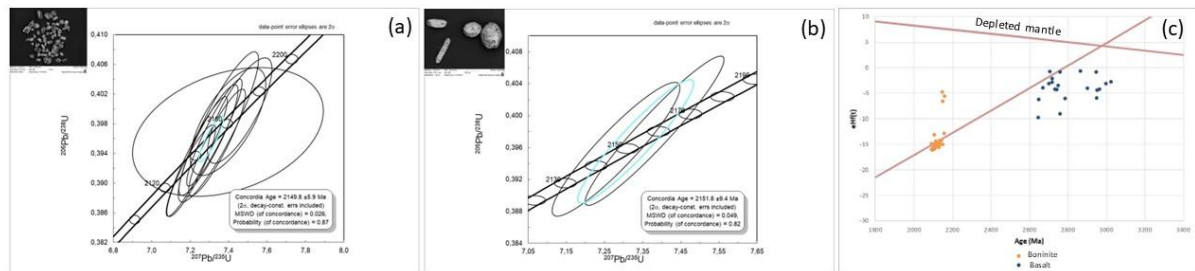


Figure 2: (a) U-Pb LA-ICP-MS dating analyse for boninite. (b) U-Pb LA-ICP-MS dating analyse for basalt; (c) Plot of ϵ_{Hf} versus magmatic age of crystallization from boninite and basalt.

Sample	SiO ₂ [wt.%]	TiO ₂ [wt.%]	Al ₂ O ₃ [wt.%]	Fe ₂ O ₃ [wt.%]	MnO [wt.%]	MgO [wt.%]	CaO [wt.%]	Na ₂ O [wt.%]	K ₂ O [wt.%]	P ₂ O ₅ [wt.%]	LOI [wt.%]	Total [wt.%]
CRM-RO-0003	53,34	0,6	4,36	9,99	0,12	22,81	1,88	0,08	0,03	0,04	5,5	99,4
CRM-RO-0005	52,23	0,23	3,63	8	0,2	19,74	11,26	0,38	0,07	0,001	3,5	99,62
CRM-RO-0006	53,94	2,01	8,97	24,78	0,46	0,81	7	0,74	0,28	0,7	0,2	99,92
CRM-RO-0008	47,76	2,8	12,3	20,11	0,25	4,32	8,52	2,38	0,7	0,17	0,4	99,74
AL-DD-009 A	55,67	0,83	14,8	9,38	0,12	5,74	6,79	3,94	1,24	0,11	1	99,75
AL-DD-009 B	54,56	0,77	14,74	10,04	0,12	6,38	6,48	3,94	1,53	0,1	1	99,76
AL-DD-009 C	52,32	0,96	14,1	12,39	0,13	6,74	6,58	3,06	1,96	0,12	1,3	99,78
AL-DD-009 D	54,02	0,93	14,22	11,51	0,12	6,51	5,78	3,01	2,23	0,11	1,2	99,79
AL-DD-009 E	51,68	0,96	14,12	13,02	0,13	6,96	6,49	2,85	2,1	0,12	1,2	99,78
AL-DD-009 49 25m	45,93	2,82	11,87	22	0,26	4,54	8,82	2,12	0,71	0,23	0,4	99,75
AL-DD-009 54 4	45,49	1,47	12,8	21,2	0,2	6,2	7,95	1,33	1,84	0,24	0,9	99,77
CRM-RO-0017	49,08	0,85	14,36	13,09	0,19	8,29	11,14	1,64	0,2	0,04	0,8	99,76
CRM-RO-0018	46,31	1,6	15,35	16,48	0,19	6,06	8,88	2,53	0,33	0,12	1,8	99,72
CRM-RO-0019	48,23	1,75	14,15	17,68	0,22	5,24	7,76	1,05	0,26	0,14	3,2	99,75

Table 1: Whole rock analyses for the samples of boninite-basalt-andesite series studied.

Bruno, H., Heilbron, M., Valeriano, C. M., Strachan, R., Fowler, M., Bersan, S., Moreira, H., Motta, R., Almeida, J., Almeida, R., Carvalho, M., Storey, C., 2021. Evidence for a complex accretionary history preceding the amalgamation of Columbia: The Rhyacian Minas-Bahia Orogen, southern São Francisco Palecontinent, Brazil, *Gondwana Research*, Volume 92, Pages 149-171.

Le Bas, M.J., 2000. IUGS reclassification of the high-Mg and picritic volcanic rocks: *Journal of Petrology*, v. 41, p. 1467–1470.

Pearce, J. A., Reagan, M. K., 2019. Identification, classification, and interpretation of boninites from Anthropocene to Eoarchean using Si-Mg-Ti systematics. *Geosphere* 15 (4): 1008–1037.

Seixas, L.A.R., Bardintzeff, J.M., Stevenson, R., Bonin, B., 2013. Petrology of the high-Mg tonalites and dioritic enclaves of the ca. 2130 Ma Alto Maranhão suite: evidence for a major juvenile crustal addition event during the Rhyacian orogenesis, Mineiro Belt, Southeast Brazil. *Precambrian Res.* 238, 18–41.

Teixeira, W., Ávila, C.A., Dussin, I.A., Neto, A.C., Bongioiolo, E.M., Santos, J.O., Barbosa, N.S., 2015. A juvenile accretion episode (2.35–2.32 Ga) in the Mineiro belt and its role to the Minas accretionary orogeny: Zircon U–Pb–Hf and geochemical evidence. *Precambrian Res.* 256, 148–169.

MINING EXPLORATION AND GEOLOGICAL MAPPING BY REMOTE SENSING THE WESTERN PART OF THE GARA TIBERT COPPER-RICH VEINS (OUMJRANE, EASTERN ANTI-ATLAS)

OUASKIOUD Khalid¹.and IBOUH² Hassan².

¹: Department of Geology, FSSM, Cadi Ayyad University, Marrakesh, Morocco; ouaskioudkhalid84@gmail.com;

²: Laboratory L3G, Faculty of Sciences and Techniques, Cadi Ayyad University, Marrakesh, Morocco; h.ibouh@uca.ac.ma;

Introduction: The geological mapping is the basic professional work of geologists. It consists of traditional techniques such as field observations and the study of outcrops. Today, the availability of aerial photography, satellite imagery (remote sensing), and geographic information systems (A. Balasubramanian, 2007), are used for digital geological mapping and mining exploration replacing many older techniques.

Remote sensing is a technique and scientific activity, which uses sophisticated sensors to measure the amount of electromagnetic energy exiting an object or geographic area from a distance (John R. Jensen. 2015). This energy is transmitted through the atmosphere to instruments mounted on the remote sensing platform, which beams the data back to the Earth where it is then processed into image products (Richards, J., Jia, X. 2006).

Problematic and objectives: There are many Lower Paleozoic cover-hosted copper ore deposits within the Oumjrane-Boukerzia mining district. Whereas, their extension is still weakly understood, and more remote sensing studies, detailed geological mapping, and mining exploration surveys are required. We have selected the Gara Tibert deposit for the present detailed study (Fig.1c').

Using remote sensing technology, this project aims to regionally map the lithological units and hydrothermal alteration zones in the Oumjrane mining district and its vicinity (Fig.1c and Fig.2). The main goal is to explore the western extension of the Gara Tibert copper-rich veins, using remote sensing combined with fieldwork and detailed digital geological mapping.

Methodology: We used Advanced Spaceborne Thermal Emission and Reflection Radiometer (Aster) (14 channels from the visible through the thermal-infrared regions) and Landsat 8 Operational Land Imager OLI/TIRS (11 bands) remote sensors data, and applied many images preprocessing and processing methods using ERDAS IMAGING v 2014, Envi v 5.3, and ArcGis v 10.8.2 softwares. Geomatica v 2014 was used to conduct automated lineament extraction. For verifications and mapping of the geological features in the area, 10 days of fieldwork have been done. Digital geological mapping has been performed using QGIS v 3.26.3 and Qfield (QGIS professional mobile app) for collecting the data on the field.

Remote sensing: Multiple image processing techniques and algorithms were applied to Aster and Landsat 8 images to map and delineate lithological units and hydrothermal alteration zones. Including color composites (Fig.2), Principal Component Analysis PCA, and band ratios (for iron oxides, alteration, carbonates, clay, NDVI...).

For mapping of the lineaments and structural elements, we used the convolution process to apply directional filters for the Landsat 8 OLI band 8 (panchromatic band), in NS, EW, NW-SE, and NE-SW directions (with a window of 3*3) to enhance and classify the lineaments in the study area. 220 fractures have been mapped within the region.

Fieldwork and digital geological mapping: We undertook detailed (1: 25000) digital geological mapping of the study area (Fig.1c'), which exhibits many Ordovician age sedimentary rocks: 1st Bani sandstones and quartzites (outcropping on the west in Fig.1c'), Ktaoua Group (Sandstones, pelites, and limestones intercalation), and 2nd Bani sandstones (outcropping on the east).

Our mapping has yielded and characterized more than 70 NE, EW, and WNW trending lineaments (including faults and veins) mapped across the study area. Some of these are grouped into sets aligned along same directions, revealing that these sets belong to major faults which may constitute the extension of the Gara Tibert copper veins to the west. The NE and EW trending faults are mainly affecting the Ktaoua Group formations, and are mainly infilled with siderose and siderite (iron carbonates), limonite, iron oxides, quartz, and rare copper carbonates traces. The WNW- trending veins are rich in baryte with copper carbonates and quartz, and are affecting the 1st Bani formations.

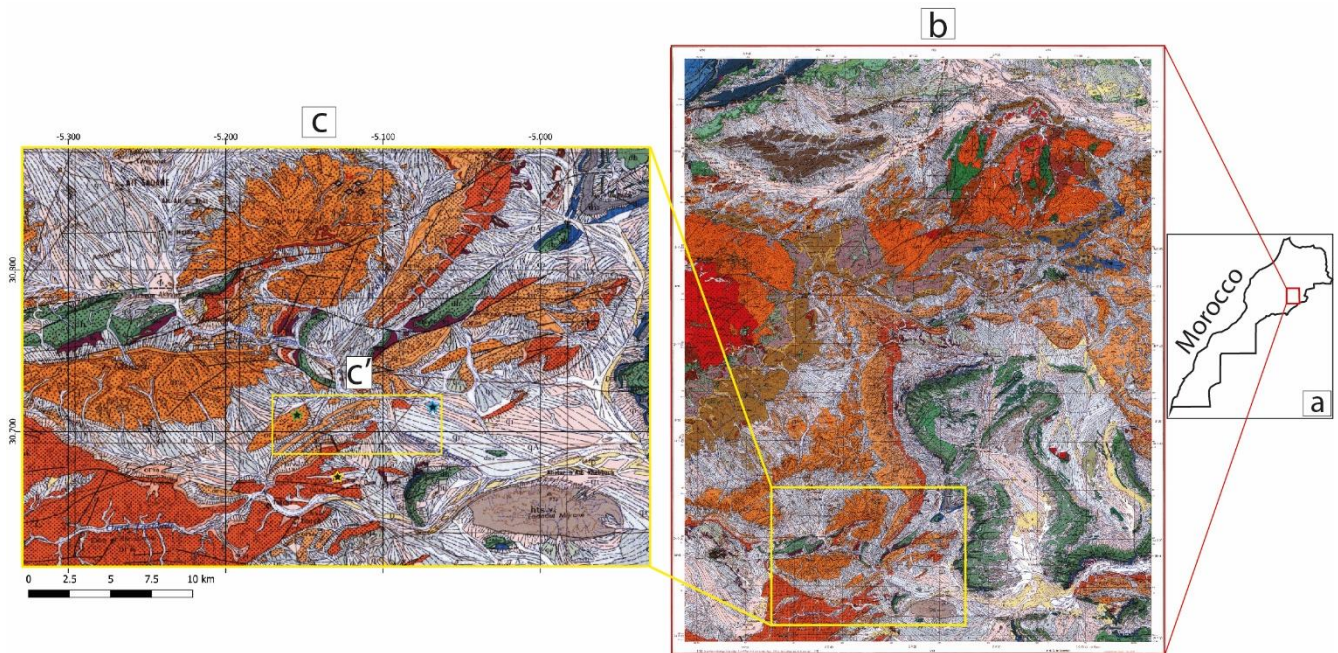


Figure 1. Diagram showing the location of the study area. *a*: the location in Morocco; *b*: geological map of the Todrha Ma'der (1: 200000); *c*: the area covered by remote sensing study; *c'*: yellow box showing the study area, with the yellow star indicating the BouN'has mining site, the blue star indicating the Gara Tibert deposit, and the green star showing the Tizgarhine formation.

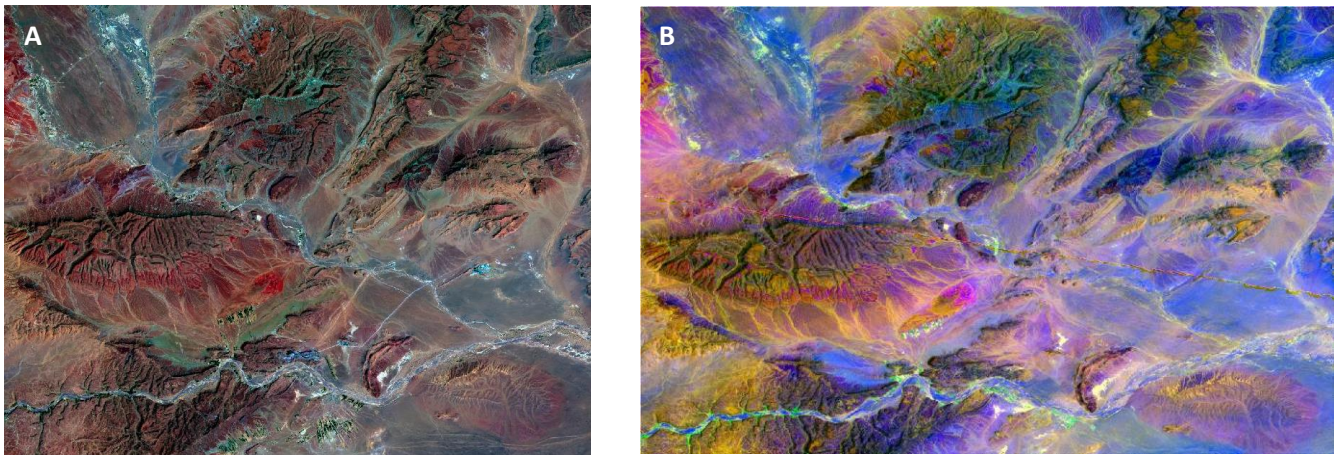


Figure 2. *A*: Color-composite (RGB= bands 7, 3, 1) of Landsat 8 OLI, *B*: Color-composite (RGB= bands 5, 3, 11) of Advanced Spaceborne Thermal Emission and Reflection Radiometer (ASTER).

References:

- Balasubramania A., (2007). *Geological Mapping Procedures*, Technical report,
 Richards, J. and Jia, X. (2006). *Remote Sensing Digital Image Analysis: an introduction*. 4th Edition. Berlin: Springer. 43 p.
 John R. Jensen. (2015). *Introductory Digital Image Processing: A Remote Sensing Perspective*. 4th Edition. Prentice Hall. 623 p..

Petrogenesis of the late Ediacaran A-type granites of the western part of the Moroccan Anti-Atlas belt: Insights from U-Pb dating, geochemistry and Sr-Nd isotopes of the Sidi El Houssein, Tafraout and Taourgha intrusions.

Mohamed Ougadire^{1,2}, Fatiha Askkour¹, Alexiane Favier², Mehdi Ousbih¹, Moha Ikenne¹, Yves Géraud²

¹: Laboratory of Applied Geology and Geo-Environment, Department of Earth Sciences, Faculty of Sciences Agadir, Ibn Zohr University, Morocco.

²: GeoRessources, ENSG - University of Lorraine, Rue du Doyen Marcel Roubault 54500 Vandoeuvre-lès-Nancy, France.

The U–Pb zircon age carried out on three distinct late Ediacaran granites through the Anti-Atlas yielded $^{207}\text{Pb}/^{235}\text{U}$ ages of $584 \pm 2.29/ 579 \pm 3.83$ Ma for Sidi El Houssein granite (Zenaga Inlier), 581 ± 2.05 Ma for Tafraout granites (Kerdous inlier) and 580 ± 3.02 Ma for the Taourgha intrusion (Bas-Drâa inlier). Geochemically, these pink granites display high SiO₂ contents that range from 69.19 to 77.3 wt. %. They are ferroan, mainly peraluminous to weak metaluminous and high-K calc-alkaline with LILE (Rb, K, Th) and HFSE (Ta, Zr, Hf) enrichment, with depletions in Ba, Nb, Sr, and Ti. These rocks have relatively high zircon saturation temperatures (700–900°C), high Zr + Nb + Ce + Y contents >350 ppm, and $10,000 \times \text{Ga}/\text{Al}$ ratios > 2.6 that are typical of A-type granites. Isotopic compositions show that the granitoids have variable ($^{87}\text{Sr}/^{86}\text{Sr}$)_i ratios (0.67–0.73), $\epsilon\text{Nd}(t)$ values (-2.9 to -7.63) and T_{DM} model ages of 1.49 to 2.53 Ga. suggesting that they were derived from the partial melting of a continental crust with moderate mantellic contribution. These granitic intrusions are subcontemporaneous to the widespread volcanic and volcano-detrital rocks from Ouarzazate Group (580-545 Ma), marking the post-collisional transtensional period in the Anti-Atlas. All these data provide evidence of an emplacement of these late Neoproterozoic granitoids during a transtensional regime due to an asthenosphere upwelling that follows the lithospheric delamination related to the collapse of the Panafrikan belts.

Keywords: Anti-Atlas, Morocco, A-type granites, Ediacaran, U/Pb-SIMS, Zircon, Sr-Nd isotopes.

DYKE SWARM HISTORY OF WESTERN JOKWA LINEA GROOVE BELT, SE STANTON QUADRANGLE (V-38), VENUS: PROPOSED PART OF TRIPLE JUNCTION RIFT SYSTEM

R. Oukhro¹, H. El Bilali^{2,3}, R.E. Ernst^{2,3}, J.W. Head⁴, N. Youbi^{1,3}

¹ : Department of Geology, Faculty of Sciences-Semlalia, Cadi Ayyad University, Marrakesh, Morocco;

² : Department of Earth Sciences, Carleton University, Ottawa, Ontario, Canada;

³ : Faculty of Geology and Geography, Tomsk State University, Tomsk, Russia

⁴ : Department of Earth, Environmental and Planetary Sciences, Brown University, Providence, Rhode Island, USA.

Lineae are elongated regional features on Venus that are associated with extensional lineaments that occur together in narrow elongated topographic highs. Lineae have also been referred to as fracture belts, densely lineated material, and more recently, groove belts (see summary of nomenclature in Ivanov & Head (2011, 2015). An extensional origin is emphasized in many interpretations (Ivanov & Head 2015), although a recent interpretation suggest they can represent deformation belts (exhibiting both extensional and compressional features) between small crustal blocks (Byrne et al. 2021). Excellent examples of groove belts (Antiope, Hippolyta, and Molpadia Lineae) are described from Lavinia Planitia (e.g. Ivanov & Head (2001); Fernández et al., 2010). Detailed mapping of linea will provide more precise constraints on their origin.

We focus on Jokwa linea which extends for 1700 km from within southeastern Stanton Quadrangle, V-38 and eastward into the adjacent Taussig Quadrangle, V-39 where it has been previously mapped at 1:5,000,000 scale (Brian et al., 2005). However, there is no quadrangle scale mapping for V-38. More than 18,750 extensional lineaments have been mapped. These are mainly interpreted as grabens overlying dykes, although some lineaments parallel to the general ENE-WSW trend of the Jokwa linea are likely to be normal faults associated with rifting. Six magmatic centres were defined on the basis of their radiating dyke swarms, and most are associated with a central magmatic centre; the largest is Koliyas Corona. Topographic profiles along and across Jokwa linea reveal a generally flat topography outside Jokwa (in Wawalag Planitia both to the north and south), but within Jokwa linea there is rift formation with associated uplift on the flanks of the rift ('rift flank uplift'), and locally higher topography along the rift where the magmatic centres are located. The highest topography is associated with Koliyas Corona (2800 meters). Jokwa linea bifurcates to the east of our map area and the overall linea pattern suggests triple junction rifting. The association of a major magmatic centre, Koliyas Corona centre, at the focus of the triple junction rifting is suggestive of a link with an underlying mantle plume centred at Koliyas Corona.

References

Byrne, P. K., Ghail, R. C., Gilmore, M. S., Şengör, A. C., Klimczak, C., Senske, D. A., ... & Solomon, S. C.

(2021). Venus tesserae feature layered, folded, and eroded rocks. *Geology*, 49(1), 81-85.

Fernández, C., Anguita, F., Ruiz, J., Romeo, I., Martín-Herrero, Á. I., Rodríguez, A., & Pimentel, C. (2010).

Structural evolution of Lavinia Planitia, Venus: Implications for the tectonics of the lowland plains. Icarus, 206(1), 210-228.

Ivanov, M. A., & Head, J. W. (2001). *Chryse Planitia, Mars: Topographic configuration, outflow channel continuity and sequence, and tests for hypothesized ancient bodies of water using Mars Orbiter Laser Altimeter (MOLA) data. Journal of Geophysical Research: Planets*, 106(E2), 3275-3295.

Ivanov, M. A., & Head, J. W. (2011). *Global geological map of Venus. Planetary and Space Science*, 59(13), 1559-1600.

Ivanov, M. A., & Head, J. W. (2015). *The history of tectonism on Venus: A stratigraphic analysis. Planetary and Space Science*, 113, 10-32.

Stofan, E. R., Brian, A. W., & Guest, J. E. (2005). *Resurfacing styles and rates on Venus: Assessment of 18 Venusian quadrangles. Icarus*, 173(2), 312-321.

Structuring of Triassic basins in the north-western Meseta (Morocco) : A tectonic hint of the central Atlantic opening.

Said Oumouaa ^{a*}, Ayoub Aabi ^b, Abdellah Nait-Bba ^c, Younes Hejja ^d, Lahssen Baïdder ^a

^a Geosciences Laboratory, Department of Geology, Faculty of Sciences Ain Chock, Hassan II University, BP 5366 Maarif, Casablanca, Morocco

^b Department of geology, Ecole Normale Supérieure, Mohammed V University, BP 5118, 10000 Rabat, Morocco

^c Mineral Deposits, Hydrogeology & Environment Laboratory, Department of Geology, Faculty of Sciences, Mohammed I University, 60000, Oujda, Morocco

^d Managem, Twin Center, Tour A, Angle Bd Zerktouni-Abdelkarim Khattabi, Casablanca, Morocco

The northwestern Moroccan Meseta constitutes an important tectonic segment of the Variscan belt in North Africa. The basement is formed mainly by Paleozoic terranes which appear as inliers, generally metamorphosed and tectonically deformed during the Variscan orogeny. This basement is unconformably overlain by the Meso-Cenozoic cover. The Mesozoic formations record key tectonic features of the occurrence of the Triassic basins. Extensive field investigation within this cover shows that the NE-SW trending faults exhibit a distinct extensional tectonic pattern which may have been formed by the reactivation of pre-existing Hercynian structures. However, the NW-SE trending one displays typical characteristics of strike-slip structures. The latter are interpreted as transverse major faults directly related to the extensional tectonics associated with the opening of the central Atlantic in response to NW-SE extension. The synchrony of these two fault systems constitutes the major mechanism controlling the development of numerous tilted blocks and then the occurrence of the Triassic basin (e.g., Berrechid and Rommani-Khemissèt basins). Synsedimentary tectonics was also active along both of these systems, resulting in significant thickness variation of sedimentary deposits (e.g., conglomerates and red beds) and leading to the emplacement of the CAMP Triassic basalts during the Pangea breakup.

Petrological and geochemical evidences for magma mixing and mingling in the Saghro granitoids, Anti-Atlas belt, Morocco

Omar Outaoui¹, Ezzoura Errami^{1,2}, Jamal El Kabouri¹, Abdellatif Jouhari¹, Nasser Ennih², Abdelmalek ouadjou³, Salmi Saber¹

¹*Faculté des Sciences, Université Chouaïb Doukkali, EGGPG, B.P. 20, 24000 El Jadida, Maroc*

²*Faculté Polydisciplinaire de Safi, Université Cadi Ayyad, GOT, B.P. 4162, 46 000 Safi, Maroc*

³*Groupe Managem, Twin Center, A BP5199, Casablanca, Maroc*

Saghro massif consists of an extensive ediacaran plutono-volcanic complex. The Saghro massif can be divided into a 590-550 Ma plutonic covered by a ca.570-540 Ma volcano-sedimentary series. In particular, the granitic and granodioritic plutons display microgranular mafic enclaves (MME) that provide insight into the process of magmatogenesis during the late Pan-African orogeny. This contribution presents a multidisciplinary study of MME, including field investigation, petrographic and geochemical data from the Saghro pluton.

The petrographic study indicates that Saghro plutons consists of granodiorite, quartz monzonite and monzogranite (charnockite). Within the host rocks, MMEs are widespread and vary between gabbro to quartz diorite, MMEs are formed by orthopyroxene, clinopyroxene, amphibole, sieved and concentric zoned plagioclase, biotite, K-feldspath, and opaque minerals and acicular apatite. Field observations show that MMEs are 2 cm to 1 m in size, fine to medium grained with rounded, elliptical or swarmed shapes and are generally in sharp contact with host rocks. In addition, MMEs may contain host rock fragments, plagioclase and K-feldspar xenocrysts. This observation suggests that MMEs were formed by injection of a high-temperature, low-viscosity mafic magma into a low-temperature, high-viscosity felsic magma. The mineralogical transfer between the mafic and felsic magmas, together with vein injections of the host rocks into the MMEs, suggests that the MMEs were likely formed by the mixing of mafic and felsic magmas.

Geochemical data show that the host rocks are calc-alkaline to high potassic calc-alkaline and peraluminous with high SiO₂ contents values and deficient in MgO. In multi-elements spider normalized, they are enriched by LREEs and LILEs, and depleted in Nb, Ta, and Ti. MMEs are metaluminous ($0,74 < A/CNK < 1,2$) with calc-alkaline affinity. However, MMEs are further characterized by low SiO₂ (42.23-56.18%) and high Al₂O₃ (15.37-18.03%), Fe₂O_{3t} (6.7-9.4%), MgO (3.07-7.87%), CaO (3.95-7.97%) and TiO₂ (0.92-1.48%). In multi-elements spider normalized to primitive mantle, MMEs are enriched in incompatible elements e.g., Rb, Ba and Th with negative anomalies in Nb and Zr. REE normalized to chondrite of the host rocks and MMEs are parallel with enrichments of LREE with respect to HREE (La/Sm = 3,94 and et La/Yb = 7,18) with negative anomaly in europium (Eu/Eu* = 0,33). This indicates that host rocks and MMEs share the same magmatogenesis process. chemical element ratios e.g., Nb/La values for the MMEs are 0.42–0.81, while those for the primitive mantle are 1.04 and the Nb/La value in the lower crust is 0.4. The Nb/La values for the MMEs are therefore intermediate between those of the lower crust and the primitive mantle. The Nb/Ta values for the mafic enclaves (12.65-20.33) also show a partially similar trend, mostly falling between the lower crust (Nb/Ta = 8.3) and the primitive mantle (Nb/Ta = 17.4). This shows that the mafic enclaves record the characteristics of mafic-felsic magma interaction.

U-Pb geochronology, geochemistry and geodynamic significance of mafic dyke swarms of Douar Eç-çour-Assarag (High Atlas and Anti-Atlas, Morocco).

Palassia, M. ¹; El Moume, W. ^{1,2}; Ait Malek, M. ¹; Ait Lahna A. ¹; Hadimi I. ¹; Moutbir, O. ¹; Gärtner, A. ³; Linnemann, U. ³; Youbi, N. ^{1,4}; Ikenne, M. ²; Boumehdi, M.A. ^{1,5}; Bensalah, M.K. ^{1,5}

¹: Department of Geology, Faculty of Sciences-Semlalia, Cadi Ayyad University, Prince Moulay Abdellah Boulevard, P.O. Box 2390, Marrakech, Morocco.

²: Department of Geology, Faculty of Sciences, Ibnou Zohr University, P.O. Box 28/S, Agadir, Morocco.

³: Senckenberg Naturhistorische Sammlungen Dresden, Museum für Mineralogie und Geologie, Sektion Geochronologie, GeoPlasma Lab, Königsbrücker Landstraße 159, 01109 Dresden, Germany.

⁴: Faculty of Geology and Geography, Tomsk State University, 36 Lenin Ave, Tomsk 634050, Russia.

⁵: Instituto Dom Luiz (IDL), Faculdade de Ciências, Universidade de Lisboa, Campo Grande, 1749-016, Lisboa, Portugal

A number of conspicuous mafic and felsic dyke swarms cross-cut the Precambrian basement of the Ouzellarh-Sirwa promontory in the High Atlas (Douar Eç-çour) and Anti-Atlas (Assarag). Here, they are named the Douar Eç-çour-Assarag dyke swarms. The Douar Eç-çour mafic dyke swarms show a NNE, NE to ENE-trending, whereas the trends are E-W, NS, NNE, NE, NNW and NW-in Assarag. Some of the mafic dykes show in Douar Eç-çour show co-mingling magmatic textures with the Askaoun granodiorite of the Assarag suite (579 ± 7 Ma, U-Pb on zircon by SHRIMP method). One of the NE trending doleritic dykes (Sample YIG2a, X: W 7.56526° ; Y: N 31.15968°) yields an approximate zircon/titanite U-Pb age of 554 ± 10 Ma (LA-ICP-MS method). In the Anti-Atlas (from Assarag to Taliouine via Askaoun), the Assarag mafic dykes yield an apatite U-Pb age of 557 ± 14 (LA-ICP-MS method) for a N-S trending dyke (Sample ASYN01c, X: $7^\circ 46' 42.60''$ W, Y: $30^\circ 39' 44.30''$ N). This age is a minimum age of emplacement and could be older. Furthermore, a zircon U-Pb concordia age of 600.6 ± 5.6 Ma (lower intercepts at 572 ± 41 and 542.8 ± 9.9 for titanite and apatite, respectively) was recognized for an E-W trending dyke (Sample ASYN12, X: $7^\circ 45' 39.40''$ W, Y: $30^\circ 38' 34.00''$ N). The ca. 600-554 Ma Douar Eç-çour-Assarag mafic swarms plot in three compositional groups: calc-alkaline, tholeiitic, and alkaline. We interpret these geochemical groups to represent three distinct pulses of the plumbing system (“feeder dykes”) of the Ouarzazate Group volcanic pile, since the three dyke compositions match the chemistry of the three successive eruptive cycles (syn-extensional calc-alkaline, tholeiitic Continental Flood Basalts, and alkaline) recognized in the Anti-Atlas (El Moume et al., 2020). The studied dolerite dyke swarms were formed during the fragmentation of Rodina (Pannotia) leading to the opening of the Central Iapetus Ocean and therefore, are compared to coeval, rift-related extrusive/intrusive rocks found in the Jebel Saghro Massif, Ougnat, and other inliers in the Anti-Atlas. The dykes belong to the Central Iapetus Magmatic Province (CIMP) and provide a window into the late Ediacaran mantle, and also shed light on early magmatic processes accompanying the breakup of the West African Craton.

References

El Moume, W., Youbi, N., Marzoli, A., Bertrand, H., Ikenne, M., Boumehdi, M.A., Ernst, R.E., El Hachimi, H., Bensalah, M.K., Mata, J., Madeira, J., Bento Dos Santos, T. M., Martins, S. (2020). Geochemistry of mafic dyke swarms of Douar Eç-çour (High Atlas, Morocco): the farthest record of the Central Iapetus Magmatic Province (CIMP) into West African Craton. *Geonovas (a revista anual da APG (Associação Portuguesa de Geólogos, the Portuguese Association of Geologists). Volume 33, Issue 1 of Geonovas 33 - Nº 1, Pages 95–12.*

Kuonamka Siberian Mesoproterozoic LIP: new paleomagnetic and geochemical data

Pasenko Aleksandr¹, Pazukhina Anna¹

¹:Adress: Schmidt Institute of Physics of the Earth, 123242, B.Gruzinskaya, 10-1, Moscow, Russia

It is believed (Ernst et al., 2016) that dikes and sills of the Kuonamka Large Igneous Province (LIP) are widespread in the northern part of the Siberian Platform. They are exposed on the Anabar massif, as well as on the Olenek uplift in the valley of the Sololi River.

In our research, we studied samples of the most southwestern intrusive bodies belonging to the Kuonamka LIP. We are somewhat increase the base of paleomagnetic and geochemical data for the magmatic bodies of the Kuonamka LIP, whose age can be estimated at 1501 Ma. We collected a sample collection from the 11 sills in the middle parts of the Koty River south of the mouth of the Kotuikan River, on the western slope of the Anabar massif. We also presenting the first paleomagnetic and geochronological data on the ~1500 Ma magmatism of the Udzha aulacogen, which is located between the Anabar massif and the Olenek uplift.

The Koty River magmatic rocks, which we were study, are represented by fine- and medium-grained dolerites with a characteristic ophite and poikilophitic texture. The rock-forming minerals are clinopyroxene (35-40%) and plagioclase (labrador, andesine, 45-50%). Ore minerals are represented by ilmenite and titanomagnetite (8-10%). Apatite is present in rocks as an accessory mineral. The degree of secondary alteration in rocks is different. The rocks can be both fresh and highly altered: propylitization, chloritization, sericitization, are noted.

The petrogenic oxides concentrations were measured by the XRF-method on the S8 TIGER X-ray fluorescence spectrometer, the concentrations of trace elements were measured by the ICP-MS method on the Agilent 7900 quadrupole mass spectrometer at the Geodynamics and Geochronology Research Center (Panteeva et al., 2003). The studied rocks are characterized by a temperate content of SiO₂ (from 46.3 to 50.3 wt. %), temperate MgO content (5.0-7.3 wt. %) and have the alkalis K₂O+Na₂O (2.3-4.3 wt. %). In the TAS diagram (Le Bas et al., 1986), all figurative points of rocks fall into the field of basalts, in the AFM diagram – into the field of tholeiites. Among the rocks there are both low-titanium and high-titanium differences: TiO₂ values vary from 1.5 to 5.1 wt. %.

The trace elements spectra normalized to the primitive mantle (Sun & McDonough, 1989) and are similar in shape to the spectra of IAB (island arc basalts) and OIB (ocean arc basalts). They are characterized by a slight slope in the REE area, variable enrichment with incompatible elements with negative Ta-Nb anomalies and variable values of U and Th. (Sm/Yb) and (La/Sm) ratios indicate a low degree of melting of rocks at shallow depths, and the diagram Th/Yb vs. Nb/Yb (Pearce, 2008) indicates a minor involvement of the crust component in the mantle-source or a metasomatic change in the lithospheric mantle.

We compared our new paleomagnetic data with the North and West Anabar intrusions poles (WAI and NAI) (Evans et al., 2016). Despite the fact that the bodies studied by us geographically belong to the WAI, their pole coincides with the NAI-pole. Also, the paleomagnetic determination for the Unguokhtakh formation (Pasenko, Malyshev, 2020) of the Udzha uplift confidently coincides with the NAI and Sololi poles. The volcano-sedimentary Unguokhtakh Formation formed 1459±16 Ma (Malyshev et al., 2022). These data were obtained by the age of the youngest zircons in the tuffs of the formation. At the moment, we cannot reliably separate the paleomagnetic definitions for Siberia for the time of 1470-1500 Ma.

However, if we use the age grouping approach and group the WAI intrusions with our new data (1501 Ma) and the NAI pole with Unguokhtakh and the Sololi poles, then the difference between the two paleomagnetic definitions becomes obvious. The new paleomagnetic data for the West Anabar Intrusions of the Siberian platform for the age of 1503 million years has coordinates: N=44; Plat = -27°; Plon = 65°; A95 = 3°. Paleomagnetic data for Unguokhtakh tuffs (1459±16 Ma), associated basalts and tuff siltstones coincide with paleomagnetic data for North Anabar Intrusions (1483±17 Ma) and Sololi-Kyutingde sill (1473 ± 24 Ma) (Evans et al., 2016; Pasenko, Malyshev, 2020). The average new paleomagnetic pole for the ~1470 Ma is: N=4; Plat = -31°; Plon = 76°; A95 = 8°.

Our data indicate that there may have been two different magmatic events in the north of the Siberian platform with ages of ~1500 Ma and ~1470 Ma. This significantly clarifies the history of the evolution of the Siberian platform in the Mesoproterozoic in the 1500-1450 Ma interval.

The work was supported by the RSF project № 22-77-00052.

References:

- Ernst R., Okrugin, A., Veselovskiy R., Kamo S.L., Hamilton M., Pavlov, V.E., Söderlund U. Chamberlain K., Rogers C., 2016. *The 1501 Ma Kuonamka Large Igneous Province of northern Siberia: U-Pb geochronology, geochemistry, and links with coeval magmatism on other crustal blocks. Russian Geology and Geophysics. 57. 653-671. 10.1016/j.rgg.2016.01.015.*
- Evans, D.A.D., Veselovsky, R. V., Petrov, P.Y., Shatsillo, A. V., Pavlov, V.E., 2016. *Paleomagnetism of Mesoproterozoic margins of the Anabar Shield: A hypothesized billion-year partnership of Siberia and northern Laurentia. Precambrian Res. 281, 639–655. <https://doi.org/10.1016/j.precamres.2016.06.017>*
- Le Bas, M.J., Le Maitre, R.W., Streckeisen, A., Zanettin, B., 1986. *A Chemical Classification of Volcanic Rocks Based on the Total Alkali-Silica Diagram. J. Petrol. 27, 745-750. <https://doi.org/10.1093/petrology/27.3.745>*
- Lipenkov G. V., Mashchak M. S., Kirichenko V. T., Larichev A. I., Nazarov D. V., Bigun I. V., Kondakova E. A., Khabarov A. N., Gerasicheva A.V., Zavarzin I. V., Litvinova I. V., Surnin A. I. (2015). *Geological map of the Russian Federation scale 1:1000 000, Anabaro-Vilyuiskaya series, sheet R-48-Khatanga. Saint-Petersburg: VSEGEI Cartographic Factory. 2015 (in Russian)*
- Malyshev, S. V., Pasenko, A.M., Khudoley, A.K., Ivanov, A. V., Priyatkina, N.S., Pazukhina, A.A., Marfin, A.E., DuFrane, A.S., Sharygin, I.S., Gladkochub, E.A., 2022. *What is the age of the Udzha paleorift?: U-Pb age of detrital zircons from Udzha basin terrigenous succession, northern Siberia. Vestn. Saint Petersburg. Univ. Earth Sci. 67. <https://doi.org/10.21638/spbu07.2022.401>*
- Panteeva S.V., Gladkochub D.P., Donskaya T.V., Markova V.V., Sandimirova G.P. *Determination of 24 trace elements in felsic rocks by inductively coupled plasma mass spectrometry after lithium metaborate fusion // "Spectrochimica Acta Part B: Atomic Spectroscopy", 2003, Vol.58, 2, p. 341-350*
- Pasenko, A.M., Malyshev, S. V., 2020. *Paleomagnetism and Age Correlation of the Mesoproterozoic Rocks of the Udzha and Olenek Uplifts, Northeastern Siberian Platform. Izv. Phys. Solid Earth 56, 864–887. <https://doi.org/10.1134/S1069351320050067>*
- Pearce, J.A., 2008. *Geochemical fingerprinting of oceanic basalts with applications to ophiolite classification and the search for Archean oceanic crust. Lithos 100, 14–48. <https://doi.org/10.1016/j.lithos.2007.06.016>*
- Sun, S., McDonough, W., 1989. *Chemical and isotopic systematics of ocean basalts: Implications for mantle composition and processes, in Magmatism in the Ocean Basins. Geol. Soc. Spec. Publ. 423, 313–345.*

Significant apparent paleolatitude changes of West Africa Craton revealed by magnetostratigraphy of the Ediacaran Ouarzazate Group, Bou Azzer Inlier, Morocco

James Pierce ^{1,*}, David Evans ¹, Nasrddine Youbi ², Justin Strauss ³, Brenhin Keller ³, Achraf Mohamed Mediany ², Jihane Ounar ², Rachid Oukthro ²

¹ Department of Earth and Planetary Sciences, Yale University, New Haven, CT 06511, USA

² Department of Geology, Cadi Ayyad University, Marrakech, P.O. Box 2390, Morocco

³ Department of Earth Sciences, Dartmouth College, Hanover, NH, 03755, USA

* Email: james.pierce@yale.edu

The first evidence for widespread metazoan life and appearance of complex biological strategies is found in fossils from the Ediacaran Period (635-539 Ma). Accurately reconstructing paleogeography during this period has important implications for nutrient cycling, climate, and the proliferation of life on Earth. A sparsity of reliable paleomagnetic evidence from the middle Ediacaran to the early Cambrian has long presented problems when reconstructing paleogeography. Paleomagnetic poles from this period suggest rapid movement of continents and are at odds with our current understanding of plate tectonics. True polar wander, where the solid Earth rotates uniformly about an equatorial axis, has been invoked to account for discrepancies in the paleomagnetic record. Alternatively, a weak and rapidly reversing magnetic field has been invoked. To investigate these discrepancies, we sampled Ediacaran rocks from the Bou Azzer inlier, part of the Ouarzazate Group on the West African Craton (WAC). Previous work by Robert et al, (2017) shows the WAC to move rapidly from high to low latitude during the Ediacaran and back to high latitude by the Cambrian which the authors propose to be caused by true polar wander. However, Robert et al (2017) did not observe both high and low latitude paleomagnetic directions within the same stratigraphic section. Our preliminary results from Bou Azzer rocks of similar age show both high and low latitude directions within the same stratigraphic section (BA01). These rocks provide the ideal geologic context to study the position of the WAC during this crucial period. As part of a multi-year project we will sample for magnetostratigraphy at high-precision throughout Anti-Atlas Mountains. This strategy samples paleosecular variation (PSV) rather than taking spot measurements such as in igneous rocks and can assess geomagnetic reversal rates. This will allow us to understand the movement of the WAC during the Ediacaran when the magnetic field was likely to have been chaotic. In context with reliable preexisting paleomagnetic data from the WAC and other cratons, this approach will allow us to achieve our overarching goal: reconstructing paleogeography across the Ediacaran-Cambrian transition and understanding the circumstances that led to the appearance of the Ediacara Biota and the Cambrian explosion of animal diversity. This presentation will discuss preliminary paleomagnetic results from the Ouarzazate Group and their paleogeographic and geodynamic implications.

Robert, B., Besse, J., Blein, O., Greff-Lefftz, M., Baudin, T., Lopes, F., Meslouh, S., & Belbadaoui, M. (2017). Constraints on the Ediacaran inertial interchange true polar wander hypothesis: A new paleomagnetic study in Morocco (West African Craton). *Precambrian Research*, 295, 90–116.

Element mobility in shear zones with a focus on the Rare Earth Elements (REE): The case of the Derraman peralkaline granite (Ouled Dlim Massif, Morocco)

Qillech F.¹, Essaifi A.¹, Corsini M.², Haissen F.³, Errami A.⁴.

¹ Département de Géologie, Université Cadi Ayyad, BP. 2390, Marrakech, Morocco

² Geoazur, CNRS UMR6526, Université Nice Sophia Antipolis, Valbonne, France

³ Département de Géologie, Faculté des sciences Ben-Msik, Université Hassan-II, Casablanca, Morocco

⁴ Office National des Hydrocarbures et des Mines, 5 Avenue Moulay Hassan, Rabat, Morocco.

The Ouled Dlim Massif, located west of the Archean part of the Reguibat Rise of the West African Craton, consists of metamorphic nappes stacked during the Mauritanides (Variscan) orogeny. The Derraman granites outcrop in the Eastern Archean sector, a structural domain that overthrusts unmetamorphosed Upper Ordovician to Devonian sedimentary rocks separating the Ouled Dlim Massif from the Cratonic Reguibat Shield. The East Archean Sector is composed of Archean gneisses (Buluated gneisses) and micaschists (Leglat micaschists) and the Derraman Alkaline granites. The Derraman granites form two distinct kilometer-sized bodies, namely North Derraman and the Derraman Highs, encased in the leucocratic gneisses of Bulautad and the Leglat micaschists. The granites have a SHRIMP U-Th-Pb zircon age of approximately 525 Ma (Haissen et al. 2018).

The Derraman granites are medium- to coarse-grained leucocratic rocks composed of dark clots of mafic minerals within a gray matrix of quartz and mesoperthitic alkali feldspar. The mafic minerals consist of blue amphibole (Ca-rich riebeckite to Na-rich ferrorichterite), green aegirine-augite, and anitic biotite, locally muscovitized. The accessory minerals include ilmenite, magnetite, fibrous stilpnomelane, muscovite, fluorite, zircon, apatite, calcite, monazite, fergusonite, aeschynite, and samarskite. The granites are highly siliceous ($\text{SiO}_2 > 75\%$), subaluminous, with low levels of Al_2O_3 and MgO , moderately high levels of Na_2O and K_2O , and a high $\text{FeOT}/(\text{FeOT} + \text{MgO})$ ratio. The agpaitic index ($(\text{Na}_2\text{O} + \text{K}_2\text{O}) / \text{SiO}_2$) ranges from 0.94 to 1.12, and approximately 40% of the analyzed samples are peralkaline. Their trace element composition is consistent with A-type affinity. They exhibit low concentrations of alkali and alkaline-earth trace elements but moderate to high concentrations of highly incompatible elements, particularly Nb and Zr. According to Bea et al. (2015), all the Derraman granites can be classified as A₁-Type (anorogenic granites with a geochemical signature similar to OIB Oceanic Island Basalts).

The Derraman granites are variably deformed, with the rocks in the Derraman Highs being more deformed than those in North Derraman. The deformation in the Derraman Highs is characterized by the development of centimeter- to meter-scale shear zones that cross cut the granites. The dominant shear zones are sub-horizontal, top to the East, thrust shear zones. They are interconnected by steeply dipping shear zones. This deformation is similar to that described in the country rocks and that was related to Variscan tectonics. Within the shear zones, the grain size decreases and the granite is transformed into mylonites and ultramylonites.

Because the alkaline granites have a mineral potential in the heavy REE, the main aim of this work is to study element mobility in the shear zones that cross cut the Derraman granite. We especially focus on the behaviors of the rare earth elements, and determine which accessory minerals control the REE uptake/loss during mylonitization and fluid/rock interaction.

Reference:

- Bea, F., Montero, P., Haissen, F., Molina, J.F., Michard, A., Lazaro, C., Mouttaqi, A., Errami, A., Sadki, O., 2016. First evidence for Cambrian rift-related magmatism in the West African Craton margin: The Derraman Peralkaline Felsic Complex. *Gondwana Res.* 36, 423–438.
- Haissen, F., Montero, P., Cambeses, A., Bea, F., Molina, J. F., Mouttaqi, A., ... & Errami, A. (2018). Petrogenesis of Derraman Peralkaline granite (Ouled Dlim Massif, West African Craton Margin, Morocco): New constraints from zircon Hf and O isotopic compositions. *Comptes Rendus Geoscience*, 350(6), 236-244.

Geological mapping using Landsat OLI imagery in Tata inlier (South-West Morocco).

Rahimi Abdelmejid¹, El Hachimi Hind¹, Kholaiq Mariame¹, Nasrddine Youbi², Hassan Ibouh³

¹Laboratory of Geodynamics and Geomatics (L2G), Dept. of Geology, Faculty of Science El Jadida, Chouaib Doukkali University, Morocco. e-mail: rahimi.am@ucd.ac.ma

²Geology Department, Faculty of Sciences-Semlalia, Cadi Ayyad University, Prince MoulayAbdellah Boulevard, P.O. Box 2390, Marrakech, Morocco, e-mail: youbi@uca.ac.ma

³Geology Department, Faculty of Sciences and Techniques, Cadi Ayyad University, A. Khattabi Boulevard, P.O. Box 549 ; Marrakech, Morocco, e-mail: ibouh@fstg-marrakech.ac.ma

Geological mapping is an indispensable tool in the exploration and exploitation of natural resources. Optical satellite images with high spatial resolution, such as Landsat 8 OLI, can meet this need, especially in arid areas where bedrock is well exposed. In the Tata inlier case, the subject of this work. This study's main objective is to map the different lithological facies and the structural lineaments from Landsat 8 OLI/TIRS satellite images and SRTM Digital Terrain Models. Thus, the application of three Machine Learning algorithms (Maximum Likelihood, Support Vector Machine, Random Forest) has allowed, because of the variation in lithological hues between adjacent units, not only the excellent discrimination of the different formations in the geological map established by Benziane and Yazidi (1982) but also a significant improvement of the latter. The mapping of linear structures (lineaments) was carried out on SRTM digital elevation models (DEM) and raw images and their derivatives from previous treatments. These techniques allowed the manual extraction (by photo interpretation) of the different lineaments. This extraction resulted in establishing a very detailed fracturing map that can be used for future mining or hydrogeological prospecting surveys.

Geochemical study of the felsic volcanic rock of the central Jbilets and Guemassa domain (Morocco): Contribution to the exploration of Volcanogenic Massif Sulphide deposits

L.Salama¹, E.M.Mouguina¹, A.Ouadjou²

¹Laboratory "Dynamics of the Lithosphere and Genesis of Resources "DLGR".

Department of Geology. Faculty of Sciences Semlalia M.B.2390. Cadi Ayyad University. 40000 Marrakesh, Morocco (leilafssm@gmail.com).

²Managem Group, Twin Center Casablanca, Morocco

Moroccan Volcanogenic Massive Sulphide (VMS) deposits are hosted in the Paleozoic of the central Jbilets and Guemassa. Draa Sfar deposit is the most with more than 14M. These economic deposits are generally formed in association with acid magmatism (Rhyodacites and Rhyolites). Several types of exploration studies have been carried out in the provinces of Jbilets and Guemassa, but geochemical exploration has not been well developed. This study uses, firstly, rhyolitic and rhyodacitic rocks to determine their fertility, which will help to delineate the mineralized zones. The geochemical study of alterations rocks which could give us more reliability to the expected results. The geochemical classification of rhyolites and rhyodacites from the Hercynian massifs of Guemassa and Jbilets showed that they belong to four different types. Thus, FI characterizes the rhyolites of Hajjar and Draa Sfar; FII is found in Khwadra, Hajjar, Draa Sfar, Nzala, Koudiat Aicha and Kechnet; FIIIa in Hajjar, Draa Sfar, Nzala and Lalla Takerkoust and finally FIV in Hajjar and Frisem. The geochemistry of FII-FIII-FIV felsic volcanic rocks is influenced by the mineralogy and composition of the source, the pressure and temperature of the primary melting process and, to a lesser extent, any subsequent fractionation processes. At Draa Sfar and Hajjar, whose geodynamic context is that of a back-arc basin, there is a preferential association of VMS deposits with felsic volcanic rocks FII, FIII and FIV. In Frisem, FIV type rocks have more affinity with those of Draa Sfar. On the alteration side, the results show that almost all the samples are in the alteration domain; that the degree of alteration is similar between Draa Sfar and Frisem and finally that all the samples are in the VMS domain. From these preliminary results, one could deduce that Frisem could be a favorable area for the existence of VMS.

Numerical fluid modeling of the Hercynian Draa Sfar Massive Sulfide Deposit, Central Jbilets, Morocco: Contribution to the exploration

Laila Salama¹, El Mostafa Mouguina¹, Essaid El Bachari², Larbi Rddad³

¹ *Laboratory Dynamics of the Lithosphere and the Genesis of Resources (DLGR), Faculty of Sciences Semlalia, University Cadi Ayyad, Av Abdelkrim Khattabi, BP 511, 40000 Marrakech, Morocco. (leilafssm@gmail.com).*

² *Laboratory of Information Systems Engineering (LISI), Faculty of Sciences Semlalia, University Cadi Ayyad, Marrakech, Morocco*

³ *Earth and Planetary Division, Department of Physical Sciences, Kingsborough Community College of the City University of New York, 2001 Oriental Boulevard, Brooklyn, New York, NY 11235-2398, USA*

Draa Sfar is a polymetallic (Zn-Pb-Cu) volcanogenic massive sulfide deposit with an actual resource of 13 Mt at 4.0% Zn and 1.3% Pb. It is part of the central Jbilets area known for its several Cu-Zn ore deposits. The ore is hosted in the upper Visean-Namurian sedimentary formation. Owing to the complexity of the geology of the ore deposits, numerical simulation approach was attempted to shed light into the temperature distribution, the circulation of the hydrothermal fluid and the genesis of massive sulfide ore bodies by evaluating the permeability, porosity, and thermal conductivity. On the basis of this simulation approach, the ore is predicted to be deposited at a temperature ranging between 230 and 290°C. This temperature range is dependent on the pre-existing temperature of the discharge area where a metal-rich fluid precipitated the ore. The duration of the Draa Sfar ore body formation is predicted to be 15, 000 to 50, 000 years.

Based on geological studies of Draa Sfar deposit together with the aforementioned results of the simulation approach, an ore genetic model for the massive sulfide ore bodies is proposed. In this model, the supply of ore-forming fluids is ensured by the combination of seawater and magmatic waters. Magma that generated rhyodacite dome acted as the heat source that remobilized the circulation of these ore-bearing fluids. The NW-SE trending faults acted as potential pathways for both the downward and upward migration of the ore-forming fluids. Due to their high permeability, the ignimbritic facies, host rocks of Draa Sfar ore bodies, have favored the circulation of the fluids. The mixing between the ore-forming fluids of magmatic origin and the descending seawaters and/or in situ pore waters led to the formation the ore bodies in 35,000 years.

The position and size of the ore body, determined by the simulation approach, is consistent with the actual field geological data.

Structural architecture of veins in the Ait-Ahmane ore deposits (Bou Azzer, Central Anti-Atlas, Morocco)

Saber Salmi¹, Ezzoura Errami^{1,2}, Jamal El Kabouri¹, Abdellatif Jouhari¹, Jamal El Kabouri¹, Nasser Ennih^{1*}, Omar Outaaoui¹, Abdelhak Karfal³, Younes Moundi³, Lhou Maacha³, Said Ilmen⁴

¹Faculté of sciences, Chouaib Doukkali University, EGGPG, B.P. 20, 24000 El Jadida, Maroc

²Polydisciplinary Faculty of Safi, Cadi Ayyad University, GOT, B.P. 4162, 46 000 Safi, Maroc

³Groupe Managem, Twin Center, A BP5199, Casablanca, Maroc

⁴CAG2M research team, polydisciplinary faculty of Ouarzazate, Ibn Zohr University, Morocco
s.ilmen@uiz.ac.ma

***To the treasured memory of Pr. Nasser Ennih**

The syn-orogenic emplacement of the Ait-Ahmane pluton at the Pan-African suture zone makes the interpretation and analysis of tectonic features challenging, given the high connectivity and density of fractures, often with parallel mirrors showing signs of different deformations events. This contribution aims to present new observations at the outcrop and microscopic scale to highlight the relationship between faults trends and extension rates within mineralized structures baren quartz-carbonate veins.

The tectonic structures in the Ait-Ahmane zone are organized into three major directions : N130 ; N070 and N030. These structures are filled with quartz-carbonate and display economically significant mineralization. The veins exhibit various morphologies such as single veins, multiple veins, composite veins, etc., and they also exhibit diverse textures including crack-seal-slip, brecciated, syntectonic, antitaxial, crust-forming, etc.

The N130 and N030 faults preserve both dextral and sinistral movements with a dominant normal component, respectively, and have a 50E to 80E dip. The N030 faults represent secondary fractures within the N130 strike-slip corridor. The opening rate of the N030 structures increases significantly at the contact zones of the N130 faults with the serpentinite-quartz diorite, forming more deformed and altered zones at the hanging walls of the N030 veins. These intersecting zones between the two fault trends are of the receptacle of the mineralizing fluids.

These observations are essential for understanding the regional tectonic context that facilitated fracturing and fluid circulation within this massif. This investigation highlights the significance of the N030 faults in the circulation of mineralizing fluids at the contact zones of the N130 fault structures, which brought together mantle rocks and syn-collisional plutons.

GEOLOGY OF THE LATMIKAIK AND XCACAU CORONAE IN THE HENIE (V-58) QUADRANGLE, VENUS.

J. Shackman¹, K.J.E. Boggs¹, R.E. Ernst^{2,3}, E.M. Bethell⁴, H.G. Wehnes¹, E. Varg¹, C. Pendleton¹, W. Jans¹, J. Hall¹, R.C. Dietrich¹, L. Dham¹, J. Demorcy², B. Dear¹, M. Chowdhury¹, H.N. Bley¹, B. Beckie¹, and M. Becerra De Rosales¹.

¹ Department of Earth and Environmental Sciences, Mount Royal University, 4825 Mount Royal Gate SE, Calgary, Alberta, Canada T3E 6K6;

² Department of Earth Sciences, Carleton University, 1125 Colonel By Drive, Ottawa, Ontario, Canada K1S 5B6;

³ Faculty of Geology and Geography, Tomsk State University, 36 Lenin Avenue, Tomsk, Russia 634050;

⁴ Department of Earth and Environmental Sciences, University of Ottawa, 75 Laurier Avenue E, Ottawa, Ontario, Canada K1N 6N5.

Keywords: Planetary Science, Planetary Geology, Volcanology, Venus, Coronae, Henie (V-58) Quadrangle, Latmikaik Corona, Xcacau Corona.

Introduction: Latmikaik Corona (345 km x 650 km) and Xcacau Corona (120 km x 165km) are both elongated N-S and constrained by annulus material defined by dense swarms of radar bright, linear and curvilinear subparallel lineaments. Annulus material defines a topographic high around the edge of Latmikaik Corona with the core material slightly raised and defining an overall W-W shaped topographic profile. Xcacau Corona has a less well-defined annulus and a sunken core giving it a U-shaped profile. Tellervo Chasma extends between the two coronae (striking 050-230°). Six densely packed graben swarms (011-191°; 010-190°; 340-160°; 325-145°; 337-157°). One graben system (025-205°) extends the length of the chasma but does not appear to extend significantly past the margins of the chasma. One radiating graben system originates from an enigmatic feature at the southeastern corner of Xcacau Corona. Two further graben systems (331-151°; 015-195°) were mapped south of Xcacau Corona. A further five graben swarms cut across the southern end of Latmikaik Corona (022-202°; 027-207°; 055-235°; 353-173°; 005-185°). The W-W shaped profile of Latmikaik Corona suggests that this corona is in a regressive stage and the sunken U-shaped profile of Xcacau Corona also suggests a regressive stage. The densely packed graben are interpreted to be the surficial expression of underlying dyke swarms. The complex system of up to 14 swarms that cut across the coronae and Tellervo Chasma suggest a prolonged history of magmatism and extension, possibly related to the formation of these two coronae and more distal magmatic centers in response to underlying mantle plumes.

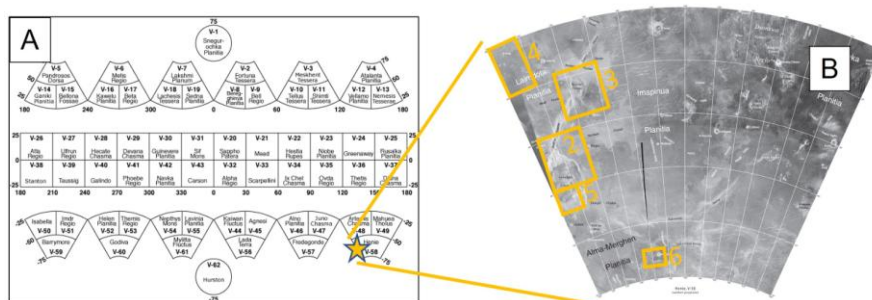


Figure 1: Study Area. The Henie (V-58) Quadrangle is located in southern Venus.

Methodology: Geological features traced out in ArcGIS (1:500,000) on files downloaded from the Planetary Data System for Magellan data. Mapped geological features categorized by defining characteristics such as orientation and trend.

Results: Both Coronae elongate N-S, constrained by annulus material (radar bright with dense swarms of subparallel lineaments; Figs. 2, 3) Latmikaik (Fig. 2) - 345 km wide, 650 km long Core – radar dull mottled, nearly devoid of fractures, radar bright flow material. Annulus forms a topography high around edge with core material raised giving an overall W-profile^[1] Xcacau (Fig. 3) - 120 km wide, 165 km long, and core sunken, less well-defined annulus Graben systems – at least three swarms (e.g. Table) cross Xcacau corona.

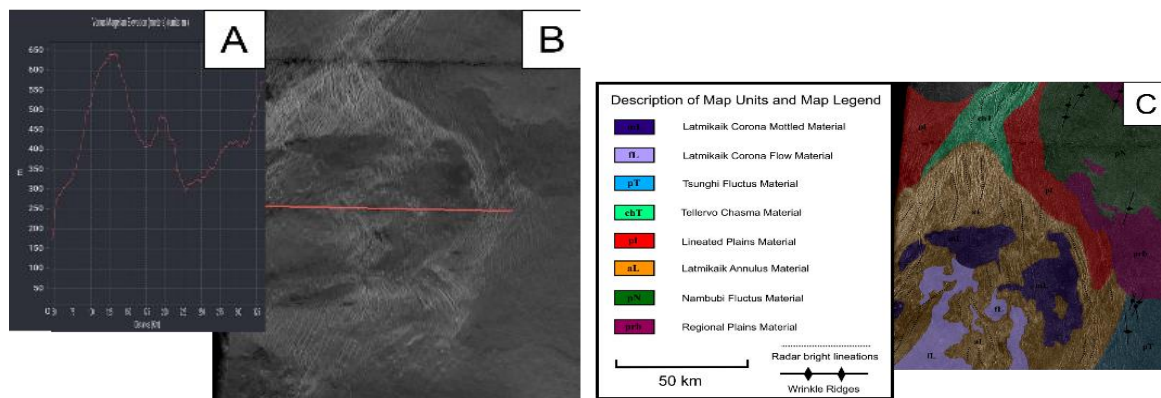


Figure 2: Morphology and Geology of the Latmikaik Corona. A topographic profile is presented on the left (“A”), the uninterpreted Magellan mission data in the middle (“B”) and the mapped geology on the right (“C”). This corona has a “W-W profile” suggestive of a regressive stage in corona development^[1], with the elevated portions defined by the intensely grooved annulus (brown in Fig. 1C).

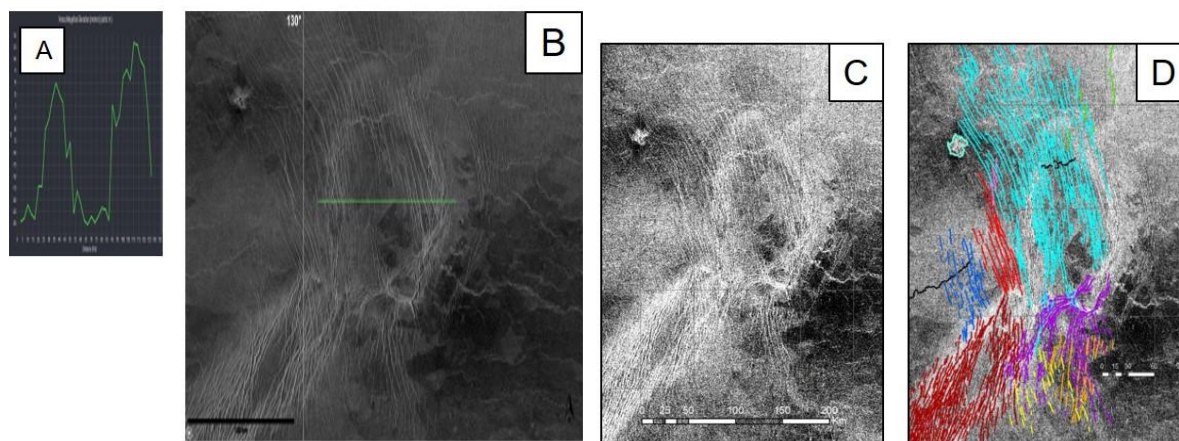


Figure 3: Morphology of the Xcacau Corona and associated Grabens. The topographic profile is presented on the left (“A”), and the uninterpreted Magellan mission data in the middle (“B”, “C”). The Xcacau Corona has a sunken core which is interpreted to represent a regressive stage. The mapped grabens in “D” are interpreted to represent underlying dyke swarms.

Discussion and Conclusions: Latmikaik Corona is considered regressive due to its W-W shaped profile. Xcacau Corona is considered regressive due to sunken U-shaped profile.^[1] Densely packed grabens – surficial expression of underlying dyke swarms. Complex system (up to 15) graben swarms - cut across the coronae and Tellervo Chasma suggest a prolonged history of extension.

Acknowledgements: Acknowledgements to the USGS Astropedia data source for supplying radar images of Venus collected by the Magellan spacecraft.

References: ^[1] Guseva, E. N., Ivanov, M. A. Structures of Coronae on Venus: Results of Topographic and Geologic Analysis. // Solar System Research. 2020, V. 54. N. 6. P. 529-536.

Application of Rb-Sr mica LA-ICP-MS dating for the determination of the age of emplacement of mafic rocks on the example of the mafic dykes in the Ukrainian Shield

Shumlyansky L.^{1,2}, Rankenburg K.³, Gatsenko V.^{4,5}

¹ School of Earth and Planetary Sciences, Curtin University, Perth, GPO Box U1987, WA 6845, Australia; Leonid.Shumlyansky@curtin.edu.au

² Institute of Geological Sciences, Polish Academy of Sciences (ING PAN), Research Centre in Kraków, Senacka 1, PL-31002 Kraków, Poland

³ John de Laeter Centre, Curtin University, GPO Box U1987, Perth, WA 6845, Australia

⁴ M.P. Semenenko Institute of Geochemistry, Mineralogy and Ore Formation of the National Academy of Sciences of Ukraine.

⁵ Armed Forces of Ukraine

Isotope dating of mafic dykes is not a trivial task due to the rarity of suitable minerals. Zircon, commonly used for U-Pb dating of various rocks, occurs in mafic rocks only at the late stages of their crystallization, when zircon saturation can be achieved. Moreover, zircon in the mafic rocks can be captured by the intruding mafic melts from the country crustal rocks. There were numerous cases when the zircon population in the mafic dykes was dominated by xenogenic crystals that yielded too old ages (e.g., Shumlyansky et al., 2016). Baddeleyite is the most trustful mineral for dating mafic rocks, but it is also commonly lacking, or its recovery from the rock is fraught with difficulties. However, the main advantage of the syngenetic zircon and baddeleyite in mafic rocks is their high closure temperatures, close to the temperature of the rock crystallization. Perovskite is another mineral suitable for U-Pb dating. It was successfully used for the dating of kimberlite and alkaline rocks worldwide, but it is uncommon in other rock types.

Other promising candidates for dating mafic rocks are mica group minerals (biotite, phlogopite, muscovite, phengite). Due to the high K contents, these minerals are amenable to the ⁴⁰Ar/³⁹Ar dating, which can produce reliable results, but is time-consuming and expensive. Due to the high (and variable) concentration of Rb (which readily substitutes for K), these minerals can also be dated using the Rb-Sr isochron method. Until recently, the application of this method was hampered by the necessity of the separation of the required amount of mica sufficient to perform at least several Rb-Sr isotope measurements using the TIMS or MC-ICP-MS technique. As long as the chemical separation of Rb and Sr is involved, this method is also relatively time-consuming and not cheap, although it still represents the “gold standard” for precision and accuracy.

The Rb-Sr mica dating method has several limitations, which restrict its application. The main ones are the relatively low closure temperature, which varies from ~ 500 °C for muscovite to 300 °C for biotite (Waight, 2013 and references therein); and susceptibility to subsequent alteration. The Rb-Sr isotope system in mica can be disturbed by moderate heating, or relatively low-temperature processes such as weathering, hydrothermal alteration and deformation. In view of the laboriousness of the Rb-Sr isotope studies using the TIMS technic, its application for the mica dating was very limited, although there were several cases of successful application of mica Rb-Sr dating for establishing ages of the igneous rocks (e.g., Yutkina et al., 2005).

The application of the LA-ICP-MS technic for Rb-Sr dating of mica was not possible until recently due to the isobaric interference of ⁸⁷Rb on ⁸⁷Sr. However, introducing the QQQ reaction cell technique allowed for resolving this problem (Zack and Hogmalm, 2016), and now the Rb-Sr LA-ICP-MS mica method can be routinely applied for the dating of various rock types. Regarding igneous rocks, the most suitable target for dating would be a fresh unaltered rock that experienced fast cooling. In addition to the isotope age, the ⁸⁷Sr/⁸⁶Sr initial ratio which bears important petrological information, is also obtained.

Micas often occur in mafic rocks as an accessory phase. They usually form at the very late stages of magmatic crystallization and fill in the interstitial space. Mafic dykes, exceeding a few meters in thickness, and emplaced in the upper crust, will cool fast enough to achieve the mica closure temperature soon after the emplacement, but slow enough to allow the formation of crystals of sufficient size.

We applied the LA-ICP-MS Rb-Sr mica dating method for the determination of the ages of several mafic dykes in the Ukrainian Shield. The first dyke is composed of mica-rich kimberlite that belongs to the Prutivka-Novogol large igneous province (Shumlyansky et al., 2016; 2021). The age of kimberlite dykes in

this area has been previously established by TIMS Rb-Sr mica dating at 1770 ± 9.4 Ma (Yutkina et al., 2005). Our new age for kimberlite is 1770 ± 6 Ma ($^{87}\text{Sr}/^{86}\text{Sr}_i = 0.7076 \pm 0.0012$) (Fig. 1).

The second dated dyke belongs to the Devladove dyke swarm that extends for ca. 50 km in the E-W direction and is located in the Middle Dnieper Domain of the Ukrainian Shield. The swarm comprises 11 individual dykes having up to 400 m in width and reaching 10-15 km in length and are composed of mica-bearing peridotites. Their Sm-Nd CHUR model ages are 2.78 and 2.57 Ga (Shumlyanskyy and Velikanova, 2007), and the youngest rocks cut by the swarm were dated at 2.85 Ga. Unlike many other mafic and ultramafic dykes in the domain, the Devladove dyke swarm do not bear indications of metamorphic overprint. The exact age of the dykes, however, is unknown. We have performed in-situ Rb-Sr mica dating of two samples of Devladove dyke peridotites, which yielded ages of 1902 ± 2 Ma ($^{87}\text{Sr}/^{86}\text{Sr}_i = 0.70987 \pm 0.00087$) and 1880 ± 6 Ma ($^{87}\text{Sr}/^{86}\text{Sr}_i = 0.8412 \pm 0.0055$), respectively (Fig. 1). As long as these rocks do not bear any mineralogical evidence of metamorphism, the obtained ages may correspond either to the true age of the emplacement or to the cooling of the rocks after moderate heating that did not cause metamorphism but resulted in a reset of the Rb-Sr isotope system in mica. The large variability of the $^{87}\text{Sr}/^{86}\text{Sr}_i$ ratio signifies the role of varying crustal contamination.

In the Azov Domain of the Ukrainian Shield, we studied micas found in the camptonite dyke that cuts through Paleoproterozoic granites in the Khibodariivka open pit. Micas in these rocks form phenocrysts and also occur in the groundmass. Zircon separated from these rocks yielded an age of 2163 ± 11 Ma, which closely corresponds to the age of host granites. In terms of chemical composition, these zircons also show affinity to granites, so we consider them as xenocrysts captured from the country rocks during the emplacement. Phenocrystic and groundmass micas yielded ages of 1650 ± 30 Ma ($^{87}\text{Sr}/^{86}\text{Sr}_i = 0.7093 \pm 0.0025$) and 1770 ± 15 Ma ($^{87}\text{Sr}/^{86}\text{Sr}_i = 0.7034 \pm 0.0016$), respectively (Fig. 1), confirming the Paleoproterozoic age of the dyke and its possible affinity to the Prutivka-Novogol LIP.

In summary, The Rb-Sr LA-ICP-MS mica dating of mafic rocks is capable to provide useful geochronological information and can be applied as an addition or substitute to the conventional $^{40}\text{Ar}/^{39}\text{Ar}$ method. However, Rb-Sr mica dating is less time-consuming and cheaper. Moreover, it provides additional geochemical information ($^{87}\text{Sr}/^{86}\text{Sr}$ initial) that can be used to constrain the origin of the rocks.

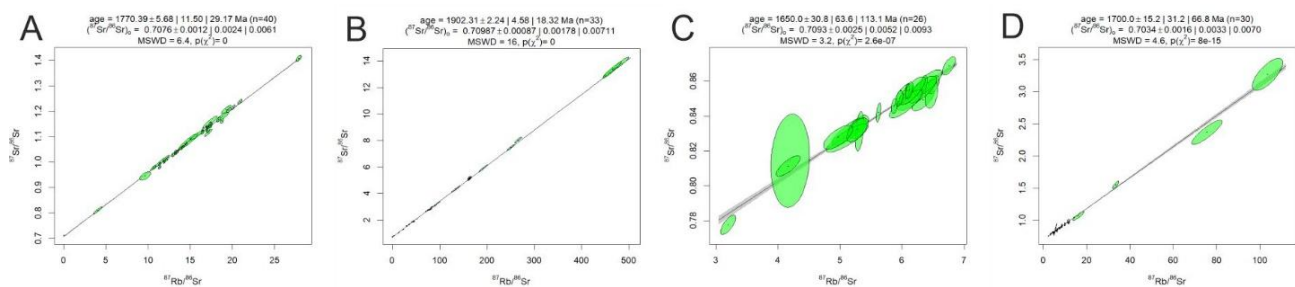


Figure 1. Results of Rb-Sr LA-ICP-MS mica dating of mafic rocks in the Ukrainian Shield. A – kimberlite dyke; B – Devladove peridotite dyke; C – Khibodariivka camptonite dyke, mica phenocrysts; D – Khibodariivka camptonite dyke, mica from the groundmass.

Shumlyanskyy L., Ernst R.E., Albekov A., Söderlund U., Wilde S.A., Bekker A. (2021) The early Statherian (ca. 1800-1750 Ma) Prutivka-Novogol large igneous province of Sarmatia: geochronology and implication for the Nuna/Columbia supercontinent reconstruction. *Precam. Res.*, 358, 106185.

Shumlyanskyy L., Mitrokhin O., Billström K., Ernst R., Vishnevskaya E., Tsymbal S., Cuney M., Soesoo A. (2016a) The ca. 1.8 Ga mantle plume related magmatism of the central part of the Ukrainian shield. *GFF*, 138, 86-101.

Shumlyanskyy L., Nosova A., Billström K., Söderlund U., Andréasson P.-G., Kuzmenkova O. (2016b) The U-Pb zircon and baddeleyite ages of the Neoproterozoic Volyn Large Igneous Province: implication for the age of the magmatism and the nature of a crustal contaminant. *GFF*, 138, 17-30.

Shumlyanskyy L., Velikanova O.Y. (2007) New data on the petrology of rocks of the Devladove dyke swarm and Ternivka syncline, the Middle Dnieper Domain of the Ukrainian Shield. *Proceedings of the IFS*, p. 83-94 (In Ukrainian).

Waight, T. (2013). Rb–Sr Geochronology (Igneous Rocks). In: Rink, W., Thompson, J. (eds) *Encyclopedia of Scientific Dating Methods*. Springer, Dordrecht.

Yutkina E.V., Kononova V.A., Tsymbal S.N., Levskiy L.K., Kiryanov N.N. (2005) Isotope-geochemical specialisation of the mantle source of kimberlites of the Kirovograd complex, Ukrainian Shield. *Doklady Akademii Nauk*, 402, 87–91 (In Russian).

Zack T., Hogmalm K. J. (2016) Laser ablation Rb/Sr dating by online chemical separation of Rb and Sr in an oxygen-filled reaction cell. Chem. Geol., 437, 120–133.

Timing of Paleoproterozoic carbonatitic magmatism by U-Pb ID-TIMS dating of calcic garnets

M.V. Stifeeva¹, Yu.V. Plotkina¹, E.B. Salnikova¹, A.B. Kotov¹, K.A. Savko²

¹Institute of Precambrian Geology and Geochronology RAS, 199034 Makarova emb. 2, St.Petersburg, Russia

²Voronezh State University, 394018 Universitetskaya Square 1, Voronezh, Russia

Early Precambrian alkaline-carbonatitic complexes often underwent by large-scale accretionary and collisional reworking, strongly transforming primary igneous associations, thus complicating geochronological and petrogenetic reconstructions.

We provide U–Pb geochronological data on Ca-Fe garnet, zircon and titanite from two metamorphosed Paleoproterozoic alkaline–carbonatite complex from the the Kursk block of Sarmatia and the Aldan shield.

The Dubravinsky alkaline-carbonatite complex is located within the Kursk-Besedino domain, which, together with the Azov block, forms the Paleoarchean core of eastern Sarmatia (Azov-Kursk domain) (Bogdanova et al., 2016; Savko et al., 2021). The Dubravinsky massif consists of clinopyroxenites, carbonatites (together with silicocarbonatites and phoscorites) and syenites (including alkaline granites).

Zircons in silicocarbonatite have short-prismatic or dipyrmidal habit typical for many carbonatite rocks. Zircon crystals are euhedral and subhedral, semitransparent and transparent, of gray color, sometimes square in shape or with smoothed, almost rounded tips, 50–80 μm in size. In CL images most crystals show a zonal structure - lighter inhomogeneous centres with a very dark high-uranium regions occupying up to 50% area, and dark gray rims 10–15 μm as wide. The U-Pb isotope system in carbonatitic zircons is disturbed, which suggests influence of superimposed events.

The ages of titanite 2071 ± 11 Ma and andradite 2075 ± 12 Ma from the alkaline pyroxenite, as well as of titanite from carbonatite 2080 ± 13 Ma (Albekov et al., 2017) The closing temperatures of the U–Pb titanite isotope system in the range of 650–700 $^{\circ}\text{C}$ (Frost et al., 2000, Wu et al., 2010) are close to the peak temperatures of metamorphism (~ 650 $^{\circ}\text{C}$), precluding choosing one of interpretations. However, for calcium garnet with a grain size of 100 μm from the alkaline rocks and carbonatites, the closing temperature is 750–800 $^{\circ}\text{C}$ (Yang et al., 2018). This suggests that the U-Pb age of andradite from the alkaline pyroxenites of the Dubravinsky massif corresponds to the age of its crystallization from the melt.

U–Pb (ID-TIMS) garnet and U–Th–Pb (LA-ICP-MS) zircon geochronological studies were performed for the carbonatites veins from the Late Archaean Ukduska alkaline-carbonatitic massif, Aldan shield. Zircons extracted from carbonatite are subeuhedral crystals with prismatic habits. Zircon crystals are usually fractured, opaque, and dark cherry colored. Their structure is characterized by the brown-color zoned cores and two generations of rims. The U–Th–Pb (LA-ICP-MS) studies were carried out in the core and rims of zircon grains. The average ages (207Pb/206Pb) of the cores are 2708 ± 14 Ma (MSWD = 0.36), the first-generation rims are 2645 ± 17 Ma, and, finally, the second-generation rims are 1865 ± 16 Ma (MSWD = 0.36). U-Pb age of andradite from the Ukduska carbonatite is at 1881 ± 8 Ma (MSWD = 0.70).

Hence, two formation stages of Early Precambrian carbonatites can be distinguished in the southeastern part of the Chara–Olyokma geoblock. The first of them includes the formation of carbonatites related to the Late Archean alkali potassic and ultrapotassic magmatism with an age of 2719 ± 14 Ma (Tabuns et al., 2004). The second stage carbonatites form dikes and veins developed in the Early Proterozoic (1881 ± 8 Ma).

Therefore U-Pb ID-TIMS ages obtained for Ca-Fe garnets demonstrate the advantages that these minerals offer to geochronological study of Precambrian carbonatites affected by metamorphic alteration.

The investigations were supported by RSF (grant № 22-17-00211).

Albekov, A.Yu., Chernyshov, N.M., Ryborak, M.V., Kuznetsov, V.S., Salnikova, E.B., Kholin, V.M., 2017. U-Pb isotopic age of apatite-bearing carbonatites in the Kursk Block, Voronezh Crystalline Massif. *Dokl. Earth Sci.*, 473, 271–272.

Bogdanova, S.V., Gorbatshev, R., Garetsky, R.G., 2016. EUROPE/East European Craton. Reference Module in Earth Systems and Environmental Sciences, Elsevier. <https://doi.org/10.1016/B978-0-12-409548-9.10020-X>.

Frost, B.R., Chamberlain, K.R., Schumacher, J.C., 2000. Spinel (titanite): phase relations and role as a geochronometer. *Chemical Geology* 172, 131–148.

Savko K.A., Samsonov A.V., Larionov A.N., Chervyakovskaya M.V., Korish E.H., Larionova Yu.O., Bazikov N.S., Tsybulyaev S.V. *A buried Paleoproterozoic core of the Eastern Sarmatia, Kursk block: U-Pb, Lu-Hf and Sm-Nd isotope mapping and paleotectonic application// Precambrian Research 353. 2021. 106021*

Tabuns E.V., Sal'nikova E.B., Kovach V.P., Kotov A.B., Yakovleva S.Z., Fedoseenko A.M., Tolkachov M.D., Plotkina Yu.V., Kovalenko V.I. *Late Archean initial potassic magmatism of the Aldan shield (Ukduska massif): evidence from U-Pb single zircon dating. 2004. Doklady Earth Sciences. 398, 7, 943-946.*

Wu, F.Y., Yang, Y.H., Marks, M.A.W., Liu, Z.C., Zhou, Q., Ge, W.C., Yang, J.S., Zhao, Z.F., Mitchell, R.H., Markl, G., 2010. *In situ U-Pb, Sr, Nd, and Hf isotopic analysis of eudialyte by LA-(MC)-ICP-MS. Chemical Geology 273, 8-34.*

Yang Y.H., Wu F.Y., Yang J.H., Mitchell R.H., Zhao Z.F., Xie L.W., Huang C., Ma Q., Yang M. and Zhao H. 2018. *U-Pb age determination of schorlomite garnet by laser ablation inductively coupled plasma Mass spectrometry. Journal of Analytical Atomic Spectrometry, 33, 231-239.*

Geological and geostatistical studies of Eburnean Tri-k orogenic gold deposits (Siguiri basin-Guinea)

Zerhouni ^aN., Mougouina ^bE.M., Machuca ^cD., Maacha ^aL., Zouhair ^aM., Mounji ^dD. and Outaghat ^dH.

^a *Reminex Company of Managem. Morocco.*

^b *Laboratory DLGR, Department of Geology, FSSM, Faculty of Sciences Semlalia. Cadi Ayyad University, Marrakesh, Morocco.*

^c *SRK Consulting. Canada*

^d *Mandiana Mining Company of Managem. Guinea*

This work is related to the “TRI-K” Eburnean orogenic gold deposits in NE of Guinea (Siguiri basin). The deposit hosts 94Mt at 1.30 ppm of gold and 4Moz of gold metal. It's consisting of two deposits, Koulekoun and Kodieran, owned by Managem group, through its subsidiary SMM (Mining Company of Mandiana). The aims of this study are to recognize the regional and local geological framework of these deposits and to estimate their mineral resources.

Koulekoun and Kodieran deposits are located in the North East of Guinea in the Birimian lands of the Siguiri sedimentary basin. This region is characterized by a predominance of Birimian-green belt which are essentially volcanics and volcano-sedimentary rocks, quartzites and greywacks. These rocks are metamorphosed to greenschist facies intruded by plutons and porphyritic dykes. The Birimian Formation is in abnormal contact with the Granitoid archaeans. All these formations are structured along a NNE and NNW direction during the Eburnean orogeny. The Koulekoun and Kodieran deposit are mainly hosted in a porphyritic dyke oriented NW-SE. The granodiorites and dacites are linked to gold mineralization. Other mineralization is associated with ductile shear zones NE-SW affecting volcanic, volcano-sedimentary and porphyry dykes NW SE. The most important gold concentrations are located in the intersection of the two directions NE-SW and NW- SE. The mineralization is carried by quartz veins and veinlets in the form of shear veins and tensional slots. These veins are most abundant in the dykes and become sporadic in the sediments. The weathering is very extensive and the outcrops of the bedrock are very rare. The source rock is overworked by a pile of saprolite reaching up to 50m or more in places. The hydrothermal alteration is predominated by the silicification, sericitization and chloritization of the host rocks. Gold at Tri-k occurs in two forms: native gold in quartz veins and veinlets, and gold associated with sulfides, mainly pyrite, which occurs in disseminated form in dykes and sedimentary rocks. The sulfides consist mainly of crystals of pyrite with gold inclusions and chalcopyrite. Pyrite is deformed and turns into arsenopyrite. Galena occurs as isolated crystals along the contact joints between these last two minerals. The structural, hydrothermal and mineralogical characteristics make the Tri-k orogenic gold deposit similar to the West African deposits.

On another hand, geostatistical study and estimation of the mineral resources are performed with ordinary kriging method using Datamine software. Variography was used to assess the spatial continuity of the gold data and to assist in the selection of estimation parameters. The variographic study yielded variograms with very large ranges and a low nugget effect ($\text{Gamma} = 0.15 + \exp(0.77 \cdot 5/4/2) + S(0.08 \cdot 120/80/15)$) indicating good continuity and distribution of gold grades in both deposits. The ellipsoids are oriented along the directions and dips of the mineralized structures and their sizes reflect the ranges of the variograms. Mineral Resources have been classified in accordance with the CIM Definition Standards for Mineral Resources and Mineral Reserves (2014). Mineral Resources are reported at an appropriate cut-off grade that takes into account mining scenarios and processing recoveries. Mineral Resources are reported in conceptual pits. The Mineral Resource statement for the Tri-K deposits is reported at different in-situ cut-off grades, which is explained by the different oxidation levels and slightly different economic parameters for the two deposits.

IDENTIFICATION OF PEGMATITES IN THE SIDI BOU OTHMANE AREA (CENTRAL JEBILET, MOROCCO) USING LANDSAT OLI 8 IMAGERY

Wissale Aba sidi¹, Amina Wafik², Abdessamad Najine¹, Yousra Morsli³

¹ Applied Geophysics, Water and Environment Laboratory, *Faculty of Sciences and Technics Beni-Mellal* 23000, Morocco

² *DLGR Laboratory, URAC 43, Semlalia Faculty of Sciences, Cadi Ayyad University (UCA), Marrakesh, Morocco*

³ *Geosciences and Applications Laboratory, Faculty of Sciences Ben M'sik, Hassan II University of Casablanca, B.P. 7955, Sidi Othmane, Casablanca, Morocco.*

Remote sensing has become an indispensable tool in various scientific disciplines, including geology, offering a multitude of techniques for mapping geological features. In particular, pegmatites, characterized by their coarse-grained and enriched composition, pose a significant interest due to their rare element content and economic potential. This study uses ratios and band combinations proposed in published literature to leverage remote sensing techniques to identify and map pegmatitic structures in the Sidi Bou Othmane (SBO) area.

To accomplish this objective, the Landsat OLI 8 data were subjected to a series of transformations and calculations, including Minimum Noise Fraction (MNF), Principal Component Analysis (PCA), and Ratio-based (RB) methods. Additionally, an extensive list of combinations proposed for mapping pegmatites was explored to identify the most effective approach.

Multiple tests were conducted to evaluate the performance of various techniques. Among them, the RGB color composition consisting of specific band ratios (1/3; 1/4; 2/5) emerged as particularly effective. This composition successfully identified the pegmatitic structures within the SBO area and provided a high level of detail, accurately reflecting the ground reality. Furthermore, it facilitated the interpretation of the main structural geology and tectonic forces influencing the area.

The resulting map generated from the selected band combination was validated by comparing it with field data, ensuring its accuracy and reliability. The map exhibited a comprehensive distribution of pegmatites, highlighting their spatial arrangement and variations within the study area. The integration of remote sensing techniques and field validation enabled a robust interpretation of the geological features and provided valuable insights into the pegmatitic structures in the SBO region.

This study demonstrates the significant contribution of remote sensing in mapping pegmatites and its potential for surpassing traditional methods. The identified RGB color composition with specific band ratios offers a practical and efficient approach for accurately delineating pegmatitic structures. The findings provide a foundation for future geological investigations, mineral resource assessments, and land management strategies in areas where pegmatites are prevalent.

Biography

Professors honored

Henry Halls Biography



Emeritus Professor
University of Toronto
Department of Earth Sciences
University of Toronto at Mississauga

After obtaining B.Sc. (Geology) and M.Sc. (Geophysics) degrees at the Universities of Sheffield and Durham (UK), I obtained my Ph.D. in 1970 in the Department of Geology at the University of Toronto, under the supervision of Gordon West, Department of Physics. The topic of my dissertation was The Geology and Geophysics of the Lake Superior Basin. I have been a faculty member at the University of Toronto in Mississauga since 1970, where I have held the rank of Emeritus Professor since 2010. My general field of research is the application of geophysical methods (gravity, magnetics and paleomagnetism) to the solution of geological problems, mainly involving major tectonic units of the Canadian shield. More recently, I have concentrated on the integrated paleomagnetic, geochronological and geochemical study of Precambrian dyke swarms worldwide in an effort to understand their origins and their use as links between dispersed Precambrian terranes. I have authored or co-authored over 90 refereed papers in internationally-recognized journals.

In 1985 I organized the first International Dyke Conference which brought together more than 100 scientists from 20 countries, the results of which were published as a Geological Association of Canada Special Paper 34 "Mafic Dyke Swarms" (Halls & Fahrig 1987). Since this inaugural meeting, International Dyke Swarm Conferences have been held approximately every five years. The sixth meeting (IDC6) was held February 4-7, 2010 in Varanasi, India, and a volume of papers presented at this meeting has been published by Springer Verlag (2011). The last meeting (ICD7) was held 18-20 August, 2016 in Beijing, China. The next meeting in Marrakesh, Morocco, will be held in 2020.

In 1988 I was elected the international leader of IGCP (International Geological Correlation Program) Project 257 on Mafic Dyke Swarms from which more than 30 publications including two books were produced. In the last five years about 30 dyke swarms from about 15 Precambrian cratons worldwide have been the subject of completed or ongoing studies by research groups from many countries including Canada, China, Australia, Finland, Russia, India, and Brazil. The last 10 years has seen a burgeoning of papers on dykes and particularly on the recognition of "giant radiating dyke swarms". This term was first used in the title of a Special Session I convened at the Geological Association of Canada Annual Meeting in Toronto in 1991. The session entitled "Giant Radiating dyke swarms and mantle plumes" drew more than 100 participants (standing room only!) and has been an important influence on subsequent thinking.

Prof. Hervé BERTRAND (France) Biography



Born in 1950, 73 years old

1975 : PhD « The Moroccan dolerites and the Atlantic opening: a petrological and geochemical study »

Position: Associate Professor at University of Lyon (retired since 2015)

Teaching activity:

Mainly petrology, geochemistry, volcanology, field geology

1972 – 2015: teaching at University of Lyon

1988 – 2015: teaching at Ecole Normale Supérieure de Lyon

Diffusion of knowledge:

Since 1990 : in charge of Earth Science for the Open University of Lyon (about 10 lectures/year)

Since 2008 : Leader of worldwide geological trips (France, Italy, Iceland, Canarias, Cyprus, Greece, Morocco, Ethiopia, Namibia, Cape Verde, Oman, Indonesia, Kamtchatka, Ecuador).

Research activity:

Since 1972 : Research at Laboratory of geology, Lyon

195 publications, h-index: 51, 8450 citations

Main research domain: Large igneous provinces (field investigations, petrology, geochemistry, geochronology, implications for mass extinctions):

- Central Atlantic Magmatic Province (CAMP) in France, Spain, Portugal, Morocco, Algeria, Mauritania, Mali, Guinea, Sierra Leone, Canada, USA, Guyana, Brazil, Bolivia.
- Karoo (South Africa, Botswana, Namibia, Zimbabwe)
- Yemen traps
- Parana (Brazil, Uruguay)
- Patagonia
- Deccan

Other research domains:

- Active volcanoes (Vanuatu, Erta Ale)
- Genesis of carbonatites
- Oceanic volcanism (Tyrrhenian Sea, Atlantic Ocean)



Professor Dr. Emeritus El Hassane CHELLAI

He was born in Jerada, north-east Morocco, a city renowned for the exploitation of Westphalian Coal.

After obtaining his Baccalaureate at the Omar Ibn Abdelaziz-Oujda High School, he flew to Toulouse to continue his university studies. These good results allowed him to have a scholarship.

He studied geology at Paul Sabatier Toulouse University, France, and obtained his 1st doctorate (PhD degree) in 1982 from Mediterranean Geology Laboratory at the same university and under the direction of Prof. Dr. Michel Durand-Delga.

He then created a research group in the Geology Department of the Semlalia Faculty of Sciences, Cadi Ayyad University-Marrakesh, Morocco.

He obtained his second doctorate (PhD degree) in the same institution in co-supervision with the University of Grenoble, France in 1995, after a two-year postdoctoral internship supervised by Prof. Jacques Perriaux at the Laboratory of Sedimentary Geology in Grenoble, France.

He obtained the position of Professor at the University of Marrakech.

He has published more research articles in the indexed journals.

He has supervised more thesis in geology.

He has directing several research projects within the framework of North-South and South-South cooperation.

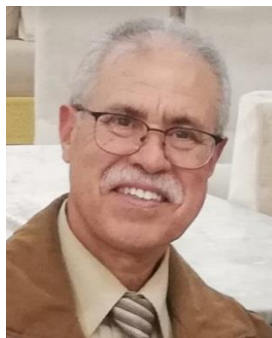
He has hosted several conferences in America, Europa, Asia, Australia (Pacific) and Africa.

He has received numerous awards from universities and learned societies “sociétés savantes”.

Some dreams come true:

- 1- A walk through: the High Atlas, the Rif, the Anti Atlas, the Meso-cenozoic (Tunisia), the Pyrenees (France-Spain), the Alps (Italy-Switzerland), Massif of Gresigne (France), The C/T (Portugal), Ophiolites (Serbia), Corals reefs (Mallorca, Zanzibar, New Caledonia, Cuba...), Mn mine (Japan), Mesozoic (China), source and reservoir rock (Nigeria, Côte d'Ivoire, Sénégal, Afrique du Sud,...), Glacial deposits (Canada), Lucy museum (Ethiopia), Phosphorite (Egypt), Thermalism (Algeria)... !!
- 2- From a pebble we were able to build a universe!!

Biographie Pr Ahmed CHALOUAN



CHALOUAN Ahmed (date de naissance 14/11/1953)

Etat civil : Marié, 2 enfants

Ex-Professeur d'enseignement supérieur (C). Faculté des sciences ;

Rabat-Université Mohammed V (1/12/1975 to 31 Août 2019)

chalouan@yahoo.com ; ahmed.chalouan@gmail.com –

Tel. Mobile: 0666187130

- *Le premier marocain qui a soutenu une thèse d'état en géologie en France.*

Etudes et Diplômes

DEA	Géologie en 1975	Université Louis Pasteur de Strasbourg
Doctorat 3 ^e cycle en	Géologie Structurale en 1977	Université Louis Pasteur de Strasbourg
Doctorat d'état	Géologie Structurale en 1986	Université Louis Pasteur de Strasbourg

- Doctorat 3^e cycle en 1977 (sur la Meseta varisque) sous la direction d'A. Piqué et A. Michard
- Doctorat d'Etat en 1986 (sur la chaîne du Rif), sous la direction d'A. Michard.

Expérience professionnelle :

1975-1977 : Assistant à la Faculté des Sciences de Rabat

1977-1986 : Maître-assistant à la Faculté des Sciences de Rabat

1986-1990 : Maître de conférences à la Faculté des Sciences de Rabat

1990-2019 : Professeur à la Faculté des Sciences de Rabat

Spécialité et thèmes de recherche :

- Géologie structurale et analyse tectonique des déformations ductiles et cassantes
- Géologie régionale et l'évolution tectonique de la chaîne alpine du Rif
- Néotectonique et tectonique active
- l'aspect appliqué de la géologie structurale (Cartographie, barrages, matériaux...).
- Etudes de subsurface par des méthodes géophysiques (sismique réflexion et magnéto-tellurique) en collaboration avec les Universités de Grenade, de Madrid, de Barcelone, de Rice-USA et l'Office National des Hydrocarbures et des Mines du Maroc (ONHYM).

Responsabilités scientifiques et administratives :

- Fondateur du laboratoire de Géologie structurale de la Faculté des Sciences de Rabat qu'il a dirigé durant une vingtaine d'années,
- Chef du département de Géologie de la Faculté des Sciences de Rabat (1982-1990) ;
- Chef du département de Géologie de la Faculté des Sciences de Tétouan (1982-1985)
- Expert et membre des comités scientifiques dans le domaine des Sciences de la Terre et de l'univers au CNRST entre janvier 2008 et janvier 2014 (2 mandats).
- Responsable d'études et de plusieurs programmes de recherche nationaux et de coopération internationale sur l'évolution tectonique de la chaîne du Rif.
- Organisation et co-organisation de rencontres, colloques et congrès internationaux au Maroc et en Europe.

Productions scientifiques :

Publications

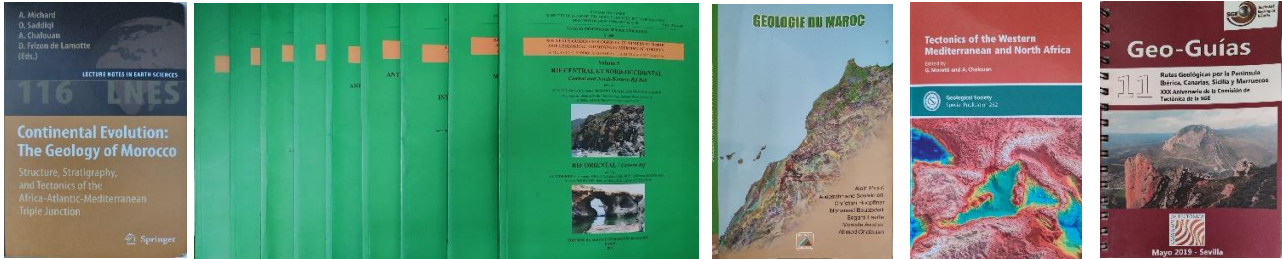
Une centaine de publications dans des revues indexées. Le dernier article scientifique publié: « A. Chalouan & al., 2023, cGPS Record of Active Extension in Moroccan Meseta and Shortening in Atlasic Chains under the Eurasia-Nubia Convergence. Sensors 2023, 23, 4846. <https://doi.org/10.3390/s23104846>».

Co-auteur d'Ouvrages de recherche :

- Co-auteur du livre « Les paysages du Rif marocain : Maroc Mémoire de la Terre ». **Ouvrage** Edit. Mus. Nat. d'Hist. Nat., Paris, pp166-179 (1999).
- Co-auteur du livre : « Géologie du Maroc » (2007). A. Piqué, A. Soulaïmani, C. Hoepffner, M. Bouabdelli, E. Laville, M. Amrhar & A. **Chalouan**. Edition GEODE. Maroc. ISBN 9954-8697-1-9. 287 pages.
- Co-auteur du livre : *Geo-Guias 11, Rutas Geológicas por la Península Ibérica, Canarias, Sicilia y Marruecos. XXX Aniversario de la Comisión de Tectónica de la SGE. Publicado por la Sociedad Geológica de España, 2019 (Mayo 2019 – Sevilla) ; 332 pages.*

Co-auteur et coéditeur d'Ouvrages et de Revues de recherche

- MORATTI, G. & CHALOUAN, A. (éditeurs) 2006. *Tectonics of the Western Mediterranean and North Africa. Geological Society, London, Special Publications, 262, Ouvrage de 384 pages ISBN. 1-86239-202-1.*
- Co-auteur et co-éditeur: du livre: Michard, O. Saddiqi, A. Chalouan and D. Frizon de Lamotte, 2008: *Continental Evolution: The Geology of Morocco: Structure, Stratigraphy and Tectonic of the Africa-Atlantic-Mediterranean Triple Junction. Springer Eds. Berlin. ISBN: 978-3-540-77075-6; 424 p.*
- Co-auteur et co-éditeur: du livret-Guide: Rif central et Nord-Occidental (Central and north-western Rif Belt). 2011- A. Chalouan, A. Michard, K. El Kadiri, O. Saddiqi, M. Durand-Delga, P. Olivier & M. L. Bouybaouene. *Notes et Mémoires du Service géologique. N° 560, 89 pages.*
- Coéditeur de : **9 Nouveaux Guides géologiques et miniers du Maroc** (New Geological and Mining Guigebooks of Morocco) en 9 volumes. 2011- A. Michard, O. Saddiqi, A. Chalouan, E. Rjimati & A. Mouttaqi (Eds). *Notes et Mémoires du Service géologique. N° 556 à 564.*
- **Co-auteur de 5 cartes géologiques du Maroc aux échelle 1/50.000 ; 1/100.000 et 1/1000.000 :**



Encadrement de thèses de doctorat :

Encadrement et Co-encadrement d'une **quarantaine** de thèses :

- une **vingtaine** de thèses de troisième cycle,
- une **quinzaine** de thèses d'Etat et
- **six** thèses de doctorat.

Autres Activites :

Société Géologique du Maroc	depuis 1992	Membre du bureau, Vice-Président
Groupe "Permo-Trias marocain"	depuis 1996	Membre
Moroccan Association Petroleum Geologists (MAPG)		Membre du bureau, Editeur entre 1997 et 2003
Moroccan Association Petroleum Geologists (MAPG)		Membre du bureau, Vice-Président entre 2004-2009
Association Marocaine des Géosciences (AMG)		Vice-Président depuis janvier 2014

Dr. Ahmed El Hassani

Hassan II Academy of Sciences and technology Succinct biography



Ahmed El Hassani got his Master in Natural Sciences (1977) at the Faculty of Sciences (Mohammed V University, Rabat); then his Ph.D., in 1980, at the Aix-Marseille University (France). Later, in 1990, he obtained the highest level in Science (Doctorat d'Etat) at Louis Pasteur University of Strasbourg (France). In September 1980, he joined the Scientific Institute as Senior Lecturer. In addition, he participated in several teaching programs of Geology (teaching and field trips) at the Mohammed V University and in Doc-training. The research he has undertaken is related to the Paleozoic of Morocco (mapping and structural geology).

He participated in several international meetings in Europe, the USA, and the MENA region.

In addition, he published his numerous data in national journals (e.g., Bulletin of the Scientific Institute, Notes and Memoirs of the Geological Survey of Morocco) and international ones (e.g., Science, Tectonophysics, P3, Facies, Geology, CRAS Paris, Cretaceous Research.). Furthermore, within the framework of international collaboration has developed very successful cooperation with several foreign universities: American (UTA Arlington-Dallas; Louisiana), German (Göttingen, Frankfurt, Berlin, Muenster), Belgium (Brussels, Liege), French (Marseille, Strasbourg, Brest, Montpellier), Spanish (Oviedo, Madrid) and Portuguese (Lisbon). Similarly, his work on Devonian of Morocco, an international reference, enabled him to organize several international meetings (1999, 2004, 2013, and 2018), which allowed him to be elected in 2004 as Vice-President of the Subcommittee of Devonian System (SDS-IUGS). In addition, he contributes to several International Geological Correlation Programs (IGCP-UNESCO) as a full member.

In 1995 he was granted a Fulbright scholarship to develop his Internet knowledge, which allowed him to develop the Scientific Institute Network.

-In January 2006, HM King Mohammed VI nominated him as Director of the Scientific Institute of the Mohammed V University of Rabat, which he led from 2006 to 2014. HM King Mohammed VI nominated him on May 18, 2006, as a Resident Member of the new Hassan II Academy of Science and Technology, where he has led the College of Science and Technology of Environment, Earth and the Sea since that until today.

-En 2022, Le Dr. A. El Hassani à capitaliser ces vastes et larges connaissances de la géologie du Maroc dans un Livre : intitulé : « Le paradis des Géologues : un voyages à travers le temps dans le royaume du Maroc, *Hassan II Academy Press* »

For further scientific works: https://www.researchgate.net/profile/Ahmed_El_Hassani

